



Margarida Maria Correia Alves Lopes

Mestre em Clima e Ambiente Atmosférico

Ultrafine Particle Levels Monitored at Different Transport Modes in Lisbon

Dissertation for obtainment of Doctor degree in
Environment and Sustainability

Advisor: Francisco Manuel Freire Cardoso Ferreira, PhD,
Associate Professor, FCT/UNL

Co-Advisor: Célia Marina Pedroso Gouveia, PhD, Assistant
Professor, IDL-FCUL

Presidente: Prof. Doutor António Nóbrega de Sousa Câmara

Arguente(s): Prof. Doutor Julio Lumbreras

Prof. Doutora Margarida Maria Correia Marques

Vogais: Prof. Doutor António Nóbrega de Sousa Câmara

Prof. Doutor Francisco Manuel Freire Cardoso Ferreira

Prof. Doutor Pedro Manuel da Hora Santos Coelho



FACULDADE DE
CIÊNCIAS E TECNOLOGIA
UNIVERSIDADE NOVA DE LISBOA

July 2019

Ultrafine Particle Levels Monitored at Different Transport Modes in Lisbon

Copyright © Margarida Maria Correia Alves Lopes,

Faculdade de Ciências e Tecnologia da Universidade Nova de Lisboa, Universidade Nova de Lisboa.

A Faculdade de Ciências e Tecnologia e a Universidade Nova de Lisboa têm o direito, perpétuo e sem limites geográficos, de arquivar e publicar esta dissertação através de exemplares impressos reproduzidos em papel ou de forma digital, ou por qualquer outro meio conhecido ou que venha a ser inventado, e de a divulgar através de repositórios científicos e de admitir a sua cópia e distribuição com objectivos educacionais ou de investigação, não comerciais, desde que seja dado crédito ao autor e editor.

To my daughter

Acknowledgments

This work started late in 2010. After many “ups and downs”, with a forced interruption of four years, it finally came to a conclusion. During these past eight years, there are many ones whom I’m deeply thankful, both in personal and professional levels. These lines won’t be enough to pay them my appreciation... still, I will do my best.

The first one I would like to thank is my supervisor, Prof. Francisco Ferreira. Thank you for the opportunity, for the precious guidance, for helping me through scientific research, for the freedom you gave me to find my own path and all the support to accomplish the work which make this thesis possible. Thank you for your infinite patience and contributions during the thesis writing stage, from its structure definition to contents discussion, and finally its proof reading. Thank you for helping me through all difficult moments and facing all the adversities without losing hope. A very special thanks to my co-supervisor, Prof. Célia Gouveia. Your complementary knowledge, perspectives, objectivity and insightful comments allowed me to widen my research and enrich this work.

Secondly, I want to thank the Air Quality research group in the FCT-NOVA, for their friendship, for all the help and for being always there for me throughout this work and Ana Russo, from Instituto Dom Luiz, Faculty of Sciences of the University of Lisbon. Joana Monjardino, a precious co-author in my first paper, thank you for all the fresh viewings, perspectives, advices and precious guidance throughout my first scientific peer reviewed paper; Ana Russo, was a crucial co-author in both my scientific peer reviewed papers. Thank you so much for helping me with writing, analysis, review and corrections and answers to reviewers. Paulo Pereira and Sofia Teixeira, for the support and for being in the field helping me collecting traffic data; Luísa Mendes for the support on getting meteorological data and Hugo Tente, for some fresh ideas and perspectives.

Thank you, Helena Pandamo and Sandra Ferreira, for all the patience, competence and availability to solve all the administrative issues that came along this journey.

A very special thanks to my daughter, to whom I dedicate this work. Thank you so much for being such a grown up, independent and comprehensive person, now a 13 years old young “woman”. I will try to make it up for you over the coming years for all the time together we had to abdicate during this task. This is also your work and I hope it can make you proud. Thank you! My grand-mother, Herminia Correia, wherever you are... you were a force of Nature and I always took you as an example and a life guidance. Wherever you are, I am sure you are feeling very proud and I am truly thankful for the privilege of learning from you and have you as my model guide. My mother and my father for the all support. My mother suffered as much as I did during this task and kept me confident throughout this job; my father... well, I learnt from him that “it is only impossible until it is done” and he never doubt I would accomplish this goal. My family’s care and love were, are and they will always be, my strength. And, as bizarre as it might seems, I want to thank my cats. Unconditional love and they had always found a way to make me laugh whenever I was stressed and needed a good laugh. Also, a thank to my “Karate family”, for helping me keeping physically and mentally healthy and for the support with logistics, whenever Joana needed it for attending all the tournaments that I could not go.

Another very special thanks to my Master advisor, Prof. Corte Real. I am so sorry you are no longer among us to enjoy this achievement! You were born to teach and had inspired so many students along your teaching years. And I am so proud for the privilege of had being one of them!

Lastly but not least, I want to thank my friends for all the support, help, confidence and friendship. You were all pillars and had your unique and precious role. I highlight Inês Filipe, what can I say? You’re the best friend anyone can ask for; Dulce Castro, for the companionship during sampling, exchanging of ideas and different approaching; Alexandra Simplício, my newest friend. An exceptional human being who always found the right words and actions to keep me grounded and confident. Thank you so much

for believing in me, even when I doubted that I would accomplish this task in time. Fernando Cunha, my former teacher and dear college and friend, whom I am extremely thankful for being always available to exchange ideas and points of view. I cannot forget Isabel Henriques, who introduced me to Paulo Veiga, an expert on analysis with Pivot Tables; his guidance and lessons were crucial to accomplish data analysis. Bruno Silva, thanks for the help with R Studio. Andrea Espinheira, for choosing me as your advisor in your final project of graduation and forcing me to be up time with road traffic data and analysis.

This work would not have been possible without the support of the following institutions who provided data and/or the means to get it and to whom I am deeply grateful for the support:

- the Portuguese Institute for Sea and Atmosphere (IPMA), for the wind data;
- the Municipality of Lisbon (CML), responsible for the GERTRUDE system, for the traffic data provided;
- the Regional Development and Coordination Commission of Lisbon Tagus Valley (CCDR-LVT), responsible for the air quality dataset provided;
- Transtejo and Soflusa (TTSL) for giving us access to a private location for measurements in the ferries station of Montijo.

Abstract

Ultrafine particles (UFP) are defined as particulate matter with a diameter smaller than 0.1 μm . Because of their reduced size and consequently very low mass, they are usually expressed in particle number concentration (PNC), in particles per cubic centimetre (pt.cm^{-3}). There have been growing evidences that long-term exposure to UFP may induce or aggravate pulmonary and cardio-respiratory health conditions and are linked to increased hospitalization and mortality rates. More recently, they have also been linked to neurological diseases and to children cognitive development issues.

Airports, road traffic and maritime transport have been identified as significant sources of ultrafine particulate matter. There is lack of information regarding PNC in the vicinity of airports. In the case of Lisbon Airport (LA), located within the city and surrounded by housing areas, offices, schools, hospitals and sport and recreational complexes, knowing their levels assumes vital relevance. In-land passenger ferries are also a source of UFP, far less addressed. A significant fraction of a person's total daily exposure to fine and ultrafine particles occurs during home-work commuting periods. Therefore, microenvironments influenced by different transport modes are particularly relevant. Thus, to associate their contribution with to UFP concentrations is important and allows the estimation of their contribution to air quality degradation within the city and the degree of population exposure.

This work aims to assess the effect on UFP concentrations from road, air and river traffic modes, in Lisbon. UFP monitoring campaigns were carried out between July 2017 and December 2018, for a 36 non-consecutive days period, complying approximately 160 hours of suitable measurements. Concerning road traffic, three sites were chosen with different traffic patterns, vehicle circulation, legal restrictions and different flow intensity of pedestrians close-by. Regarding air traffic, the monitoring network was designed to include several sampling sites in the vicinity of LA and a set of sites further away, under the landing and take-off path. Finally, to assess the in-land ferries-related UFP levels, the sampling sites were chosen in order to maximize measurements under downwind conditions and allow the association between ferry operations and PNC response.

Based on the information collected, the obtained levels were analysed and several statistical analysis were performed, particularly searching for correlations between UFP concentrations and the three different traffic activity modes. Concerning road traffic, in Av. da Liberdade, results show high peak values of 1-minute PNC mean (up to $75 \times 10^3 \text{ pt.cm}^{-3}$). This avenue (downtown, in the most striker Low Emission Zone (LEZ1)) presents the higher PNC levels and dispersion ($18.2 \pm 13.2 \times 10^3 \text{ pt.cm}^{-3}$) followed by a high-speed road (2nd Circular, $15.0 \pm 12.2 \times 10^3 \text{ pt.cm}^{-3}$). The lowest values were found at an interception close to LEZ2 boundary (Entrecampos, $10.3 \pm 5.1 \times 10^3 \text{ pt.cm}^{-3}$). Moreover, the results of analysis of variance (ANOVA) show that PNC levels are statistically different among the sampled locations. Results suggest that PNC are strongly dependent on the type and age of vehicles: light-duty vehicles, taxis and buses. PNC peak values were mainly associated with vehicles prior to the Euro 3/III Standard. Finally, results show a strong

positive correlation, statistically significant, between hourly mean values of PNC and PM_{10} ($r = 0.76$, $p < 0.01$) and a moderate positive correlation between PNC and nitrogen oxides (r coefficients of 0.55, 0.51 and 0.59, with all p -values lower than 0.01, for NO , NO_2 and NO_x , respectively). Regarding air traffic, results show the occurrence of high UFP concentrations in LA vicinity. Considering 10-minutes means, the particle counting increases by 18 to 26-fold at downwind locations near the airport, and by 4-fold at locations up to 1 km distance to LA. Results show that particle number increases with the number of flights and decreases with the distance to LA. Finally, concerning ferries, data show that UFP emitted contributes to PNC increase in the surrounding area. Results show an increase in PNC, ranging from 25 to 197% during the third minute before an arrival or departure of a ship, with moderate to positive correlations, statistically significant, between PNC values and the number of ferry operations ($r = 0.79$ to $r = 0.94$). Moreover, negative correlations ($r = -0.85$ to $r = -0.93$) between PNC and wind intensity were also found.

This work, based on Lisbon study-case, show that people working, living or spending a considerable amount of time close to intense traffic roads, nearby the airport or close to ferries' stations or downwind to their cruising path are exposed to high UFP concentrations with a magnitude which may lead to considerable health risks.

Keywords: Air pollution; Particle number concentration (PNC); Lisbon; Monitoring; Road traffic; Airport vicinity; In-land passenger ferries.

Resumo

As partículas ultrafinas (UFP) definem-se como material particulado com diâmetro inferior a $0.1\ \mu\text{m}$. Devido ao seu tamanho reduzido e, conseqüentemente, reduzida massa, são geralmente expressas como concentração do número de partículas (PNC), em partículas por centímetro cúbico (pt.cm^{-3}). Existem evidências crescentes de que a exposição prolongada a UFP pode induzir ou agravar as condições de saúde pulmonar e cardiorrespiratória estando associada ao aumento das taxas de hospitalização e mortalidade. Mais recentemente, têm também sido associadas a doenças neurológicas e a problemas no desenvolvimento cognitivo das crianças.

Os aeroportos, tráfego rodoviário e transporte marítimo foram identificados como fontes significativas de partículas ultrafinas. A informação sobre PNC nas imediações dos aeroportos é reduzida. No caso do Aeroporto de Lisboa (LA), localizado dentro da cidade e rodeado por zonas habitacionais, escritórios, escolas, hospitais e complexos desportivos e recreativos, o seu conhecimento assume uma enorme relevância. Os barcos de transporte fluvial de passageiros (ferries), são igualmente uma fonte de UFP, cujo conhecimento é muito limitado. Uma fração significativa da exposição diária total de uma pessoa a partículas finas e ultrafinas ocorre durante os períodos de deslocação, nomeadamente casa-trabalho. Portanto, os microambientes influenciados por diferentes modos de transporte são particularmente relevantes. Desta forma, associar a sua contribuição às respetivas concentrações de UFP nas proximidades é importante, para além de permitir estimar a sua contribuição na degradação da qualidade do ar na cidade e o grau de exposição da população.

Este trabalho tem como objetivo avaliar o efeito do tráfego rodoviário, aéreo e fluvial na concentração de UFP na cidade de Lisboa. Foram realizadas campanhas de monitorização de UFP entre Julho de 2017 e Dezembro de 2018, por um período de 36 dias não consecutivos, perfazendo aproximadamente 160 horas de medições válidas. No que respeita ao tráfego rodoviário foram selecionados três locais apresentando diferentes perfis de tráfego, restrições de circulação automóvel e fluxos pedestres próximos. Relativamente ao tráfego aéreo, a rede de monitorização foi projetada para incluir vários locais de amostragem na vizinhança do LA e um conjunto de locais mais distantes do aeroporto, sob as rotas de aterragem e descolagem. Finalmente, para avaliar os níveis de UFP relacionados com os ferries, foram escolhidos locais de amostragem por forma a maximizar as medições sob condições a jusante do vento, permitindo associar movimentos de ferries à respetiva resposta de PNC.

Com base nas medições efetuadas, avaliaram-se os níveis obtidos e aplicaram-se diversas análises estatísticas, em particular procurando identificar a existência de correlações entre concentrações de UFP e o nível de atividade dos três diferentes modos de tráfego. Relativamente ao tráfego rodoviário, na Av. da Liberdade, os resultados mostram elevados valores de pico das médias de 1-minuto de PNC (até $75 \times 10^3\ \text{pt.cm}^{-3}$). Esta avenida (baixa citadina, na Zona de Emissões Reduzidas (LEZ1) mais exigente) apresenta os níveis e dispersão de PNC mais elevados ($18.2 \pm 13.2 \times 10^3\ \text{pt.cm}^{-3}$), seguidos por uma via

de alta velocidade (2^{a} Circular, $15.0 \pm 12.2 \times 10^3 \text{ pt.cm}^{-3}$). Os menores valores foram registados num cruzamento próximo do limite da LEZ2 (Entrecampos, $10.3 \pm 5.1 \times 10^3 \text{ pt.cm}^{-3}$). Adicionalmente, os resultados da análise de variância (ANOVA) mostram que os níveis de PNC identificados são estatisticamente diferentes entre os locais amostrados. Os resultados sugerem que a PNC é fortemente dependente do tipo e idade dos veículos: veículos comerciais ligeiros, táxis e autocarros. Os valores de pico de PNC estão principalmente associados a veículos anteriores à Norma Euro 3/III. Finalmente, os resultados mostram uma correlação positiva forte, estatisticamente significativa, entre os valores médios horários de PNC e PM_{10} ($r = 0.76$, $p < 0.01$) e correlação positiva moderada entre PNC e óxidos de azoto (coeficientes r de 0.55, 0.51 e 0.59, para NO , NO_2 e NO_x , respetivamente, com todos os valores p inferiores a 0.01). Em relação ao tráfego aéreo, os resultados mostram a ocorrência de concentrações elevadas de UFP na vizinhança do LA. Considerando médias de 10 minutos, a contagem de partículas é 18 a 26 vezes superior aos valores de fundo em locais próximos ao aeroporto, a jusante do vento, e quatro vezes em locais até 1 km de distância do LA. Os resultados mostram que o número de partículas aumenta com o número de voos e diminui com a distância ao LA. Finalmente, relativamente aos ferries, os dados mostram que as UFP emitidas contribuem para o aumento da PNC na área circundante. Os resultados mostram um aumento na PNC variando de 25 a 197% durante o terceiro minuto antes ou após o movimento de chegada ou partida de um barco, com correlações moderadas a positivas, estatisticamente significativas, entre os valores de PNC e o número de operações de ferries ($r = 0.79$ a $r = 0.94$). Foram também encontradas correlações negativas ($r = -0.85$ a $r = -0.93$) entre a PNC e intensidade do vento.

O presente trabalho, com base no caso de estudo de Lisboa, indica assim que pessoas que trabalham, vivem ou passam uma quantidade considerável de tempo perto de estradas de tráfego intenso, perto do aeroporto ou perto dos locais de atracação de barcos de passageiros ou ferries ou ainda a jusante do vento na rota de navegação, estão expostas a elevadas concentrações de UFP com uma magnitude que constitui à partida um risco considerável para a sua saúde.

Palavras-chave: Poluição atmosférica; Lisboa; Concentração do número de partículas (PNC); Monitorização; Tráfego rodoviário; Aeroporto; Ferries.

CONTENTS

1	INTRODUCTION	21
1.1	BACKGROUND	21
1.2	RESEARCH QUESTIONS AND OBJECTIVES.....	24
1.3	STRUCTURE OF THE THESIS.....	25
2	LITERATURE REVIEW	27
2.1	AIR QUALITY IN URBAN AREAS	27
2.1.1	Road Traffic	29
2.1.2	Airports	31
2.1.3	Maritime Traffic.....	33
2.2	AIR QUALITY GUIDELINES	35
2.3	AIR QUALITY MONITORING.....	41
2.4	CLASSIFICATION, FORMATION AND COMPOSITION OF PARTICULATE MATTER	43
2.5	IMPACTS OF PARTICULATE MATTER	48
2.5.1	Human Health.....	48
2.5.2	Climate	52
2.6	INFLUENCE OF METEOROLOGICAL CONDITIONS ON AIR QUALITY	53
3	BACKGROUND AND METHODOLOGY	55
3.1	MAIN SOURCES OF PARTICULATE MATTER IN LISBON.....	55
3.1.1	Road Traffic	56
3.1.2	Lisbon Humberto Delgado Airport	64
3.1.3	In-Land Passenger Ferries	65
3.2	SAMPLING EQUIPMENT	68
3.3	ROAD TRAFFIC	69
3.3.1	Monitoring Campaigns	71
3.3.2	Meteorological Data.....	71
3.3.3	Data Analysis.....	72
3.4	LISBON AIRPORT	73
3.4.1	Monitoring Campaigns	75
3.4.2	Meteorological Data.....	75

3.4.3	Data Analysis.....	75
3.5	IN-LAND PASSENGER FERRIES	76
3.5.1	Monitoring Campaigns	76
3.5.2	Data Analysis.....	78
4	RESULTS AND DISCUSSION	81
4.1	ROAD TRAFFIC.....	81
4.1.1	Overall Statistical Analysis	82
4.1.2	Traffic Characterization and PNC Levels	83
4.1.3	Correlation between PNC and other atmospheric pollutants	87
4.1.4	Correlation between PNC and meteorological parameters	89
4.2	LISBON AIRPORT	91
4.2.1	Statistical Analysis	93
4.2.2	Influence of Wind and Mixing Layer's Height on PNC.....	99
4.3	IN-LAND PASSENGER FERRIES	103
5	CONCLUSIONS	111
5.1	ROAD TRAFFIC.....	111
5.2	LISBON AIRPORT	112
5.3	IN-LAND PASSENGER FERRIES	113
5.4	ANSWERS TO RESEARCH QUESTIONS	113
5.5	MAIN CONSTRAINTS AND SUGGESTIONS TO FUTURE WORKS	116
6	REFERENCES	119

LIST OF FIGURES

Figure 1.1: Schematic representation of the structure of the thesis.	26
Figure 2.1: Diagram representation of air pollutants path in atmosphere, from their emission to their impacts on people and environment (https://www.eea.europa.eu/publications/explaining-road-transport-emissions).	27
Figure 2.2: Health effects of air pollution regarding the seriousness of the effects and the number of people affected (adapted from EEA, 2014).	28
Figure 2.3: EU urban population exposed to air pollutant concentrations above air quality standards of the EU Air Quality Directive (top) and WHO air quality guidelines (bottom). (Adapted from EEA, 2018a).	38
Figure 2.4: Daily PM ₁₀ concentrations in Europe, in 2016. The map shows the 90.4 percentile of the PM ₁₀ daily mean concentrations, representing the 36 th highest value in a complete series. It is related to the PM ₁₀ daily limit value, allowing 35 exceedances of the 50 µg.m ⁻³ threshold over 1 year. Red and purple dots indicate stations where concentrations were higher than the daily limit value (50 µg.m ⁻³). (EEA, 2018a).	39
Figure 2.5: Annual PM ₁₀ concentrations in Europe, in 2016. Red and purple dots indicate stations where concentrations were higher than the daily limit value (40 µg.m ⁻³). Green dots indicate stations reporting values below the WHO AQG for PM ₁₀ (20 µg.m ⁻³). Only stations with more than 75 % of valid data have been included in the map (EEA, 2018a).	40
Figure 2.6: Annual PM _{2.5} concentrations in Europe, in 2016. Red and purple dots indicate stations where concentrations were higher than the daily limit value (25 µg.m ⁻³). Green dots indicate stations reporting values below the WHO AQG for PM _{2.5} (10 µg.m ⁻³). Only stations with more than 75 % of valid data have been included in the map (EEA, 2018a).	40
Figure 2.7: European AQMN showing air quality index in Europe on the 24 th April 2019 at 11:00 UTC (http://airindex.eea.europa.eu/).	41
Figure 2.8: Classification of particulate matter (PM ₁₀ , PM _{2.5} and PM _{0.1} or UFP) and its common sources (Mühlfeld et al., 2008).	43
Figure 2.9: Schematic representation of PM according to its size (https://www.epa.gov/pm-pollution/particulate-matter-pm-basics).	44
Figure 2.10: Typical engine exhaust size distribution in mass, surface and number weightings (adapted from Kittelson, 1998).	45
Figure 2.11: Total concentrations of trace elements and metals bounded to PM _{0.25} found in two different locations of Los Angeles. Error bars represent standard deviation (from Shirmohammadi et al., 2018).	48
Figure 2.12: Diagrammatic representation of inhaled particulate matter of variable sizes and PM-linked respiratory, cardiovascular, and neurological diseases (adapted from Zaheer et al., 2018).	49
Figure 3.1: PM ₁₀ (top) and NO ₂ (bottom) relative emissions, in Lisbon, 2014, by source (FCT-NOVA, 2017).	55
Figure 3.2: AQMN in Lisbon and respective air quality index on the 24 th April 2019 at 11:00 UTC (http://airindex.eea.europa.eu/).	56
Figure 3.3: Annual average concentrations of PM ₁₀ and NO ₂ in Av. da Liberdade (AL) and Entrecampos (EC) AQMS and limit value established in EU (2008).	57
Figure 3.4: Annual average concentrations of PM _{2.5} in Olivais (OLI) and Entrecampos (EC) AQMS and limit value established in EU (2008).	58
Figure 3.5: Daily average concentrations of PM ₁₀ in Av. da Liberdade, in 2017. The red line represents the LV (EU, 2008).	59
Figure 3.6: Daily average concentrations of PM ₁₀ in Entrecampos, in 2016. The red line represents the LV (EU, 2008).	59
Figure 3.7: Hourly average concentrations of NO ₂ in Av. da Liberdade, in 2017. The red line represents the LV (EU, 2008).	59

Figure 3.8: Hourly average concentrations of NO ₂ in Entrecampos, in 2017. The red line represents the LV (EU, 2008).	60
Figure 3.9: Number of exceedances of daily PM ₁₀ and annual NO ₂ limit values in Av. da Liberdade and Entrecampos between 2010 and 2017. The red line represents the annual number of exceedances allowed for each one of the pollutants (35 and 18 days for PM ₁₀ and NO ₂ , respectively) (EU, 2008).	60
Figure 3.10: LEZ geographical extent and location (adapted from Ferreira et al., 2015).	61
Figure 3.11: Distribution of vehicles by type and zone in 2015 (adapted from Henriques, 2015).	62
Figure 3.12: Relative distribution of Euro Standard by type of vehicle and zone in 2015 (adapted from Henriques, 2015).	63
Figure 3.13: Distribution of NO _x and PM emission by type of vehicle in Av. da Liberdade in 2015 (adapted from Henriques, 2015).	64
Figure 3.14: Distribution of light passenger and light duty vehicles by engine capacity (adapted from Henriques, 2015).	64
Figure 3.15: Representation of Lisbon Airport (dashed contour) on map (Maps source: https://www.google.pt/maps).	65
Figure 3.16: Map of the network of ferry stations connecting the northern and southern shores of Tagus River (Maps source: https://www.google.pt/maps , last accessed on December 2018).	66
Figure 3.17: Power, in kW, by type of ferry of the fleet operating in Tagus River, in LMA.	67
Figure 3.18: Hourly number of ferries cruising in Tagus, LMA, by week-day, Saturday and Sunday/Holiday.	67
Figure 3.19: Annual average trips in 2018 associated with the different connections.	67
Figure 3.20: Particle number counter device, P-Trak®.	68
Figure 3.21: LEZ geographical extent and location of the three analysed sites (black dots) (adapted from Ferreira et al., 2015).	69
Figure 3.22: Representation of sampling sites. The star indicates the AQMS and sampling sites (a) Avenida da Liberdade, site 1; (b) Entrecampos, site 2 and (c) 2 nd Circular, site 3, where dots indicate the two different locations (Torres de Lisboa and Escola Alemã, sites 3.1 and 3.2, respectively). (Maps source: https://www.viamichelin.pt/web/Mapas-plantas).	71
Figure 3.23: Representation of LA and sampling sites. The thin arrow indicates the main runway and direction of landings and take-offs, the dashed line shows the landing and take-off route, and the thick arrow, on top left, indicates the predominant wind direction. (Maps source: https://www.google.pt/maps).	74
Figure 3.24: Location of the ferry-related sampling sites (dots). Arrows indicate the downwind directions to cruising paths; Shadow triangles indicate the manoeuvring area; continuous lines indicate the ferry path. Top left – Cacilhas; top right – Barreiro; bottom left – Montijo and bottom right – Seixal. (Maps source: https://www.viamichelin.pt/web/Mapas-plantas# , last accessed on December 2018).	77
Figure 4.1: Boxplot of 1-minute PNC mean distribution by traffic site. (1 st quartile, average (x), median (-), 3 rd quartile and outliers (dots)).	82
Figure 4.2: Traffic characterization by type of vehicle in Av. da Liberdade over two periods during sampling. (PC – passenger cars; LD – light-duty vehicles; T – taxis; B – buses; HD – heavy-duty vehicles; G – gasoline; D – diesel; HE – hybrid or electric).	83
Figure 4.3: Traffic characterization by Euro Standard and type of vehicle . (PC – passenger cars; LD – light-duty vehicles; T – taxis; B – buses; HD – heavy-duty vehicles; G – gasoline; D – diesel; HE – hybrid or electric) in Av. da Liberdade.	84
Figure 4.4: Association between 1-minute PNC peaks and specific observed vehicles in Av. da Liberdade. The black arrow denotes a period where measurements were discarded due to another source of contamination.	85
Figure 4.5: 1-hour means of PNC vs. buses and light-duty vehicles, in Av. da Liberdade.	86
Figure 4.6: Statistical outputs for regression analysis with 95% confidence level between PNC 1-hour averages and the number of vehicles, in Entrecampos.	86

Figure 4.7: Association between 1-minute means of PNC peaks and specific observed vehicles in Entrecampos.	87
Figure 4.8: Statistical outputs for regression analysis with 95% confidence level between PNC 15-minutes averages and air pollutants (NO, NO ₂ , NO _x and PM ₁₀) monitored in AQMS of Av. da Liberdade. Regression for nitrogen oxides was done with PNC 15-minutes averages and with 1-hour averages for PM ₁₀	88
Figure 4.9: Statistical outputs for regression analysis with 95% confidence level between PNC 1-hour averages and PM ₁₀ monitored in AQMS of Entrecampos.	89
Figure 4.10: Statistical outputs for regression analysis with 95% confidence level between PNC 1-hour averages and wind speed, in Av. da Liberdade.	90
Figure 4.11: As in Figure 4.10 but respecting to Entrecampos.	90
Figure 4.12: 10-minute PNC averages obtained under impact wind direction (blue) and non-impact wind direction (grey). Sites are ordered by distance to runway and type of location.	94
Figure 4.13: Overall statistical outputs for regression analysis with 95% confidence level between PNC 10-minutes averages and the number of landings.	96
Figure 4.14: As in Figure 4.13 but respecting to the number of take-offs.	97
Figure 4.15: As in Figure 4.13 but respecting to the number of flights (landings and take-offs).	97
Figure 4.16: As in Figure 4.13 but respecting to wind intensity.	97
Figure 4.17: Boxplot of 10-minutes PNC mean distribution by site ordered by location and increase distance to LA (please see sites spatial distribution in Figure 3.23b). (1 st quartile, average (x), median (-), 3 rd quartile and outliers (dots)).	98
Figure 4.18: LA-related PNC geographical distribution: minimum, average and maximum (PNC expressed in pt.cm ⁻³).	99
Figure 4.19: PNC concentrations at five sites located in LA landing route vicinity, ordered by increasing distance to the runway (a), and corresponding wind speed and ML height (b).	100
Figure 4.20: UFP concentration at sampling site 5 (LA vicinity) and LTO cycles differentiated by long-haul flights and low/medium-haul flights.	101
Figure 4.21: (a) 10-minutes UFP average concentration, number of flights and wind direction, in LA vicinity (site 5) (b) Geographical detail of sampling site: relative position to the beginning of the runway (small dashed red arrow) and to aircrafts idling to take-off (pointed orange arrow). The runway is represented by the black arrow and idling path by the large dashed blue line.	102
Figure 4.22: UFP concentration at sampling site 13 (landing path, far from LA), wind direction and number of landings during a 10-minutes period.	103
Figure 4.23: Boxplot of 1-minute PNC mean distribution by ferry-related site, under downwind conditions. (1 st quartile, average (x), median (-), 3 rd quartile and outliers (dots)).	105
Figure 4.24: Site by site PNC during the immediate eight minutes before/after ferry operations (blue), eight minutes before departures (grey), eight minutes after arrivals (yellow).	106
Figure 4.25: Average PNC of ferries from/to Barreiro measured in Seixal as function of wind speed and under wind direction range from N to NE.	107
Figure 4.26: Detail of Barreiro and Seixal geographical location. Plumes emitted by Barreiro's ferries affect PNC on Seixal when wind direction range from NE to NW. Shadowed triangle shows the wind direction range in which only plumes emitted by Barreiro's ferries are measurable in Seixal; the continuous and dashed lines show the ferries paths from Barreiro and Seixal, respectively.	108
Figure 4.27: PNC rose pollution in each ferry station (pt.cm ⁻³ x 10 ³).	109
Figure 4.28: Obtained PNC average for different class of ferry operating among the four stations studied, downwind.	109

LIST OF TABLES

Table 2.1: Implementation of Euro Standards by vehicle's category.....	31
Table 2.2: Average dimension (nm) and concentration (pt.cm ⁻³) of atmospheric particles in European cities (adapted from Hofman et al. (2016) and Kumar et al.).	32
Table 2.3: LTO cycle phases defined by ICAO (ICAO, 2011).	33
Table 2.4: Air quality standards under the EU Air Quality Directive and WHO air quality guidelines (adapted from EEA, 2018b).....	36
Table 2.5: National ambient air quality standards established by USEPA (adapted from https://www.epa.gov/criteria-air-pollutants/naaqs-table).	37
Table 2.6: Premature deaths and years of life lost (YLL) attributable to PM _{2.5} and NO ₂ exposure in EU-28 and in 41 European countries, in 2015 (adapted from EEA, 2018a).....	52
Table 3.1: Technical characteristics of Lisbon urban AQMS (http://www.ccdr-lvt.pt/pt/avaliacao-da-qualidade-do-ar-na-rlvt/8085.htm#D1).	57
Table 3.2: Emissions of PM ₁₀ and PM _{2.5} in 2014 regarding the four main ferry connections between Lisbon and South Tagus shore.	66
Table 3.3: P-Trak® technical characteristics (adapted from P Trak®, 2013).	69
Table 3.4: Geographic coordinates of traffic-related sites.	70
Table 3.5: Geographic coordinates of each LA-related site.....	74
Table 3.6: Geographic coordinates of each ferry-related site.....	77
Table 3.7: Technical characteristics of the portable meteorological station WatchDog 2700.....	78
Table 3.5: Technical data of the ships identified during sampling periods (https://ttsl.pt/terminais-e-frota/frota/).....	79
Table 4.1: Sampling dates and periods for each road traffic-related site and the corresponding height of the mixing layer (ML), wind speed (v) and direction, temperature (T), relative humidity (RH) and measured minimum (Min), mean, mode, and maximum (Max) PNC values.	81
Table 4.2: Obtained average, mode and standard deviation (SD) of PNC on traffic-related sites, in pt.cm ⁻³ x 10 ³	82
Table 4.3: Single factor ANOVA for PNC sampled values among the four traffic sites	83
Table 4.4: Summary of statistical outputs for regression analysis with 95% confidence level between PNC and other pollutants and meteorological parameters, in Av. da Liberdade and Entrecampos.	91
Table 4.5: Sampling date and period for each airport-related site and the corresponding height of the Mixing Layer (ML), wind speed (v) and direction, temperature (T), relative humidity (RH) and measured minimum (Min), mean, mode, and maximum (Max) PNC values.	92
Table 4.6: Average, mode and standard deviation (SD) of PNC on airport-related sites, in pt.cm ⁻³ x 10 ³ . Sites are arranged by location and distance to the airport.	93
Table 4.7: Impact wind directions (IWD, in °) by site.....	94
Table 4.8: Single factor ANOVA among all sites.	95
Table 4.9: Single factor ANOVA among sites with similar characteristics.	96
Table 4.10: Sampling date and period for each ferry-related site and the corresponding height of the Mixing Layer (ML), wind speed (v) and direction, temperature (T), relative humidity (RH) and measured minimum (Min), mean, mode, and maximum (Max) PNC values.	104

Table 4.11: Obtained average, mode and standard deviation (SD) of PNC on ferry-related sites, in $\text{pt.cm}^{-3} \times 10^3$	104
Table 4.12: Obtained results of PNC increase with ferry operations, regression analysis between PNC averages and ferry occurrences and wind speed and ANOVA analysis between periods with and without ferry operations.	107

1 INTRODUCTION

1.1 BACKGROUND

Air pollution, mainly in great urban areas, had become a major problem over the past years. Urban air pollution is mostly associated with the transport sector. The main primary pollutants are airborne particulate matter (PM), nitrogen oxides (NO_x, mostly nitrogen monoxide, NO, and nitrogen dioxide, NO₂, often expressed as NO₂), uncombusted hydrocarbons (HC) and carbon monoxide (CO) (Kousoulidou *et al.*, 2008). Many studies identify road traffic related emissions as the main responsible for air quality degradation in urban areas (e.g. Anenberg *et al.*, 2017). Even with improved exhausting systems, due to higher traffic levels, air pollution should keep an increasing tendency in certain regions of the world (WHO, 2005). Also, some authors have been studying other contributions, such as tire-road interference in ultrafine particulate emissions. Ultrafine particles are generated under extreme driving conditions, i.e., full stop braking, at the tire road interface (Mathissen *et al.*, 2011). Considering other transport modes, such as airports, maritime traffic and in-land passenger ferries currently using combustion engines are also responsible for emissions of particulate matter, nitrogen oxides, carbon monoxide and volatile organic compounds (VOC) which contribute for a deterioration of air quality (Anenberg *et al.*, 2017; Hagler *et al.*, 2010; Kousoulidou *et al.*, 2008; López-Aparicio *et al.*, 2017; Sardar *et al.* 2005; Stafoggia *et al.*, 2016; Zhu *et al.*, 2002a,b).

According to the World Health Organization (WHO) particulate matter database, more than 80% of people living in urban areas where air pollution is monitored are exposed to air pollution that exceeds WHO's air quality limits (WHO, 2018). The database, which currently covers 4300 cities in 108 countries, points that 97% of cities in low and middle-income countries with more than 100 000 inhabitants do not meet WHO air quality guidelines, whereas in high-income countries the percentage decreases to 49%. The increase in air pollution levels monitoring recognizes their association with health impacts: as urban air quality declines, the risk of stroke, heart disease, lung cancer, and chronic and acute respiratory diseases, including asthma, increases for the people who live there. Moreover, WHO estimates a worldwide 4.2 million deaths every year as a result of exposure to ambient air pollution and that 91% of the world's population lives in areas where air quality exceeds the global defined guidelines limits for PM₁₀ and PM_{2.5} (particulate matter with aerodynamic diameter less than 10 µm and 2.5 µm, respectively) annual means: 20 µg.m⁻³ for PM₁₀ and 10 µg.m⁻³ for PM_{2.5}. (WHO, 2006). Coarse particles (PM₁₀) are inhalable, and they can easily reach people's lungs and fine particles (PM_{2.5}) may even enter the bloodstream.

Over the past years, specific components of PM came into focus: ultrafine particulate matter (UFP), which consists in particles with aerodynamic diameter less than 0.1 µm (100 nm). The urban main source of UFP is also combustion engines and they are able to reach cellular level and cause intracellular damages (Carosino *et al.*, 2015). However, the impact of UFP on human health is still under studying and the results

are inconclusive, despite the possibility of being even more harmful than fine particles (PM_{2.5}) (Lanzinger *et al.*, 2016).

Behind particulate matter, nitrogen oxides, carbon monoxide, volatile organic compounds and tropospheric ozone (O₃) must also be taken in consideration due to their negative and sometimes synergetic impacts on air quality (AQ). Nitrogen oxides are linked to respiratory problems, mucous tissues irritation and central nervous system damages. In particular, nitrogen oxide, has been linked to premature mortality and morbidity in result of cardiovascular and pulmonary diseases. Carbon monoxide is considered toxic once it may connect to haemoglobin and disable its ability to bloodstream transport oxygen from lungs to cells. Depending on their chemical nature, VOCs effects on human health may vary from simple olfactive discomfort to breathing problems and even carcinogenic effects. Ozone is a secondary pollutant and therefore in urban areas, is mainly produced in the presence of sunlight (wavelength less than 400 nm) by photochemical reactions where volatile organic compounds are oxidized by nitrogen oxides, both emitted by combustion engines. Moreover, ozone is the major component of photochemical smog and it is related to respiratory diseases such breathing problems, asthma and reduced lung function. Aside these health issues, tropospheric ozone is a short-lived greenhouse gas. Additionally to their role as ozone precursors, VOC and NO_x are dangerous air pollutants themselves (<http://www.ccdr-lvt.pt/pt/o-ar-e-os-poluentes-atmosfericos/8082.htm>). Furthermore, particulate matter interferes with the radiative budget and albedo and therefore has impact on climate; nitrogen oxides are responsible for acidification and both ozone and volatile organic compounds are harmful to vegetation.

When speaking about air quality is not controlled exclusively by the amount of pollutants emitted. Meteorological conditions play also a crucial role in transport, transformation and dispersion processes of atmospheric pollutants. Additionally, these processes are affected by local topography and meteorological factors such as wind intensity and direction, atmospheric pressure, temperature, precipitation and solar radiation (Mu *et al.*, 2011; Pateraki *et al.*, 2012; Shen *et al.*, 2009; Tai *et al.*, 2010; Wang *et al.*, 2018),

Pollutants dispersion in the atmosphere are mainly driven by wind speed and direction. On one hand, wind speed generates mechanical turbulence, which is responsible for local dispersion. Therefore, low wind speeds lead to high pollutants concentration and moderate wind speeds promote their dispersion, lessening their ambient concentrations. On the other hand, strong wind may induce vortices' effects which might lead to high pollutants concentration in the predominant wind direction, downwind to the source(s) (Grundström, 2015; Guldman, 2011; Hudda *et al.*, 2018; Kim and Guldman, 2011; Russo *et al.*, 2014a). Regarding atmospheric pressure, low pressure systems (cyclones) are generally associated to atmospheric high turbulence, enhancing pollutants dispersion and lessening ground level pollutants concentration. On the contrary, high pressure systems (anticyclones), characterized by weak winds and atmospheric stability, inhibit the pollutants dispersion, increasing their ground level concentrations (Lin *et al.*, 2009). Moreover, temperature plays an important role in their vertical atmospheric dispersion by inducing ascendant convection (lessen ground level concentrations). As an example, in Summer, the high temperatures promote the

tropospheric ozone production. On the other hand, in Winter, the occurrence of thermal inversions may lead to ground-level high pollutants concentrations. The role of precipitation on pollutants dispersion is also noticeable, as precipitation is usually associated to an instable atmosphere, promoting air pollutants dispersion. Rain droplets solubilize gaseous pollutants and particulate matter, accelerating their deposition on surface (wet deposition), decreasing their atmospheric concentrations (Shen *et al.*, 2009). Finally, strong solar radiation, associated with high temperatures, promotes photochemical reactions and enhances secondary pollutants production, such as ozone.

As pointed out before, road traffic is one of the main contributors to air pollution in urban areas (Anenberg *et al.*, 2017; Lee *et al.*, 2017; Keuken *et al.*, 2016). The exhaust gases emitted close to the surface often lead to air quality degradation, once road traffic is characterized by the emission of toxic particles and gases (Russo and Soares, 2013). Despite all the efforts that have been made, Lisbon still has an intense road traffic and some areas often exceed the legal standards, mainly regarding particulate matter and nitrogen dioxide (Ferreira *et al.*, 2015). Other emission source, less addressed in previous studies, is the activity of the aviation industry where there are no detailed studies of the impact of Lisbon Airport Humberto Delgado (LA) on its surroundings regarding particulate matter concentration, namely UFP, and other atmospheric pollutants. Another transport related sector with no air quality impact information due to the lack of previous studies is in-land passenger ferries. Transport sector is also expected to be responsible for the emission of air pollutants with significant impact on air quality, namely UFP.

This thesis is focused on UFP concentration over the urban region of Lisbon and its relationship with transport-services. In the last decade, several studies have been carried out in order to characterize air quality in different European cities, namely trying to distinguish the range of average UFP concentrations in those European cities (Hofman *et al.*, 2016; Kumar *et al.*, 2014). Lisbon is a city with 547 733 inhabitants, according to the last cense (INE, 2011).

The appellative climate (temperature warm), together with its location, close to one of the major estuaries in Europe and to Atlantic Ocean, rich historical monuments and gastronomy, makes Lisbon one of the most attractive European cities. Therefore, the tourist sector is one of its main economic activity. Besides, many people travel daily to Lisbon, mostly for working and school/university formation. These conjugated factors contribute to an increase in the different transport modes, making transports (road-traffic, aircrafts and in-land passenger ferries) the main air pollution source in the city, like in many other cities, as previously pointed out by several studies (e.g. Lee *et al.*, 2017; López-Aparicio *et al.*, 2017; Stafoggia *et al.*, 2016). Furthermore, the Lisbon Airport is located within the city and there is a considerable number of passenger river transports to and from Lisbon, particularly during weekdays.

During recent years, several studies have been carried out in order to evaluate air quality in Lisbon (e.g. FCT-NOVA, 2017; Monjardino *et al.*, 2018; Lopes *et al.*, 2019a,b; Russo *et al.*, 2014a,b). Also, several measures have been implemented in areas considered critical (downtown) in order to contribute to air quality improvement (Ferreira *et al.*, 2015; Monteiro *et al.*, 2015). However, there is a lack of studies to assess UFP

levels, which are mainly emitted by combustion engines. This work intends to fill this gap and is the first work on characterization of UFP concentration in Lisbon. It will allow to evaluate not only the UFP concentrations but also to estimate the potential level of exposure of the affected population. One of the main contributors to air pollution in Lisbon is road traffic (Russo and Soares, 2013), which is characterized by the emission of toxic particles and gases. However, considering the location of Lisbon Airport and the amount of ferries crossing Tagus River, aircrafts and in-land passenger ferries are also a pertinent emission source, far less addressed in those studies.

Therefore, this study intends to fill the above-mentioned information gaps, assessing the effect on UFP concentrations of road, air and river traffic modes in Lisbon. These three sources assume special relevance due to their locations (within or close to the city centre, proximity to residential, business, services and recreational areas, schools, sport complexes, hospitals and companies, among others) and, therefore, the number of people potentially affected, particularly by peak concentrations. Furthermore, given the lack of studies in airport-related UFP concentrations in the immediate airport's vicinity, it also aims to assess the airport-related UFP concentrations in the immediate LA vicinity. This study also proposes to assess when and how much air traffic in LA affects UFP concentrations taking into consideration the aircraft types (short/medium or long-haul) and the associated movement (landing or take-off). A thorough analysis on UFP emissions on the vicinity of the LA will improve the ability and capability of alert system for air quality in Lisbon. In the case of in-land ferries, according to the literature review, there is an almost total lack of studies characterizing UFP concentrations in ferries stations and across ferries path. In Lisbon, there are no previous studies on this subject which assumes special relevance, once it is a significant transport mode used to connect Tagus shores.

Finally, the thesis will use the collection of data to provide further relevant insights on monitoring strategies of UFP and a better understanding of the relationships between UFP and other pollutants, including the decisive role of meteorological parameters during data collection and further interpretation.

1.2 RESEARCH QUESTIONS AND OBJECTIVES

The main objective of this thesis is to set up a monitoring scheme and evaluate different modes of traffic related UFP concentrations in Lisbon. For that purpose, the present work aims to access the contribution of UFP emissions of three main sources (road-traffic, aircrafts and in-land passenger ferries) to their atmospheric concentration. In this context, the research questions are:

- RQ1.** Regarding vehicles, aircrafts and ferries traffic, what are the UFP levels in Lisbon in the proximity of these sources?
- RQ2.** How can we design appropriate monitoring techniques to evaluate UFP levels at roadside, airport landing and take-off pathways, and close to ferries stations?
- RQ3.** How do meteorological conditions affect UFP monitoring?

RQ4. Is it possible to establish and quantify relationships between UFP levels and traffic intensity (vehicles, aircrafts and ferries)?

RQ5. Regarding road traffic, are there any correlations between UFP concentrations and other pollutants monitored by air quality monitoring stations in the vicinity?

To achieve the thesis objectives and answer these research questions, the following particular tasks have been accomplished:

- Collecting UFP concentrations in order to cover the different traffic sources considered and their influence;
- Compiling information on the traffic intensity associated with the different sources under research such as the number and type of vehicles, number of flights and aircraft type and movements, and number of in-land passenger ferries during sampling periods;
- Monitoring/Recording meteorological conditions during sampling periods.

1.3 STRUCTURE OF THE THESIS

This thesis is divided in five chapters as following:

- Chapter 1 – Introduction, where the aim and contextualization of the present work is defined as well as the research questions.
- Chapter 2 – Literature Review, is divided into sub-chapters according to the different contexts: air pollution in urban areas, the main air pollution sources in urban areas, guidelines and monitoring of air quality focused on particulate matter, UFP impacts on health and climate and influence of meteorology on air quality.
- Chapter 3 – Background and Methodology, begins by contextualization of our case study, Lisbon and describes the methodology applied on sampling and data analysis for each one of the three sources considered.
- Chapter 4 – Results and Discussion, as its title suggests, presents the obtained results and their discussion, also by source.
- Finally, Chapter 5 – Conclusions, presents the main achieved conclusions, both by source and global. The main limitations and suggestions for future works are also indicated.

Figure 1.1 presents the schematic structure of this document. The work developed in this dissertation resulted in one conference paper and presentation and two peer reviewed publications:

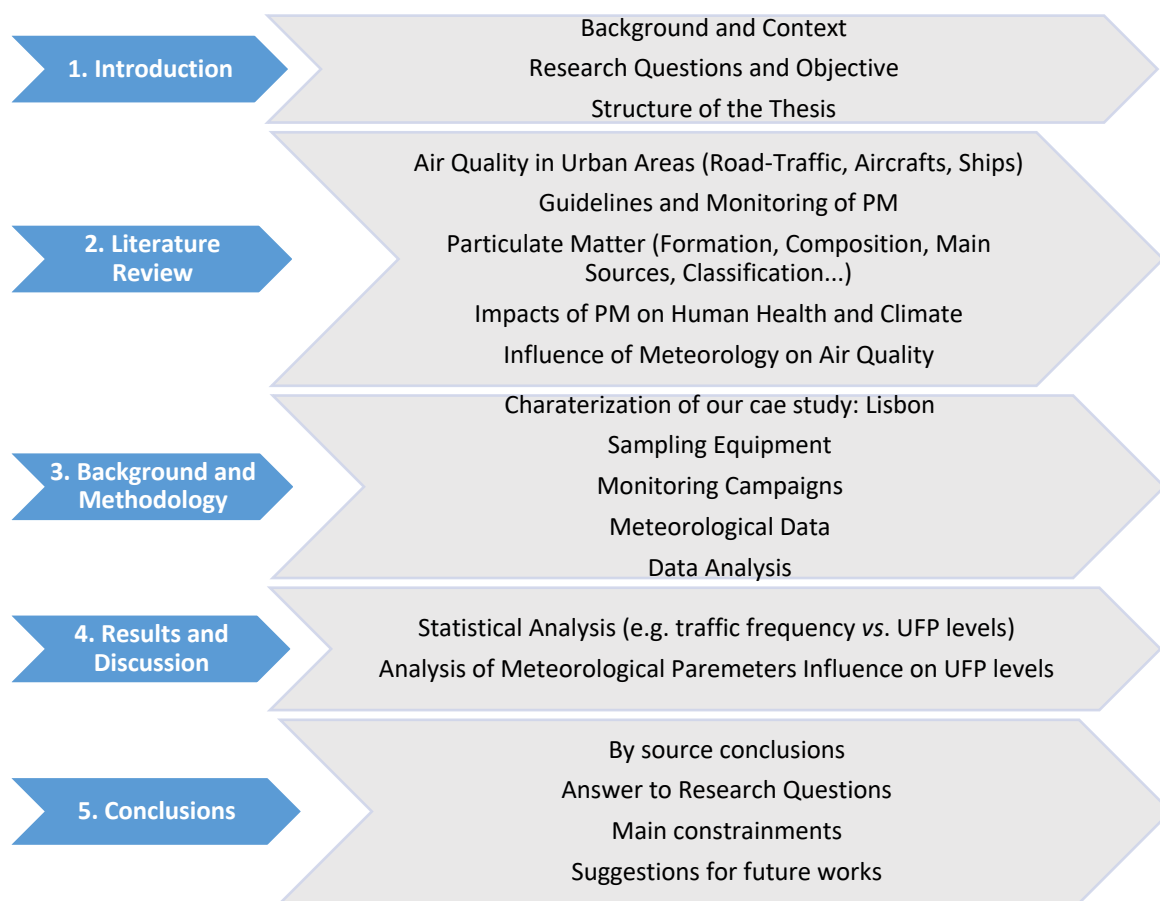


Figure 1.1: Schematic representation of the structure of the thesis.

Publications:

Lopes, M., Russo, A., Monjardino, J., Gouveia, C., Ferreira, F. (2019). Monitoring of ultrafine particles in the surrounding urban area of a civilian airport. *Atmospheric Pollution Research*. ISSN 1309-1042. <https://doi.org/10.1016/j.apr.2019.04.002>.

Lopes, M., Russo, A., Gouveia, C., Ferreira, F. (2019). Monitoring of ultrafine particles in the surrounding urban area of ferries terminals. *Journal of Environmental Protection*. Vol. 10, 838-860 <https://doi.org/10.4236/jep.2019.106050>.

Conference:

Lopes, M., Corrêa, M., Ferreira, F., “Avaliação do Impacte do Aeroporto de Lisboa na Concentração de Partículas Ultrafinas na Zona Urbana Circundante”, Livro de Atas da Conferência Internacional de Ambiente em Língua Portuguesa (CIALP), do XX Encontro da Rede de Estudos Ambientais de Países de Língua Portuguesa (REALP) e da XI Conferência Nacional do Ambiente, Aveiro, 8-10 de maio de 2018, ISBN: 978-972-789-540-3, Vol-III, pp. 235-244.

2 LITERATURE REVIEW

2.1 AIR QUALITY IN URBAN AREAS

Air quality is usually used to express the degree of pollution of the air we breathe. This pollution is caused by a mixture of chemical substances emitted in ambient air or as a result of chemical reactions among them or with ambient air constituents (Brimblecombe, 1999) as exemplified in Figure 2.1. Air pollution, mainly in great urban areas, had become a major problem over the past decades. Atmospheric pollution is mostly associated with traffic and its main primary pollutants: particulate matter, nitrogen oxides, uncombusted hydrocarbons and carbon monoxide (Kousoulidou *et al.*, 2008). Many studies identify road traffic related emissions as the main contributor to poor air quality in urban areas (Anenberg *et al.*, 2017; Kumar *et al.*, 2014; Pant and Harrison, 2013; Querol *et al.*, 2008; Stanier *et al.*, 2004a).

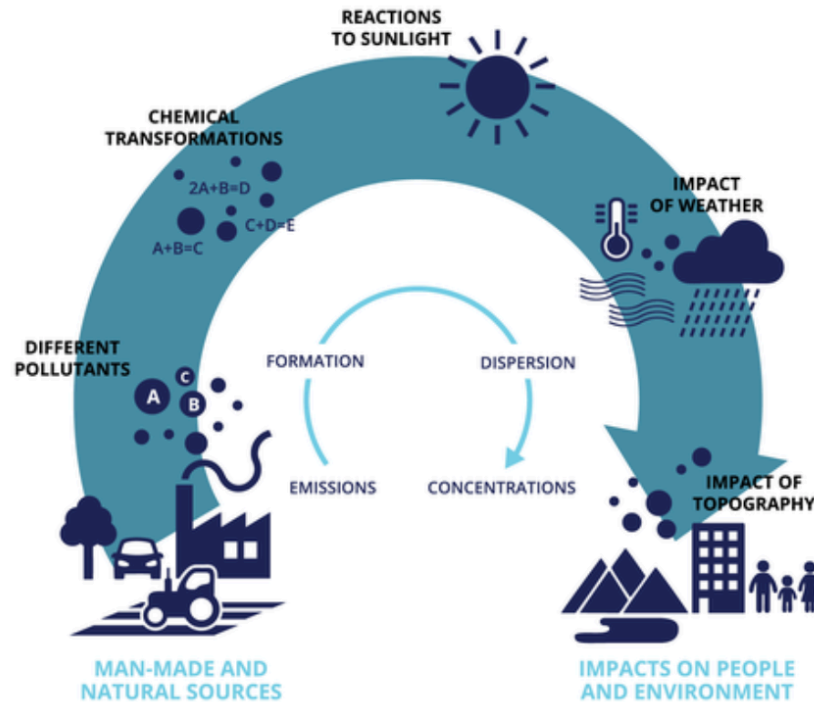


Figure 2.1: Diagram representation of air pollutants path in atmosphere, from their emission to their impacts on people and environment (<https://www.eea.europa.eu/publications/explaining-road-transport-emissions>).

Regarding Europe, the last report of European Environmental Agency (EEA) on Air Quality in Europe highlights that, in 2016, traffic-related pollutants (PM_{10} , $PM_{2.5}$, O_3 , and NO_2) exceeded both the EU limit values and the World Health Organization (WHO) guidelines (EEA, 2018a). In 2016, 13 % of EU-28 urban population resided in areas where the European Union (EU) daily limit value of PM_{10} was exceeded, 6 % of the EU-28 urban population was exposed to $PM_{2.5}$ levels above the EU limit, 12 % of the urban population was exposed

to O₃ concentrations above the EU target value threshold, and 7 % of urban population resided in areas where the annual EU limit value of NO₂ was exceeded (EEA, 2018a). According to this report, in 2015, approximately 422 000 deaths in Europe were related to PM_{2.5} (originating from long-term exposure), 391 000 of which were in the EU-28. The same report points out that, in 2016, 42 % of UE-28 urban population was exposed to PM₁₀ levels exceeding the stricter World Health Organization (WHO) air quality guidelines (AQG), 74 % of UE-28 urban population was exposed to PM_{2.5} concentrations exceeding the WHO AQG, 98 % of UE-28 urban population was exposed to O₃ levels above the WHO AQG, and 7 % of the UE-28 urban population lived in areas where the NO₂ WHO AQG was exceeded (EEA, 2018a). The health effect pyramid of air pollution is outlined in Figure 2.2.

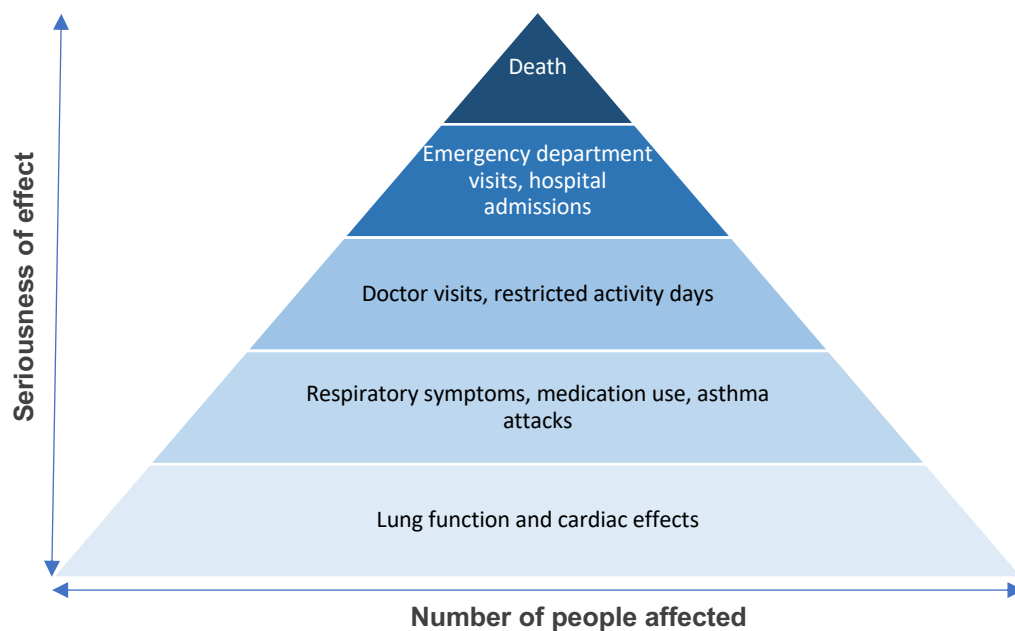


Figure 2.2: Health effects of air pollution regarding the seriousness of the effects and the number of people affected (adapted from EEA, 2014).

The WHO had recently estimated around 4.2 million deaths worldwide due to air pollution exposure (WHO, 2018). The same source points out that in 2016, 91 % of world population was living in areas where WHO air guideline levels were not met. Particulate matter (PM) is one of the major causes of premature deaths (Gakidou *et al.*, 2017). According to this study, PM is the sixth cause of death, in a list of 84 risk factors, and is pointed as the cause of 4 million deaths in 2016.

Different emission sources have different contributions on ambient air pollutants concentrations. Concentrations not only depend on the amount of pollutant emitted, but also on proximity to source, emission conditions (e.g. height and temperature) and other factors (e.g. dispersion conditions and topography). Low emission heights, such traffic, are generally associated to higher significant impact on ground concentrations than emissions from high stacks (EEA, 2018b).

Besides road traffic, other air pollution sources pointed by several authors are air traffic (e.g. Stafoggia *et al.*, 2016) and maritime transport (e.g. Westerlund *et al.*, 2015). In this last source, López-Aparicio *et al.* (2017) find domestic ferries as the main contributors to emissions among harbour ships.

2.1.1 Road Traffic

Road traffic is the most important contributor to air pollution in urban areas (Anenberg *et al.*, 2017; Keuken *et al.*, 2016; Kumar *et al.*, 2014; Lee *et al.*, 2017; Morawska *et al.*, 2008; Rönkkö *et al.*, 2017). Therefore, as referred by Joerger and Pryor (2018), people living, working or spending much time next to intense traffic roads are exposed to high traffic-related emissions and have higher risk to respiratory and cardiovascular health problems or even premature mortality (Chen *et al.*, 2008; Chen *et al.*, 2017; HEI, 2013; Hystad *et al.*, 2015; Lelieveld *et al.*, 2015). Combustion generated particles (from vehicle emissions) range from 30 nm to 500 nm (Vu *et al.* 2015). Several studies have concluded that the elevated particle number concentrations decay exponentially with increasing distances from the roadway (e.g. Zhu *et al.*, 2009). Nucleation (atmospheric formation of new particles) (Kulmala *et al.*, 2014) also plays an important role to UFP concentrations in urban areas (Brines *et al.*, 2015; Kulmala *et al.*, 2017; Stanier *et al.*, 2004b; Watson *et al.*, 2006).

Particulate matter emitted from gasoline and diesel engines consist mainly on ultrafine particles with size ranges of 20 to 60 nm and 20 to 130 nm, respectively (Karjalainen *et al.*, 2014; Morawska *et al.*, 2008;). UFP represent only 0.1 to 10% of the total particulate mass, despite might represent more than 90% of the total particle number (Giechaskiel *et al.*, 2010). Particle emission depends on the fuel, engine technology and aftertreatment devices. Compared to the standard gasoline passenger cars, gasoline direct injection technology induces an increase of UFP concentration (Köhler *et al.*, 2013; Liang *et al.*, 2013).

Research suggests that a significant fraction of a person's total daily exposure to fine and ultrafine particles occurs during commuting periods (Ham *et al.*, 2017). Transport microenvironments (MT), close to traffic emissions sources, exhibit higher traffic related pollutants concentrations (Goel and Kumar, 2014; Patton *et al.*, 2016). In their commuting to work, school and shopping, among other activities, people spend a variable, but considerable, amount of time in vehicles (cars, public transportation, motorcycles or bicycles) or close to them. Due to recurrent acceleration and deceleration of vehicles, intense-traffic areas are susceptible to have higher emissions (Goel and Kumar, 2015). A study carried out by De Nazelle *et al.* (2012) concluded that UFP concentrations in cars are 2-3 times higher than in walk or bike modes, close to roadways. Still, considering inhalation, pedestrians and cyclists' doses are comparable to car drivers. In Europe, results show that car riders are exposed to the highest levels of UFP; on the contrary, pedestrians are exposed to the lowest levels (De Nazelle *et al.*, 2017). However, in modern cars, equipped with high-efficiency filters and air recirculation, the UFP exposure levels inside vehicles are significantly lower (Spinazzè *et al.*, 2014). Still according to this study, the highest exposures were observed for walking or biking along high-trafficked routes and while using public buses.

Many air monitoring studies (Hagler *et al.*, 2010; Sardar *et al.*, 2005; Zhu *et al.*, 2002a,b) conducted near traffic roads or on-roadways has focused not only on the UFP measurements, but particularly on emissions of more conventional and well-studied pollutants such as:

- Carbon monoxide (CO): the adoption of emission control technologies and regulations allowed ambient concentrations of this pollutant to decline over the past years. However, mostly light-duty and gasoline vehicles remain as the primary source of CO at most locations.
- Nitrogen oxides (NO_x): diesel vehicles are responsible for the majority of NO_x emissions. The majority of NO_x exhaust occurs as NO (primary emissions). Once in atmosphere, NO is rapidly oxidized to NO₂ (a secondary pollutant), which is the focus of concern in terms of health effects. Heavy-duty diesel engines with after-treatment equipment may contain a greater ratio of NO₂/NO.
- Particulate matter (PM₁₀, PM_{2.5}): significant near-roadway sources of PM mass include direct emissions from vehicle combustion engines (predominantly PM_{2.5}), brake and tyre wear, and resuspension of dust from the road surface (mostly PM₁₀ and larger). PM_{2.5} atmospheric concentration is mostly affected by contributions from regional sources. Therefore, the impact of direct emissions from motor vehicles is generally small in near-roadway environments.
- Volatile organic compounds (VOC) and carbonyls: these compounds are emitted from both natural and anthropogenic sources, including vehicles engines. They are involved in the photochemical formation of tropospheric O₃. Moreover, some of them have been associated with toxic health effects. VOC of concern for near-road monitoring include benzene, toluene, ethylbenzene, xylenes, styrene, formaldehyde, acetaldehyde, and acrolein.
- Black or elemental, carbon (BC or EC): often referred to as “soot,” is a common constituent emitted by vehicles engines. BC represent the black (graphitic) portion of PM. Though heavy-duty diesel engines are often pointed as the main sources of BC, all combustion engines emit BC. A study conducted by Liggio *et al.* (2012) has shown that BC emissions from light-duty gasoline vehicles are expected to be at least a factor of 2 to 9 times higher than formerly supposed. In urban areas, the main source of BC is diesel trucks engine which rules near-roadway environments.

Aiming to minimize traffic-related air pollution in urban areas, some plans and/or particular measures have been taken to reduce air pollutant concentrations to acceptable levels, meeting the EU limit values and WHO guidelines. The implementation of Low Emission Zones (LEZ), areas where the circulation of most polluting vehicles is restricted or penalized on the basis of European class emission standards, are often used as the major component of emission control strategies. London, UK, introduced the world's largest citywide LEZ in 2008 (Mudway *et al.*, 2019). Currently, there are about 264 LEZ across Europe (Santos *et al.*, 2019). Also, in Asia, including Singapore and Tokyo, LEZ are being implemented (Mudway *et al.*, 2019). Restrictions in vehicles circulation range from only heavy duty to all type of vehicles according to their Euro Standard (Table 2.1).

Table 2.1: Implementation of Euro Standards by vehicle's category.

Vehicle Category		Euro Standard					
		Euro 1	Euro 2	Euro 3	Euro 4	Euro 5	Euro 6
Passenger Cars		July 1992	January 1996	January 2000	January 2005	September 2009	September 2014
Light Duty	(≤ 1305 kg)	October 1994	January 1998	January 2000	January 2005	September 2010	September 2014
	(> 1305 kg)	October 1994	January 1998	January 2001	January 2006	September 2010	September 2015
Heavy Duty and Heavy Passenger		January 1993	October 1995	October 1999	October 2005	October 2008	January 2013
Motorcycle		July 2000	July 2005	July 2007	---	---	---

2.1.2 Airports

The past 20 years have seen European airports evolve from mere infrastructure providers into businesses, directly contributing to the employment of people and also to the nearest cities' development (ACI, 2018). During the past decades, air traffic registered a significant global increase, which is expected to continue over the coming decades. Data from the International Airports Council shows that, in Europe, between 1990 and 2014, there was an 80% increase in the number of flights, and it is estimated that this figure will increase by about 50% over the next 20 years. Furthermore, an increase in aircraft age and travelled distance is also expected (ACI, 2016). These factors together contribute significantly to the worsening of the impacts associated with air traffic, namely local air quality, noise levels and greenhouse gas emissions. Air quality is particularly affected by the large quantities of particulate matter emitted by airplanes, with consequent implications on air quality, as some studies have showed (e.g. Mazaheri *et al.*, 2009). PM is one of the most harmful pollutants to human health (ACI, 2016; EEA, 2016) leading to health impacts on populations, living close to airports, and workers (Cattani *et al.*, 2014). Several studies identify airports as a significant source of several pollutants, such as: fine particles (PM_{2.5}) and ultrafine particles, nitrogen dioxide and volatile organic compounds. They also reveal significant increases in UFP concentrations in the vicinity of several airports (Hudda *et al.*, 2014; Hsu *et al.*, 2013; Hsu *et al.*, 2014; Keuken *et al.*, 2015; Stafoggia *et al.*, 2016; Westerdahl *et al.*, 2008; Zhu *et al.*, 2011) and elevated PNC were observed in areas under the influence of winds from the airport (Fuller *et al.*, 2012; Hudda *et al.*, 2016; Patton *et al.*, 2014a,b). Although clinical studies related to UFP exposure are still not enough for unequivocal conclusions, UFP are suspected to be even more harmful to human health than coarse and fine particles. In this context, together with airport locations close to urban and suburban areas, special attention should be devoted to human health in those areas. Some of these studies were conducted close to the main European airports, namely trying to distinguish the range of average UFP concentrations in those European cities (Hofman *et al.*, 2016; Kumar

et al., 2014). Table 2.2 summarizes the number of particles by cubic centimetre (pt.cm⁻³), referred as particle number concentration (PNC) for several European cities.

Table 2.2: Average dimension (nm) and concentration (pt.cm⁻³) of atmospheric particles in European cities (adapted from Hofman *et al.* (2016) and Kumar *et al.*).

City	Dimension [nm]	PNC [pt.cm ⁻³]	City	Dimension [nm]	PNC [pt.cm ⁻³]
Amsterdam (NL)	7 – 3 000	31 000	Helsinki (FI)	7 – 3 000	14 000
Amsterdam (NL)	7 – 100	759	Helsinki (FI)	10 – 10 000	19 576
Antwerp (BE)	7 – 100	1 063	Lahti (FI)	6 – 300	39 000
Antwerp (BE)	20 – 500	12 367	Leicester (UK)	7 – 100	1 112
Athens (EL)	7 – 3 000	24 000	Leicester (UK)	5 – 1 000	64 200
Barcelona (ES)	10+	59 270	Leipzig (DE)	3 – 800	17 119
Berlin (DE)	10 – 500	28 000	Linz (AT)	7+	23 400
Berna (CH)	7 – 1 000	28 032	London (UK)	7 – 100	776
Berne (CH)	10+	30 839	London (UK)	19 – 800	22 941
Birmingham (UK)	7 – 3 000	20 000	Manchester (UK)	4 – 100	27 000
Cambridge (UK)	10 – 2 500	30 200	Prague (CZ)	25 – 25 000	11 600
Copenhagen (DK)	6 – 700	19 224	Prague (CZ)	25 – 2 500	35 900
Dresden (DE)	3 – 800	36 685	Rome (IT)	10+	46 799
Essen (DE)	20 – 750	16 789	Salzburg (AT)	13 – 830	30 000
Strasbourg (FR)	7 – 10 000	39 000	Utrecht (NL)	10+	38 635
Graz (AT)	7+	22 500	Vienna (AT)	7+	26 200
Helsinki (FI)	3 – 10 000	67 000	Zurich (CH)	3+	80 000

Another gap on assessing air quality on airports is that, in the aviation sector, total emissions are given by the sum of the emissions occurred at distinct phases: taxi out and ground idle, take-off, climb, cruise, descent, final approach, landing and taxi in and ground idle. The landing and take-off cycle, short listed by LTO, includes all activities near the airport, which occur at a height of less than 914 m (ICAO, 2011). Relevant direct air quality impacts, at local and regional levels, result from emissions during LTO cycles. Above this altitude aircraft engine emissions also have an impact on air quality, but they are of a global nature. Table 2.3 resumes the different phases of the LTO cycle (ICAO, 2011).

Moreover, the landing and take-off cycle (LTO) includes all activities near the airport, which occur bellow 914 m. Relevant direct air quality impacts, at local and regional levels, result from emissions during LTO cycles. Above this altitude, aircraft engine emissions also have an impact on air quality, but they have a distinct nature and spatial scale of influence. Besides the evident LTO activities, there are others, such as, passenger and luggage transport, aircrafts maintenance and fuel supply, auxiliary power operations and engines start up, also responsible for UFP emissions.

Table 2.3: LTO cycle phases defined by ICAO (ICAO, 2011).

Operating Phase	Time-in mode (min)	Thrust setting (%)
Approach (bellow 915 m)	4	30
Landing, taxi and ground idle	7	7
Taxi and ground idle to take-off	19	7
Take-off (ground - 450 m)	0.7	100
Climbing (450 – 915 m)	2.2	85

2.1.3 Maritime Traffic

Air pollution associated to maritime transportation (MT) has been widely studied and it is recognized for the emission of air pollutants, namely UFP. Therefore, it is expected that passenger ferries are also responsible for UFP emissions. Maritime transportation is widely used for passenger carriage, for touristic purposes and for international or intercontinental transport of goods. According to the United Nations Conference on Trade and Development, more than 80% of world trade is carried by sea (UNCTAD, 2018). During the past decades MT registered a significant global increase which is expected to continue over the coming decades (Marmer *et al.*, 2005; US-EPA, 2009), leading to the increase of research on its environmental impacts (e.g. López-Aparicio *et al.*, 2017; Becerril-Valle *et al.*, 2017; Viana *et al.*, 2014; Westerlund *et al.*, 2015; Zimmerman *et al.*, 2016). Shipping emerged as an important source of air pollution in coastal areas (Van der Zee *et al.*, 2012; Westerlund *et al.*, 2015) mainly associated with the large quantities of particulate matter (PM) emitted and the consequent implications on air quality and human health. Fu *et al.* (2013) found that large amounts of UFP smaller than 10 nm appear for manoeuvring mode, affecting regional air quality.

Recent results indicated that 30 to 40% of the particulate matter from shipping is emitted as a primary source and 60 to 70% as secondary (Viana *et al.*, 2014). Shipping PM consists mainly on fine to ultrafine fraction (e.g. elementary or black carbon (BC), nickel (Ni), vanadium (V), etc.) or results from chemical reactions between exhaust gases and particles in the atmosphere (Reche *et al.*, 2011). Besides PM, shipping also emits gaseous pollutants, such as nitrogen oxides (NO_x), sulphur dioxide (SO₂) and smaller amounts of carbon monoxide (CO) and volatile organic compounds (VOCs) (Zhang *et al.*, 2016). Maritime traffic is also a relevant source of greenhouse gases (GHG), namely carbon dioxide (CO₂) and small amounts of nitrous oxide (N₂O) and methane (CH₄) (López-Aparicio *et al.*, 2017). Beyond health consequences, PM emissions are climate forcing agents (Becerril-Valle *et al.*, 2017; Fiore *et al.*, 2012; Liggio *et al.*, 2012; Zimmerman *et al.*, 2016). They affect mainly the radiative balance and cloud formation, since they act as water condensation nuclei (Booth and Bellouin, 2015; Hodnebrog *et al.*, 2014). Ice and clouds albedo are also affected, although the uncertainty of the global effect is still high.

Maritime traffic's impacts should also be evaluated in the context of harbour locations (e.g. close to urban and suburban areas), as air quality in the surroundings is particularly affected with consequences to

human health for populations living in coastal urban areas (Viana *et al.*, 2014). It is estimated that 70% of ship's emissions occur close to the coast, within 400 km from land (Endresen *et al.*, 2003) and disperse directly onto mainland, which worsens the environmental impacts associated with maritime traffic (e.g. local air quality) affecting both human health and ecosystems (Lonati *et al.*, 2010; Miola and Ciuffo, 2011). Research suggests that, in certain cases, ships in harbour may contribute to about 55 to 77% of total emissions within their vicinity (Cullinane and Cullinane, 2013; Hulskotte and Gon, 2010;). Regarding European coastal areas, shipping emissions contribute to 1.7% of PM₁₀ air concentrations, 1.14% of PM_{2.5} concentrations and at least 11% of PM₁ (aerodynamic diameter less than 1 µm) concentrations (Viana *et al.*, 2014). In the western Mediterranean region, the Barcelona's harbour contributes to 31% of PM₁₀ average mass (Pey *et al.*, 2013). A more recent study carried out by Pérez *et al.* (2016) suggests that in the harbour, ship emissions are responsible for 9-12% of PM₁₀ and 11-15% of PM_{2.5} concentrations in the Barcelona urban area. Other studies identified lower values for PM_{2.5}, namely in the harbour industrial area of Brindisi (Italy) where the primary in-harbour shipping emissions of PM_{2.5} are approximately 3% while the average ship traffic related is reported to be ~7% (Cesari *et al.*, 2014; Donateo *et al.*, 2014). More recently, a study focused in Oslo's harbour estimates oceangoing vessels as the main emission source of air pollution, contributing 63 to 78% of the total NO_x, PM₁₀, SO₂ and CO_{2e} emissions (López-Aparicio *et al.*, 2017). The authors highlight international ferries, cruises and container vessels as the main contributors among oceangoing vessels. Ledoux *et al.* (2018) estimated the impact of shipping in Calais harbour on average concentrations to be 51% for SO₂, 35% for NO, 15% for NO₂ and 2% for PM₁₀. According to the same study, the in-port ships average impact on PM₁₀ concentrations are estimated to be +28.9 µg.m⁻³, from which 40% are PM₁. The authors also found that, under certain circumstances, punctually PM₁₀ concentration can reach a concentration value close to 100 µg.m⁻³. Furthermore, the daily limit value established in the European Directive 2008/50/EC of 21 May 2018 (EU, 2008) - 50 µg.m⁻³ - was exceeded for several days.

On a wider-range, Alver *et al.* (2018) summarized the results of several studies concerning ship-related emissions inventories for different worldwide countries. Considering PM₁₀ emissions in European countries, the authors accounted emissions ranging from 10 to 1500 t/year. This report also highlights Portugal's emissions as the highest, quoting a study conducted on four Portuguese harbours (Nunes *et al.*, 2017).

PM in its different typologies (PM₁₀, PM_{2.5} and PM₁) is one of the most harmful pollutants to human health (ACI, 2016; EEA, 2016), leading to health impacts on populations exposed to them such as people living close to harbours or in coastal urban areas, or shipyard workers (Kukkonen *et al.*, 2016; Ledoux *et al.*, 2018; López-Aparicio *et al.*, 2017; Westerlund *et al.*, 2015). Healy *et al.* (2009) concluded the vast majority of freshly emitted ship exhaust particles lie in the ultrafine mode, communally designated by UFP (particles, with an aerodynamic diameter less than 0.1 µm). Apart from the above mentioned and more common reference to PM₁₀, PM_{2.5} and PM₁ emissions from ships, UFP have been also addressed in studies related to shipping emissions (e.g. González and Rodríguez, 2013; Kopanakis *et al.*, 2018; Kukkonen *et al.*, 2016; Merico *et al.*, 2017). Regarding heavy fuel oil used by ships, emission factors for particle number were found

in the range 5×10^{15} to 1×10^{17} pt.kg⁻¹_{fuel} (Moldanová *et al.*, 2013). Westerlund *et al.* (2015) found out emission factors of 2.79 ± 0.19 vs. $2.35 \pm 0.20 \times 10^{16}$ pt.kg⁻¹_{fuel} for cargo and passenger ships, respectively. The influence of shipping and harbours was found to be relevant for Helsinki, Oslo, Rotterdam and Athens (Kukkonen *et al.*, 2016). Two studies carried out in Santa Cruz de Tenerife City found UFP linked to ship emissions of $15\text{--}45 \times 10^3$ pt.cm⁻³ (González and Rodríguez, 2013) and $35\text{--}50 \times 10^3$ pt.cm⁻³ when meteorological conditions allowed ship plumes inland transport by sea breezes (González *et al.*, 2011). Another study, concerning Brindisi and Venice (Italy), Patras (Greece) and Rijeka (Croatia), concluded that shipping and harbours contributions to UFP emissions have an impact 2 to 4 times larger than PM₁₋₁₀ (Merico *et al.*, 2017). In Crete, Kopanakis *et al.*, (2018) found high UFP concentrations related to aviation and shipping emissions transported from the nearby airport and harbour.

Furthermore, within urban areas, the main source of UFP is the direct emission from combustion processes; the new particle formation (NPF) is a main provider to particulate pollution, being a secondary source of UFP (Lyu *et al.*, 2018). NPF occurs by nucleation of gas precursors and posterior growth by condensation on the formed particles is a common atmospheric process, being recurrently referred by several studies as an important process in maritime areas (Hama *et al.* 2017a; Hofman *et al.*, 2016; Pushpawela *et al.*, 2018). NPF events are common in coastal areas once the combined mixing of clean marine air and UFP enriches urban air and leads to appropriate conditions for particle formation (Babu *et al.*, 2016). Therefore, UFP concentration can significantly be increased in coastal urban areas (Liu *et al.*, 2008; Rodríguez *et al.*, 2018). Additionally, NPF events have been studied regarding to meteorological variables (temperature, relative humidity, solar radiation, wind speed and direction) to identify the conditions that improve particle nucleation. Although the impact of temperature is still ambiguous, several authors point that NPF is enabled by higher solar radiation (Lyu *et al.*, 2018), moderate relative humidity (Hama *et al.*, 2017b; Huang *et al.*, 2017) and, considering coastal areas, it is likely to take place during sea breeze (Babu *et al.*, 2016; Mordas *et al.*, 2016).

Although there are many studies evaluating the effects on shipping-related coarse and fine PM concentrations, and fewer regarding the effects on ship-related UFP concentrations, there is a lack of studies on passenger in-land ship transport-related UFP emissions, namely in estuaries in the vicinity of European capitals, specifically in the Mediterranean. López-Aparicio *et al.* (2017) identify domestic ferries as the main contributors to emissions among harbour vessels. Merico *et al.* (2016) highlight that UFP represent an important fraction of low-sulphur fuel emissions and the need for future policies to take this factor into account.

2.2 AIR QUALITY GUIDELINES

Despite all the efforts made to improve air quality in EU, the air quality standards established in Air Quality Directive (EU, 2008) for PM, O₃ and NO₂ are still not being accomplished in large parts of EU (EEA, 2018b). According to the same report, these widespread exceedances of PM, O₃ and NO₂ in urban areas,

make the air quality standards goals for 2020 unlikely to be achieved. Furthermore, WHO guidelines are much further away from being achieved. European air quality standards (EU, 2008) and WHO air quality guidelines (WHO, 2006) are presented in Table 2.4. The corresponding National Ambient Air Quality Standards (NAAQS) established by the United States Environmental Protection Agency (USEPA) are presented in Table 2.5. Primary Standards stipulate pollutant concentrations for public health protection, taking in account the denominated “sensitive” populations (children, elderly and asthmatics). Secondary Standards provide public wellbeing protection (visibility, animals, crops, vegetation, and buildings) (from <https://www.epa.gov/criteria-air-pollutants/naaqs-table>). USEPA has set NAAQS for six pollutants: the five presented in Table 2.5 plus lead.

Table 2.4: Air quality standards under the EU Air Quality Directive and WHO air quality guidelines (adapted from EEA, 2018b).

Air Quality Directive				WHO Guidelines	
Pollutant	Averaging Period	Objective	Comments	Objective	Comments
PM _{2.5}	One day	Limit value: 25 µg.m ⁻³		25 µg.m ⁻³	99 th percentile (3 days/year)
	Calendar year			10 µg.m ⁻³	
PM ₁₀	One day	Limit value: 50 µg.m ⁻³	Not to be exceeded on more than 35 days per year	50 µg.m ⁻³	99 th percentile (3 days/year)
	Calendar year	Limit value: 40 µg.m ⁻³		20 µg.m ⁻³	
O ₃	Maximum daily 8-hour mean	Target value: 120 µg.m ⁻³	Not to be exceeded on more than 25 days per year, averaged over three days	100 µg.m ⁻³	
NO ₂	One hour	Limit value: 200 µg.m ⁻³	Not to be exceeded on more than 18 days per year	200 µg.m ⁻³	
	Calendar year	Limit value: 40 µg.m ⁻³		40 µg.m ⁻³	
CO	One hour	Limit value: 10 mg.m ⁻³		30 µg.m ⁻³	
	Maximum daily 8 hour mean			10 mg.m ⁻³	

Table 2.5: National ambient air quality standards established by USEPA (adapted from <https://www.epa.gov/criteria-air-pollutants/naaqs-table>).

Pollutant	Standard Type	Averaging Period	Level	Form
CO	Primary	1 hour	35 ppm	Not to be exceed more than once per year
		8 hours	9 ppm	
PM_{2.5}	Primary	1 year	12 µg.m ⁻³	Annual mean, averaged over 3 years
	Secondary	1 year	12 µg.m ⁻³	
	Primary and secondary	24 hours	35 µg.m ⁻³	98 th percentile, averaged over 3 years
PM₁₀	Primary and secondary	24 hours	150 µg.m ⁻³	Not to be exceed more than once per year on average over 3 years
O₃	Primary and secondary	8 h	0.070 ppm	Annual fourth-highest daily maximum 8-hour concentration, averaged over 3 years
NO₂	Primary	1 hour	100 ppb	98 th percentile of 1-hour daily maximum concentrations, averaged over 3 days
	Primary and secondary	1 year	53 ppb	Annual mean

Air pollutant concentrations can be expressed in mass of pollutant by air volume units, usually in µg.m⁻³, or volume by volume units, ppm (10⁻⁶) or ppb (10⁻⁹). Once the volume depends on temperature and pressure, the conversion between these units (Eq. 1) must take in account those parameters (Eq. 2):

$$MC = VCx \frac{M}{V} \quad [1] \quad \text{and} \quad V = 22.41 \times 10^{-3} x \frac{T}{273} x \frac{1013}{p} \quad [2]$$

Where:

MC – mass concentration [µg.m⁻³]

V – molecular volume [m³]

VC – volume concentration [ppm]

T – absolute temperature [K]

M – molecular mass

p – atmospheric pressure [hPa]

Most of the air pollutants have anthropogenic sources and derive from combustion processes of fossil or biomass fuels used in several sectors: industry, transport, agriculture and domestic, among others (EEA, 2018a). In urban areas, where over 70 % of European population lives (Eurostat, 2016), many researchers point out road traffic as air pollutants main source (e.g. Anenberg *et al.*, 2017; Lee *et al.*, 2017). It is estimated that more than 400 000 premature deaths per year in the EU are related to air pollution (EEA, 2018b). Figure 2.3 presents the percentage of urban population exposed to air pollutant concentration above EU Air Quality Directive (top) and WHO Air Quality Guidelines (WHO AQG), more stringent (bottom). One eighth of EU citizens living in urban areas are exposed to higher of one or more air pollutants concentrations established by EU standards. Moreover, considering WHO guidelines, up to 96 % of EU urban citizens are exposed to air pollutant levels of one or more air pollutants considered harmful to health (EEA, 2018c).

As it can be seen in Figure 2.3, between 2006 and 2016, EU's urban population exposure to fine particulate matter levels above EU limit value decreased from 16 to 5 %. Considering WHO guidelines, the decrease was from 97 to 74 %, although exposure level was much higher. Since 2011, both percentages have a decreasing trend and reached the lowest value in 2016. Regarding coarse PM, between 2000 and 2016, exposure to levels above EU standards also decreased from 32 to 13 %. The highest value, 43 %, was recorded in 2003. Comparison with WHO stricter values, it was recorded a decrease from 84 to 42 % and the highest value, 91 %, was also observed in 2003.

Regarding ozone, the current target value was often exceeded. In the considered period, 8 % (2014) to 55 % (2003) of the EU urban population was exposed to concentrations exceeding the target value. Once again, considering the stricter WHO guidelines, 94 to 99 % of EU urban population was exposed to levels higher than recommended and there is no apparent change over time.

Finally, concerning nitrogen dioxide, the percentage of EU urban population exposed to levels above both the EU limit and WHO guideline values, progressively decreased to values lower than 10 %, over the same period. Once again, the highest value was recorded in 2003 (32 %) and the lowest, 7 %, in 2014 and 2016.

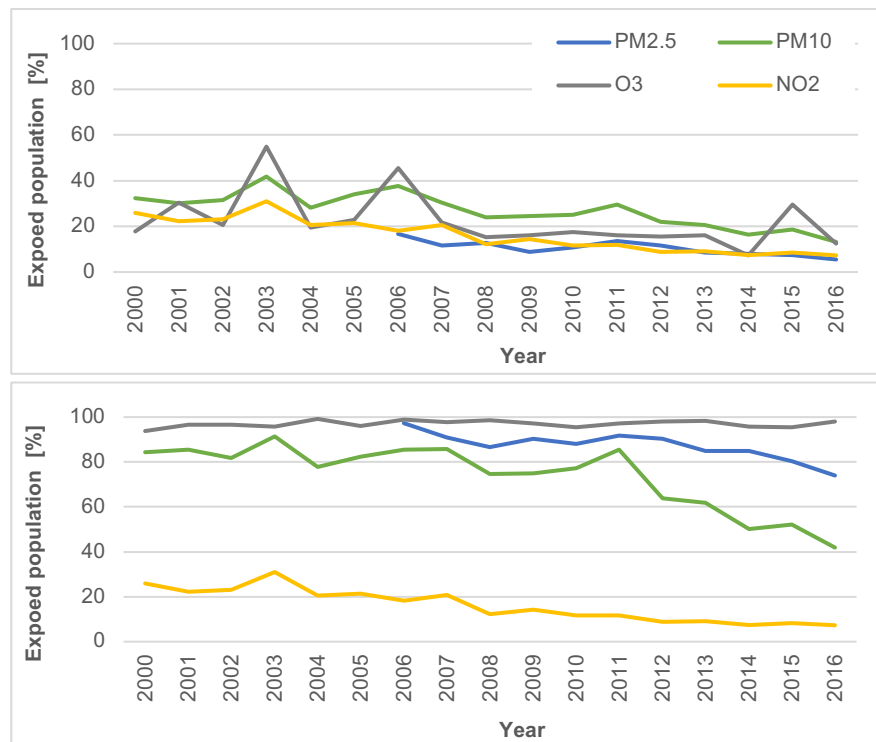


Figure 2.3: EU urban population exposed to air pollutant concentrations above air quality standards of the EU Air Quality Directive (top) and WHO air quality guidelines (bottom). (Adapted from EEA, 2018a).

Air Quality in Europe EEA report (EEA, 2018a) highlights that the PM₁₀ daily limit value was exceeded in 19 % of the reported air quality monitoring stations in 19 countries of EU-28 and eight other reporting countries (Figure 2.4). Many of these exceedances were reported during high PM₁₀ pollution events in

winter, spring and autumn, 2016. PM₁₀ concentrations above the annual limit value were reported in 6 % of all monitoring air stations (Figure 2.5). PM_{2.5} concentration higher than the annual limit value were also registered in 5 % of reporting stations in four EU-28 and another four reporting countries (Figure 2.6). Regarding the long-term WHO air quality guideline for PM₁₀, there were reported exceedances at 48 % of the stations of all reporting countries except for four (Estonia, Iceland, Ireland and Switzerland). Also, the long-term WHO air quality guideline for PM_{2.5} was exceeded at 68 % of the reporting countries except for Estonia, Finland, Hungary, Norway and Switzerland. In this context, the report stresses that, in 2016, 13 % of EU-28 urban population was exposed to PM₁₀ concentrations above the daily limit value; considering the stricter WHO guidelines, this value rises to 42 %. Regarding PM_{2.5}, exposed EU-28 urban population to levels above EU limit value was 6 % and 74 % for WHO guidelines. UFP ambient concentrations are not yet targeted both in EU legislation and WHO guidelines.

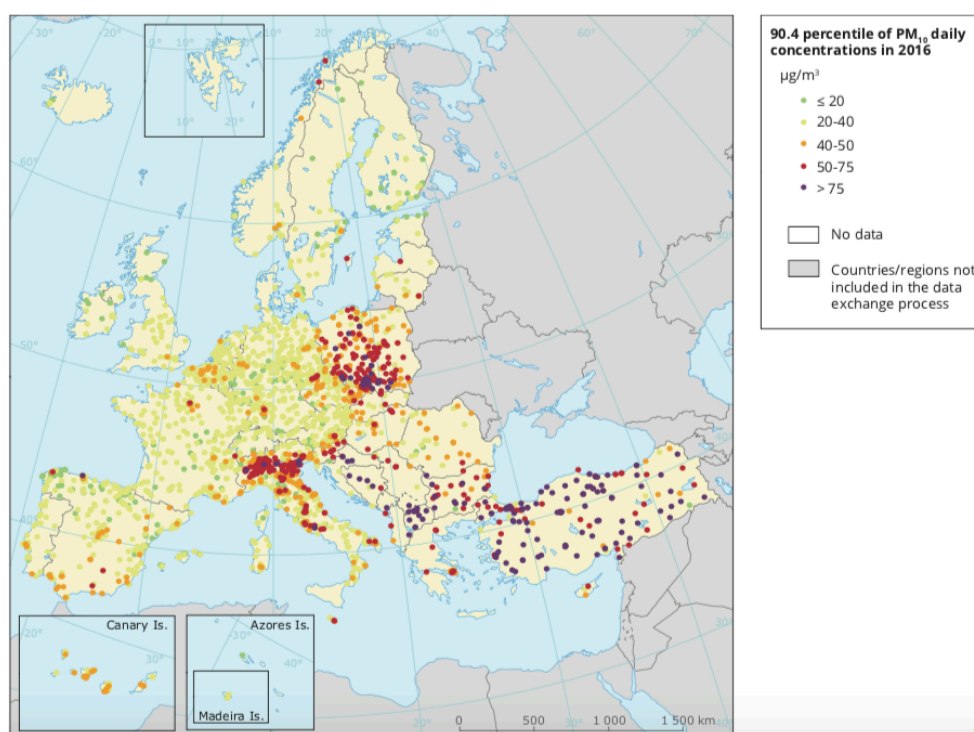


Figure 2.4: Daily PM₁₀ concentrations in Europe, in 2016. The map shows the 90.4 percentile of the PM₁₀ daily mean concentrations, representing the 36th highest value in a complete series. It is related to the PM₁₀ daily limit value, allowing 35 exceedances of the 50 µg.m⁻³ threshold over 1 year. Red and purple dots indicate stations where concentrations were higher than the daily limit value (50 µg.m⁻³). (EEA, 2018a).

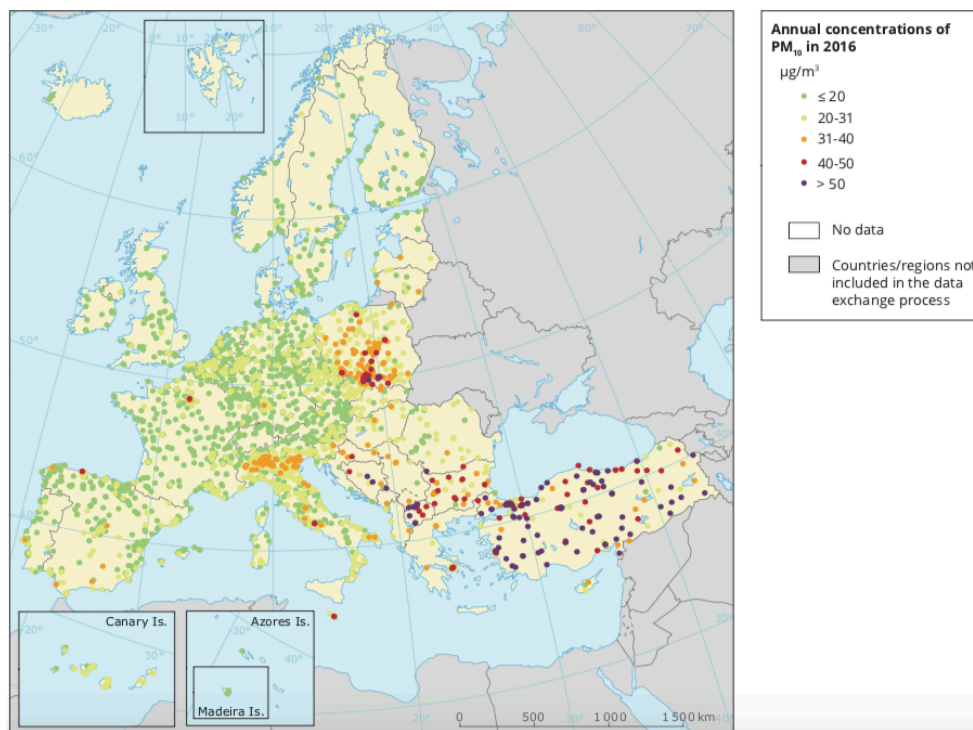


Figure 2.5: Annual PM₁₀ concentrations in Europe, in 2016. Red and purple dots indicate stations where concentrations were higher than the daily limit value (40 $\mu\text{g}\cdot\text{m}^{-3}$). Green dots indicate stations reporting values below the WHO AQG for PM₁₀ (20 $\mu\text{g}\cdot\text{m}^{-3}$). Only stations with more than 75 % of valid data have been included in the map (EEA, 2018a).

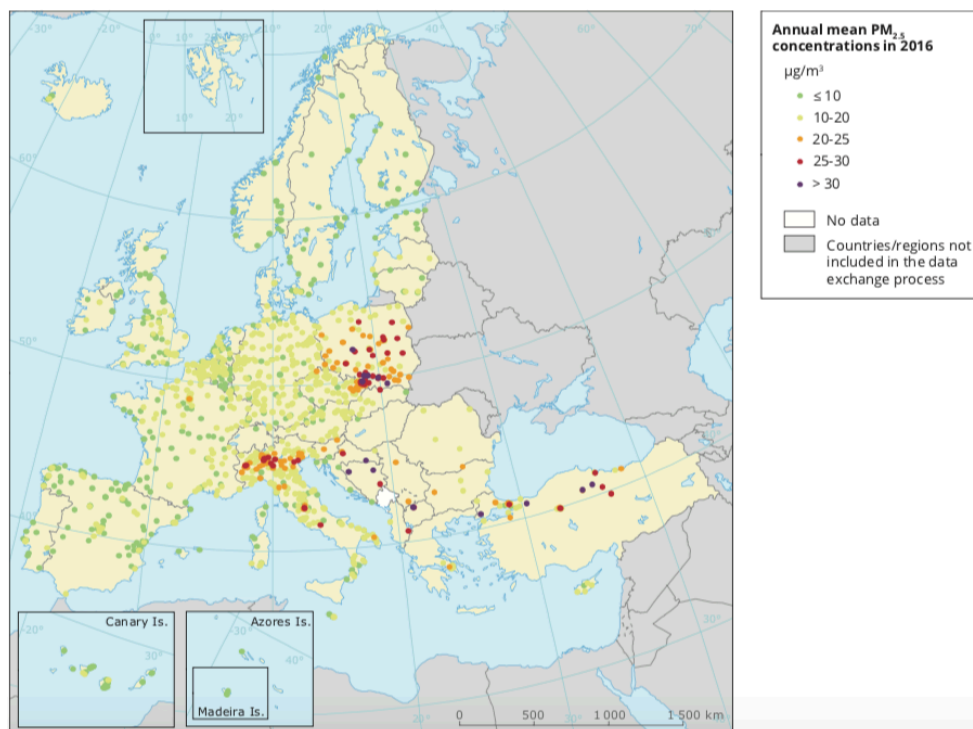


Figure 2.6: Annual PM_{2.5} concentrations in Europe, in 2016. Red and purple dots indicate stations where concentrations were higher than the daily limit value (25 $\mu\text{g}\cdot\text{m}^{-3}$). Green dots indicate stations reporting values below the WHO AQG for PM_{2.5} (10 $\mu\text{g}\cdot\text{m}^{-3}$). Only stations with more than 75 % of valid data have been included in the map (EEA, 2018a).

2.3 AIR QUALITY MONITORING

Air quality monitoring is assured by an Air Quality Monitoring Network (AQMN) composed by Air Quality Monitoring Stations (AQMS). European AQMNT provides near on-time air quality information over Europe as it can be seen in Figure 2.7 (<http://airindex.eea.europa.eu/>). These stations are mostly concentrated in urban and sub-urban areas, where most of the people live.

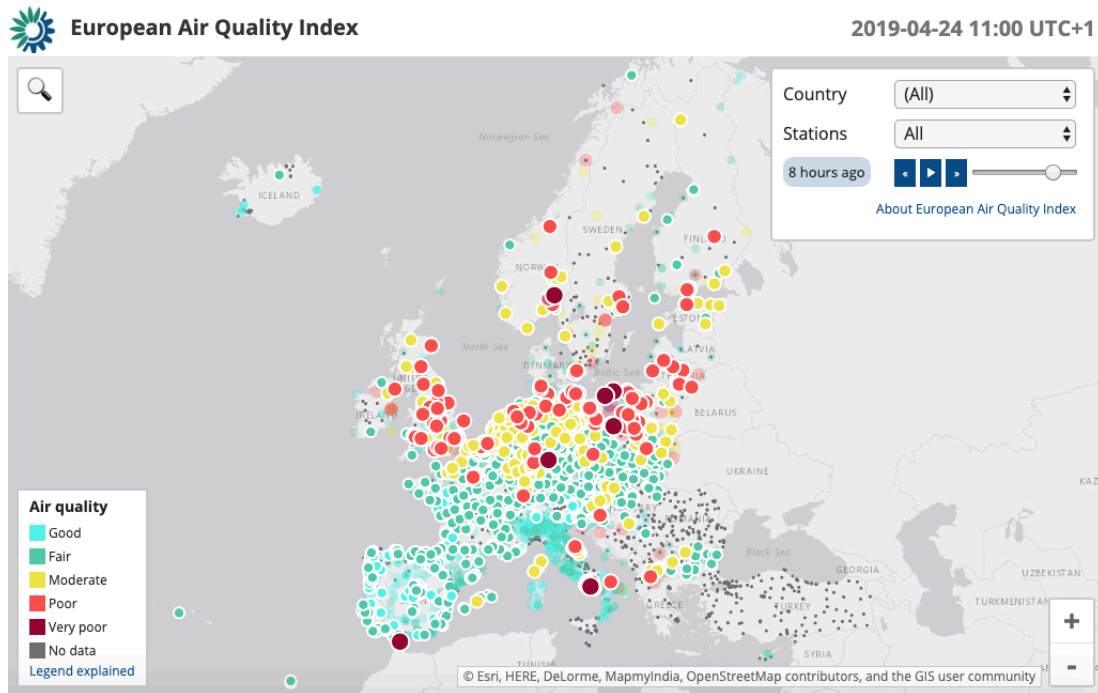


Figure 2.7: European AQMN showing air quality index in Europe on the 24th April 2019 at 11:00 UTC (<http://airindex.eea.europa.eu/>).

PM₁₀ is monitored in all AQMS and PM_{2.5} is monitored by the majority of AQMS, in mass concentration. The evaluation is accomplished by gravimetric collection of atmospheric particles on polytetrafluoroethylene (PTFE) filter over the specified sampling period (e.g. 24 h, according to Directive 2008/50/CE). The air flow rate is specified (e.g. European Standards EN 12341:1998 and EN 14907:2005 for PM₁₀ and PM_{2.5}, respectively). The filters are weighted before and after the sampling period (after a proper moisture and temperature conditioning). PM is determined by the quotient of mass balance and the total volume of sampled air, in micrograms per cubic meter of air ($\mu\text{g}\cdot\text{m}^{-3}$).

When rural and remote areas are left without air quality information, satellite measurements may mitigate this lack of information over these areas. In the last ten years, there were conducted a significant number of studies using satellite measurements of Aerosol Optical Depth (AOD) to predict ground-level PM concentrations over places or periods without air quality measurements (Di *et al.*, 2016; De Hoogh *et al.*, 2018; Lee *et al.*, 2016; Stafoggia *et al.*, 2016). AOD quantifies the amount of light absorbed or scattered by

suspended particles, often designated by aerosols. Therefore, although representing a relevant parameter to predict PM variability, it is not an accurate one, once it is an atmospheric column estimative and PM concentrations are measured at ground level. Restrictions such cloud coverage, snow or water glint contamination, satellite calibration manoeuvres or lost data transmission are often responsible for missing AOD data. Researchers developed techniques to fill the gaps in PM predictions such as kriging, spatiotemporal interpolation or geographic weighted regression. (Zhu *et al.*, 2017). However, satellite AOD measurements are useful as a first indicator of PM concentrations at ground level (Chu *et al.*, 2003; Engel-Cox *et al.*, 2004; Gupta *et al.*, 2006; Wang and Christopher, 2003; Zhang *et al.*, 2009) and, for areas without air quality network coverage, satellite measurements may be the only way to estimate PM concentrations. Better PM concentrations predictions may be achieved by merging satellite AOD measurements with meteorological parameters (Gupta and Christopher, 2009) and land-use type (Hoek *et al.*, 2008), known to be strongly correlated with surface air quality, such as meteorology. Moreover, regarding meteorological parameters, temperature and humidity are the two strongest meteorological predictors of PM_{2.5} in the eastern United States (Zhang *et al.*, 2017). A recent study developed a high-fidelity PM_{2.5} ground level concentration prediction, by combining ground monitoring, satellite data and chemical transport, with high special resolution (1 x 1 km²), temporal resolution (daily) and spatial coverage (larger than 2 000 000 km²) (Goldberg *et al.*, 2019).

Lastly, concerning ambient air monitoring of UFP, the main pollutant object of this work, it is performed using two different equipment – a Condensation Particle Counter (CPC) and a Scanning Mobility Particle Sizer:

- Condensation Particle Counter (CPC): it counts, in real time, the total number concentration of particles above a lower size limit (3 to 20 nm, depending on manufacturer and model). Condensation in a controlled super-saturated environment is used to grow UFP to larger sizes. These larger particles are then measured, by counting, by means of a photodetector. Condensing liquids are usually alcohol or water. These particle counters are the most commonly used instruments in most applications. Yet, they do not provide any information on the original size of the particles counted. This type of equipment was used in many studies, including the present work (e.g. Hudda *et al.*, 2014; Hsu *et al.*, 2012; Lopes *et al.*, 2019a,b; Ren *et al.*, 2016, Riley *et al.*, 2016; Stafoggia *et al.*, 2016).
- Scanning Mobility Particle Sizer (SMPS): it consists of a combination of a particle counter and electrostatic classifier. The electrostatic classifier separates airborne particles according to their size, allowing to characterize the particle size distribution of UFP. Typically, for particles as small as 10 nm, these devices provide size distribution data in almost real-time. SMPS was used in several studies (e.g. Buonanno *et al.*, 2015; Keuken *et al.*, 2015; Masiol *et al.*, 2016; Shirmohammadi *et al.*, 2017; Zhu *et al.*, 2011).

2.4 CLASSIFICATION, FORMATION AND COMPOSITION OF PARTICULATE MATTER

Figure 2.8 illustrates the details of particulate matter classification (PM) according to its aerodynamic diameter in:

- PM_{10} – inhalable particles with $d \leq 10 \mu m$
- $PM_{2.5-10}$ – coarse particles with $2.5 \mu m \leq d \leq 10 \mu m$
- $PM_{2.5}$ – fine inhalable particles with $d \leq 2.5 \mu m$
- UFP or $PM_{0.1}$ – ultrafine particles with $d \leq 0.1 \mu m$.

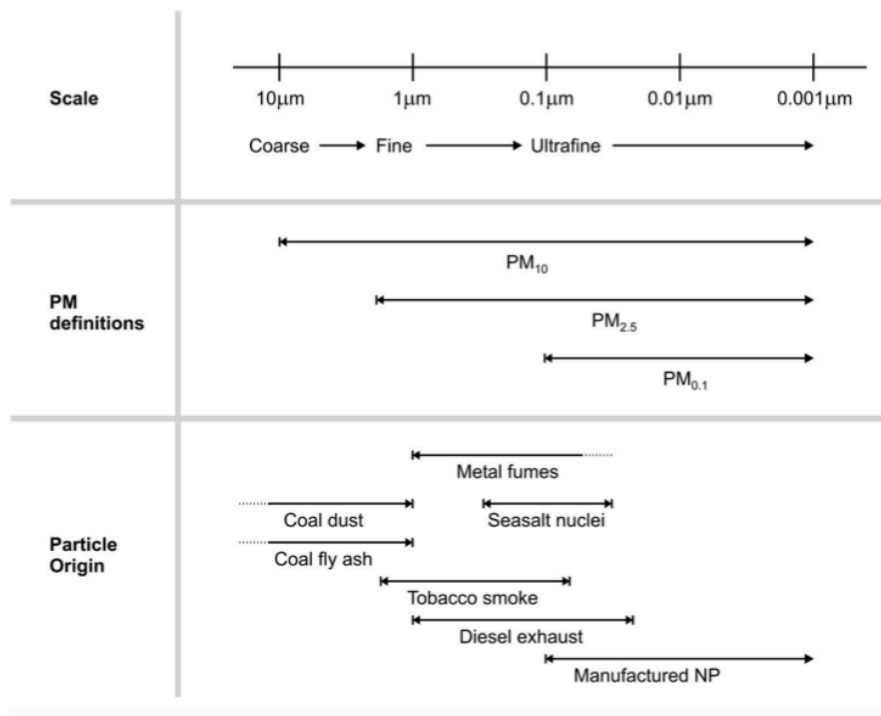


Figure 2.8: Classification of particulate matter (PM_{10} , $PM_{2.5}$ and $PM_{0.1}$ or UFP) and its common sources (Mühlfeld *et al.*, 2008).

Figure 2.9 presents the relative particles dimensions compared to a human hair which measures about $70 \mu m$. PM_{10} are seven times smaller than the human hair, $PM_{2.5}$ are about 30 times smaller and UFP are 700 times smaller.

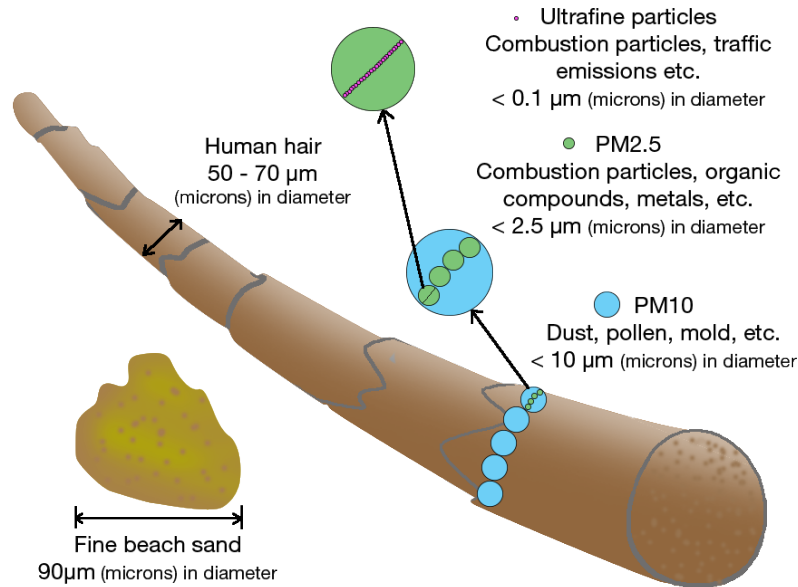


Figure 2.9: Schematic representation of PM according to its size (<https://www.epa.gov/pm-pollution/particulate-matter-pm-basics>).

Back in the late 1990s, Kittelson (1998) conducted a pioneering research on identifying three size categories for particles found in diesel engine emissions:

- 1) coarse mode ($1 \mu\text{m} < d \leq 10 \mu\text{m}$),
- 2) accumulation mode ($\sim 0.05 \mu\text{m} < d \leq 1 \mu\text{m}$), and
- 3) nuclei mode ($d \leq 0.05 \mu\text{m}$).

As shown in Figure 2.10, UFP, particularly in nuclei mode govern the total number concentration (blue line). Currently, the definition of fine particles according to their range size is (Argyropoulos *et al.*, 2016):

- Nucleation mode ($< 20 \text{ nm}$) - nucleated particles that have grown by condensation of gaseous precursors. They are mainly composed by sulphate particles and semi-volatile organic compounds.
- Aitken mode (20 to 100 nm) - also essentially composed by sulphate particles and semi-volatile organic compounds.
- Accumulation mode (100 to 1000 nm) - mostly includes soot and non-volatile organic compounds resulting from the combustion process. Sulphate particles and semi-volatile organic compounds may also be present. This mode is predominantly associated with exhausting gases of diesel engines.

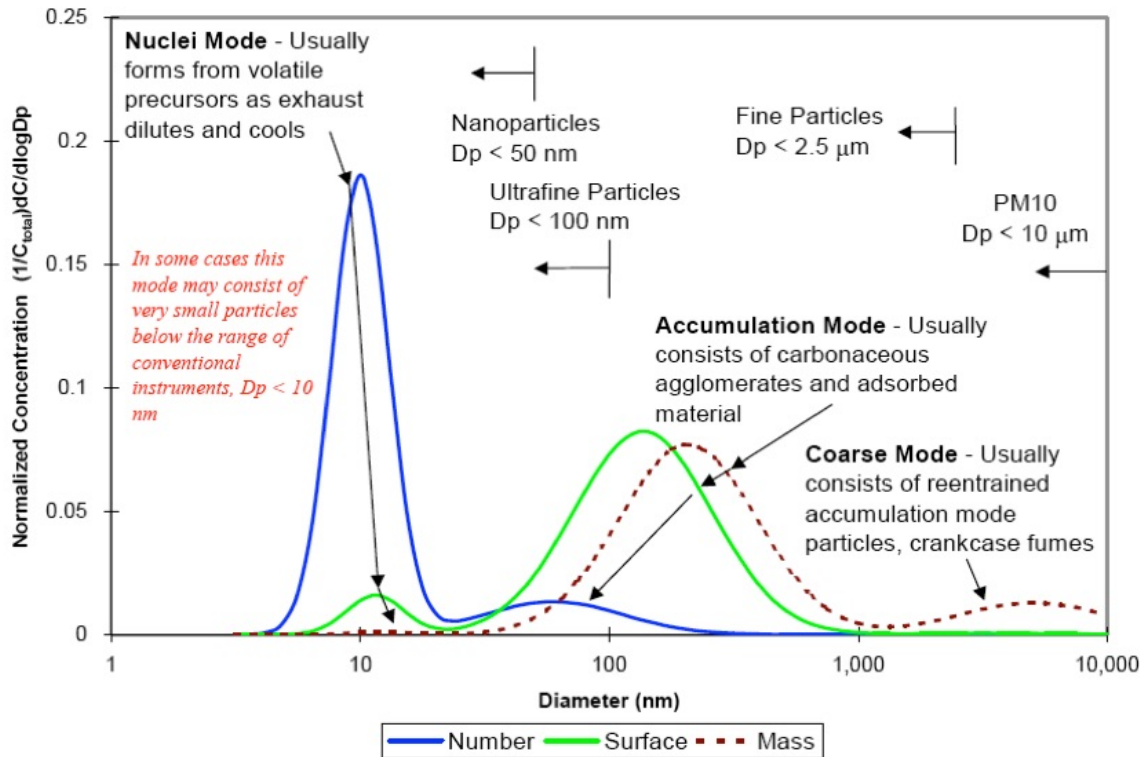


Figure 2.10: Typical engine exhaust size distribution in mass, surface and number weightings (adapted from Kittelson, 1998).

Particulate matter smaller than 1 μm appears to dominate the total PM emissions from combustion processes. Particularly, a large majority of particles emitted from urban area sources are smaller than 50 nm (Saha *et al.*, 2019), which might have greater health effects than background particles.

Yet, as mentioned in previous sub-chapter, particles smaller than 2.5 μm are not monitored and there are still no guidelines for its ambient concentrations.

PM emitted by vehicle engines can be divided into two categories, regarding the location of their formation:

- Primary combustion particles: formed in the engine or tailpipe. These particles are mostly sub-micrometre agglomerates of solid carbonaceous material ranging from 30 to 500 nm. They may also contain metallic ash (from lubricating oil additives and engine wear), adsorbed or condensed hydrocarbons, and sulphur compounds (Morawska *et al.*, 2008).
- Near-tailpipe UFP: the hot exhausting gases expelled from the tailpipe quickly cool and condense on existing particles or nucleate, forming large numbers of very small new particles. They are mainly composed by hydrocarbons and hydrated sulfuric acid, and generally 30 nm or less in diameter. These are the most commonly observed UFP near busy freeways, particularly those where a large fraction of heavy-duty diesel vehicles is present (Keskinen and Rönkkö, 2010; Ntziachristos *et al.*,

2007; Westerdahl *et al.*, 2005). The formation of these particles is very fast, and they are distinct from UFP derivative from photochemical nucleation processes which occur in atmosphere, further away from the source (Stanier *et al.*, 2004b).

Once released into the atmosphere, UFP are diluted with ambient air and undergo to chemical reactions and physical processes, namely evaporation, condensation, and coagulation (Putaud *et al.*, 2010). Thus, particles measured away from sources (e.g. roadways) have generally different characteristics than those measured close to the sources, immediately after their formation (Kim *et al.*, 2018). Moreover, UFP concentrations strongly depend on the local sources (Kumar *et al.*, 2010) and decline with the distance to source (Karner *et al.*, 2010). Physiochemical processes (dilution, coagulation, evaporation, condensation) (Karner *et al.*, 2010; Saha *et al.*, 2018a,b; Zhang *et al.*, 2004) contribute to high spatial variability of UFP concentrations within urban areas (Kumar *et al.*, 2014). Particle number concentrations are 2–3 times more spatially heterogeneous than PM_{2.5}. The observed order of spatial heterogeneity is UFP > NO₂ > CO > PM_{2.5} (Saha *et al.*, 2019). UFP concentration is ruled by non-linear processes such as coagulation which reduces UFP concentrations by promoting its growing to more than 100 nm. Traffic is a major UFP source in nucleation mode and higher UFP concentrations occur in winter during morning traffic rush hours, and at night. Photochemical nucleation has a relatively low frequency, but it yields for very high UFP concentrations (Agudelo-Castañeda *et al.*, 2019).

As mentioned before, the mass of UFP is very small. Therefore, the amount of UFP mass available for chemical analysis is reduced. Moreover, most studies were conducted using different equipment, different measurement protocols, UFP sampling in distinct size ranges, and focused on diverse properties of their chemical composition (Morawska *et al.*, 2008). Therefore, the author concludes that chemical composition of UFP is not yet fully known. However, it is clear that combustion engines produce gaseous emissions such as SO₂ and NO_x, and that nucleation of these pollutants into sulphate and nitrate particles plays an important role in the mechanism that leads to the increase in particle formation near sources (e.g. roads, airports, harbours).

Pakkanen *et al.* (2001) investigated UFP chemistry, elemental composition included, at two sites (urban and rural) in Helsinki, Finland. In both sites, the most important trace elements were Ca (calcium), Na (sodium), Fe (iron), K (potassium) and Zn (zinc) (present in higher concentrations), and Ni (nickel), V (vanadium), Cu (copper), and Pb (lead) (known as heavy metals). These measured elements accounted for less than 1% of the total UFP mass. Kuhn *et al.* (2005) concluded that UFP samples collected in Pittsburgh downtown, were mostly composed of organic matter (45 to 55% in mass) and salts of ammonium and sulphate (35 to 40%).

Sardar *et al.* (2005), conducted a study at two sites (urban and inland) in Los Angeles, and found that organic carbon (the amount of carbon present in the collected organic material) ranged from 32 to 69% (by mass), elemental carbon (an indicator of diesel PM and closely related to black carbon) from 1 to 34%, sulphate from 0 to 24% and nitrate from 0 to 4%. Organic material was found to comprise the larger fraction

of UFP mass, particularly in summer, when photochemical formation of organic aerosol is higher. Reche *et al.* (2011), found out that shipping PM consists mainly on fine to ultrafine fraction (e.g. elementary or black carbon (BC), Ni, V, etc.) or results from chemical reactions between exhaust gases and particles in the atmosphere. Saffari *et al.* (2013), in a year-long study at 10 different locations in Los Angeles basin, identified road dust (influenced by vehicular emissions as well as re-suspended soil), vehicular abrasion and residual oil combustion as major sources of trace elements and metals in PM_{0.25} ($d \leq 0.25 \mu\text{m}$, also known as quasi-UFP). Studies over the past two decades have linked many of the PM chemical components to oxidative potential, including, yet not limited to, polycyclic aromatic hydrocarbons (PAH) (Cheung *et al.*, 2010; Cho *et al.*, 2005; Janssen *et al.*, 2014), elemental carbon (EC) and organic carbon (OC), water-soluble organic carbon (WSOC), and transition metals (Decesari *et al.*, 2017; Saffari *et al.*, 2013; Shirmohammadi *et al.*, 2018).

The composition of PM widely varies and is strictly dependent on the emission source, particle size, geographic location, atmospheric chemical transformations, and meteorological conditions (Putaud *et al.*, 2010). Metals and trace elements such as Ba (barium), Cu, Fe and Pb usually result from abrasion of brakes, tyre abrasion, and resuspension of road dust (Lough *et al.*, 2005, Pant and Harrison, 2013). Metals and trace elements may also result from lubricating oil additives and engine wear debris accumulated in the oil (Gustafsson *et al.*, 2008, Schauer *et al.*, 2006). Particulate matter is greatly increased by the emission of unburned or partially combusted lubricating oil, which is expected to be complemented by an increase in metal emissions (Schauer *et al.*, 2006). Previous laboratory studies of diesel particulate matter emissions showed that lubricating oil is the dominant source of increased emission rates of many metals (Schauer *et al.*, 2006). Other studies have reported the formation of UFP as a consequence of abrasion and resuspension of road dust due to the tire-pavement interaction, with a peak in number size distribution at 40 nm and mean particle number in the 15 to 50 nm diameter range of (Dahl *et al.*, 2006, Gustafsson *et al.*, 2008).

Overall, UFP chemical composition differs significantly from place to place and it depends on the types of local sources and their relative contributions. Studies conducted by Shirmohammadi and co-workers (2016, 2017, 2018) allowed additional knowledge of chemical species bounded to quasi-UFP (Figure 2.11). Besides elemental and organic carbon (EC and OC), S (sulphur), K, Al (aluminium), Fe, Na and Ca were the most abundant elements found at both locations, Na, S, V and As (arsenicum) presented higher concentrations at LAX (Los Angeles International Airport). Elements associated with abrasion of brake and tyre wear (e.g. Ba, Cu, Fe, Mn (manganese), Pb and Zn (zinc) (Pant and Harrison, 2013)) and elements associated with re-suspension of road dust (e.g. Al, Ca, K and Ti (titanium) (Marcazzan *et al.*, 2001)) were higher at the site in centre of Los Angeles.

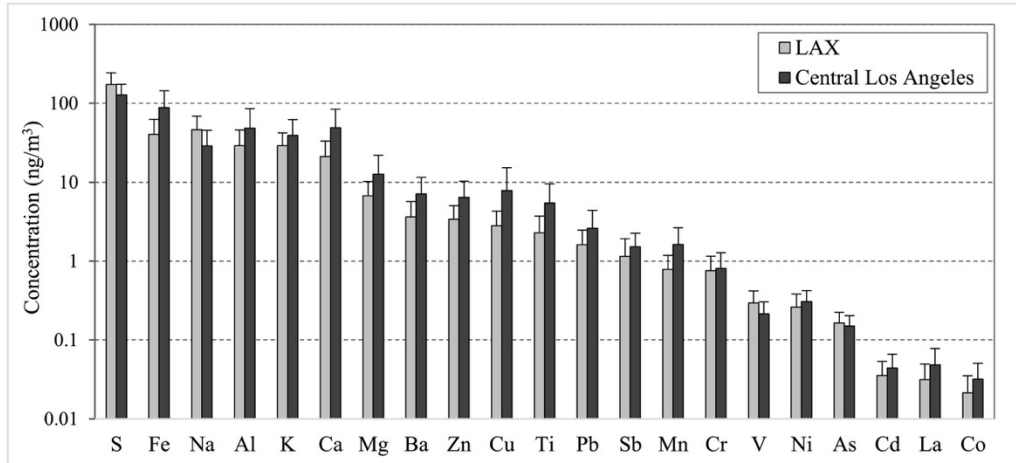


Figure 2.11: Total concentrations of trace elements and metals bounded to PM_{0.25} found in two different locations of Los Angeles. Error bars represent standard deviation (from Shirmohammadi *et al.*, 2018).

2.5 IMPACTS OF PARTICULATE MATTER

2.5.1 Human Health

During the last decades, many epidemiological studies consistently reported adverse health effects of PM exposures, both from short-term (e.g. daily variability) and long-term (e.g. annual averages) (Atkinson *et al.*, 2014; Beelen *et al.*, 2015; Cesaroni *et al.*, 2013; Raaschou-Nielsen *et al.*, 2013; Samoli *et al.*, 2013; Stafoggia *et al.*, 2013). These studies were mainly conducted in major cities, where air monitoring networks allow more accurate measurements and models of spatiotemporal PM variability.

Fine particulate matter is widely recognized for being particularly harmful and many studies demonstrated that its toxicity is considerably greater than coarse particles (e.g. Leliveld *et al.*, 2015). While the impacts on health of PM₁₀ and PM_{2.5} are well scientifically recognized, studies on UFP health impacts are scarce (Kumar *et al.*, 2013). The UFP input into the human body is mainly processed through three ways: respiratory, dermal and ingestion (Albuquerque *et al.*, 2012). Because of their small size, they rapidly reach the bloodstream and spread through all organs (WHO, 2013). Compared to fine particles, and because of their smaller size (ultrafine particles are generally associated with higher numerical concentrations), they have a much higher specific surface area, which can be associated with increased reactivity and toxicity (Ezz *et al.*, 2015; Sioutas *et al.*, 2005). Ultrafine particles can also cross the cell membranes and damage intracellular proteins, organelles and DNA (Carosino *et al.*, 2015; Geiser *et al.*, 2005; Penttinen *et al.*, 2001; Peters *et al.*, 1997; Semmler *et al.*, 2004). Figure 2.12 shows a schematic representation of inhaled PM and its main effect on human health (Zaheer *et al.*, 2018).

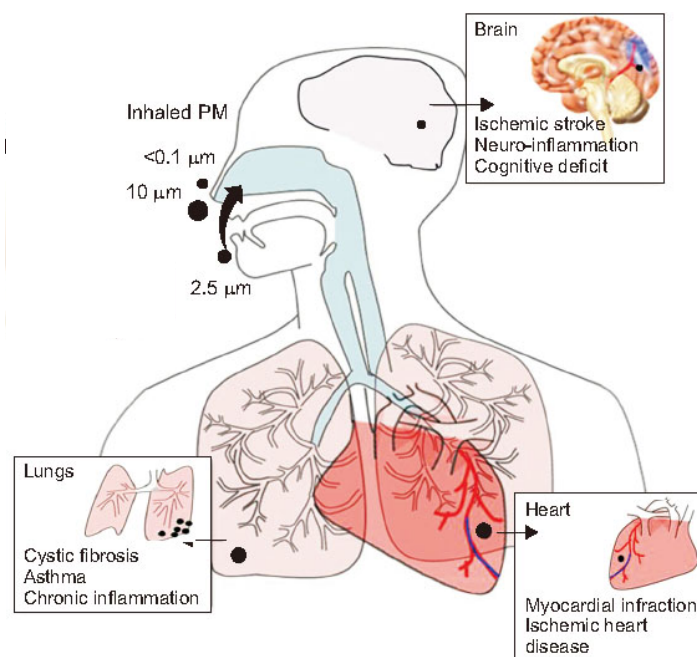


Figure 2.12: Diagrammatic representation of inhaled particulate matter of variable sizes and PM-linked respiratory, cardiovascular, and neurological diseases (adapted from Zaheer *et al.*, 2018)

Unlike the health effects of $\text{PM}_{2.5}$ and PM_{10} , the conclusions regarding the effects of UFP are limited because they are not usually measured (Lanzinger *et al.*, 2016). The same study also notes that the few epidemiological studies carried out on the effect of UFP on the mortality rate have revealed inconsistent results. A positive correlation, even though not statistically significant, has been observed between prolonged exposure to UFP and mortality due to breathing problems. The authors claim that more years of studies are needed to draw more precise conclusions. However, recently, UFP (50-500 nm) were associated with cardiovascular mortality in Ruhr area, Germany (Hennig *et al.*, 2018). Given their minimal size and high spatial variability, UFP are not strongly correlated with $\text{PM}_{2.5}$ (Baldauf *et al.*, 2016; Kumar *et al.*, 2010). However, there is growing concern that the adverse health effects of exposure to UFP may be worse from those of larger particles (HEI, 2013). Moreover, there is growing evidence and concern that short-term exposures to high UFP levels may also have important and adverse health effects (Stafoggia *et al.*, 2017a). Nevertheless, results from previous studies suggest that prolonged exposure to high concentrations of UFP may be responsible for reduced lung function and/or aggravation of respiratory diseases, such as asthma or chronic obstructive pulmonary disease (Carosino *et al.*, 2015; Ferreira *et al.*, 2013; Stanek *et al.*, 2011; Slezakova *et al.*, 2012; Terzano *et al.*, 2010).

Although clinical studies related to UFP exposure are still not enough for unequivocal conclusions regarding its toxicity, they make clear that its effects should not be neglected (Gomes *et al.*, 2012). Respiratory and cardiopulmonary problems, increased hospitalization (César *et al.*, 2016), and mortality

rates, especially due to lung cancer, are already associated with exposure to particulate matter (PM₁₀ and PM_{2.5}) (Buonanno, 2015; Grana *et al.*, 2017; WHO, 2013). In 2013, the International Cancer Research Agency, classified diesel engines exhaust particulate matter, as a Group I carcinogen (IARC, 2014). The exposure to PM_{10-2.5} during gestation, regardless gestational stage, was associated with below-average birth weight infants (Ebisu *et al.*, 2016). The economic costs associated with treating these health problems could be considerably reduced by decreasing the atmospheric concentration of particulate matter (Holland *et al.*, 2014; Shah *et al.*, 2013). Therefore, as referred by Joerger and Pryor (2018), people living, working or spending much time next to intense traffic roads are exposed to high traffic-related emissions and have higher risk to respiratory and cardiovascular health problems or even premature mortality (Chen *et al.*, 2008; Chen *et al.*, 2017; HEI, 2013; Hystad *et al.*, 2015; Lelieveld *et al.*, 2015;).

Several studies have shown that UFP are also able to constrain phagocytosis (Renwick *et al.*, 2001), and to stimulate necrosis and apoptosis (Pan *et al.*, 2009, Sydlík *et al.*, 2006), inflammation (Müller *et al.*, 2009), and oxidative stress (Gasparotto *et al.*, 2013). The brain is also affected by the PM, depending upon the particulate size and charge (Bharadwaj *et al.*, 2018); particularly, UFP has neurological effects (Daher *et al.*, 2013). The potential biological effects are determined by PM characteristics (Wu *et al.*, 2018) which vary according to their sources. Wu *et al.* (2018) showed that the size of PM regulates its potential to cause injury, or oxidative, inflammatory responses, among other biological reactions.

Moreover, recent studies associate airborne PM to cardiovascular diseases and an increase cause of stroke (Kolpakova *et al.*, 2017; Lee *et al.*, 2018; Pinault *et al.*, 2017). Cardiovascular issues are linked to arise from changes in blood composition and pressure and increases in PM concentrations were linked to increase chance for myocardial infarction (Tsai *et al.*, 2003). Additionally, recent studies implied that PM can attack the brain parenchyma inducing neurodegenerative and vascular dementia diseases such as Alzheimer's disease, Parkinson's disease (Chen *et al.*, 2017; Oudin *et al.*, 2016) and may have significant impact on central nervous system of children developing brain (Annavarapu and Kathi, 2016).

A recent global burden of disease study (Gakidou *et al.*, 2017), found that, in 2016, exposure to air pollution caused an estimated 6.1 million premature deaths worldwide, of which 4.1 million deaths were attributed to exposure to ambient particulate matter. Mousavi *et al.* (2019) highlighted the toxicity and oxidative potential of quasi-UFP emitted by Ports of Los Angeles and Long Beach, as well as road traffic, particularly heavy-duty vehicles. Combustion generated particles (from vehicle emissions) range from 30 nm to 500 nm (Vu *et al.* 2015).

Airport-related particles have been shown to be considerably toxic, even at low exposure concentrations (He *et al.*, 2018). The results of this study suggest that airport emission as source of PM_{0.25} may also contribute to the adverse effects on public health attributable to PM. The potency of such particles is in the same range as those collected at a site in urban area impacted heavily by traffic emissions. Exposure to airport-related UFP has an increased acute systemic inflammation (Habre *et al.*, 2018). A recent study in

Los Angeles airport, shown that the mean diameter of particles from the airport is around 20 nm, considerably smaller than particles emitted from the urban traffic area with mean diameter around 35 nm (Shirmohammadi *et al.*, 2017). These airport-related nanoparticles result in a higher surface area/mass ratio, when compared to micro-particles. Therefore, more organic and inorganic species are able to be adsorbed and/or absorbed on these UFP which is expected to increase their toxicity.

Nanotoxicology is a recent investigation field which allows a better understanding of toxicity mechanisms of airborne UFP in air pollution. Considering the evidences from particulate matter and nanotoxicology areas, distinct to fine particulate matter, UFP is suspected to have much more impacts on human health (Chen *et al.*, 2016). The authors claim that UFP plays a major role in adverse impacts on human health. Therefore, further investigation in toxicological research of air pollution is required. A recent review (Ohlwein *et al.*, 2019) concludes that the evidence suggests adverse associations of short-term UFP exposure with pulmonary and systemic inflammation, autonomic tone and blood pressure, which may be at least partly independent of other pollutants. For the other studied health outcomes (e.g. morbidity and mortality), the evidence on independent health effects of UFP remains inconclusive or insufficient. The authors recognize road traffic-related exposures and the exposure to UFP in the vicinity of airports as relevant issues. They claim that research is still at the beginning, and new exposure assessment methods need to be defined and employed in epidemiological studies. Finally, the conclusions achieved are similar in previous evaluation (HEI, 2013).

The results of health impact assessment in Europe, 2015 (both global and EU-28) are presented in Table 2.6. Globally, there were registered 422 000 premature deaths attributable to fine particulate matter exposure and 79 000 premature deaths attributable to NO₂. In EU-28, these figures drop to 391 000 and 76 000, respectively. Regarding the number of years of life lost, 4 466 000 YLL are attributable to PM_{2.5} exposure and 821 000 to NO₂, considering all European countries. In EU-28, these figures decrease to 4 150 000 and 795 000, respectively (EEA 2018a). Premature deaths and years of life loss are defined in EEA (2018a) as:

- **Premature deaths** are deaths that occur before a person reaches an expected age. This expected age is typically the life expectancy for a country stratified by sex. Premature deaths are considered to be preventable if their cause can be eliminated.
- **Years of life lost (YLL)** are defined as the years of potential life lost due to premature death. It is an estimate of the average number of years that a person would have lived if he or she had not died prematurely. YLL takes into account the age at which deaths occur and is greater for deaths at a younger age and lower for deaths at an older age. It gives, therefore, more nuanced information than the number of premature deaths alone.

Table 2.6: Premature deaths and years of life lost (YLL) attributable to PM_{2.5} and NO₂ exposure in EU-28 and in 41 European countries, in 2015 (adapted from EEA, 2018a).

Countries	Population (1000)	PM _{2.5}		NO ₂		PM _{2.5}		NO ₂	
		Annual Mean ^(a)	Premature Deaths ^(b)	Annual Mean ^(a)	Premature Deaths ^(b)	YLL	YLL/10 ⁵ inhabitants	YLL	YLL/10 ⁵ inhabitants
EU-28	506 030	13.9	391 000	18.9	76 000	4 150 000	820	795 000	157
Total	538 278	14.1	422 000	18.8	79 000	4 466 000	830	821 000	153

(a) Expressed in µg.m⁻³.

(b) Total and EU-28 premature deaths are rounded to the nearest thousand.

2.5.2 Climate

Recently, the fifth Assessment Report of the Intergovernmental Panel on Climate Change has identified the Mediterranean area as one of the most vulnerable hot spots to climate change for the 21st century (IPCC, 2014). On the other hand, the heat and air pollution have synergetic effects on mortality (Scortichini *et al.*, 2018). According to these authors, taking in account the predicted increase of frequency and/or intensity of heat waves events in Mediterranean areas, special concerns and prevention public health heat prevention plans should be implemented.

Behind health problems, airborne particulate matter is a climate forcing agent (Becceril-Valle *et al.*, 2017; Fiore *et al.*, 2012; Liggio *et al.*, 2012; Zimmerman *et al.*, 2016), as they modulate the warming effects of CO₂ and other greenhouse gases (Wang *et al.*, 2019). PM affects mainly the radiative balance and ice and clouds albedo, although the uncertainty of the global effect is still high. Additionally to their adverse effects on public health, anthropogenic aerosols, or PM, are the most important short-lived climate forcers (Boucher *et al.*, 2013; Myhre *et al.*, 2013). Aerosols interfere with terrestrial radiative budget both directly and indirectly. In the absence of clouds, the direct effect is scattering or absorbing the shortwave incoming solar radiation (Ramanathan *et al.*, 2001), and thus inducing a negative or positive radiative forcing, respectively. Moreover, aerosols promote the absorption of longwave radiation emitted by the surface and thus the heating of low atmosphere (positive radiative forcing) (Haywood and Boucher, 2000). Indirectly radiative forcing results of addition of cloud condensation nuclei and subsequent alteration of clouds properties (Lohmann and Feichter, 2005). It can also be considered a semi-direct radiative forcing once the evaporation of clouds is enabled in the presence of absorbing aerosols such as black carbon (Ackerman *et al.*, 2000). Moreover, the black carbon fraction exerts strong absorption and a positive radiative forcing (Wang *et al.*, 2019). The magnitude of direct radiative forcing depends on several properties of the aerosols such as particle diameter and chemical composition (Bohren and Huffman, 1998) as well as shape, state of mixture, and hygroscopicity (Zieger *et al.*, 2013). Particle number size distribution and their light absorption coefficient are helpful parameters to predict the direct radiative forcing based on in situ measurements. Although the uncertainties of aerosol radiative forcing remain high, Simon and co-workers (2008) found that direct aerosol forcing in urban atmosphere is mainly driven by the absorbing black carbon aerosols. The same study also concluded

that the mean heating rate within the urban boundary layer is considerably enhanced, by 4.57 K day^{-1} , due to the presence of absorbing aerosols.

2.6 INFLUENCE OF METEOROLOGICAL CONDITIONS ON AIR QUALITY

High concentrations of air pollutants depend not only on emission sources but also on dilution processes, transport and chemical reactions of the emitted pollutants. These processes are highly dependent on meteorological conditions (Russo *et al.* 2014a). Meteorological parameters such as temperature, wind speed and direction, relative humidity, precipitation and mixing layer height are determinant to air quality (Russo *et al.*, 2014a). Mainly, wind speed and mixing layer height strongly affect the accumulation/dispersion of air pollutants, namely by traffic in urban areas (Grundström, 2015).

Horizontal (wind) and vertical (turbulence) air movements affect the mixing and transport of air pollutants and so, their concentrations (Kim and Guldmann, 2011). Wind speed plays a crucial role in pollutants dispersion: low intensity winds (intensity inferior to 5 m.s^{-1}) tend to lead to high pollutants, such PM, concentrations once dispersion is not promoted (Russo *et al.*, 2014a). However, for higher wind speed, PM concentrations may increase, highlighting the ability of higher wind speeds, associated to high mechanical turbulence, to transport and re-suspend PM (Grundström, 2015). For buoyant plumes, such as plumes emitted by aircrafts, higher wind speeds promote faster ground arrival which counterbalances the dispersion (Hudda *et al.*, 2018). Moreover, wind direction is determinant once locations downwind to emission source will present higher concentrations (Kim and Guldmann, 2011).

Other important meteorological parameter is the mixing layer height which corresponds to the lowest atmospheric layer where air constituents are mixed by convection and mechanical turbulence (Chou *et al.*, 2007). This ability of mixing is critical to keep air quality acceptable in the vicinity of emission sources (Wallace *et al.*, 2010). Once the majority of emissions occur close to the ground, the mixing layer is usually the layer showing high pollutants concentrations, mainly in urban areas (Chou *et al.*, 2007). Therefore, the mixing layer height defines the upper level of the layer close to surface where the pollutant mixing take place (Cimini *et al.*, 2013).

In urban areas is frequent the occurrence of thermal inversions close to the surface. A thermal inversion occurs when the vertical temperature profile increases with high in opposition to tropospheric vertical temperature profile (Rédon *et al.*, 2014), leading to static stable atmospheric conditions which inhibits convection ascendant movements. Therefore, pollutants become trapped in this layer (Wallace *et al.*, 2010), promoting eventual extreme pollution events (Russo *et al.*, 2014a) and air quality degradation (Wallace *et al.*, 2010). Stable inversions have been associated with the frequent occurrence of the extreme $\text{PM}_{2.5}$ levels in middle-south plain of Hebei province (Wang *et al.*, 2018). This study highlights the boundary layer and inversion conditions, closely related with topography, as great contributors to high $\text{PM}_{2.5}$.

Previous research has concluded that meteorological variables (temperature, relative humidity (RH), atmospheric boundary height, wind intensity and direction and precipitation) were decisive parameters for pollutant diffusion and dilution (Pateraki *et al.*, 2012; Tai *et al.*, 2010). Moreover, absorption and dry deposition on surface (vegetation, soil, and structures) induce PM_{2.5} concentration reduction (Beckett *et al.*, 1998; Janhäll, 2015). Also, it has been shown that PM concentration increases with relative humidity, under stable atmospheric conditions, low wind speed or thermal inversion conditions. (Mu *et al.*, 2011). Regard PM_{2.5}, RH strongly enhances secondary reactions leading to an increasement in PM_{2.5} concentrations (Liu *et al.*, 2016). Lou *et al.* (2017) reported an inverted U-shaped curve for the relation between RH and PM_{2.5}.

On the other hand, several works have highlighted the role played by temperature and precipitation. Generally, high (low) values of temperature are responsible for intense (lessen) convection of pollutants (Lin *et al.*, 2009) and consequently leading to higher (lower) PM concentrations. On the other hand, precipitation enhances wet deposition and decreases PM concentrations (Shen *et al.*, 2009).

3 BACKGROUND AND METHODOLOGY

3.1 MAIN SOURCES OF PARTICULATE MATTER IN LISBON

The atmospheric emissions inventory for the Lisbon and Tagus Valley Region (FCT-NOVA, 2017), clearly identified transport modes as the main sources of PM₁₀ and NO₂ emissions in Lisbon, during the five years covered period, 2010-2014. Results for 2014, presented in Figure 3.1 identify road traffic as the main PM₁₀ and NO₂ source, accounting for 87 % and 57% of their emissions, respectively. Maritime traffic is responsible for 9 % of PM₁₀ emission of which 2 % are related to in-land passenger ferries. This transport mode is responsible for 20 % of NO₂ emissions, of which 6 % are associated with in-land passenger ferries. Air traffic is responsible for 2 % of PM₁₀ emissions and 17 % of NO₂ emissions. The remaining 2 % and 6 % of PM₁₀ and NO₂ emissions, respectively, are related to other sources including electricity production, industry, trade and services, domestic and biogenic sectors.

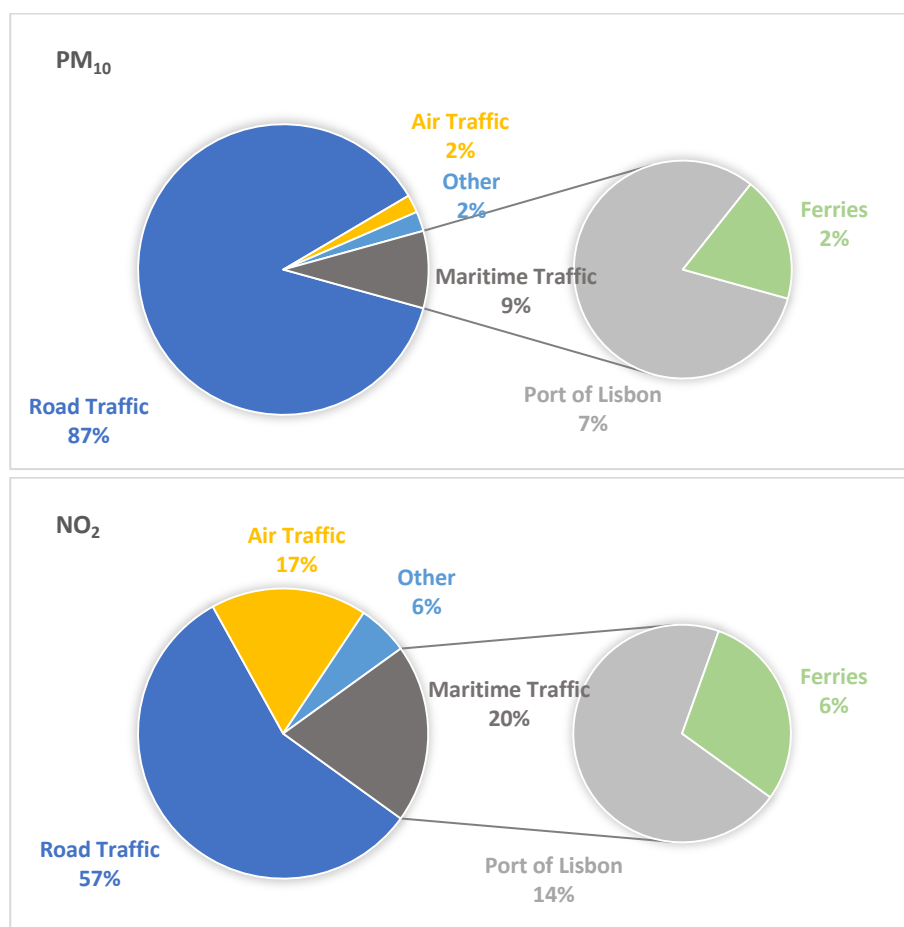


Figure 3.1: PM₁₀ (top) and NO₂ (bottom) relative emissions, in Lisbon, 2014, by source (FCT-NOVA, 2017).

3.1.1 Road Traffic

In the city of Lisbon, air quality is monitored by five AQMS shown in Figure 3.2. Their characteristics and measured pollutants are presented in Table 3.1 (<http://www.ccd-r-lvt.pt/pt/avaliacao-da-qualidade-do-ar-na-rlvt/8085.htm#D1>). As it can be seen, PM_{2.5} is not measured in three stations and continuous monitoring of UFP by AQMN is currently not performed.

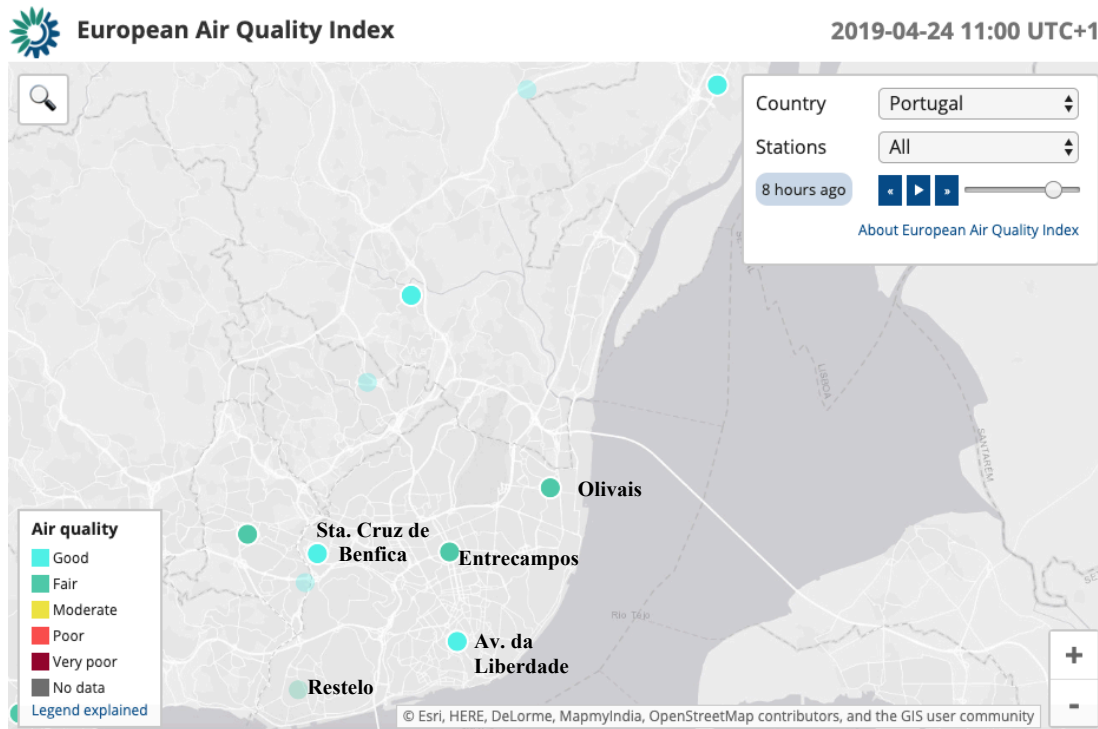


Figure 3.2: AQMN in Lisbon and respective air quality index on the 24th April 2019 at 11:00 UTC (<http://airindex.eea.europa.eu/>).

Lisbon has an intense road traffic with diversified characteristics, from low speed narrow streets to high-speed roads and highways. Due to this intensive road traffic, the air quality limit values established by European Union and Portuguese legislation, particularly for NO₂ and PM₁₀, have been often exceeded. Figure 3.3 presents NO₂ and PM₁₀ annual averages over the period 2010-2017 (APA, 2019). The red dot line denotes the annual limit value (LV), 40 µg.m⁻³, for both pollutants. While the measured values at Av. da Liberdade (AL), NO₂ consistently exceeds this LV, in Entrecampos (EC), it is regularly close to the LV or above it. On the other hand, PM₁₀ does not present many exceedances. However, over the last four years of the considered period, all series present a slightly increasing trend.

Table 3.1: Technical characteristics of Lisbon urban AQMS (<http://www.ccdr-lvt.pt/pt/avaliacao-da-qualidade-do-ar-na-rlvt/8085.htm#D1>).

Station	GPS coordinates	Type	Start Measuring Date	Monitored Pollutants
Av. da Liberdade	38°43'13.140" N 09°08'45.036" W	Traffic	January, 1994	PM ₁₀ , NO, NO ₂ , NO _x , CO
Entrecampos	38°44'52.137" N 09°08'59.037" W	Traffic	March, 1992	PM ₁₀ , PM _{2.5} , NO, NO ₂ , NO _x , O ₃ , SO ₂ , CO, C ₆ H ₆
Olivais	38°46'08.415" N 09°06'29.338" W	Background	March, 1992	PM ₁₀ , PM _{2.5} , NO, NO ₂ , NO _x , O ₃ , CO, SO ₂
Restelo	38°42'17.813" N 09°12'37.145" W	Background	February, 2002	PM ₁₀ , NO, NO ₂ , NO _x , O ₃ , CO
Sta. Cruz de Benfica	38°44'52.681" N 09°12'09.334" W	Traffic	December, 2008	PM ₁₀ , NO, NO ₂ , NO _x , CO, SO ₂ and Pb, Ni, Cd, As in PM ₁₀

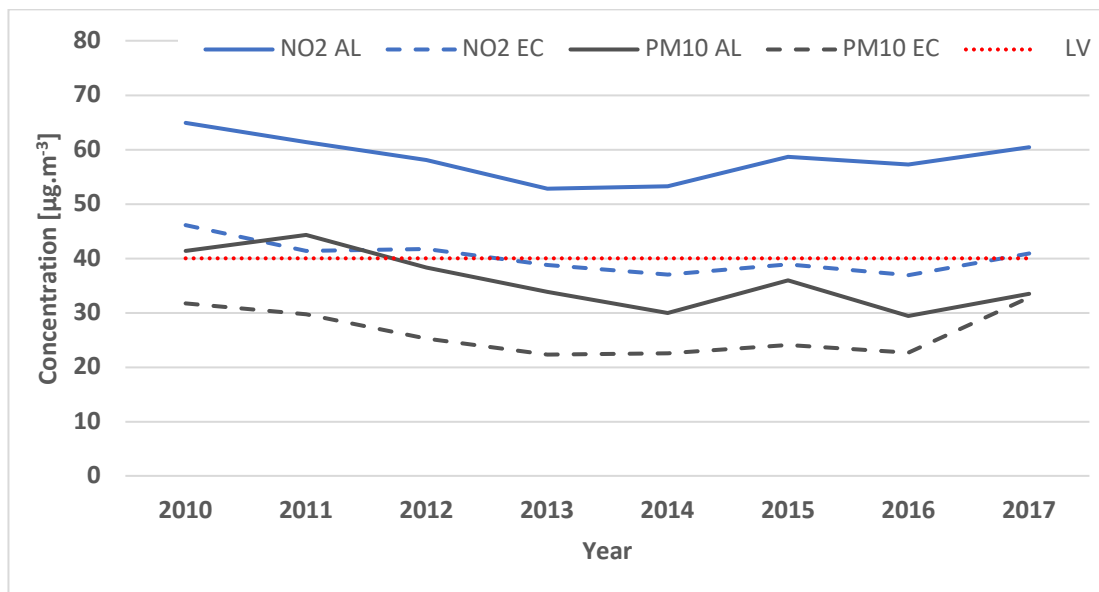


Figure 3.3: Annual average concentrations of PM₁₀ and NO₂ in Av. da Liberdade (AL) and Entrecampos (EC) AQMS and limit value established in EU (2008).

Although its harmful effects on human health, PM_{2.5} is not monitored in Av. da Liberdade AQMS. Therefore, we are only able to present its annual evolution between 2010 and 2017 in Entrecampos and a background air quality monitoring station, Olivais (OLI). As it can be seen in Figure 3.4, the annual limit value (25 µg.m⁻³) has not been exceeded in both stations. Still, over the last four years of the considered period, PM_{2.5} annual concentrations present an increasing trend, to values close to the limit value.

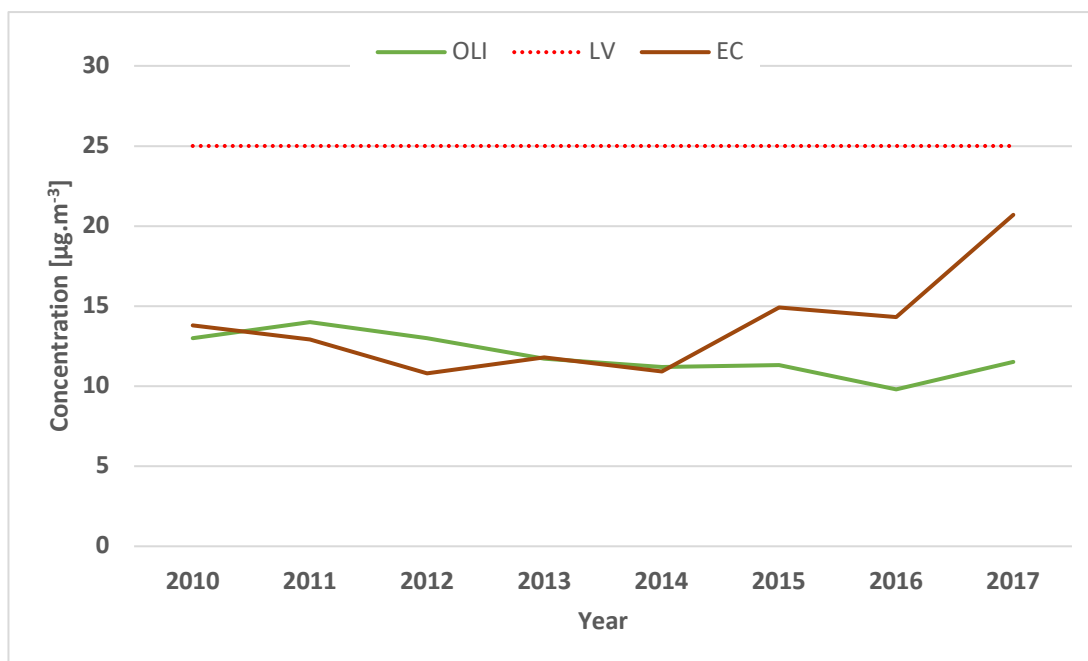


Figure 3.4: Annual average concentrations of PM_{2.5} in Olivais (OLI) and Entrecampos (EC) AQMS and limit value established in EU (2008).

Daily mean values of PM₁₀ in Av. da Liberdade and Entrecampos are presented in Figure 3.5 and Figure 3.6. In 2017, AQMS of Entrecampos presents only 15.9 % of validated data of PM₁₀. Therefore, we chose the previous year, 2016. In 2017, in Av. da Liberdade, the daily limit value for PM₁₀ is often exceeded, mostly from Fall to Spring. In Entrecampos, the limit value is accomplished most of the time, although some exceedances have been recorded. Hourly mean values of NO₂ in Av. da Liberdade and Entrecampos in 2017 are presented in Figure 3.7 and Figure 3.8. The hourly limit value for NO₂ is accomplished most of the time in both locations. In Av. da Liberdade, this value is exceeded more often, mainly from October to December. The number of annual exceedances of these two pollutants, in the considered sites and years, is presented in Figure 3.9.

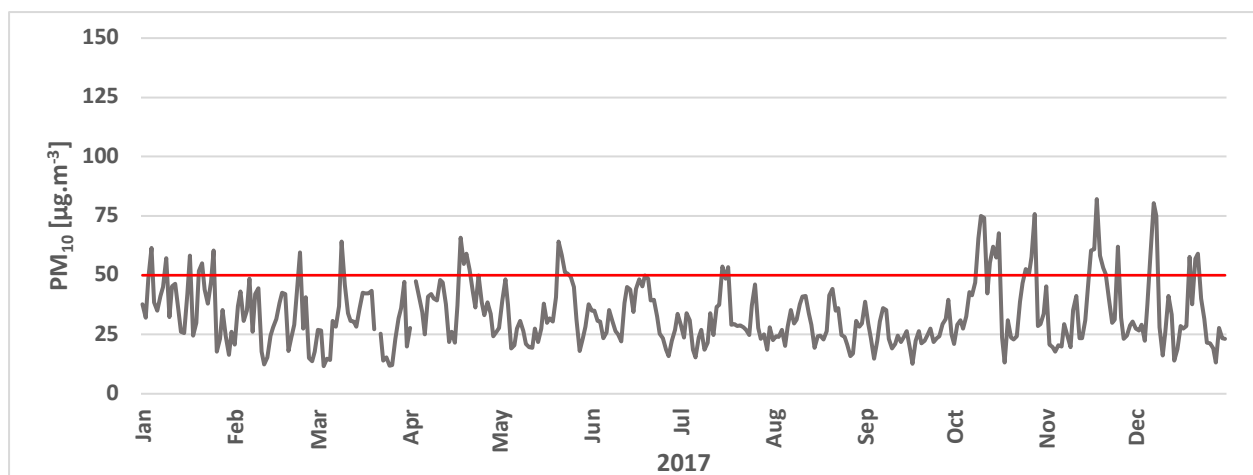


Figure 3.5: Daily average concentrations of PM₁₀ in Av. da Liberdade, in 2017. The red line represents the LV (EU, 2008).

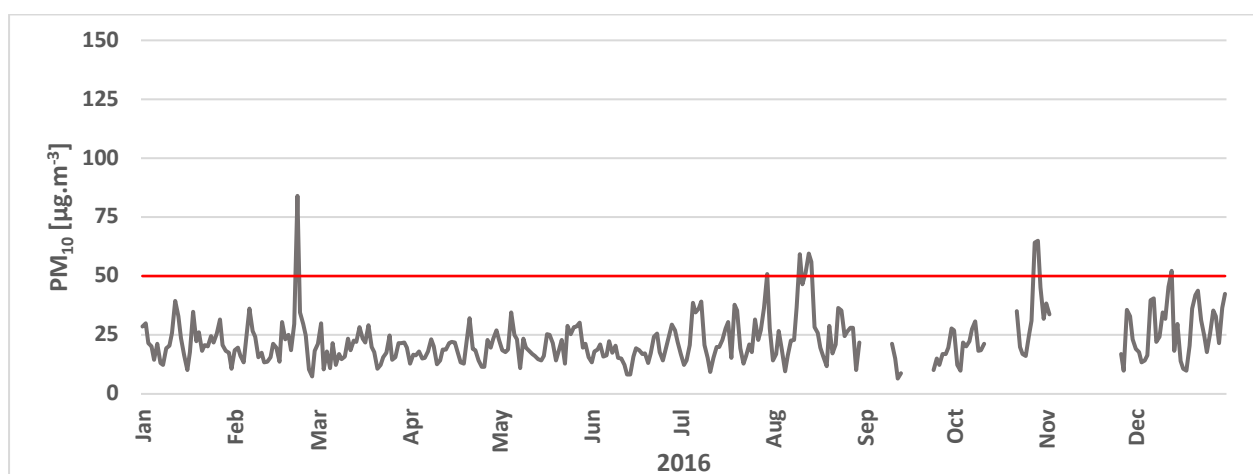


Figure 3.6: Daily average concentrations of PM₁₀ in Entrecampos, in 2016. The red line represents the LV (EU, 2008).

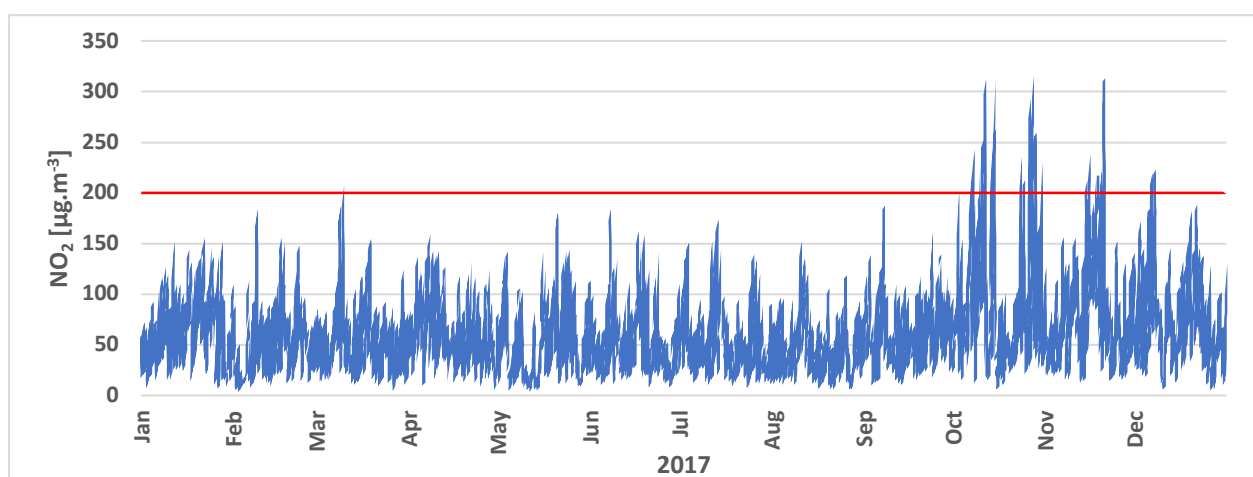


Figure 3.7: Hourly average concentrations of NO₂ in Av. da Liberdade, in 2017. The red line represents the LV (EU, 2008).

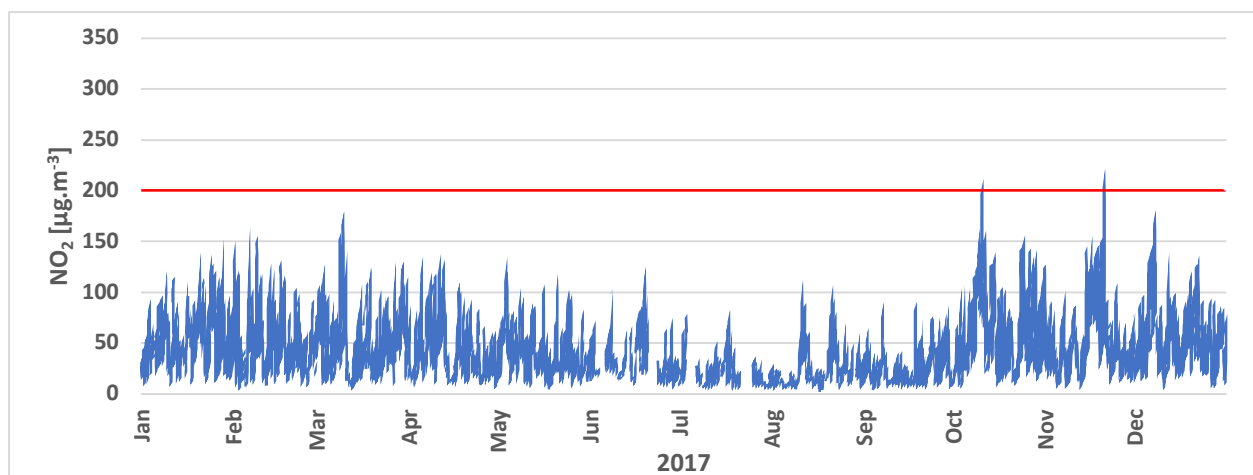


Figure 3.8: Hourly average concentrations of NO₂ in Entrecampos, in 2017. The red line represents the LV (EU, 2008).

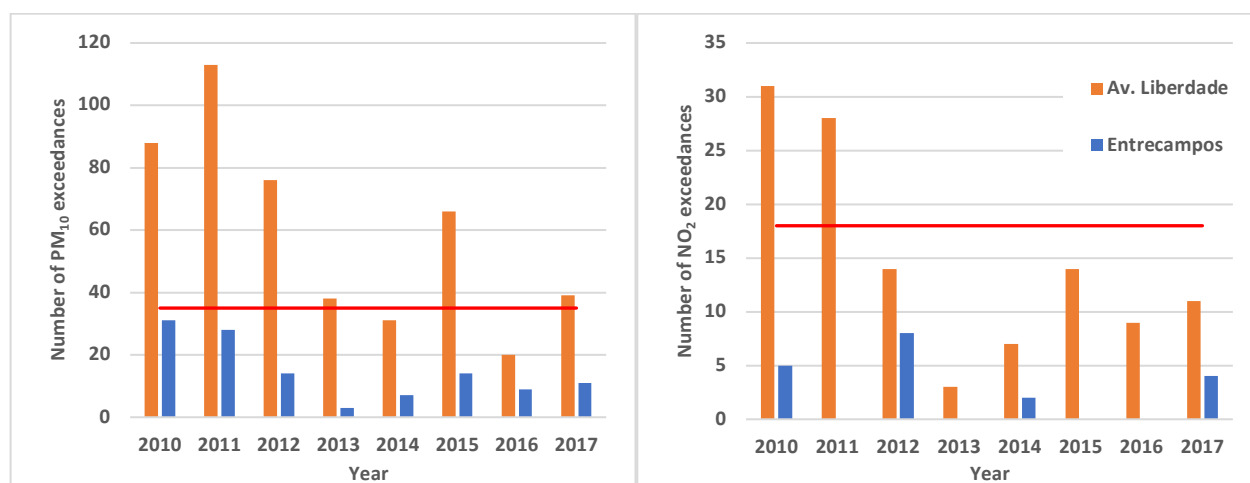


Figure 3.9: Number of exceedances of daily PM₁₀ and annual NO₂ limit values in Av. da Liberdade and Entrecampos between 2010 and 2017. The red line represents the annual number of exceedances allowed for each one of the pollutants (35 and 18 days for PM₁₀ and NO₂, respectively) (EU, 2008).

In order to mitigate the exceedances of both NO₂ and PM₁₀, Low Emissions Zones (LEZ) were implemented. Lisbon's LEZ, shown in Figure 3.10, were implemented through phases: the first stage started in 2011, July 4th, at Marquês de Pombal/Terreiro do Paço axis, zone 1 (LEZ 1), where pre-Euro (prior to 1992) vehicles circulation was banned during weekdays between 8:00 h and 20:00 h. The 2nd stage begun in 2012, April 1st, covering a larger area (about one third of the city), zone 2 (LEZ 2), where pre-Euro vehicles were not allowed to circulate. Simultaneously, in zone 1, the circulation restrictions were extended to vehicles accomplishing Euro 2 and the time period, weekdays from 7:00 h to 21:00 h (Ferreira *et al.*, 2015). Finally, the 3rd stage begun in 2015, January 15th, covering the same area but with circulation restrictions extended to vehicles accomplishing Euro 3, in zone 1, and Euro 2, in zone 2, during weekdays between 7:00 h and 21:00 h (CML, 2015).

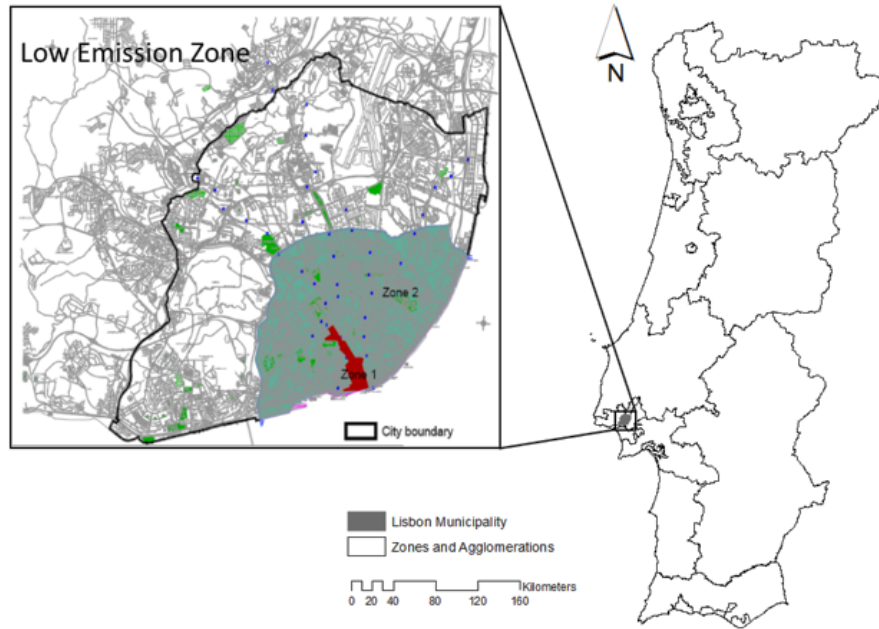


Figure 3.10: LEZ geographical extent and location (adapted from Ferreira *et al.*, 2015).

Figure 3.11 illustrates the distribution of vehicles by type in Lisbon in 2015, out of LEZ and in zones 1 and 2 of LEZ. Light passenger cars account for the major parcel of the vehicles followed by taxis, except for out of LEZ area, where light duty vehicles occupy the second position. The frequency of light passenger cars is also higher, compared to the figures recorded in LEZ. Public passenger transport is more frequent in LEZ than in the remaining area.

The relative distribution by Euro standard and type of vehicle is presented in Figure 3.12. Globally, with exception for taxis, about 60 % of the vehicles accomplish Euro 4 or stricter. Considering LEZ 1, this figure increases to 70 % for light passenger and light duty vehicles. Still, taxis and buses only achieve a little more than 50 % of vehicles accomplishing Euro 4 standard being the worst performance for taxis. There were not recorded heavy duty vehicles in LEZ 1. A higher frequency of buses accomplishing, at least, Euro 4 in LEZ 2 (70 %) than in LEZ 1 (55 %) was recorded. In LEZ 1, during the counting periods, no heavy-duty vehicles were recorded which highlight the reduced number of this type of vehicles presently circulating in LEZ 1. Nevertheless, it is clear that circulation restrictions in LEZ are not being entirely fulfilled which may reduce their impact on air quality improvement. However, these results must be interpreted simply as indicative, since counting was performed by students, with an academic purpose and, therefore, their representativeness and quality is not fully assured.

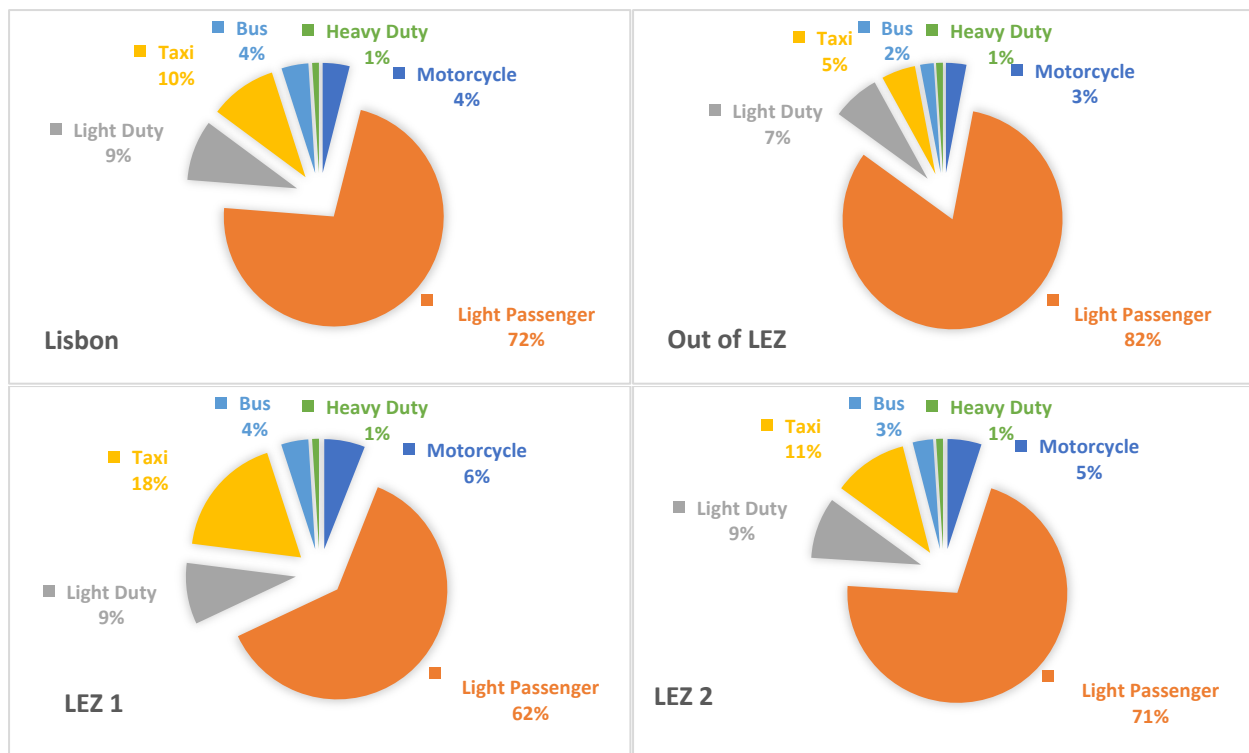


Figure 3.11: Distribution of vehicles by type and zone in 2015 (adapted from Henriques, 2015).

Real traffic levels are monitored by the GERTRUDE system managed by Lisbon Municipality. This system provides automatic counting of traffic at different parts of Lisbon, but it does not provide vehicle age nor traffic type distribution (Góis *et al.*, 2007).

Several campaigns of traffic characterisation in Lisbon have been carried out to evaluate the effect of LEZ implementation on air quality improvement (Ferreira *et al.*, 2013; Ferreira *et al.*, 2015; Monjardino *et al.*, 2018; Santos *et al.*, 2019). After the third stage of LEZ implementation, an extensive campaign was carried out with the purpose of counting and charactering the vehicles, in terms of age (and so Euro emission standard) as well as in terms of typology (passenger cars, light duty or heavy vehicles, buses, taxis and motorcycles). This campaign was conducted in 2015, covering 18 locations within LEZ1, LEZ2 and out of LEZ. It allowed the characterisation of 37 117 vehicles: 6 446 within de LEZ 1, 17 931 in LEZ 2 and 12 739 out of LEZ. The counting resulted from *in-situ* observations, for several periods during the day (morning rush hour, lunchtime and afternoon rush hour). It was performed by counting teams who also registered type of vehicle and fuel. Moreover, the engine manufacturing year of 14 830 vehicles was also recorded: 2 224 in LEZ 1, 7 392 in LEZ 2 and the remaining 4 915 out of ZER areas). Vehicle typology was directly observed and evaluated, while vehicle age was assessed by observation of the license plate (which in Portugal contains the month and year of construction of the vehicle's engine).

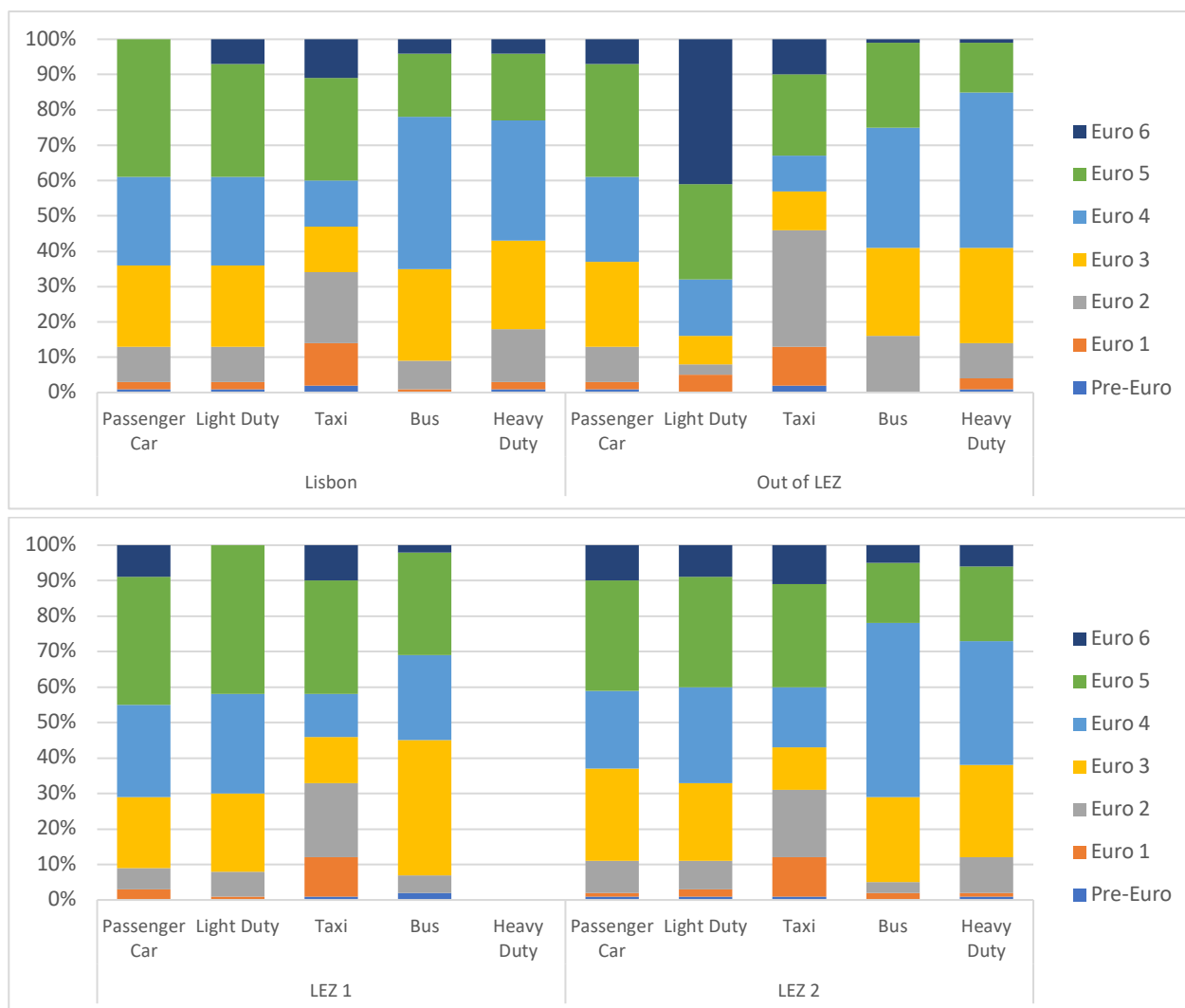


Figure 3.12: Relative distribution of Euro Standard by type of vehicle and zone in 2015 (adapted from Henriques, 2015).

The estimated emissions of directly traffic-related pollutants, NO_x and PM, in Av. da Liberdade are presented in Figure 3.13, where 35 % of NO_x emissions are linked to public transports (buses) followed by light passenger (28 %) vehicles. Taxis account 13 % in NO_x emissions. Thus, passenger transport accounts for 73 % of NO_x emissions. Regarding particulate matter, light passenger vehicles account for 30 %, closely followed by buses (28 %) while taxis account for 20 %. Once again, passenger transport is the main source (78 %).

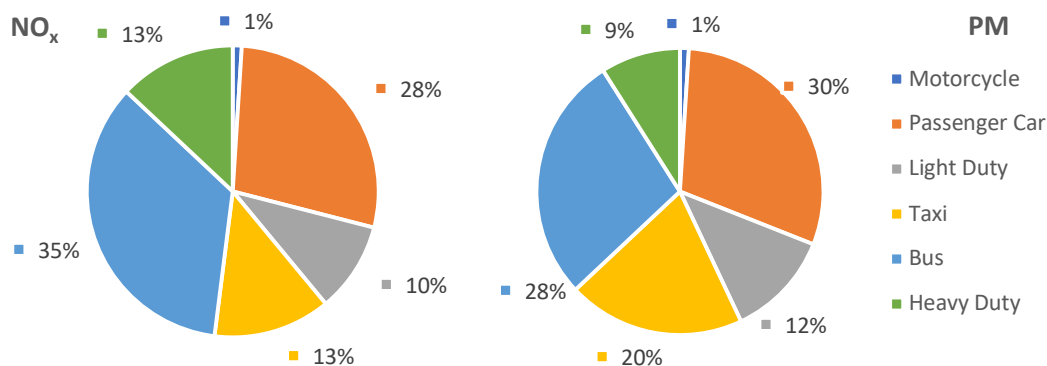


Figure 3.13: Distribution of NO_x and PM emission by type of vehicle in Av. da Liberdade in 2015 (adapted from Henriques, 2015).

Finally, the analysis by fuel and engine capacity for light passenger and light duty vehicles in Lisbon, 2015, is illustrated in Figure 3.14. Data is identical for Av. da Liberdade. Nearly half of light passenger vehicles use gasoline while the fuel majority consumed by light duty vehicles is diesel (77 %). 24 % of the gasoline passenger vehicles have engine capacity lesser than 1.4 L and 41 % of diesel cars have engine capacity lesser than 2.0 L. For light duty vehicles, 18 % of gasoline vehicles have engine capacity lesser than 2.0 L and, for diesel, this figure rises to 63 %.

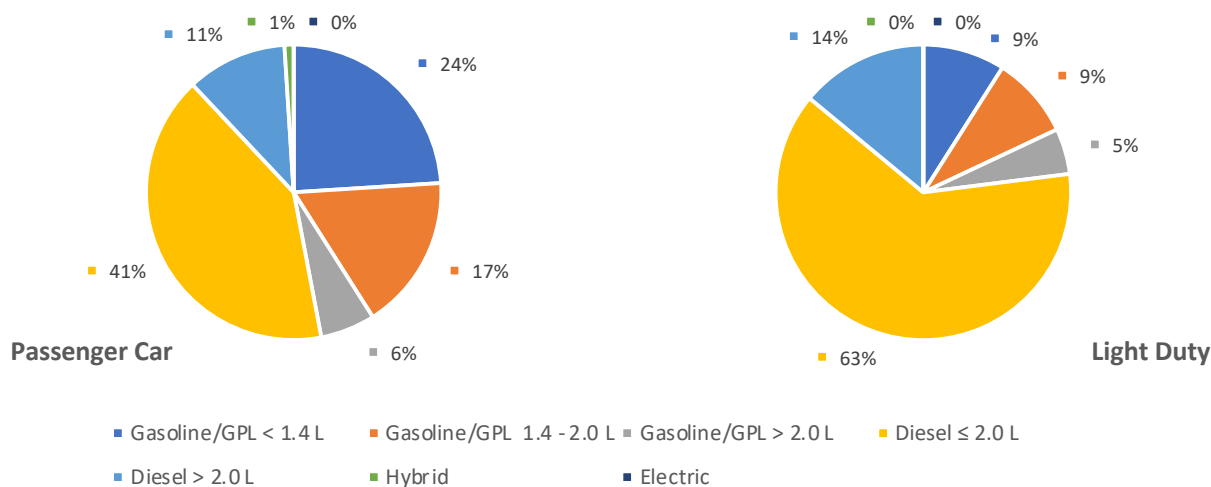


Figure 3.14: Distribution of light passenger and light duty vehicles by engine capacity (adapted from Henriques, 2015).

3.1.2 Lisbon Humberto Delgado Airport

Other emission source, far less addressed in previous studies, is the activity of the aviation sector. Up to the present, there are no detailed studies of the impact of Lisbon Humberto Delgado Airport (LA) on its surroundings, regarding particulate matter concentration, particularly UFP, and other atmospheric pollutants. This study intends to fill this gap, assessing the air traffic in LA activities effect on UFP concentrations, which

assumes special relevance due to LA's location: within the city centre, surrounded by residential, business, services and recreational areas, schools, sport complexes, hospitals and companies, among others.

The Lisbon Airport is the Portuguese larger and busiest airport, with an increasing number of passengers (100% between 2009 and 2017) and consequent increase in number of flights (Pordata 2018). According to the most recent data, in 2017, the LA registered approximately 183 000 flights and it is close to reach its full capacity (185 000 flights/year). Currently, LA has only one active runway. It is aligned approximately SSW-NNE. Once the predominant winds are from North, most of the landings and take-offs take place from South to North (runway 03). For South wind conditions, landings and take-offs use the same runway, but in opposite direction (runway 21). As shown in Figure 3.15, LA (dashed contour) is located within the city, surrounded by housing, commercial, offices and school complexes.



Figure 3.15: Representation of Lisbon Airport (dashed contour) on map (Maps source: <https://www.google.pt/maps>).

3.1.3 In-Land Passenger Ferries

There are several studies evaluating the effects of shipping-related UFP concentrations. However, in-land passenger ferries are also a pertinent emission source, far less addressed in those studies in the best of our knowledge. Nevertheless, the bottom-up approach used in the atmospheric emissions inventory for the Lisbon and Tagus Valley Region (FCT-NOVA, 2017), considering the four main ferry connections between Lisbon and Tagus South shore (Cacilhas, Barreio, Montijo and Seixal), point for relevant emissions

of PM₁₀ and PM_{2.5} in the year 2014 as presented in Table 3.2. These results stress the increased need for a detailed analysis and evaluation of the UFP emissions.

Table 3.2: Emissions of PM₁₀ and PM_{2.5} in 2014 regarding the four main ferry connections between Lisbon and South Tagus shore.

Connection	Cacilhas	Barreiro	Montijo	Seixal
PM _{2.5} [t/year]	1.0	7.2	2.2	2.0
PM ₁₀ [t/year]	1.0	7.7	2.3	2.1

Passenger ferries provide a fast and comfortable alternative to cars, buses and trains for crossing the Tagus river. Ferry services play a particularly important role in the Lisbon Metropolitan Area (LMA), connecting North and South shores in Tagus Estuary, the largest in Western Europe. Data from April 2018 (https://www.amt-autoridade.pt/media/1655/relatorio-final_ação-fiscalização_soflusa.pdf) indicates that in 2016, commuter ferries provided service to 16 million passengers, shuttling them between the nine ferry stations serving this network, shown in Figure 3.16. This service is provided by TTSL (Transtejo e Soflusa). The longest itinerary is between Montijo and Cais do Sodré (13.8 km), followed by Barreiro – Terreiro do Paço (9.3 km), Trafaria – Porto Brandão – Belém (9.3 km), Seixal - Cais do Sodré (8.5 km) and Cacilhas – Cais do Sodré (2.2 km).

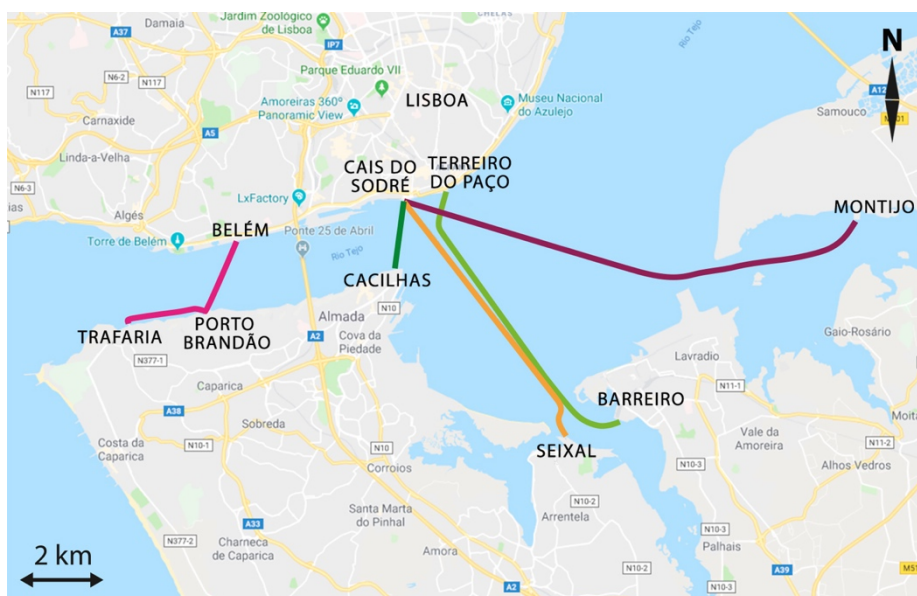


Figure 3.16: Map of the network of ferry stations connecting the northern and southern shores of Tagus River (Maps source: <https://www.google.pt/maps>, last accessed on December 2018).

Currently, the fleet is composed by 28 vessels: 18 catamarans, three ferries (catamaran) for passenger and cars, five passenger ferries (named “cacilheiros”) and two monohull (<https://tsl.pt/terminais-e-frota/frota/>). The power of the different vessels is presented in Figure 3.17. The hourly number of ferries

cruising in Tagus by week-day, Saturday and Sunday/Holiday is presented in Figure 3.18, and the annual average trips associated with the different connections is presented in Figure 3.19.

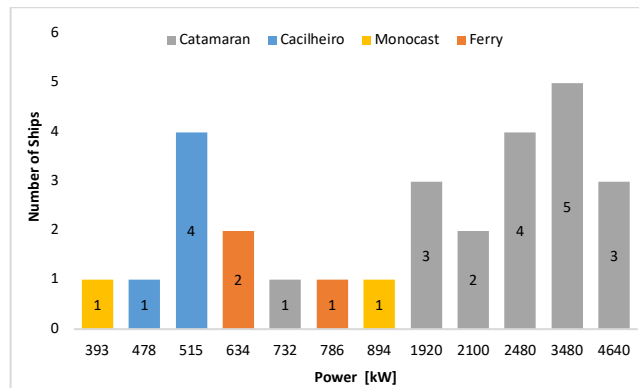


Figure 3.17: Power, in kW, by type of ferry of the fleet operating in Tagus River, in LMA.

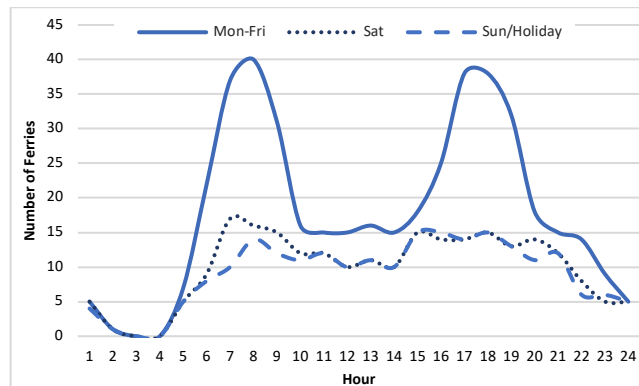


Figure 3.18: Hourly number of ferries cruising in Tagus, LMA, by week-day, Saturday and Sunday/Holiday.

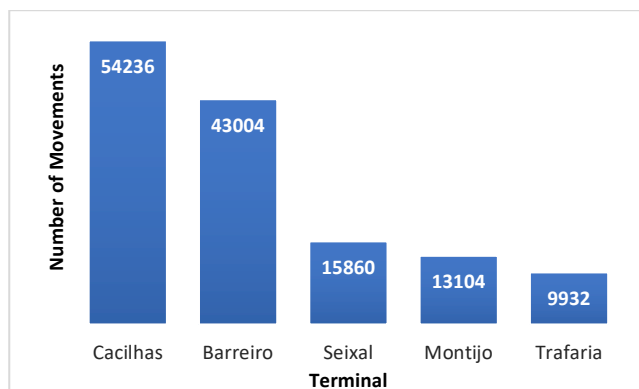


Figure 3.19: Annual average trips in 2018 associated with the different connections.

During weekdays, the number of ferries cruising the Tagus river rounds 40 ships during the morning and evening rush hours (8:00 h and 18:00 h, respectively), when most people uses this type of public transportation for commuting to work/school and back home. Nevertheless, even on weekends and holidays

the number of commutes is between 10 and 15 ships each hour. Only during the night period, from 0:00 h to 5:00 h, operations are less than five, or even null. Connections between Cacilhas – Lisbon and Barreiro – Lisbon are from far the most frequent.

3.2 SAMPLING EQUIPMENT

Aiming to assess the influence of road, aircraft and in-land passenger ferries traffic on urban and suburban air quality, particularly on UFP concentrations, three monitoring campaigns were designed accordingly to the emission source considered. Measurements were carried out with one portable particle number counter, P-TRAK®. Except for two sites related with the aircrafts monitoring campaign, where the equipment was installed in residences, all measurements were carried out in open-air environment, where the monitoring equipment was handled by an expert.

Ultrafine particles concentration is expressed as the number of particles by cubic centimetre (pt.cm^{-3}). UFP concentrations measurements were performed with the particle counter “*P-Trak® Ultrafine Particle Counter, 8525*”. As shown in Figure 3.20, P-track is a portable measuring device which detects and counts, each second, particles with less than $1\ \mu\text{m}$ diameter present in a cubic centimetre volume of air by an optical method. Consequently, the particle number counting (PNC) is expressed in pt.cm^{-3} . The particles captured in the inlet stream are mixed with alcohol vapour (isopropyl) allowing the microscopic particles in the air growth into larger droplets, easier to detect and count. This mixture passes through a condenser which promotes the condensation of the alcohol on the particle’s surface, forming a droplet with enough size to diffuse visible light. Then the droplets pass through a laser beam where a light detector counts the number of light flashes produced. Each flash corresponds to a particle. Before sampling, it is mandatory to verify that the counter is operating normally. For this purpose, it is used an HEPA zero filter (P-Trak®, 2013). This filter is attached to the counter and it should register zero in a few seconds. P-Trak® concentration range is 0 to $5 \times 10^5\ \text{pt.cm}^{-3}$ for particles range size 0.02 to $1\ \mu\text{m}$. Its sampling flow is $100\ \text{cm}^3.\text{min}^{-1}$ and operation temperature range is 0 to $38\ ^\circ\text{C}$ (Figure 3.20).



Figure 3.20: Particle number counter device, P-Trak®.

Table 3.3: P-Trak® technical characteristics (adapted from P Trak®, 2013).

Concentration range	0 to 5 x 10 ⁵ pt.cm ⁻³
Particle size range	0.02 to 1 µm
Operation temperature range	0 to 38 °C
Sample flow rate	100 cm ³ /min

Although P-Trak® measures particles less than 1 µm size, and UFP are defined as particles with a diameter less than 100 nm, interference will be minimal. Unlike mass concentrations, PNC consists mainly of particles smaller than 0.1 µm (Kumar *et al.*, 2011). Further details about the sampling equipment may be found in P Trak®, 2013.

Several studies in Europe have shown that air masses from the Northern Africa and/or the Mediterranean Sea transport particulates rich in Saharan dust (e.g. Querol *et al.*, 2009). During all the sampling periods, no episodes associated with air masses transporting dust from Sahara were registered.

3.3 ROAD TRAFFIC

Aiming to assess the influence of road traffic on urban air quality, specifically on UFP concentrations, similarly to what was done in other studies (Dos Santos-Juusela, 2013; Goel and Kumar, 2015; Grana *et al.*, Hudda *et al.*, 2014; 2017; Joerger and Pryor, 2018; Rahman *et al.*, 2017; Simon *et al.*, 2017; Van Popel *et al.*, 2012; Wang *et al.*, 2008), a monitoring campaign was designed by choosing sampling sites in three locations with distinct traffic modes. The three options have different traffic patterns (low/medium or high speed) and restrictions in vehicles circulation (Figure 3.21).

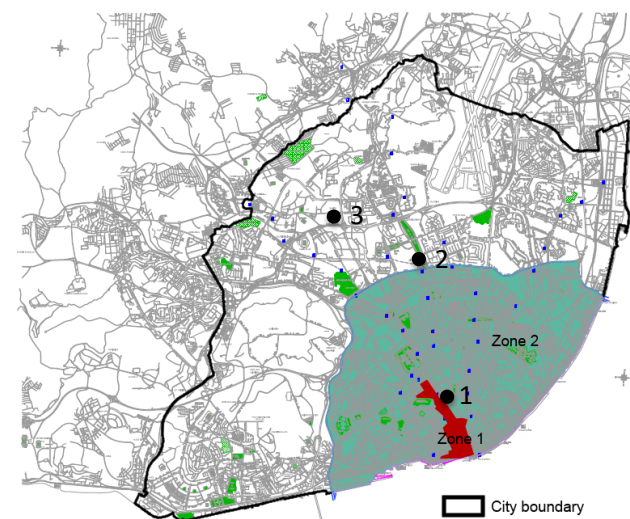


Figure 3.21: LEZ geographical extent and location of the three analysed sites (black dots) (adapted from Ferreira *et al.*, 2015).

Site 1, in Avenida da Liberdade, nearby the air quality monitoring station (AQMS), is considered a traffic hotspot in LEZ, zone 1. Site 2, in Entrecampos, is also considered a traffic hotspot, close to the boundary of LEZ, zone 2, but out of it, also close to an AQMS. The purpose of monitoring UFP close to AQMS was to establish eventual correlations between PNC and some pollutants monitored by the respective AQMS. Furthermore, we aimed to find differences in PNC between zones with and without road traffic circulation restrictions. Finally, site 3, close to a high-speed road, 2nd Circular, where UFP concentrations were measured in two different locations, Torres de Lisboa (site 3.1) and Escola Alemã (site 3.2). The sites locations are presented in Figure 3.22. Each sampling site was properly geo-referenced (Table 3.4).

Table 3.4: Geographic coordinates of traffic-related sites.

Site	Latitude	Longitude
Av. da Liberdade	38.720968	-9.146171
Entrecampos	38.748500	-9.148763
Escola Alemã	38.757659	-9.175148
Torres de Lisboa	38.757714	-9.163447

Av. da Liberdade, in downtown and Lisbon's historical centre, is characterized by intensive commercial and offices complexes, as well as cultural spaces, hotels and residences. Therefore, it is daily visited by thousands of people, mainly workers, service's clients and tourists. Entrecampos, close but out of the LEZ boundary, is characterized by the confluence of four major avenues (Avenida das Forças Armadas, Avenida da República, Avenida Estados Unidos da América e Campo Grande). Plus, it is an important transport commuting zone with offices complexes, residences and schools. Finally, 2nd Circular, subdivided in Torres de Lisboa and Escola Alemã, has no restrictions to vehicle's circulation. It is characterized by its proximity to a major high-speed road, surrounded by commercial and offices complexes, schools and residences.

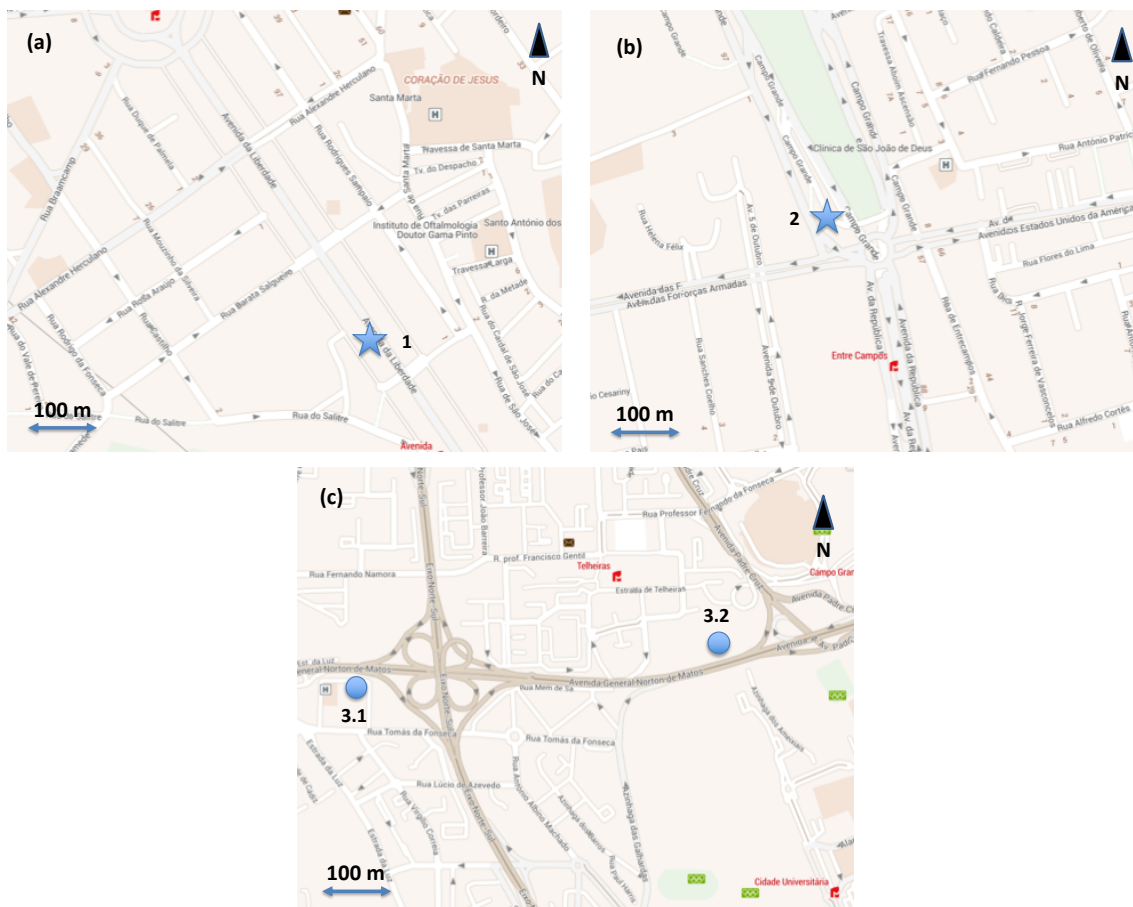


Figure 3.22: Representation of sampling sites. The star indicates the AQMS and sampling sites (a) Avenida da Liberdade, site 1; (b) Entrecampos, site 2 and (c) 2nd Circular, site 3, where dots indicate the two different locations (Torres de Lisboa and Escola Alemã, sites 3.1 and 3.2, respectively). (Maps source: <https://www.viamichelin.pt/web/Mapas-plantas>).

3.3.1 Monitoring Campaigns

Three campaigns were carried out starting in July 2017 covering two different seasons, different sampling periods and three different sampling sites, presented in Figure 3.22. The first UFP monitoring campaign was carried out in the Summer of 2017 (2-days monitoring period), the second in Spring of 2018 (4-days, March to May 2018), and the third in the Summer of 2018 (3-days, August 2018), accomplishing 38 hours of suitable measurements. More detailed information can be found in Table 4.1.

3.3.2 Meteorological Data

Meteorological conditions during sampling were collected from Portuguese Institute for Sea and Atmosphere (<http://www.ipma.pt/en/otempo/obs.superficie/>). The height of the Mixing Layer was compiled from the atmospheric soundings, at 12:00 UTC over Lisbon (<http://weather.uwyo.edu/upperair/sounding.html>), for the sampling period.

In sampling sites 1 and 2, data from the respective AQMS was also recorded (APA, 2018). Aiming to assess the number and type of vehicles, 10-minute counting's of vehicles during each sampling hour were taken, discriminating passenger cars, light-duty, buses and heavy-duty vehicles.

3.3.3 Data Analysis

Regarding road traffic, this study was performed with two main purposes: understand and, if possible, quantify how does PNC vary with different vehicles and traffic intensity, and establish probable correlations between PNC and pollutants measured by AQMS, when applicable. Meteorological parameters (wind intensity (v) and direction, temperature (T) and relative humidity (RH)) were obtained from IPMA Gago Coutinho weather station (<http://www.ipma.pt/en/otempo/obs.superficie/>, last accessed on May 2018). Atmospheric pollutants monitored by AQMS (PM₁₀, CO, NO, NO_x and NO₂) were obtained from the Regional Development and Coordination Commission of Lisbon and Tagus valley (CCDR-LVT), responsible for the air quality network, with 1-hour time resolution.

3.3.3.1 Avenida da Liberdade (site 1)

Due to the high pollutant levels already described, this site is the most relevant within this traffic-related study. For the campaign purposes, 15-minute time resolution for nitrogen oxides (NO_x), nitrogen monoxide (NO) and nitrogen dioxide (NO₂) were obtained from CCDR-LVT. Plus, real-time traffic counting is compiled and registered by the GERTRUDE system, property of Lisbon Municipality (CML), also with a 15-minute time resolution. GERTRUDE's data relative to four days in which we monitored PNC was obtained from CML. Unfortunately, the vehicles counting does not distinguish their typology, fuel nor age. For these reasons, GERTRUDE's data was not used in this work. The option was to count vehicles, 10 minutes in each direction, and extrapolate to an hour. Vehicles counted were subdivided in typology (passenger cars, taxis, buses and light-duty and heavy-duty vehicles). Linear regressions considering all sampled data in this site were performed using the Least Squares Method to access correlations between:

- i) 1-hour PNC averages and number of vehicles counted by type (passenger cars, taxis, buses, light-duty and heavy-duty vehicles) and fuel (gasoline, diesel, hybrid and electric);
- ii) 1-hour PNC averages and pollutants monitored by Avenida da Liberdade AQMS normalized with the background correspondent data measured in Olivais AQMS and
- iii) 15-minute PNC averages and nitrogen oxides monitored in Avenida da Liberdade AQMS. Regressions were performed with a 95% confidence level.

Traffic was also characterized according to its:

- i) typology (passenger cars (PC), light-duty vehicles (LD), heavy-duty vehicles (HD), buses (B) and taxis (T));
- ii) fuel (gasoline (G), diesel (D), hybrid (H) and electric (E)) and

- iii) Euro Standard.

The counting for Euro Standard characterization *in situ*, took place during two different periods (morning and afternoon) in two different sampling days (26th and 30th July), lasting for about 20 minutes each one. Vehicle typology was determined by direct observation and the vehicle age by observation of the license plate (in Portugal is mandatory that the license plate specify the year and month of construction of the vehicle's engine). Additionally, 1-minute averages were also performed and plotted. The highest PNC figures were crossed with on-site observed specific traffic occurrences such as type or age of vehicles observed.

3.3.3.2 Entrecampos (site 2)

As for Avenida da Liberdade, linear regressions considering all sampled data in this site were performed using the Least Squares Method to access correlations between:

- i) 1-hour PNC averages and traffic intensity and type according to our counting;
- ii) 1-hour PNC averages and pollutants monitored by Entrecampos AQMS.

3.3.3.3 2nd Circular (site 3)

The main purpose of the choice of this site was to comparison of its PNC levels with the ones in the other two sites under analysis, with completely different traffic characteristics. ANOVA tests were applied to compare PNC among the three sites subject to this study.

3.4 LISBON AIRPORT

Aiming to assess the area of influence of air traffic activities on urban and suburban air quality, a monitoring campaign was designed by choosing several sampling sites in the vicinity of LA and a set of sites further away of the LA, under the landing or take-off path (Figure 3.23). The unique characteristics of LA, within the city and surrounded by many intense traffic roads, makes it more difficult to individualize UFP from air traffic, especially regarding the take-off path due to inaccessible monitoring locations close to the runway northern end. Measurements were limited due to geographical conditions, access restrictions to LA boundary and vicinity, equipment performance and variable meteorological conditions. Moreover, other factors that might play a role, such as engine type (Masiol *et al.*, 2014; Ren *et al.*, 2016), were not evaluated.

As shown in Figure 3.15, LA (dashed contour) is located within the city, surrounded by housing, commercial, offices and school complexes. Sampling locations, indicated by numbers, are shown in Figure 3.23. The thin black arrow indicates the only runway and main direction of landing and take-offs; the dashed black line indicates the landing and take-off path and the thick blue arrow on top left, indicates de predominant wind direction (<https://pt.windfinder.com/windstatistics/lisboa>). Each sampling site was properly geo-referenced (Table 3.5).

Table 3.5: Geographic coordinates of each LA-related site.

Site	Latitude	Longitude	Site	Latitude	Longitude
1	38.757659	-9.175148	8	38.803900	-9.124213
2	38.757714	-9.163447	9	38.778427	-9.141877
3	38.763007	-9.142951	10	38.789856	-9.135275
4	38.762705	-9.142849	11	38.756015	-9.150279
5	38.763319	-9.141713	12	38.807932	-9.123248
6	38.76107	-9.147991	13	38.724627	-9.164347
7	38.761638	-9.146628	14	38.751846	-9.146484

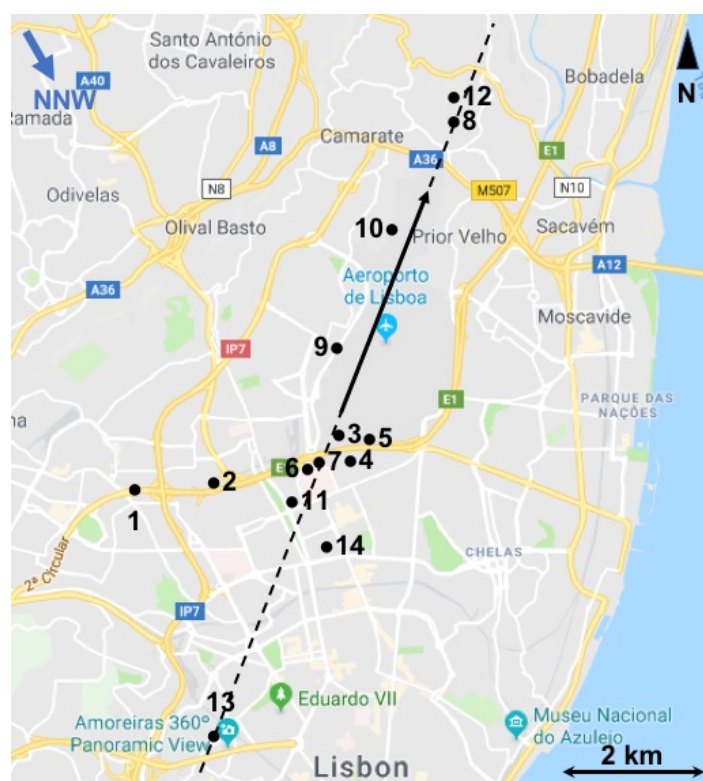


Figure 3.23: Representation of LA and sampling sites. The thin arrow indicates the main runway and direction of landings and take-offs, the dashed line shows the landing and take-off route, and the thick arrow, on top left, indicates the predominant wind direction. (Maps source: <https://www.google.pt/maps>).

The locations close to the airport allow an assessment of the effect of all operations at the airport (landings, take-offs, movement of aircrafts and other vehicles within facilities); the most remote locations are intended to assess the effect of the aircraft approaching or after the take-off. Locations 1 and 2, close to a major road (as sampling sites 3 to 5) but more distant to the airport and out of the predominant wind range, indicate the UFP concentrations expected out of the airport activities influence.

3.4.1 Monitoring Campaigns

Three campaigns were carried between July 2017 and May 2018, covering three different seasons and different sampling periods (Table 4.5):

The first UFP monitoring campaign was carried out in the summer (4-days monitoring period, in July 2017), the second in the fall (11-days, from October to December 2017) and the third in the spring (4-days, from March to May 2018), complying approximately 75 hours of suitable measurements.

When located next to intense traffic roads, the sampling periods were chosen in order to minimize the road traffic influence (weekends and holidays, or dawn). Except for sites 13 and 14, measurements were carried out on the street, where the monitoring equipment was handled by an expert. In sites 13 and 14 (residences) the monitoring equipment was left on a balcony.

All take-offs and landings during the sampling periods were identified on Flightradar24 (<https://www.flightradar24.com/data/airports/lis/>), as well as the model and age of the aircraft and destination distance type (short/medium or long-haul).

3.4.2 Meteorological Data

The meteorological conditions during sampling were collected from Portuguese Institute for Sea and Atmosphere. (<http://www.ipma.pt/en/otempo/obs.superficie/>). The height of the Mixing Layer (ML) was also compiled from atmospheric soundings, at 12:00 UTC over Lisbon, (<http://weather.uwyo.edu/upperair/sounding.html>) for the sampling period. Wind data was obtained from IPMA weather station with a 10-minutes time resolution.

3.4.3 Data Analysis

The sampling dates were chosen based on wind intensity and direction daily forecast, in order to be downwind (or close to downwind) to the airport and/or aircraft plume during each sampling collection. Furthermore, during sampling, wind speed and direction were permanently checked, both on-site and on IPMA's website. Whenever the wind conditions were not satisfactory, the sampling was cancelled. So, regardless the site, measurements were not ever done upwind which allows for a more robust analysis. Once wind direction is highly variable, and similarly to what was done by Hudda *et al.* (2016), for each site, PNC *versus* 10° wind direction ranges were plotted to find the wind direction responsible for the highest concentrations. These wind directions were called “impact wind direction” (IWD).

Linear regressions considering all sampled data, aggregated regardless of the location of the monitoring site, were performed using the Least Squares Method to access correlations between 10-minute PNC averages and (i) number of flights, (ii) meteorological parameters, namely (1) wind speed and (2) mixing layer height. In regression between number of flights and PNC, a 10-minutes time period was considered for

both variables. During that period, both the maximum number of landings and take-offs were six, whereas the maximum number of flights (landings plus take-offs) was ten. PNC averages during all 10-minutes periods were calculated per each number of flights, from zero to ten. Finally, we plotted these data and correlations between the number of flights and PNC were calculated with a 95% confidence level. Single factor ANOVA was performed among all sites and among sites with similar characteristics with a 95% confidence level.

This approach can easily be applied to other airports.

3.5 IN-LAND PASSENGER FERRIES

Aiming to assess the influence of river passenger ships on urban and suburban air quality, particularly on UFP concentrations, a monitoring campaign was designed by choosing sampling sites in the vicinity of the ferry terminals. The strong influence of emissions from road traffic, as well as the intense ferries traffic, created a challenging monitoring environment. Furthermore, measurements were limited due to geographical conditions, access restrictions to ferries stations and vicinity, equipment performance, and variable meteorological conditions.

3.5.1 Monitoring Campaigns

Measurements took place in non-consecutive 19 periods, reaching a total of approximately 45 hours of suitable measurements. Details of the sampling periods can be found in Table 4.10. Considering the goal of measuring the plume emitted by ferries at the Lisbon ferry stations (Cais do Sodré and Terreiro do Paço, (Figure 3.16), it would be mandatory winds from a southern direction. We must stress that those synoptic situations are relatively scarce in Lisbon, where predominant winds are from the northern direction. In addition, both stations are overmuch close to intense traffic roads and the frequency of number of arrivals and departures, sometimes continuous, would difficult the association between a ferry operation and its effect on UFP concentration. Furthermore, most of the available surrounding areas are public restricted. The combination of these factors disengaged any reliable measurements in Lisbon. Therefore, only the stations in Tagus southern shore were selected, namely Cacilhas, Barreiro, Seixal and Montijo. The southern stations allowed measurements from the plumes emitted by the majority of TTSL ships currently cruising the Tagus river. Also, especially for Barreiro and Cacilhas, they register high number of ferry operations and, exception for Cacilhas, they are relatively away from other UFP sources. Additionally, the location of Seixal ferry allows to assess the area of influence of ferry's path from/to Barreiro within the urban and sub-urban areas, therefore enabling the evaluation on ferry cruising on urban air quality, along the navigation path.

Details about the location of each sampling site can be seen in Figure 3.24. Continuous lines indicate the ferry paths, shadowed triangles represent the manoeuvring and hoteling area, arrows designate the wind direction which allow the ferry plume measurement during cruising on the sampling site (dot). Both Montijo and Seixal

ferry stations are located in areas relatively far away from residential areas. Barreiro is located closer to residential areas and Cacilhas is located close to restaurants and residential areas.

Aiming to maximize measurements under downwind conditions, sampling site dates were chosen according to the available meteorological forecast. Measurements were carried out on the street with one particle counter equipment. The monitoring equipment was handled by an expert. Each sampling site was properly geo-referenced (Table 3.6).

Table 3.6: Geographic coordinates of each ferry-related site.

Site	Latitude	Longitude
Barreiro	38.651139	-9.077778
Cacilhas	38.688012	-9.148781
Montijo	38.699612	-9.005861
Seixal	38.647605	-9.095500

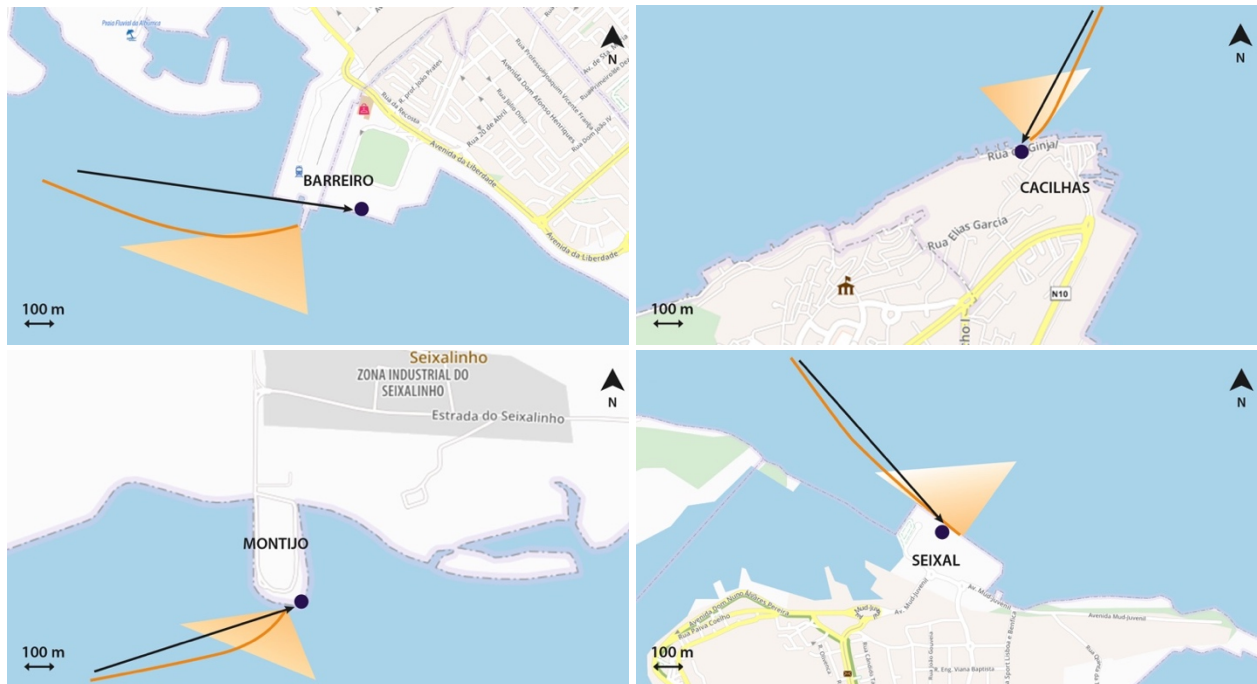


Figure 3.24: Location of the ferry-related sampling sites (dots). Arrows indicate the downwind directions to cruising paths; Shadow triangles indicate the manoeuvring area; continuous lines indicate the ferry path. Top left – Cacilhas; top right – Barreiro; bottom left – Montijo and bottom right – Seixal. (Maps source: <https://www.viamichelin.pt/web/Mapas-plantas#>, last accessed on December 2018).

The height of the Mixing Layer (ML) was compiled from the atmospheric soundings, at 12:00 UTC over Lisbon (<http://weather.uwyo.edu/upperair/sounding.html>) for the sampling periods. All departures and arrivals

during the sampling periods were checked on sight. The ferry model, technical characteristics and age were obtained from the TTSL site (<https://tsl.pt/terminais-e-frota/frota/>). Meteorological parameters (temperature, wind intensity and direction, relative humidity) were also recorded with a portable meteorological station model WatchDog 2700. Its technical characteristics are resumed in Table 3.7.

Table 3.7: Technical characteristics of the portable meteorological station WatchDog 2700.

Parameter	Range	Accuracy
Temperature	-40 °C to 125 °C	±0.3 °C at -40 °C to 90 °C
Relative Humidity	10 % to 100 %, at 5 °C to 50 °C	±3% at 20% to 100% and 25 °C
Wind Speed	0.1 to 322 km.h ⁻¹	±3 km.h ⁻¹
Wind Direction	0° to 330°, resolution 1°	±3°

Currently, from the 28 operational ferries, only 15 were identified during sampling periods. Technical data of the identified ferries are presented in Table 3.8. The exhausting system in catamarans is close to water level while in all other ships are located at the top, emitting the exhaust plume of the ferry directly into ambient air. All ferries have engines classified as Diesel/High Speed.

3.5.2 Data Analysis

Due to synoptic and geographical constrains, similarly to what was done in airport-related monitoring, measurements were mostly done downwind, allowing for a more robust analysis.

Averages of PNC were plotted considering the temporal window from 1-minute before and after arrivals/departures. Linear regressions considering site by site data were performed using the Least Squares Method to access correlations between 1-minute PNC averages and meteorological parameters, namely temperature, relative humidity, wind speed and mixing layer height. Aiming to access correlation between PNC and ferry operations, linear regressions between 1-hour PNC averages and number of ferry operations during that period were also performed. Regression was made with a 95% confidence level. Furthermore, ANOVA analysis between periods with and without ferry operations was also performed, also with 95% confidence level. Associations between PNC and different classes of ferries were also evaluated.

Table 3.8: Technical data of the ships identified during sampling periods (<https://ttsl.pt/terminais-e-frota/frota/>)

Ferry	Class	Length [m]	Entry into Service	Engine	Power [kW]	Service Speed [knot]	Propulsion
Cacilhas ↔ Cais do Sodré ⁽¹⁾							
Campolide							
Dafundo	<i>Cacilheiro</i>	29.20	1980-1982	mtu8V 396 TC	515	10	Propellers Variable Pitch
Sintrense							
S. Jorge	Monohull	49.94	1992	mtu 12 V183 TE62	478	13	Propellers of Step fixed
Barreiro ↔ Terreiro do Paço (catamaran)							
Antero de Quental							
Damião de Goes							
Fernando Namora	Damen	49.20	2003	mtu 16V4000M70	3480	22	2 Hamilton water jets
Fernando Pessoa							
Gil Vicente							
Miguel Torga							
Montijo ↔ Cais do Sodré (catamaran)							
Castelo	Transcat	45	1995	MWM TBD 616 V16	1920	22	2 water jets Lips
Aroeira	Transcat	46.25	1998	mtu 12V 396	2480	22	2 water jets Lips
Seixal ↔ Cais do Sodré (catamaran)							
Aroeira	Transcat	46.25	1998	mtu 12V 396	2480	22	2 water jets Lips
S. Julião							
Algés	Transcat	45	1995	MWM TBD 616 V16	1920	22	2 water jets Lips
Pedro Nunes	Austral	37.4	2002	mtu 12V2000M70	2100	22	2 water jets Hamilton

⁽¹⁾ During rush hours the fleet may be complemented by catamarans, class Transcat, 2480 kW.

4 RESULTS AND DISCUSSION

4.1 ROAD TRAFFIC

As mentioned in chapter 3, the three sites where PNC were measured present distinct traffic characteristics. The site with most interest is Avenida da Liberdade, not only because of its localization, in Lisbon downtown, but also because it is located in LEZ1, where the most strictly restrictions to vehicles circulation are applied. The main purpose of the two other sites, Entrecampos and 2nd Circular, close to LEZ boundary and far from it, respectively, is to perform a comparison of PNC levels.

The measurements taken at each sampling site (minimum, average and maximum PNC), the respective average meteorological parameters (mixing layer height (ML), wind intensity (v), temperature (T) and relative humidity (RH)) are summarized in Table 4.1. PNC obtained results, summarized by location, PNC average, mode and standard deviation are presented in Table 4.2.

Table 4.1: Sampling dates and periods for each road traffic-related site and the corresponding height of the mixing layer (ML), wind speed (v) and direction, temperature (T), relative humidity (RH) and measured minimum (Min), mean, mode, and maximum (Max) PNC values.

Site	Date	Period	ML	Wind		T	RH	PNC [pt.cm ⁻³] x 10 ³			
		[Time UTC]	[m]	v [km.h ⁻¹]	Direction	[°C]	[%]	Min	Mean	Mode	Max
Torres de Lisboa	11/07/17	14:49 – 19:04	617	6	NNW	28	29	3.0	14.1	10.2	233
Escola Alemã	13/07/17	13:29 – 17:49	400	6	NNW	33	32	1.4	15.9	15.6	277
Av. da Liberdade	28/03/18	14:06 – 18:03	936	15	NW	15	64	1.7	12.3	10.6	164
	05/04/18	08:40 – 12:39	919	7	E	15	70	13.8	28.5	24.6	278
	19/04/18	09:13 – 11:19	182	14	NE	15	60	7.3	21.7	12.0	145
	26/04/18	08:46 – 12:48	580	13	NW	19	65	7.6	21.0	12.0	138
	11/05/17	15:54 – 10:05	899	16	NW	17	63	3.1	10.4	11.4	11.4
	26/07/18	14:57 – 17:49	976	20	NW	25	52	4.0	20.8	15.8	235
	30/07/18	08:48 – 11:25	842	12	NW	23	62	2.6	13.0	10.1	421
Entrecampos	01/08/18	15:46 – 17:46	660	15	NW	31	45	5.4	11.9	10.2	68.9
	10/08/18	08:24 – 11:00	574	15	N	24	48	4.1	11.0	10.3	87.0
	14/08/18	09:11 – 12:02	846	9	NE	25	62	2.6	7.8	10.2	106

Table 4.2: Obtained average, mode and standard deviation (SD) of PNC on traffic-related sites, in $\text{pt.cm}^{-3} \times 10^3$.

Site	Average	Mode	SD
Torres de Lisboa	15.9	15.6	13.9
Escola Alemã	14.1	10.2	10.2
2 nd Circular ⁽¹⁾	15.0	11.8	12.2
Av. da Liberdade	18.2	11.4	13.2
Entrecampos	10.3	10.2	5.1

⁽¹⁾ It combines Torres de Lisboa and Escola Alemã.

4.1.1 Overall Statistical Analysis

As it can be observed in Figure 4.1, the highest 1-minute PNC means and dispersion were obtained in Av. da Liberdade, and the lowest were obtained in Entrecampos. In boxplot graphics, boxes delineate median, upper and lower quartiles, with the whiskers extending up from the top of the box to the largest data element that is less than or equal to 1.5 times the interquartile range (IQR) and down from the bottom of the box to the smallest data element that is larger than 1.5 times the IQR. Dots represent outliers, i.e. values beyond the ends of the whiskers. Although the most frequent values presented no significant differences among the three sites, dispersion is much higher in Av. da Liberdade, which leads to mean PNC values almost twice higher than on Entrecampos (18.2×10^3 and $10.3 \times 10^3 \text{ pt.cm}^{-3}$, respectively). This fact highlights that, in spite of all efforts made to reduce traffic-related air pollution in Av. da Liberdade, air pollution remains an issue. Even when compared to 2nd Circular (Escola Alemã and Torres de Lisboa), a very busy high-speed road with no circulation restrictions, Av. da Liberdade presents higher PNC values. Regarding mode values, Entrecampos and Escola Alemã presented the lowest values, followed by Av. da Liberdade and Torres de Lisboa (10.2 , 11.4 and $15.6 \times 10^3 \text{ pt.cm}^{-3}$, respectively). In fact, although its mean value is higher, mode value in Av. da Liberdade is considerably lower, when compared to the value obtained in Torres de Lisboa. This result indicates that peak values are more frequent and higher in Av. da Liberdade than in 2nd Circular, as it can be observed in Figure 4.1.

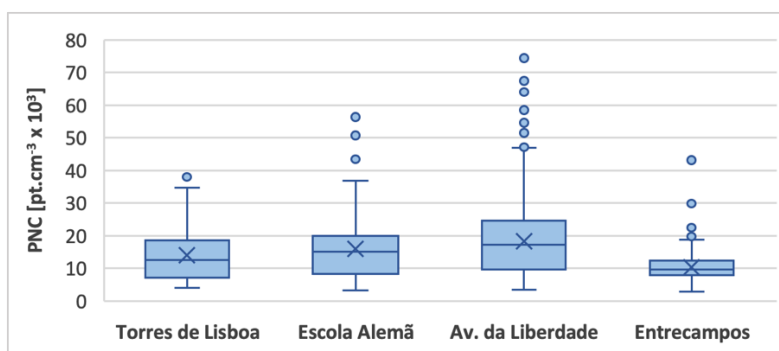


Figure 4.1: Boxplot of 1-minute PNC mean distribution by traffic site. (1st quartile, average (x), median (-), 3rd quartile and outliers (dots)).

Single factor ANOVA among sites presented is presented in Table 4.3. The obtained results clearly show statistically significant differences in the means among the sites (p-value much lower than 0.01). This result shows that at least one site presents a different mean value. When applied between two sites, covering the six possible combinations, ANOVA outputs indicate that means remain statistically different (p-values much lesser than 0.01). These results show that PNC levels are different among sites with different traffic characteristics.

Table 4.3: Single factor ANOVA for PNC sampled values among the four traffic sites

Source of Variation	SS	df	MS	F	P-value	F crit
Between Sites	1,45E+12	3	4,84E+11	3534.356	0	2.60
Within Sites	1.89E+13	137 950	136 947 684			
Total	2.03E+13	137 953				

4.1.2 Traffic Characterization and PNC Levels

4.1.2.1 Avenida da Liberdade

The traffic characterization *in situ*, took place during two different periods (morning and afternoon) in two different sampling days (26th and 30th July), lasting for about 20 minutes each one. The results by type of vehicle are presented in Figure 4.2. The majority (83 %) of vehicles in this avenue are passenger transport related. Among these, light passenger cars account for 50 % disaggregated by type of fuel in 29 % gasoline powered, 19 % diesel and 2 % hybrid or electric. Taxis account for 26 %, and buses 7 %. The remaining 17 % are duty vehicles, of which, 4 % are heavy-duty. The analysis by Euro Standard and type of vehicle is presented in Figure 4.3.

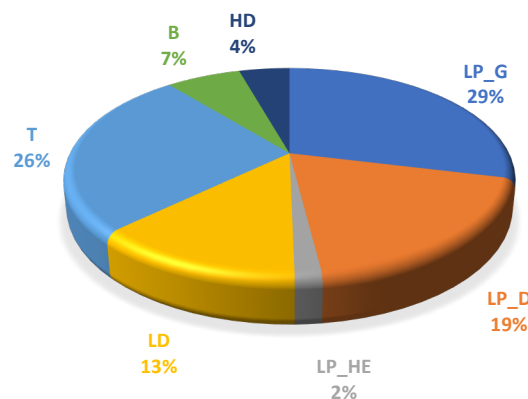


Figure 4.2: Traffic characterization by type of vehicle in Av. da Liberdade over two periods during sampling. (PC – passenger cars; LD – light-duty vehicles; T – taxis; B – buses; HD – heavy-duty vehicles; G – gasoline; D – diesel; HE – hybrid or electric).

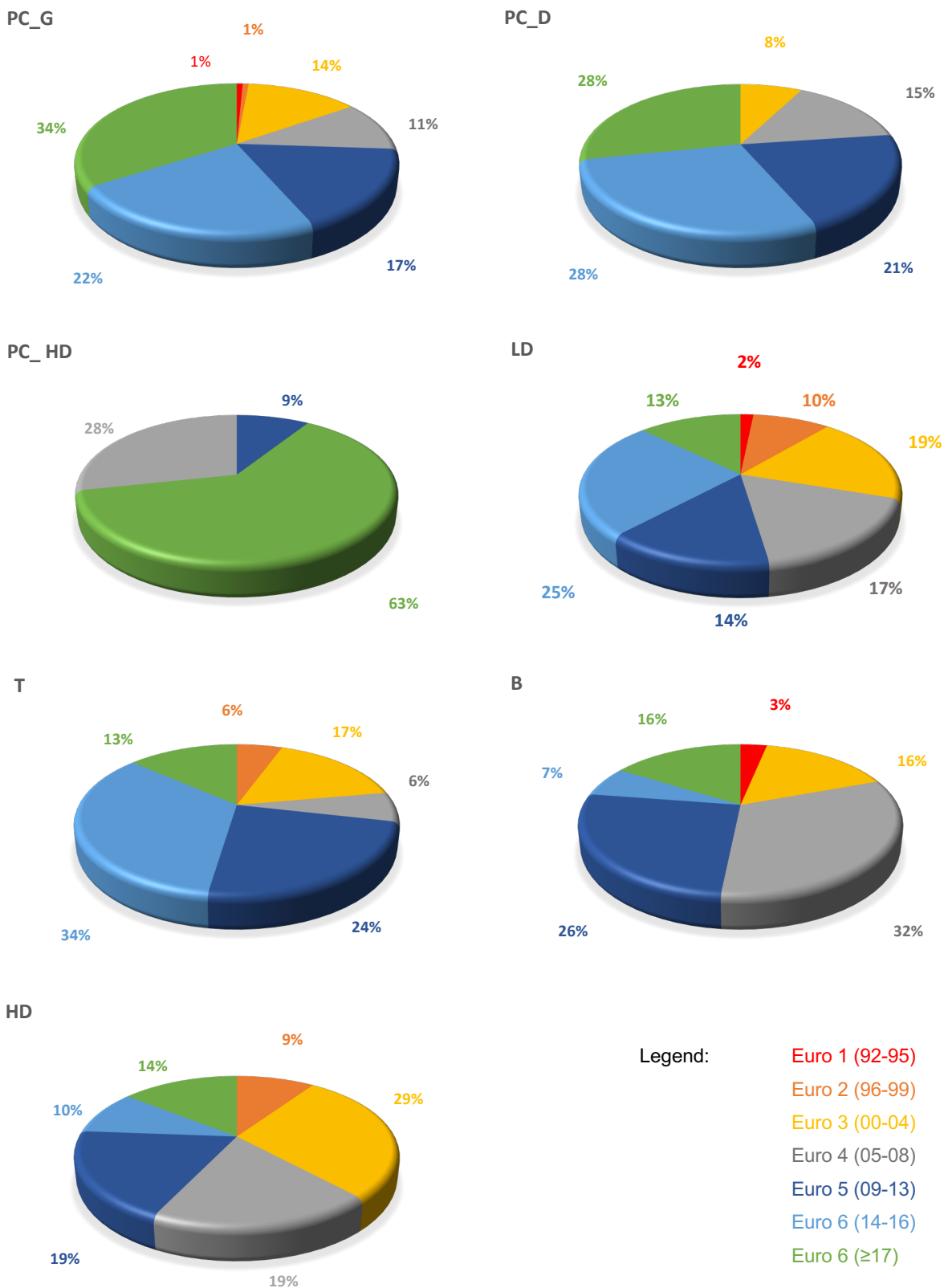


Figure 4.3: Traffic characterization by Euro Standard and type of vehicle. (PC – passenger cars; LD – light-duty vehicles; T – taxis; B – buses; HD – heavy-duty vehicles; G – gasoline; D – diesel; HE – hybrid or electric) in Av. da Liberdade.

The majority of vehicles circulating in Av. da Liberdade comply with the applied Euro restrictions to this location. However, there are still a reduced number of vehicles which do not meet the imposed restrictions, namely:

- Passenger cars, gasoline powered (PC-G) – 2 %
- Taxis (T) – 6 %
- Buses (B) – 3 %
- Light-Duty (LD) – 12 %
- Heavy-Duty (HD) – 9 %

Globally, 4 % of vehicles in circulation in this avenue do not meet the required Euro 3 Standard is still significant. Also, it is expected that PNC are higher when some of these vehicles passes close to the sampling site. In fact, as shown in Figure 4.4, the majority of 1-minute PNC peaks are associated with the event of an older vehicle, prior to 2000, mostly buses, taxis and light-duty. This result is in accordance to recent findings reported by Luengo-Oroz and Reis (2019) and Qiu *et al.* (2019). In this figure, the black arrow represents a period when a “leaf blower” device was functioning nearby the sampling spot. Due to the unusually high values, not caused from traffic-related, measurements during this period were discarded from the analysis.

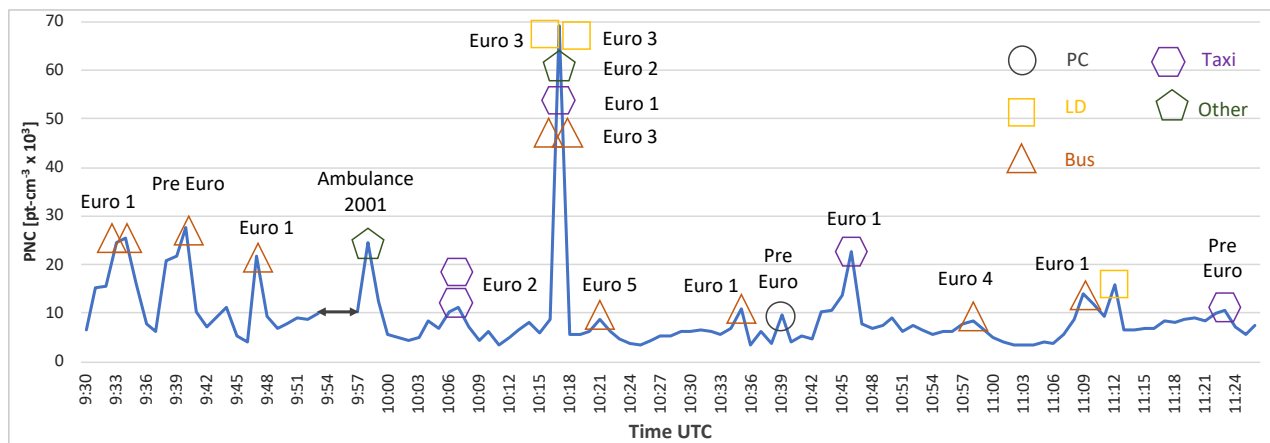


Figure 4.4: Association between 1-minute PNC peaks and specific observed vehicles in Av. da Liberdade. The black arrow denotes a period where measurements were discarded due to another source of contamination.

Unlike other studies (e.g. Qiu *et al.*, 2019), the constant and intensive traffic in this avenue, with many stops due to traffic lights, consequent breakings, accelerations and congestions, and the dependence of PNC from specific traffic events, correlations between the number of vehicles and PNC could not be established. Still, as it can be seen in Figure 4.5, 1-hour PNC mean closely follow the number of buses and light-duty vehicles. This fact suggests that these two diesel powered types of vehicles govern the UFP concentration in this avenue. This fact is in accordance with several studies (e.g. Knibbs *et al.*, 2011; Luengo-Oroz and Reis, 2019; Qiu *et al.*, 2019).

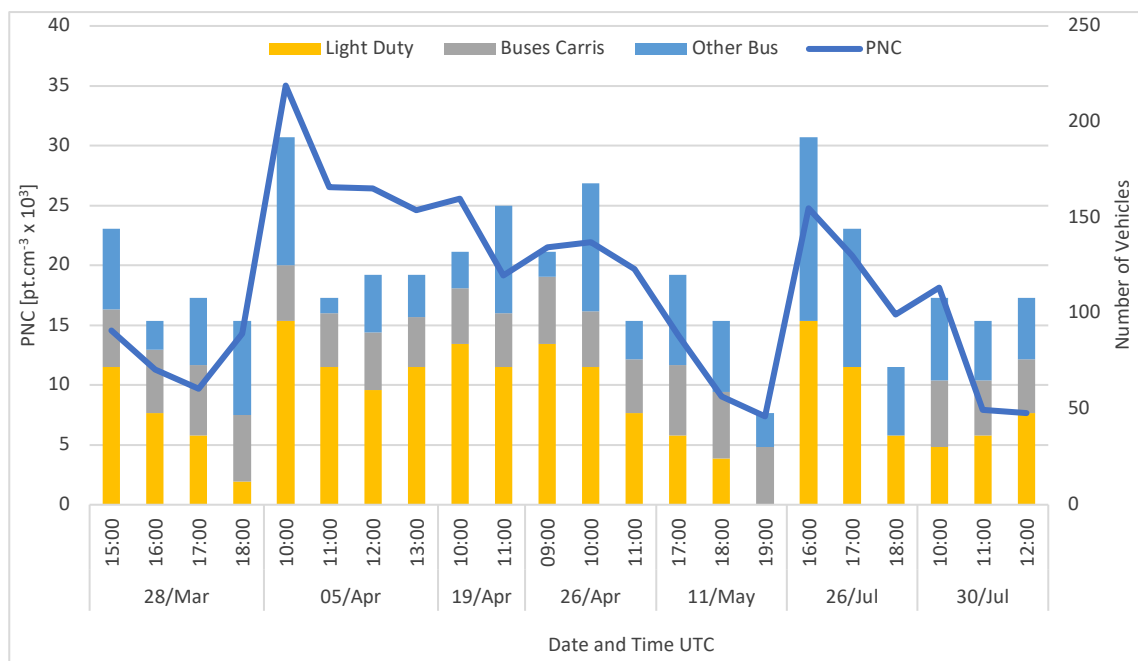


Figure 4.5: 1-hour means of PNC vs. buses and light-duty vehicles, in Av. da Liberdade

4.1.2.2 Entrecampos

In Entrecampos, the traffic characteristics are quite different from the ones in Av. da Liberdade. Although traffic is also intense, it flows much easier and with lesser traffic congestions. In spite of the reduced sampling hours, it was found a positive strong correlation statistically significant was found between 1-hour PNC means and the number of vehicles during that period ($r = 0.73$, $p = 0.04$), as shown in Figure 4.6. This result is in accordance with other studies findings (e.g. Qiu *et al.*, 2019). However, given the reduced sampling hours and consequent lack of vehicles counting between 2540 and 3240, one should be careful with the fact that the slope is determined by two points.

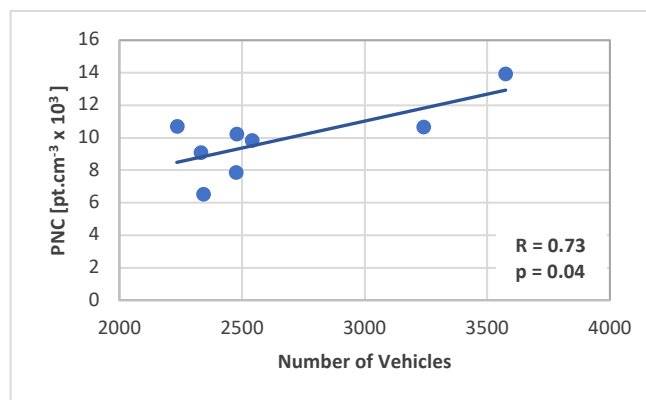


Figure 4.6: Statistical outputs for regression analysis with 95% confidence level between PNC 1-hour averages and the number of vehicles, in Entrecampos.

As mentioned before, there are no traffic restrictions in this site. Still, similarly to what was done in Av. da Liberdade, peaks of 1-minute PNC means were associated to particular observed traffic events as shown in Figure 4.7. Unequivocal identification of Euro Standard was not always possible, but most PNC peaks are associated with heavy and light-duty vehicles, buses and older passenger cars.

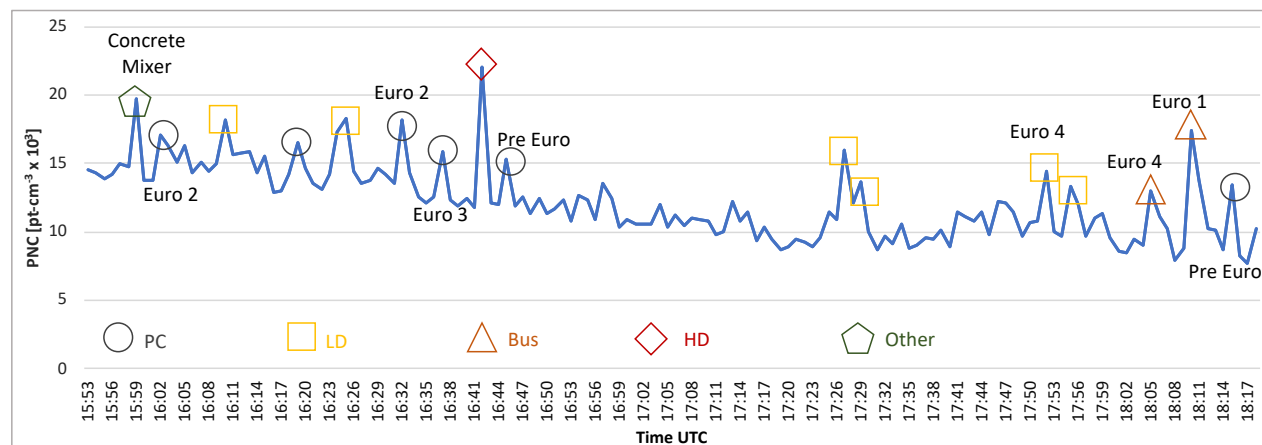


Figure 4.7: Association between 1-minute means of PNC peaks and specific observed vehicles in Entrecampos.

4.1.3 Correlation between PNC and other atmospheric pollutants

4.1.3.1 Avenida da Liberdade

As it can be seen in Figure 4.8, results show statistically significant strong positive correlation between hourly mean values of PNC and PM_{10} ($r = 0.76$, $p < 0.01$) and moderate positive correlation between PNC and nitrogen oxides (r coefficients of 0.55, 0.51 and 0.59, with all p -values lower than 0.01, for NO , NO_2 : and NO_x , respectively). Similarly to other studies (e.g. Zhang *et al.*, 2017), it was not found a correlation with CO . These results are in accordance to previous findings (e.g. Hagler *et al.* 2012; Sardar *et al.*, 2005; Wang *et al.*, 2008; Zhu *et al.*, 2002a,b). Most authors (e.g. Wolf *et al.*, 2017 and Eeftens *et al.*, 2015) found higher correlations between PNC and nitrogen oxides than between PNC and PM. Stafoggia *et al.* (2017b), found moderate correlations between PNC and other pollutants, also higher for NO_2 . On the other hand, Talbi *et al.* (2018) found strong positive correlations between PM_{10} - $PM_{2.5}$, PM_{10} - PM_1 , and $PM_{2.5}$ - PM_1 at the roadside (0.85, 0.81 and 0.88, respectively). Contrarily, some studies also observed negative correlations of PM_{10} with size fractions below 50 nm (e.g. Leitte *et al.* 2012). However, it should be stressed that the time lag in these studies was much greater (annual averages) than in our case: our results concern 15-minutes and 1-hour means for nitrogen oxides and PM, respectively. This fact might explain the discrepancies of our results.

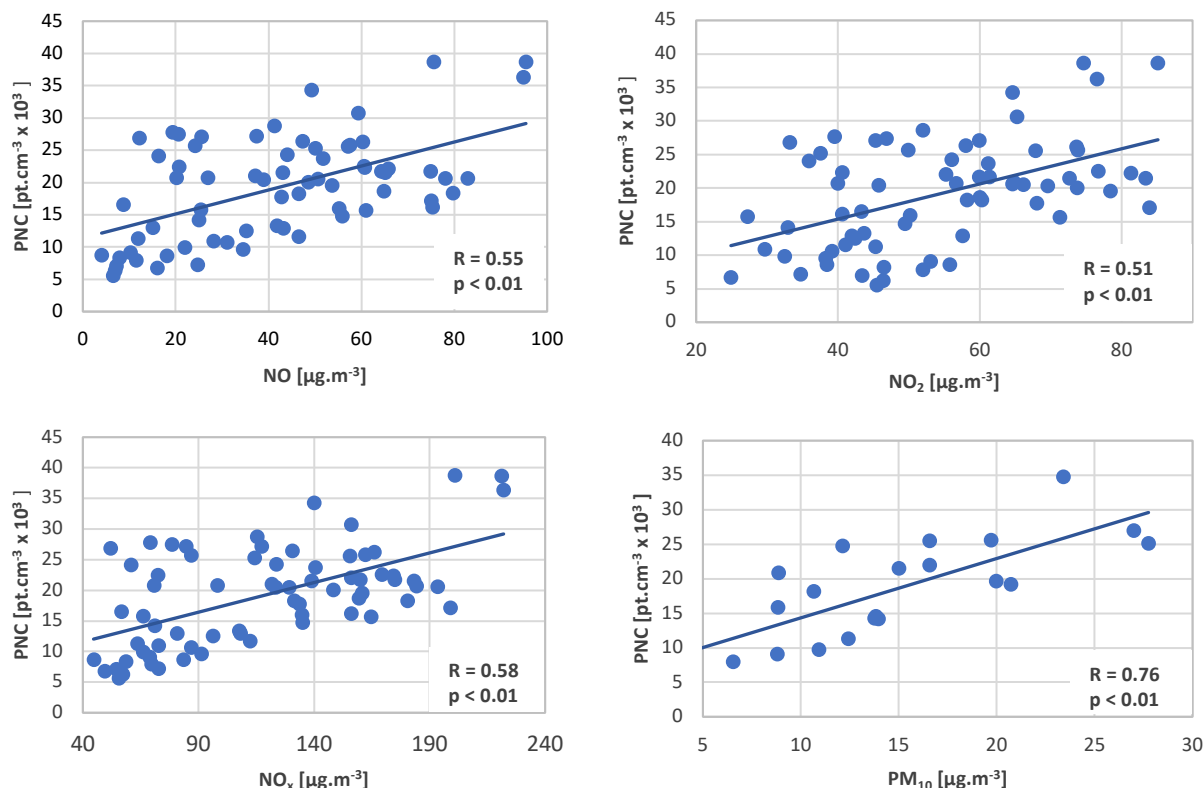


Figure 4.8: Statistical outputs for regression analysis with 95% confidence level between PNC 15-minutes averages and air pollutants (NO, NO₂, NO_x and PM₁₀) monitored in AQMS of Av. da Liberdade. Regression for nitrogen oxides was done with PNC 15-minutes averages and with 1-hour averages for PM₁₀.

4.1.3.2 Entrecampos

In this site, results of regression analysis were only statistically significant between PNC and PM₁₀ ($r = 0.76$, $p = 0.03$), as it can be seen in Figure 4.9. The Pearson coefficient was equal to the one obtained in Av. da Liberdade. However, in Entrecampos, due to the reduced sampling hours and the lack of PM₁₀ concentrations between 11 and 25 μg.m⁻³, the slope is determined by two clusters and one should be careful with this correlation coefficient. Results with other pollutants monitored at the AQMS of Entrecampos (PM_{2.5}, NO₂ and CO) were not statistically significant. The absence of correlation between PNC and PM_{2.5} is in accordance with previous findings (e.g. De Jesus *et al.*, 2019). The authors claim that PNC and PM_{2.5} are not representative of each other.

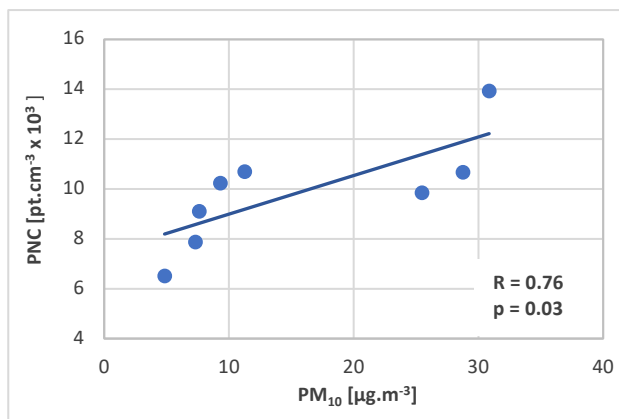


Figure 4.9: Statistical outputs for regression analysis with 95% confidence level between PNC 1-hour averages and PM₁₀ monitored in AQMS of Entrecampos.

4.1.4 Correlation between PNC and meteorological parameters

Unlike other studies (e.g. Onat *et al.*, 2019), we did not find correlations between PNC and meteorological parameters such as temperature and relative humidity. As mentioned before, the meteorological parameters were obtained with 1-hour resolution from IPMA Gago Coutinho weather station (<http://www.ipma.pt/en/otempo/obs.superficie/>), located 2.7 km in a straight line, NNE to the sampling site in a non-urbanized area, which might explain the lack of correlation. Regarding wind, in accordance with previous studies (e.g. Onat *et al.*, 2019), a moderate negative correlation ($r = -0.48$, $p = 0.03$) was obtained in Av. da Liberdade (Figure 4.10). In Entrecampos (Figure 4.11), the correlation between PNC and wind speed was positive and moderate ($r = 0.74$, $p = 0.04$). Though, once again due to the reduced sampling hours, this result must be taken with caution. Entrecampos sampling site is located approximately 2 km South to runway 03. Therefore, the plumes emitted by aircrafts when they are approaching to land can be transported to sampling site, under winds from NNW to NNE, which might explain the obtained positive correlation. For aircraft (buoyant) plumes, higher wind speeds promote faster ground arrival, counterbalancing the dispersion (Hudda *et al.*, 2018). Therefore, under these conditions (higher wind speeds and downwind to the aircraft plume), aircraft emissions are supposed to have a widespread impact on the affected area (Simon *et al.*, 2017). Still, once again, one should be careful with the fact that the slope is determined by two clusters, given the lack of wind speed between 10 and 15 km.h⁻¹.

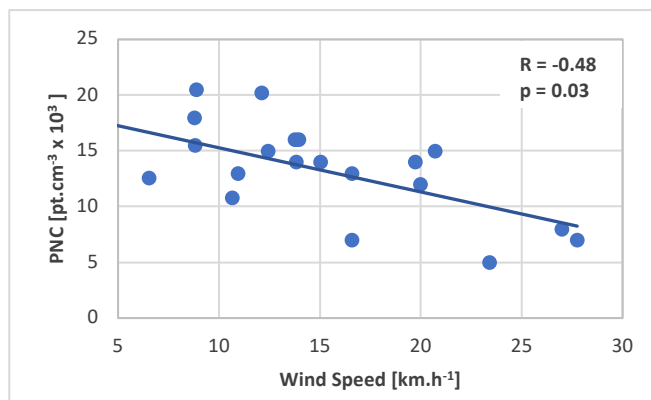


Figure 4.10: Statistical outputs for regression analysis with 95% confidence level between PNC 1-hour averages and wind speed, in Av. da Liberdade.

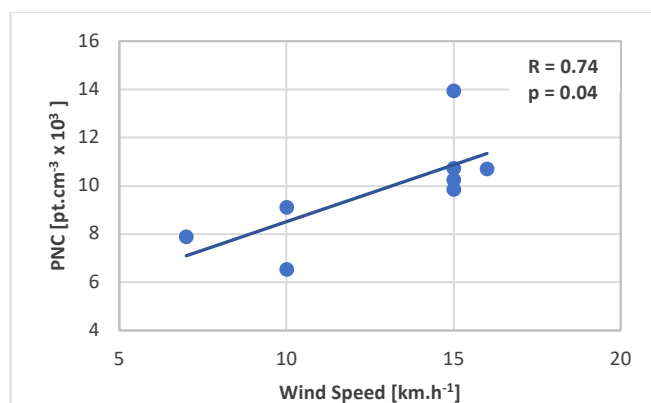


Figure 4.11: As in Figure 4.10 but respecting to Entrecampos.

High temperatures are usually responsible for intense convection which promotes the dispersion of pollutants, reducing their ground level concentration. On the contrary, low temperatures weaken convection (Lin *et al.*, 2009), which leads to higher atmospheric PM concentrations. On the other hand, precipitation enhances the wet deposition phenomenon (Shen *et al.*, 2009) promoting decreasing in PM atmospheric concentrations. Additionally, it has been shown that for stable atmospheric conditions, low wind speed (breeze) or thermal inversion layer, higher rates of RH lead to an increase of PM concentrations (Mu *et al.*, 2011). Onat *et al.* (2019) reported that UFP are significantly positively associated with RH. Moreover, a study conducted by Morawska *et al.* (2008), reported that on colder days the greater atmospheric stability (less dispersion) and lower mixing layer height probably contribute to the increase in PNC. Evidence also suggests that traffic-related average PNC is highest in cold days (Fujitani *et al.*, 2012; Pirjola *et al.*, 2006).

As in our case, Talbi *et al.* (2018) found very poor correlations between PNC and meteorological variables (temperature, wind speed, precipitation and relative humidity). The authors justify this lack of correlations with the fact that the distance between the sampling site and the road was less than five meters, which was also our case, meaning that the effect of weather conditions on PM concentration is barely

detectable. On the contrary, measurements made far from the source showed a clear dependence with positive correlations with meteorological variables.

A summary of all regression analysis outputs is presented in Table 4.4.

Table 4.4: Summary of statistical outputs for regression analysis with 95% confidence level between PNC and other pollutants and meteorological parameters, in Av. da Liberdade and Entrecampos.

Parameter	Av. da Liberdade		Entrecampos	
	r	p-value	r	p-value
PM₁₀	0.80	< 0.01	0.76	0.03
PM_{2.5}	(¹)		NSS	
NO	0.55	< 0.01	(¹)	
NO₂	0.51	< 0.01	NSS	
NO_x	0.58	< 0.01	(¹)	
CO	NSS		NSS	
Wind	-0.48	0.03	0.72	0.04
RH	NSS		NSS	
T	NSS		NSS	

NSS – Not statistically significant.

(¹) Pollutant not measured by the respective AQMS.

4.2 LISBON AIRPORT

The measurements taken at each sampling site (minimum, average, mode and maximum PNC), the respective average meteorological parameters (mixing layer height (ML), wind intensity (v), temperature (T) and relative humidity (RH)) and distance to runway are summarized in Table 4.5.

Results obtained for PNC average, mode and standard deviation are presented in Table 4.6. Except for site 3, in which most of the measurements were done under NIWD, in the vicinity of LA all sites present mode values higher than $100 \times 10^3 \text{ pt.cm}^{-3}$. Mode values in sites under the take-off path (12.3 and $13.4 \times 10^3 \text{ pt.cm}^{-3}$) are lower than the ones measured in the sites lateral to the runway (16.2 and $17.1 \times 10^3 \text{ pt.cm}^{-3}$). The differences in altitude and the height of the aircraft may explain these particularities.

Table 4.5: Sampling date and period for each airport-related site and the corresponding height of the Mixing Layer (ML), wind speed (v) and direction, temperature (T), relative humidity (RH) and measured minimum (Min), mean, mode, and maximum (Max) PNC values.

Site	Date	Period	Distance	ML	Wind		T	RH	PNC [pt.cm ⁻³] x 10 ³			
		[Time UTC]	[m]	[m]	v [km.h ⁻¹]	Direction	[°C]	[%]	Min	Mean	Mode	Max
Sites located far from the influence of LA ⁽¹⁾												
1	11/07/17	14:49 – 19:04	2 836	617	6	NNW	28	29	3.0	14.1	10.2	233
2	13/07/17	13:29 - 17:49	1 895	400	6	NNW	33	32	1.4	15.9	15.6	277
Sites located in the landing direction and/or under the influence of LA activities ⁽¹⁾												
3	18/07/17	14:05 – 18:01	314	1 000	4	NW	23	61	0.9	20.5	2.0	194
4	20/07/17	14:00 – 18:02	349	1 083	7	NNW	22	44	26.2	73.1	106	140
5	01/10/17	05:44 – 08:29	337	0	14	NNW	18	82	0.8	33.1	1.2	342
5	05/10/17	06:08 – 08:08	337	0	5	NNW	14	87	5.4	52.7	112	227
6	22/10/17	10:35 – 10:52	610	724	15	NNW	19	43	2.6	92.4	158	469
7	29/10/17	10:05 – 11:52	497	288	16	NNE	20	35	9.9	56.9	103	343
11	19/11/17	10:28 – 11:58	1 197	185	9	NNE	17	48	12.0	58.7	108	227
13	08/12/17	16:05 – 00:00	4 886	0	7	NW	14	91	3.9	14.6	14.4	120
13	09/12/17	00:00 – 04:58	4 886	0	9	NW	12	86	1.2	3.6	1.5	29.9
14	31/03/18	22:10 – 00:00	1 548	0	7	SW	12	78	3.4	5.1	5.6	8.5
14	01/04/18	00:00 – 07:52	1 548	0	5	SW-SE	10	84	2.7	6.7	7.0	13.2
14	30/05/18	23:10 – 00:00	1 548	0	14	NW	15	84	2.2	4.7	3.2	28.3
14	31/05/18	00:00 – 11:43	1 548	0-2336	8	NW	16	80	0.8	4.1	1.7	23.2
Sites located in the take-off direction ⁽²⁾												
8	11/11/17	10:32 – 12:22	821	414	7	NNE	22	46	9.1	21.1	13.4	325
12	25/11/17	09:42 – 12:03	1 272	734	7	NNE	16	89	9.5	15.2	12.3	243
Sites located laterally to the runway ⁽³⁾												
9	15/11/17	09:51 – 11:39	692	110	9	NNE	17	41	7.8	34.5	17.1	172
10	18/11/17	09:51 – 12:06	872	178	6	NNE	19	44	6.1	25.0	16.2	325

⁽¹⁾ The distance is indicated relative to the start of the runway 03, in a straight line.

⁽²⁾ The distance is indicated relative to the end of the runway 03, in a straight line.

⁽³⁾ The distance is indicated relative to the centre of the runway 03, in a straight line

Table 4.6: Average, mode and standard deviation (SD) of PNC on airport-related sites, in $\text{pt.cm}^{-3} \times 10^3$. Sites are arranged by location and distance to the airport.

Location	Site	Distance to LA [m]	Average	Mode	SD
Sites located in the landing direction and/or under the influence of LA activities ⁽¹⁾	3	314	20.5	2.0	35.7
	5	337	41.3	112	33.3
	4	349	73.1	106	32.2
	7	497	56.9	103	34.8
	6	610	92.4	158	74.8
	11	1 197	58.7	108	32.6
Sites under the take-off path ⁽²⁾	8	821	21.1	13.4	23.6
	12	1 272	15.2	12.3	4.5
Sites lateral to runway ⁽³⁾	9	692	34.5	17.1	22.3
	10	872	25.0	16.2	18.1
Sites under the landing path, in residences at the 5th floor level ⁽¹⁾	14	1 548	5.5	5.6	4.1
	13	4 886	10.4	14.4	6.6

⁽¹⁾ The distance is indicated relative to the start of the runway 03, in a straight line.

⁽²⁾ The distance is indicated relative to the end of the runway 03, in a straight line.

⁽³⁾ The distance is indicated relative to the centre of the runway 03, in a straight line

4.2.1 Statistical Analysis

Generically, the highest PNC values (average, median, standard deviation and maximum) were found at sampling sites 4, 5, 7 and 11, in LA vicinity, up to 1200 m. Figure 4.12 presents the 10-minutes PNC averages under impact wind direction and other directions (NIWD). Results show that downwind average PNC ranges from $3.3 \times 10^4 \text{ pt.cm}^{-3}$ to $5.9 \times 10^4 \text{ pt.cm}^{-3}$, and the peaks range from $2.3 \times 10^5 \text{ pt.cm}^{-3}$ to $3.4 \times 10^5 \text{ pt.cm}^{-3}$. Measurements in non-impact wind conditions or further away to LA have lower standard deviation and PNC values (Figure 4.12). Sampling sites located laterally to LA main runway (sites 9 and 10) present higher average PNC values than sampling sites located under the take-off path (sites 8 and 12): $2.5 \times 10^4 \text{ pt.cm}^{-3}$ to $3.5 \times 10^4 \text{ pt.cm}^{-3}$, and $1.5 \times 10^4 \text{ pt.cm}^{-3}$ to $2.1 \times 10^4 \text{ pt.cm}^{-3}$, respectively. Still, both locations present high peak PNC values, range from $1.7 \times 10^5 \text{ pt.cm}^{-3}$ to $3.3 \times 10^5 \text{ pt.cm}^{-3}$.

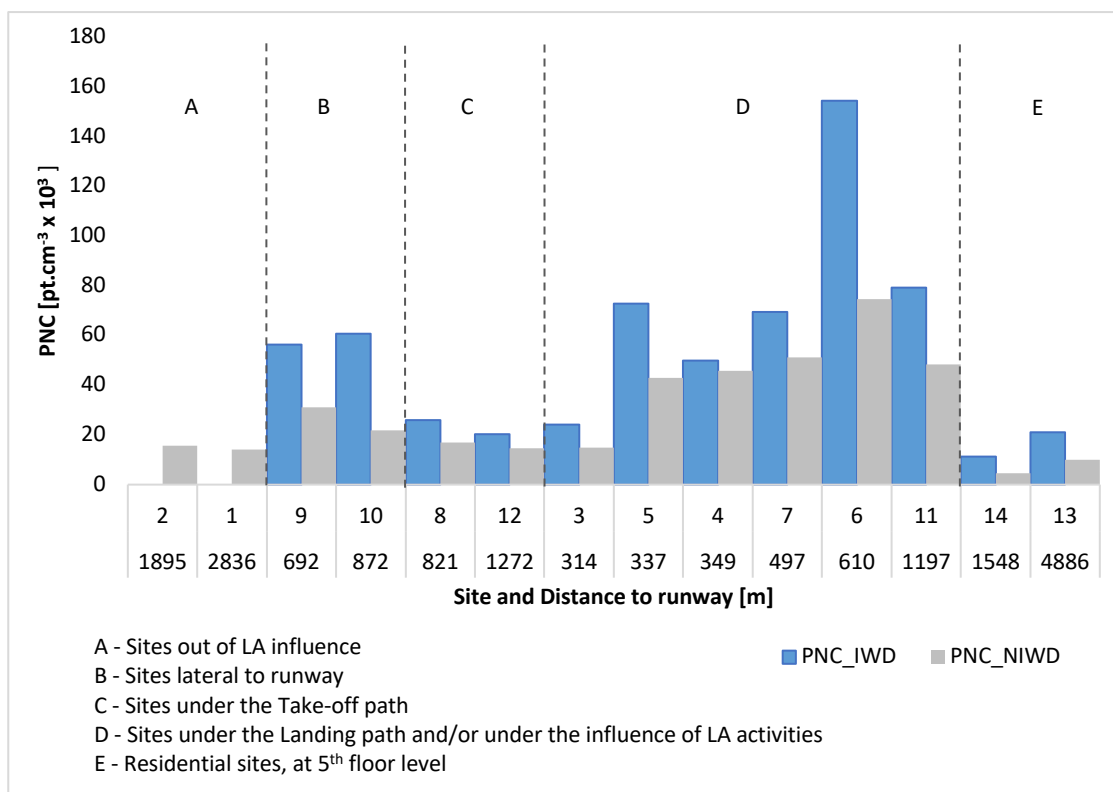


Figure 4.12: 10-minute PNC averages obtained under impact wind direction (blue) and non-impact wind direction (grey). Sites are ordered by distance to runway and type of location.

The obtained results for IWD are presented in Table 4.7. Generally, there are no relevant differences between impact wind direction and other directions values. These results show that most of the time, and regardless the site, measurements were made downwind. The highest differences occur in sites lateral to runway and site 6. Therefore, results may be slightly sub-estimated.

Table 4.7: Impact wind directions (IWD, in °) by site.

Site	IWD (°)	Site	IWD (°)
3	351 – 360	9	71 – 80
4	351 – 360	10	91 – 100
5 (Flights) ⁽¹⁾	321 – 330	11	51 – 60
5 (Idling) ⁽¹⁾	11 – 20	12	101 – 110
6	1 – 10	13	311 – 320
7	61 – 70	14	311 – 320
8	21– 30		

(1) Please see Figure 4.21.

These results are in agreement with the results by Hudda *et al.* (2014) which analysed UFP emissions in the Los Angeles International Airport, which reach the same level of the ones from the entire

city road network. According to this study, the highest UFP concentrations were found aligned downwind to the aircraft's trajectories. In this direction, at 8 km distance from the airport, concentrations over 7.5×10^4 pt.cm⁻³, were registered. Still regarding Los Angeles airport, Riley *et al.* (2016), found a 3 to 5-fold increase in UFP concentrations in transects under the landing approach path. An increase from 1.4×10^4 pt.cm⁻³ (non-downwind conditions) to 4.2×10^4 pt.cm⁻³ (downwind conditions) at 40 km distance from the Schiphol airport (Netherlands) was also observed (Keuken *et al.*, 2015). Additionally, a 2×10^4 pt.cm⁻³.min⁻¹ UFP concentration increase within 5 minutes after take-offs in Ciampino airport (Rome, Italy) was reported, being incremented by three when measurements were taken under downwind conditions (Stafoggia *et al.*, 2016). Psanis *et al.* (2017) concluded that UFP concentrations increase by two orders of magnitude during take-offs in a small airport of the Aegean Sea Insular Region. Ren *et al.* (2016) found UFP emissions during one take-off to be the twice of the UFP emissions from all gasoline passenger vehicles in Tianjin. This study was carried out up to 400 m way from Tianjin International Airport in China for particles from 10 nm to 1 µm. Authors found UFP to be the main aircraft particles emissions. It is also highlighted the lack of studies in the immediate airport vicinity (up to 400 m away) and within the airport (Ren *et al.*, 2018).

Single factor ANOVA among sites presented in Table 4.8 clearly presents statistically significant differences in the means among all sites (p-value much lower than 0.01). This result shows that at least one site presents a different mean value. However, when applied to sites with identical location, ANOVA outputs indicate that means are statistically identical.

Table 4.8: Single factor ANOVA among all sites.

Source of Variation	SS	df	MS	F	P-value	F crit
Between Sites	199145	13	15319	64,4	5.1E-92	1.7
Within Sites	101856	428	238			
Total	301001	441				

Table 4. 9 resumes the obtained p-values. Residential sites present statistically different means. However, it should be noticed that they are about 5 km distance from each other. When site 6 is added to "Landing path and/or under LA influence" group, ANOVA returns a p-value much lower than 0.01. This result highlights the particular aircraft plume dispersion conditions. This site is located close to LA (610 m from runway 03) in a terrain depression in comparison to the LA baseline. This particular orography affects the aircraft plume dispersion leading to higher PNC than the values measured in site 7, closer to LA (500 m from runway 03), but a few meters higher than site 6.

Table 4.9: Single factor ANOVA among sites with similar characteristics.

Sites	Location	p-value
1 and 2	Out of LA influence	0.42
9 and 10	Lateral to LA	0.15
8 and 12	Take-off path	0.09
13 and 14	Residences	< 0.01
4, 5, 7 and 11	Landing path and/or under LA influence	0.30

Results from regression analysis between PNC and the number of flights show significant correlation coefficients (r) between PNC and the total number of flights, as well as, between PNC and the number of landings and take-offs (Figure 4.13 to Figure 4.15). Results show higher positive correlations between PNC and the number of flights ($r = 0.90$, $p = 0.01$). Comparing the obtained results for take-offs and landings (please see Data Analysis for details), take-offs have a significant and higher positive correlation value ($r = 0.86$, $p = 0.01$) than landings, although also statistically significant ($r = 0.78$, $p = 0.04$). During landings aircraft engine power is approximately set to 30 % while it operates at 100 % power during take-off, with consequent higher emissions (ICAO, 2011). The obtained results from regression analysis between PNC and mixing layer height were insignificant. On the other hand, correlations between PNC and wind intensity (Figure 4.16) shows a moderate positive statistically significant correlation ($r = 0.57$, $p < 0.01$).

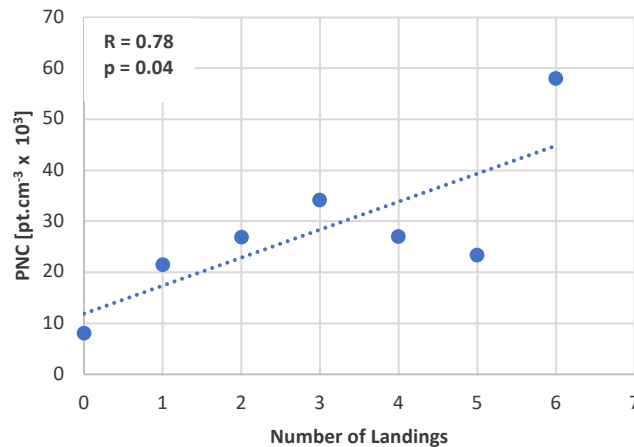


Figure 4.13: Overall statistical outputs for regression analysis with 95% confidence level between PNC 10-minutes averages and the number of landings.

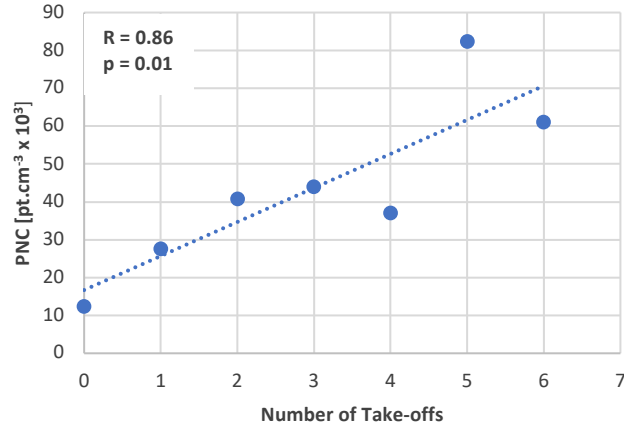


Figure 4.14: As in Figure 4.13 but respecting to the number of take-offs.

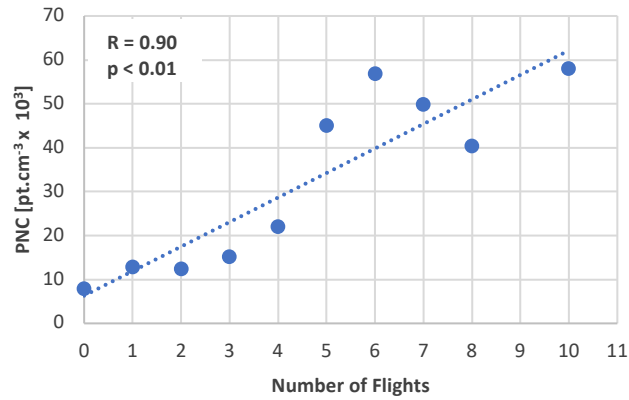


Figure 4.15: As in Figure 4.13 but respecting to the number of flights (landings and take-offs).

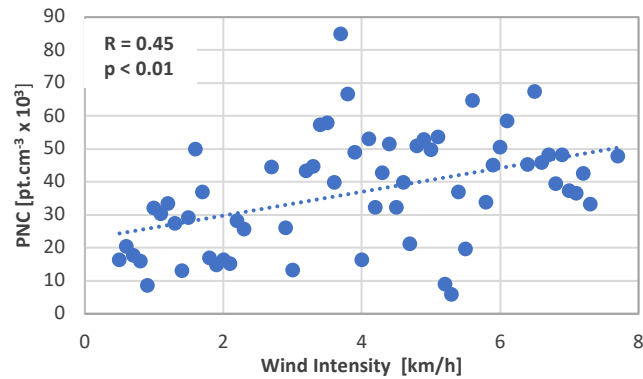
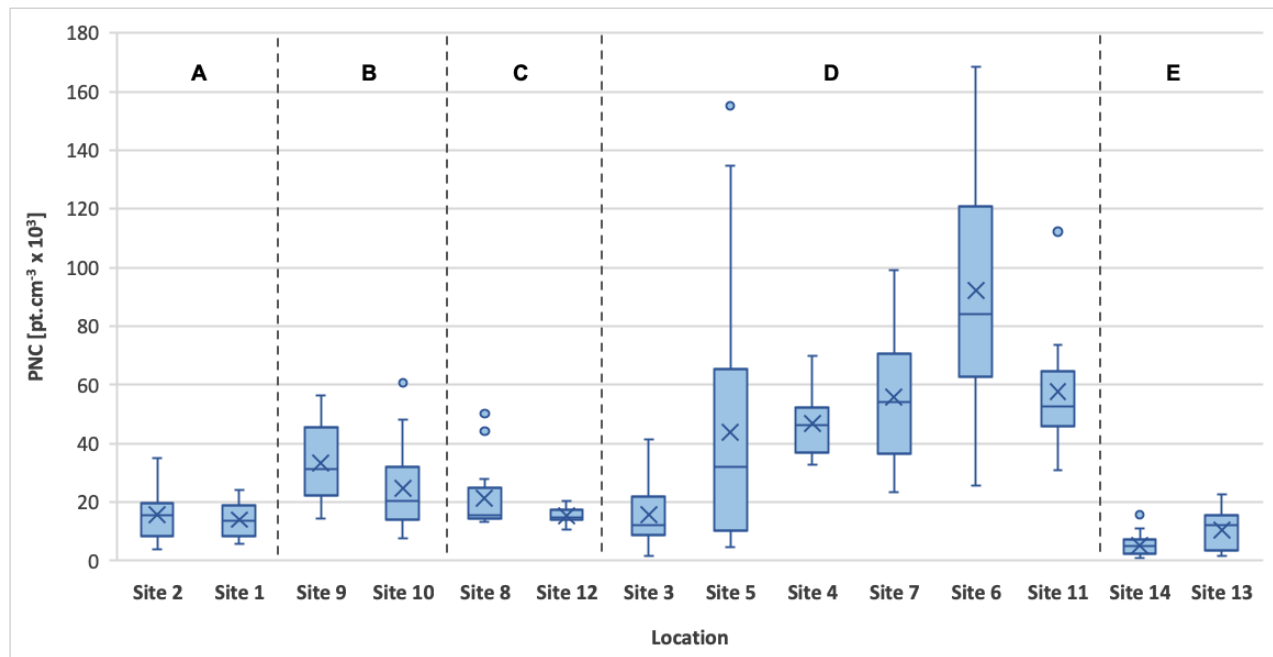


Figure 4.16: As in Figure 4.13 but respecting to wind intensity.

Obtained results are in agreement with previous studies (Campagna *et al.*, 2016; Keuken *et al.*, 2015; Psanis *et al.*, 2017; Riley *et al.*, 2016; Stafoggia *et al.*, 2016) that found significant positive correlation values between PNC and total number of flights. Additionally, the stronger relationship between PNC and take-offs

highlights that take-offs have stronger impact on PNC, also in accordance with previous studies (e.g. Ren *et al.*, 2016; Stafoggia *et al.*, 2016). Also, the moderate positive correlation between PNC and wind intensity is in accordance with previous studies. Generally, higher wind speed promotes greater dispersion and mixing, and PNC and wind speed are negatively correlated. However, for buoyant aircraft plumes, higher wind speeds promote faster ground arrival which counterbalance the dispersion (Hudda *et al.*, 2018).

The range of 10-minutes PNC average by site is plotted in Figure 4.17. Sites are ordered by typology of location and increase distance to LA. Higher dispersion values were obtained for site 5 and 6, even though with higher mean, median, quartiles and extreme values over site 6. Therefore, the highest values and range dispersion are downwind located close to the airport (Figure 4.18). Lower dispersion values were obtained for sites 12 and 14 with mean, median and quartiles very similar and lower than $20 \text{ pt.cm}^{-3} \times 10^3$. The lowest PNC were obtained during non-downwind conditions (sites 1, 2, 3, 8, 12 and 14) or further away to LA (site 13). Comparing sites far from intensive road traffic influence (sites 9, 10 and 11) to sites close to intensive road traffic influence (sites 1 and 2), higher PNC was found on sites far from intensive traffic road, downwind to LA.



Legend: A - Sites out of LA influence
 B - Sites lateral to runway
 C - Sites under the Take-off path
 D - Sites under the Landing path and/or under the influence of other LA activities
 E - Sites under the Landing path, in residences at the 5th floor level

Figure 4.17: Boxplot of 10-minutes PNC mean distribution by site ordered by location and increase distance to LA (please see sites spatial distribution in Figure 3.23b). (1st quartile, average (x), median (-), 3rd quartile and outliers (dots)).

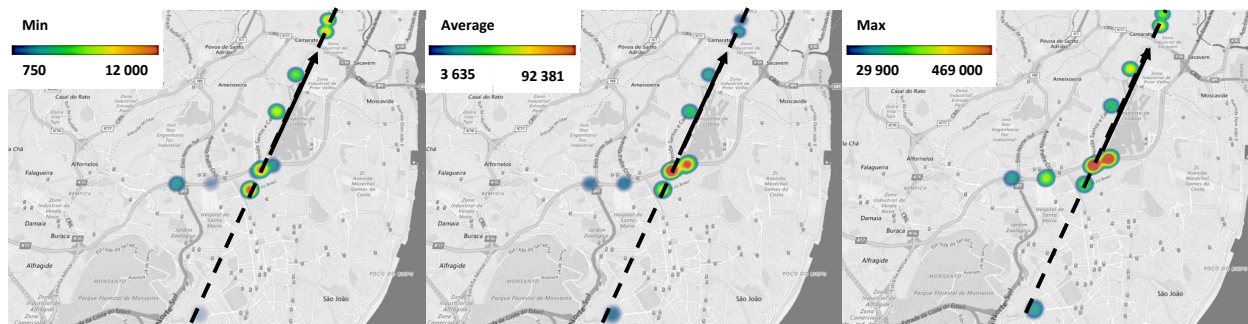


Figure 4.18: LA-related PNC geographical distribution: minimum, average and maximum (PNC expressed in pt.cm^{-3}).

Sites closer to LA present the higher PNC, except for residential sites (13 and 14). Although site 14 is much closer to LA than site 13, PNC are lower in site 14 which might be explained by the reduced power of aircraft engine when it flies near this site. All the sites in group D are close to each other. The major difference among them is the surroundings (e.g. terrain depression which is the case of site 6). Therefore, besides proximity to LA, ventilation also plays an important role in PNC.

This result highlights that air traffic contributes to elevated PNC downwind to airport, as previously concluded by several studies (e.g. Keuken *et al.*, 2015, Shirmohamadi *et al.*, 2017).

4.2.2 Influence of Wind and Mixing Layer's Height on PNC

Figure 4.19 illustrates the concentrations measured at five sites (4, 5, 6, 7 and 11) close to the landing route, near the LA (a) for different wind intensities and for different ML height (b). These particular sites were chosen for comparison because of their characteristics in the vicinity of LA and close to the same flight path (landing). The highest PNC values were obtained for higher wind intensity (higher than 14 km.h^{-1}); relation between PNC and mixing layer height is unclear. These results show that, close to LA, both wind speed and direction affect PNC values, which is in accordance to the results obtained by Ren *et al.* (2016) and emphasize that higher wind speeds lead to higher PNC peaks by promoting faster ground arrival of the plumes emitted by aircrafts, counterbalancing the dispersion (Hudda *et al.*, 2018).

The highest PNC maximum and average values were obtained in site 6, 610 m away from the start of the runway, in a straight line. These results can be explained by the terrain depression in comparison to the LA baseline. This adverse orographic conditions to aircraft plume dispersion associated with the high turbulence generated by landings, when the aircraft altitude is very low (75 m above the ground), lead to a PNC increase by 7-fold, compared to the values obtained without landings.

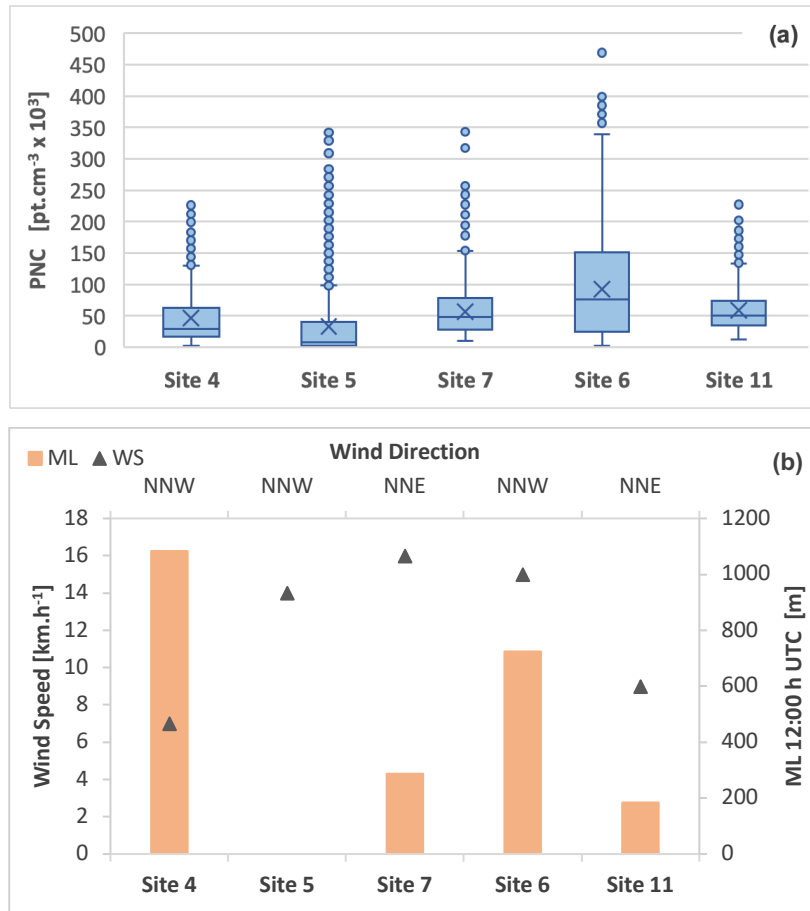


Figure 4.19: PNC concentrations at five sites located in LA landing route vicinity, ordered by increasing distance to the runway (a), and corresponding wind speed and ML height (b).

Results for sampling site 5 allow a comparison of PNC values between absence and during LTO cycles. The maximum value was recorded for the higher wind speed, which can be explained by instant plume transport, in accordance to correlation found between PNC and wind speed. In the vicinity of LA the lowest recorded value was obtained in sampling site 5 after a period of approximately 3 hours without landings or take-offs. With the beginning and intensification of air traffic, during morning period, these concentrations increase about 10 times compared to those observed after the short period without aircraft movement. The results obtained at sampling site 5, illustrated in Figure 4.20, show that the number of LTO cycles and aircraft movement in the airport, particularly when they are holding for take-off, cause a significant PNC increase. These results show an increase of PNC when the aircraft passes near the monitoring site, similarly to what Hsu *et al.* (2012) and Masiol *et al.* (2016) had also concluded.

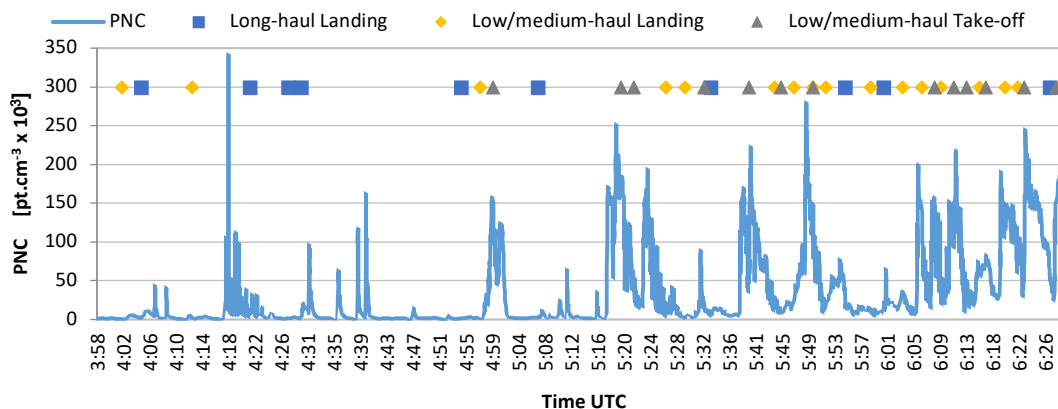


Figure 4.20: UFP concentration at sampling site 5 (LA vicinity) and LTO cycles differentiated by long-haul flights and low/medium-haul flights.

Regarding the aircraft's type (long-haul flights *versus* low/medium-haul flights), associated with large and small aircrafts, respectively, data showed no differences on PNC (Figure 4.20), in accordance with conclusions reached by Stafoggia, *et al.* (2016).

Results show that PNC increases with most of the flight occurrences, but not all, particularly for the sampling points located across the take-off route. Nevertheless, we would like to highlight that the PNC measurements are carried out at a fixed point on the ground, whereas an aircraft moves quickly and has a 3-dimensional movement and the wind suffers constant variations of intensity and direction. For these reasons, it was not always possible to establish a direct relationship between the LTO cycles and the obtained measurements, as showed by Campagna *et al.* (2016).

Figure 4.21 represents the mean of 10-minutes PNC averages by 10° ranges of wind direction and the number of LTO cycles occurred during those wind direction ranges, at sampling site 5. This site is located at approximately 350 m east to the beginning of the runway, close to the airport fence, and also near to the taxiing lane used by aircrafts to access the main runway. The impact wind direction for landings and take-offs is 320 to 329° (Figure 4.21a) is consistent with the site relative position to the beginning of the runway (black thin arrow), as indicated by the small dashed red line (Figure 4.21b). The impact wind direction for taxiing is 10 to 19° (Figure 4.21a) is also consistent with site relative position to taxiing lane (blue large dashed line) as illustrated by the orange dot line (Figure 4.21b). Aircrafts idling to take-off contribute to relevant PNC increase. However, the most notorious increase is registered with take-offs and landings.

For distinct and complementary purposes, results obtained at a 5 km distance from LA, at a 5th floor level, and under thermic inversion conditions from the ground, are presented in Figure 4.22. The PNC is given in 10-minute average and the bars represent the number of landings occurred during each 10-minute period. These results clearly show that PNC values during landing period are higher than 10 pt.cm⁻³ x 10³, with peaks of 20 pt.cm⁻³ x 10³. When the landings stop, these values fall down to 5 pt.cm⁻³ x 10³ and later to 2 pt.cm⁻³ x 10³. Thus, it is possible to conclude that, even for distances 5km far from the LA, the impact of

airplanes' landing is noticeable on PNC registries. Moreover, only when landings stop is that PNC starts to lower.

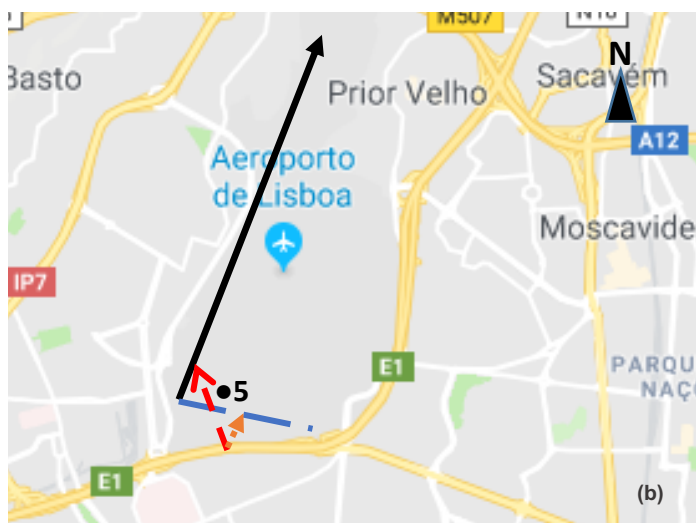
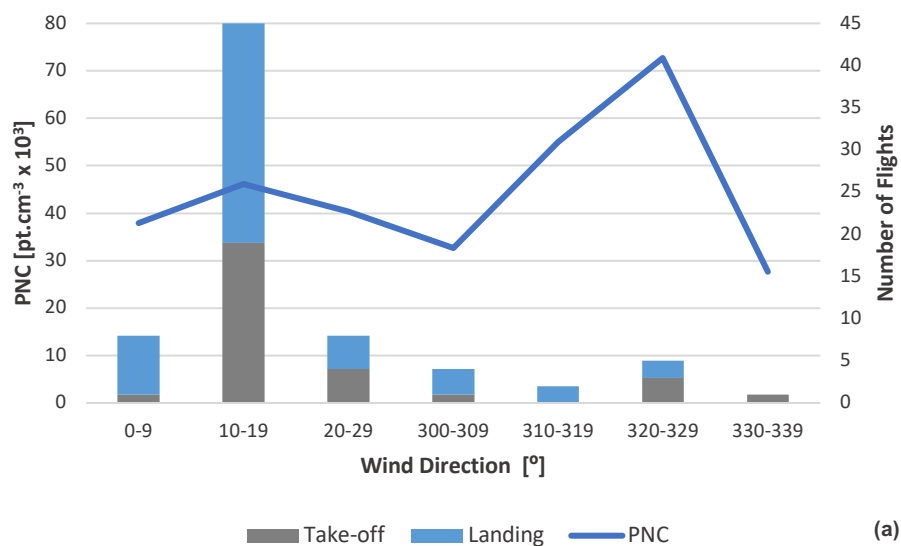


Figure 4.21: (a) 10-minutes UFP average concentration, number of flights and wind direction, in LA vicinity (site 5) (b) Geographical detail of sampling site: relative position to the beginning of the runway (small dashed red arrow) and to aircrafts idling to take-off (pointed orange arrow). The runway is represented by the black arrow and idling path by the large dashed blue line.

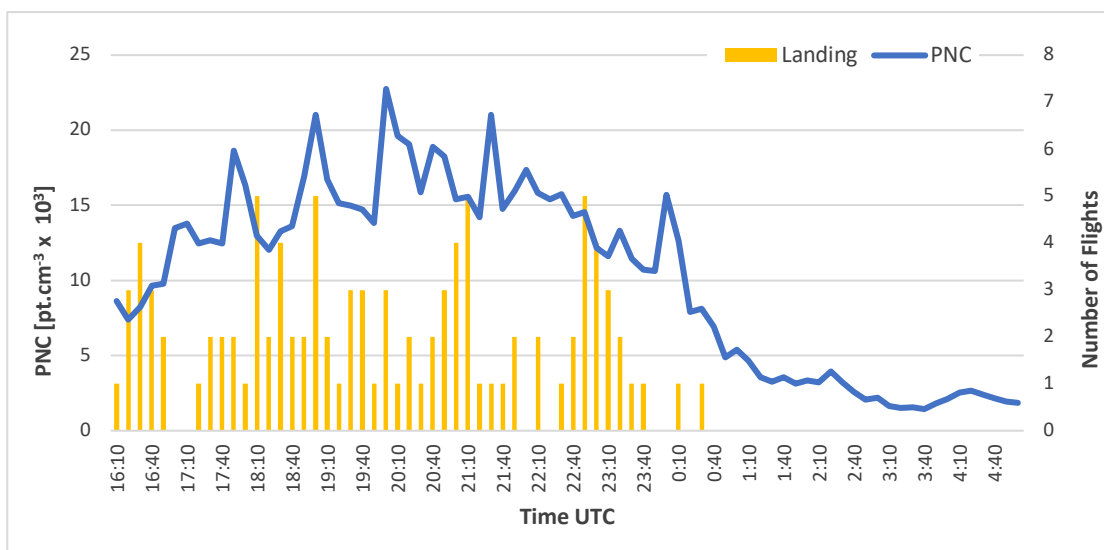


Figure 4.22: UFP concentration at sampling site 13 (landing path, far from LA) and number of landings during a 10-minutes period.

4.3 IN-LAND PASSENGER FERRIES

There are substantial different characteristics among the sampling sites. Therefore, the results and discussion will be performed by site. The measurements taken at each sampling site (minimum, average and maximum PNC), the respective average meteorological parameters (mixing layer height, wind intensity (v) and direction, temperature (T) and relative humidity (RH)) are summarized in Table 4.10. Results of PNC average, mode and standard deviation are presented in Table 4.11.

Obtained 1-minute PNC averages by site and under downwind conditions are plotted in Figure 4.23. Higher dispersion values were obtained for Cacilhas and Seixal (standard deviation (SD) $11.92 \times 10^3 \text{ pt.cm}^{-3}$ and $11.76 \times 10^3 \text{ pt.cm}^{-3}$, respectively). Higher mean and median ($21.09 \times 10^3 \text{ pt.cm}^{-3}$ and $16.2 \times 10^3 \text{ pt.cm}^{-3}$, respectively) were found in Cacilhas and the higher maximum ($70.05 \times 10^3 \text{ pt.cm}^{-3}$) was obtained in Seixal. Minimum PNC values are lower in Montijo. Cacilhas presents the highest maximum PNC. Montijo and Seixal stations present slightly higher mode values and the highest peak values are found in Cacilhas and Seixal.

Table 4.10: Sampling date and period for each ferry-related site and the corresponding height of the Mixing Layer (ML), wind speed (v) and direction, temperature (T), relative humidity (RH) and measured minimum (Min), mean, mode, and maximum (Max) PNC values.

Site	Date	Period	ML	Wind		T	RH	PNC [pt.cm ⁻³] x 10 ³			
		[Time UTC]	[m]	v [km.h ⁻¹]	Direction	[°C]	[%]	Min	Mean	Mode	Max
Barreiro	05/07/18	16:13 – 18:08	1351	0	SW	25	59	1.1	10.0	10.4	249
	17/09/18	07:40 – 11:02	235	0	WSW	25	62	1.0	8.7	10.4	77.3
	18/09/18	18:06 – 18:35	864	0	NW	28	50	1.5	15.1	14.6	31.2
	30/09/18	10:30 – 16:06	155	1	WSW	30	43	0.8	6.8	10.1	55.0
Cacilhas	06/07/18	14:49 – 16:59	896	1	NNW	27	41	3.6	10.2	10.5	66.3
	18/09/18	06:50 – 08:25	864	1.2	WNW	19	78	2.4	8.1	10.3	90.5
	19/09/18	06:30 – 11:29	524	0.3	NW	20	72	4.0	35.0	42.0	95.5
	21/09/18	06:50 – 11:07	728	2	NW	22	73	1.9	11.6	10.2	99.1
	30/09/18	08:20 – 09:35	155	0.0	ENE	22	73	3.6	11.4	11.8	61.2
	27/12/18	23:12 – 23:59	0	0.0	N	11	88	4.8	13.9	13.5	25.6
	28/12/18	00:00 – 01:13	0	0.0	W	10	89	7.4	9.5	10.1	48.4
Montijo	10/09/18	05:45 – 08:88	3301	1.0	WSW	18	82	1.3	5.9	5.6	68.7
	10/09/18	14:46 – 15:56	3301	6.1	WNW	33	28	4.1	9.9	11.7	17.9
Seixal	24/09/18	06:52 – 14.08	233	0.4	NNE	25	65	3.1	12.4	11.5	152
	27/09/18	06:48 – 11:47	1000	6.5	NE	23	77	1.1	10.4	3.7	102
	28/09/18	18:11 – 19:35	1000	7.8	ENE	25	57	3.4	15.0	11.4	123
	02/10/18	07:00 – 10:08	313	15	NW	20	43	2.9	11.7	4.4	132

Table 4.11: Obtained average, mode and standard deviation (SD) of PNC on ferry-related sites, in pt.cm⁻³ x 10³.

Sites	Average	Mode	SD
Barreiro	8.7	10.4	5.9
Cacilhas	13.0	10.1	10.2
Montijo	7.1	11.7	3.7
Seixal	11.8	11.5	13.7

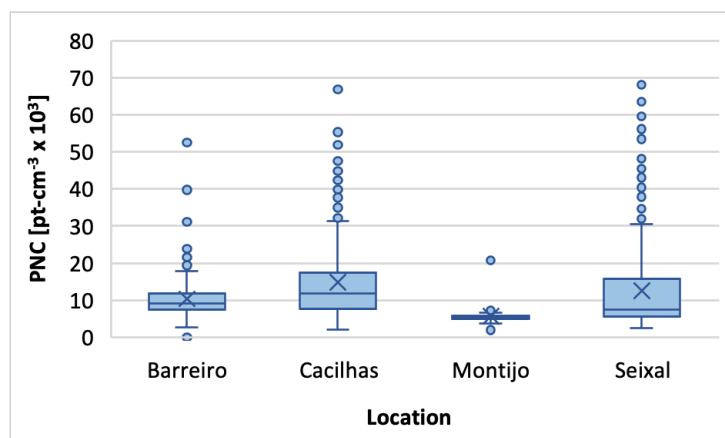


Figure 4.23: Boxplot of 1-minute PNC mean distribution by ferry-related site, under downwind conditions. (1st quartile, average (x), median (-), 3rd quartile and outliers (dots)).

PNC during the immediate eight minutes before arrivals, eight minutes after departures and eight minutes before and after ferry occurrences, are plotted in Figure 4.24. During rush periods, there are many ferry occurrences in Cacilhas and Barreiro, in average two every 10 minutes. Therefore, a time lag larger than 8 minutes would excessively overlap PNC related to ferry occurrences.

As shown in Figure 4.25, during the third minute around a ferry occurrence, PNC are considerably higher when compared to the lowest value during this 8-minute period, ranging from 25% higher in Barreiro to 197% in Cacilhas. During the same period, departures are responsible in all the ports for a higher increase in PNC than arrivals (Figure 4.25). Given the almost constant ferry operations in the Barreiro terminal, with the consequent continuous emission of UFP, departure and arrival PNC values are believed to be underestimated. Nevertheless, they clearly show an increase of PNC as a result of departures and arrivals.

Except for Montijo, results from regression analysis (Table 4.12) show high positive correlations (r) between 1-hour PNC averages and the number of ferry occurrences. This result highlights that in-land ferries contribute to elevated PNC downwind to ferry's path, as previously concluded by López-Aparicio *et al.* (2017). The non-significant correlation found in Montijo can be explained by the reduced number of ferries operating in this connection, comparatively to the other three terminals. Comparing the obtained results for departures and arrivals for the four terminals, departures have a significant and higher positive correlation value than arrivals in Barreiro, Cacilhas and Seixal, and both are statistically significant. The exception again is Montijo, which presents non-significant correlations values. The obtained results from regression analysis between 1-minute PNC averages and wind speed were different for each analysed terminal, with

- i) Montijo and Barreiro presenting not statistically significant correlations, and
- ii) Cacilhas and Seixal showing very high negative statistically significant correlations.

The correlation results in Barreiro can be explained by the reduced wind speed range during sampling periods in this site (0, 1 and 4 km.h⁻¹). Results did not show significant correlations between PNC and other meteorological parameters (temperature, relative humidity and mixing layer height).

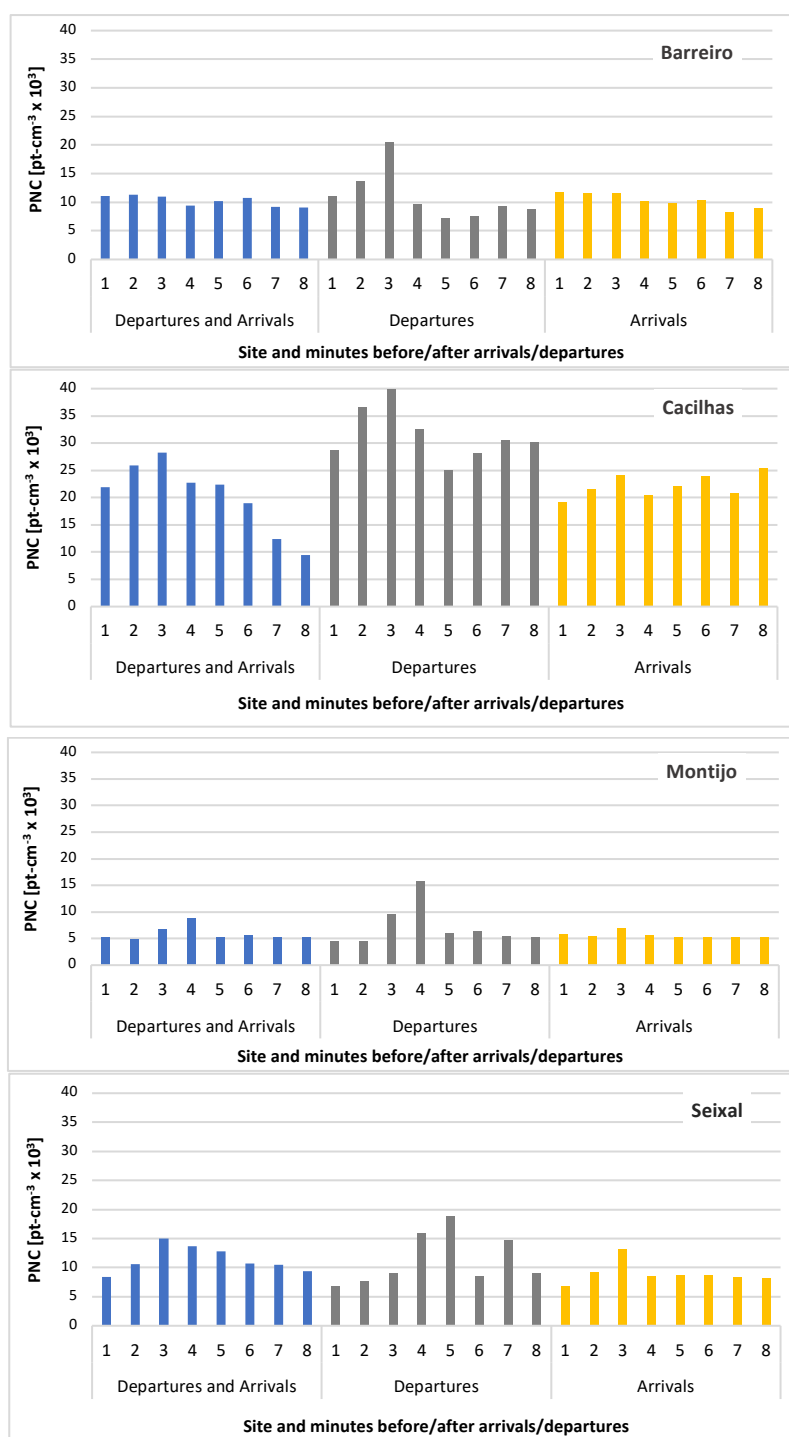


Figure 4.24: Site by site PNC during the immediate eight minutes before/after ferry operations (blue), eight minutes before departures (grey), eight minutes after arrivals (yellow).

Finally, the ANOVA analysis between measured PNC during periods with and without ferries operations show a statistically significant ($p < 0.01$) difference between PNC averages for all stations except

for Seixal. However, the lack of statistical significance in Seixal may be explained by the high frequency of Barreiro's ferries which plumes are measured in this site. This result suggests that ferries emissions are responsible for a significant PNC increase, in accordance to what was concluded for ships by González *et al.* (2011) and Merico *et al.* (2016).

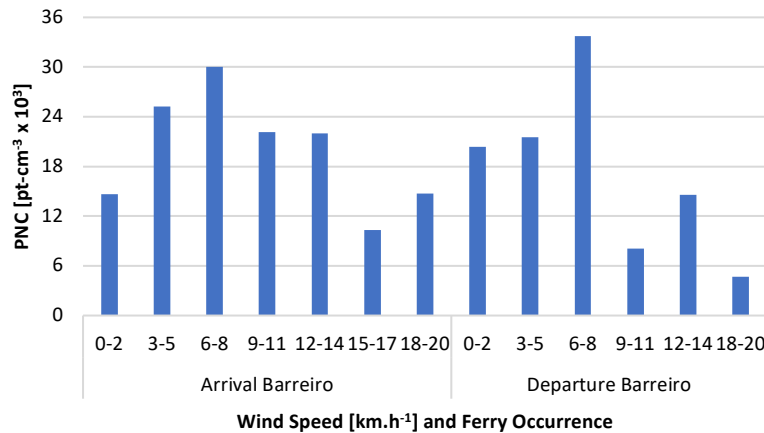


Figure 4.25: Average PNC of ferries from/to Barreiro measured in Seixal as function of wind speed and under wind direction range from N to NE.

Table 4.12: Obtained results of PNC increase with ferry operations, regression analysis between PNC averages and ferry occurrences and wind speed and ANOVA analysis between periods with and without ferry operations.

Site			Barreiro	Cacilhas	Montijo	Seixal
PNC	Ferry Occurrences		25 %	197 %	69 %	79 %
Increments	Departures		179 %	59 %	249 %	170 %
during	Arrivals		43 %	25 %	35 %	79 %
Regression Analysis	Ferry Occurrences	r	0.79	0.91	NSS	0.94
		p	<0.01	0.02		<0.01
	Departures	r	0.80	0.92	NSS	0.93
		p	<0.01	0.01		<0.01
	Arrivals	r	0.76	0.88	NSS	NSS
		p	0.01	0.02		
	Wind Speed	r	NSS	-0.93	NSS	-0.85
		p		<0.01		<0.01
ANOVA ⁽¹⁾		p	<0.01	<0.01	0.04	NSS

NSS – Not statistically significant.

⁽¹⁾ Analysis between PNC in periods with ferry operations and without ferry operations.

As shown in Figure 4.26, Barreiro and Seixal stations are located close to each other and the ferries from/to Barreiro path is close to Seixal (approximately 650 m distance). In Seixal, for wind direction range from N to NE, PNC results exclusively from plumes emitted by Barreiro's ferries. As it is shown in Figure 4.25, the maximum PNC averages are measured for wind speed range 6 to 8 km.h⁻¹. Considering this wind

speed range, PNC values obtained in Seixal are higher than PNC measured in Barreiro's terminal: arrivals, $30 \times 10^3 \text{ pt.cm}^{-3}$ in Seixal and $10 \times 10^3 \text{ pt.cm}^{-3}$ in Barreiro; departures, $35 \times 10^3 \text{ pt.cm}^{-3}$ in Seixal and $20 \times 10^3 \text{ pt.cm}^{-3}$ in Barreiro. In accordance to previous results, obtained PNC is slightly higher for departures than arrivals from/to Barreiro. This result might be explained by the way the exhaust gases are emitted, close to the water level at the rear of the ship. During cruise phase, the water flow generated is laminar and the plume is emitted into ambient air; during manoeuvring and hoteling phases, water flow generated by ferry engines is turbulent, which prevents the plume full dispersion into ambient air, leading to lower UFP emissions.

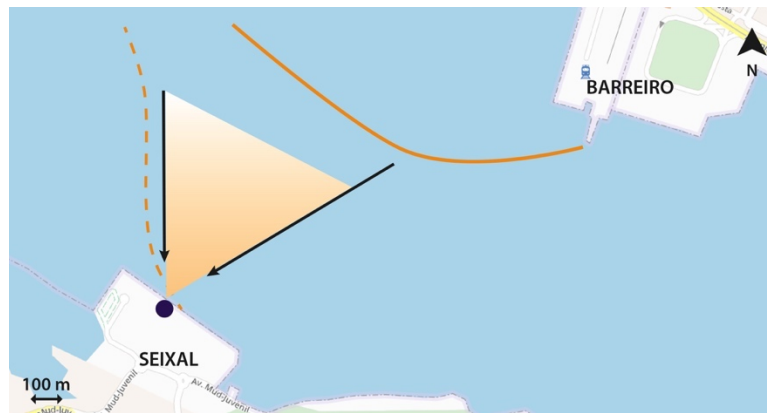


Figure 4.26: Detail of Barreiro and Seixal geographical location. Plumes emitted by Barreiro's ferries affect PNC on Seixal when wind direction range from NE to NW. Shadowed triangle shows the wind direction range in which only plumes emitted by Barreiro's ferries are measurable in Seixal; the continuous and dashed lines show the ferries paths from Barreiro and Seixal, respectively.

Figure 4.27 shows pollution roses in each ferry sampling periods, regardless of downwind or non-downwind direction. Except for Montijo, the highest PNC is obtained in downwind direction. In Barreiro, there are higher PNC levels measured from NW which are similar to the ones measured under downwind, probably resulting from de ferry cruising after shifting direction to NNE (please see Figure 3.23). In Montijo, the highest PNC was obtained for non-downwind direction, suggesting the existence of in-land UFP sources with more impact on PNC than de ferries.

PNC averages obtained in each ferry terminal, by class of ferry are presented in Figure 4.28. The highest PNC are associated with *Cacilheiros* ($30 \times 10^3 \text{ pt.cm}^{-3}$) Transcat with power of 2480 kW ($28 \times 10^3 \text{ pt.cm}^{-3}$) and monohull ($23 \times 10^3 \text{ pt.cm}^{-3}$). The other ferries present figures from $12 \times 10^3 \text{ pt.cm}^{-3}$ to $15 \times 10^3 \text{ pt.cm}^{-3}$. Nevertheless, as highlighted before, UFP emitted during cruising are expected to be higher than in stations and these figures should be interpreted only as a magnitude order.

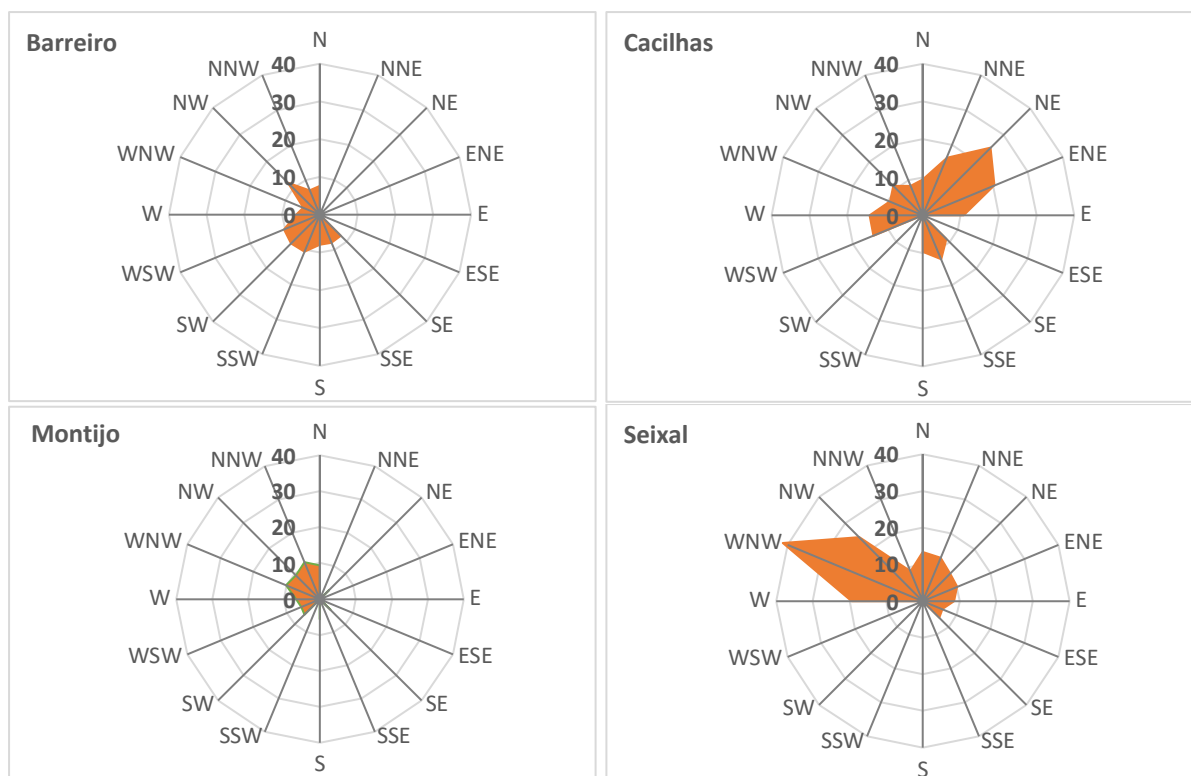


Figure 4.27: PNC rose pollution in each ferry station ($\text{pt.cm}^{-3} \times 10^3$).

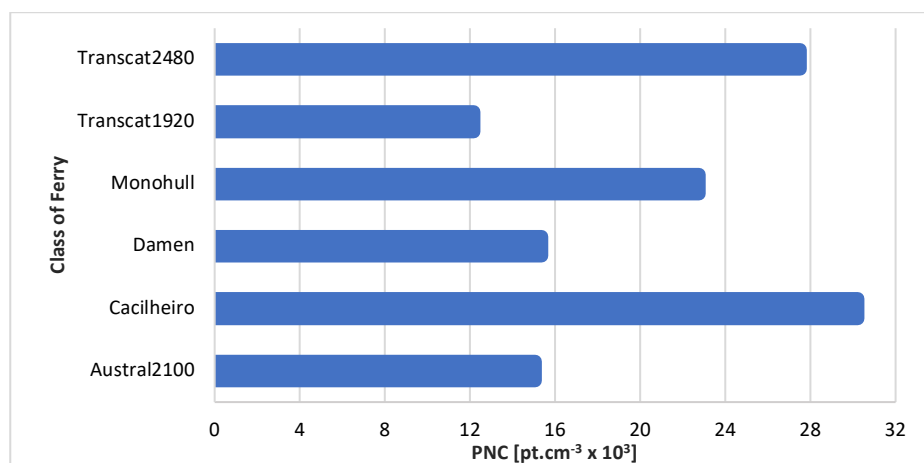


Figure 4.28: Obtained PNC average for different class of ferry operating among the four stations studied, downwind.

Our findings are in good accordance with results obtained in studies of PNC related to ship transport: increase of PNC in the vicinity and downwind to harbour (Cullinane and Cullinane, 2013; Hulscombe and Gon, 2010; Ledoux *et al.*, 2018; Pérez *et al.*, 2016; Pey *et al.*, 2013; Viana *et al.*, 2014) and in coastal areas (Ledoux *et al.*, 2018; López-Aparicio *et al.*, 2017; Viana *et al.*, 2014; Westerlund *et al.*, 2015). However, as mentioned above, there are no studies devoted to evaluating the PNC associated with in-land ferries emissions, although there are similar studies to other types of MT (e.g. Cullinane and Cullinane, 2013;

Hulskotte and Gon, 2010; Pey *et al.*, 2013). However, the dimension of the ships is completely different; this work is focused on small ferries while the mentioned studies are focused on larger ships and vessels.

5 CONCLUSIONS

The present work aimed to fulfil the lack of PNC studies in Lisbon and assess their emissions from road, air and river traffic in the city. Depending on the source under evaluation, sampling sites were chosen close to intense traffic roads with different characteristics and in the vicinity of the airport or ferry terminals. In the case of Lisbon Airport, sites further away were chosen to assess the area of influence of air traffic activities on urban and sub-urban air quality. Regarding in-land passenger ferries, one of the sampling sites (Seixal), was specifically chosen to add an evaluation of ferries' impact on PNC along shore navigation paths. The data analysis provided new insights on how to monitor the different types of traffic mentioned and some of the key factors that determine the levels found.

The next five sub-chapters will describe the main conclusions according to the source of UFP addressed in this dissertation, the answers to the "Research Questions", and the last one describes the main restraints to this work and suggestions for future work.

5.1 ROAD TRAFFIC

Results clearly show that PNC levels are different among sites with different traffic characteristics (p -values < 0.01). Although it is a strictly restricted circulation zone (LEZ1), Av. da Liberdade (downtown) presents the higher PNC levels and dispersion ($18.2 \pm 13.2 \times 10^3 \text{ pt.cm}^{-3}$) followed by a high-speed road (2nd Circular, $15.9 \pm 13.8 \times 10^3$ and $14.1 \pm 10.1 \times 10^3 \text{ pt.cm}^{-3}$, in Torres de Lisboa and Escola Alemã, respectively). The lowest values were found at an interception close to LEZ2 boundary (Entrecampos, $10.3 \pm 5.1 \times 10^3 \text{ pt.cm}^{-3}$). Mode values are higher in Torres de Lisboa ($15.5 \times 10^3 \text{ pt.cm}^{-3}$), followed by Av. da Liberdade, Entrecampos and Escola Alemã (11.4 , 10.3 and $10.2 \times 10^3 \text{ pt.cm}^{-3}$, respectively).

Both in Av. da Liberdade and Entrecampos, most of the PNC peaks were associated with older vehicle emission events, prior to 2000, mostly buses, taxis and light-duty. Unlike the downtown site, in Entrecampos results show high positive correlation between 1-hour PNC means and the number of vehicles ($r = 0.73$, $p = 0.04$). Our limited vehicle characterization by type and Euro Standard indicates that 26 % of the vehicles circulating in Av. da Liberdade were taxis, of which 6 % do not meet the imposed circulation restrictions; 13 % are light-duty vehicles, 12 % of which do not accomplish the Euro Standard required; 7 % are buses, from which 3 % are prior to 2000; and 4 % are heavy-duty, from which 9 % are previous to 2000.

The results show statistically significant strong positive correlation between PNC and PM_{10} ($r = 0.76$, $p < 0.01$) and moderate positive correlation between PNC and nitrogen oxides (NO , NO_2 and NO_x), with Pearson coefficients 0.55, 0.51 and 0.59, respectively, all statistically significant (p -values < 0.01). However, probably due to the reduced number of sampling hours, in Entrecampos correlations between nitrogen oxides and PNC were not statistically significant.

Wind speed, even though monitored at IPMA Gago Coutinho weather station which is relative far (up to a few kilometres from the sampling sites), show different associations with PNC: negative moderate correlation in Av. da Liberdade ($r = -0.48$, $p = 0.03$) and positive strong correlation in Entrecampos ($r = 0.74$, $p = 0.04$). Entrecampos is relatively close to the airport and below the landing / take-off path, which might have influenced this result. For buoyant (aircraft) plumes, higher wind speeds promote faster ground arrival, counterbalancing the dispersion and leading to higher PNC levels.

5.2 LISBON AIRPORT

The results indicate that particle count increases with the number of flights and decreases with the distance to the runway and the altitude of aircrafts relative to the sampling site. Peak values of particle number count also increase with wind speed. Results show high positive correlations between PNC values and the number of flights ($r=0.90$) and that air traffic contributes to elevated PNC values downwind to the airport, especially for take-offs. Moreover, in the vicinity of the Lisbon Airport, under the landing path, mode values are higher than $100 \times 10^3 \text{ pt.cm}^{-3}$. This statistic value drops to values lower than $20 \times 10^3 \text{ pt.cm}^{-3}$ in other sites. Close to the airport south boundary (sites 3 and 5, approximately 300 m west and east to runway, respectively) PNC 10-minutes averages increased by 18 to 26-fold, compared to the PNC 10-minutes averages recorded without landing and take-off cycles. Still in the vicinity of LA but further away, until 1200 m, the PNC increase is around 4-fold. A particular case is site 6. This site is located close to LA (610 m) in a terrain depression in comparison to the LA baseline. This particular orography affects the aircraft plume dispersion leading to PNC increases by 7-fold, almost twice the increase found in site 7, closer to LA (500 m), but a few meters higher than site 6. Even at the furthest point of LA on the landing route (site 13), at a 5th floor, far from the direct influence of road traffic and under thermal inversion conditions, the influence of aircraft traffic was reflected on the increase of the 10-minutes PNC average, by a 16-fold, compared to the period without flights.

Regarding the aircraft's type (long-haul flights *versus* low/medium-haul flights), associated with large and small aircrafts, respectively, data showed no differences on PNC.

These results highlight that people working or living nearby (up to approximately 1.5 km) the Lisbon Airport are exposed to high PNC values. Also, people working in the airport are expected to be exposed to even higher PNC levels for 8-hours periods, 5 days per week. Additionally, passengers spend considerable periods in terminals, although for shorter periods. Nevertheless, their UFP exposure were compared to be equivalent to approximately 11-hours of exposure to regular urban environment (Ren *et al.*, 2018). Furthermore, the number of flights is expected to continue increasing over the next years, leading to an increase in UFP emissions. Technical protection measures should be considered in order to improve indoor air quality in terminals. Furthermore, future airports construction should take in account these results and implement technical measures to mitigate their effect on workers, passengers and nearby population.

5.3 IN-LAND PASSENGER FERRIES

The results point out that PNC increases with the number of ferry operations during the minutes before or after arrivals or departures, respectively. The highest PNC was recorded in Cacilhas, where average PNC, three minutes after departures, was $40 \times 10^3 \text{ pt.cm}^{-3}$. The lowest was recorded in Montijo, $15 \times 10^3 \text{ pt.cm}^{-3}$, also three minutes after departures. Both Barreiro and Seixal present similar figures, approximately $20 \times 10^3 \text{ pt.cm}^{-3}$, four and five minutes after departures, respectively. Mode values among sites are similar.

Results show moderate to high positive correlations between PNC values and the number of ferry trips ($r = 0.79$ to $r = 0.94$). Ferries contribute to short-time elevated PNC values downwind to the ferries' navigation paths, especially for departures. Except for Seixal, there are significant differences in PNC averages between periods with and without ferry operations. This fact highlights that UFP emitted by ferries contribute to PNC increase. High negative correlations ($r = -0.85$ and $r = -0.93$) between PNC and wind intensity were also found.

Regarding ferries' class and age, higher PNC values were found for older engines or more powerful engines. However, the gas exhausting system in oldest ferries is located on top of the ferry, which promotes better plume dispersion. For this reason, this result must be looked at with caution. Regarding catamarans class Damen, higher PNC was found downwind and along the cruising path ($30 \times 10^3 \text{ pt.cm}^{-3}$ to $35 \times 10^3 \text{ pt.cm}^{-3}$) than in ferries' terminals. This result highlights that, for catamarans, UFP emissions during navigation are higher than during manoeuvring and hoteling. Therefore, downwind and under very weak wind (6 to 8 km.h^{-1}) conditions, PNC along shore path is expected to be higher than in ferries' terminals.

Finally, to the best of our knowledge, there are no published studies on PNC emitted by small in-land water bodies ferries. Therefore, our findings could not be properly compared to other results, and the current paper makes a unique contribution for a better understanding of the air quality impacts of this transport mode.

These results highlight that people working in ferry stations or living downwind, along the navigation path, are exposed to high PNC values. Additionally, most passengers use ferries on a daily basis as a commutant mode, although for shorter periods. Nevertheless, their exposure to UFP during the period of permanence in station should not be neglected. Obtained results reveal the possibility of using the developed methodology to monitor the exposure to ultrafine particles in the surrounding urban area of in-land passenger ferries, namely in the present context of increasing number of ferry movement on Tagus river.

5.4 ANSWERS TO RESEARCH QUESTIONS

This section presents more detailed conclusions, summarizing the answers to the research questions identified in the beginning of the research work.

RQ1: Regarding vehicles, aircrafts and ferries traffic, what are the UFP levels in Lisbon in the proximity of these sources?

This first research question was one of the main motivations for this work. Up to the date, there was no evaluation of UFP levels in Lisbon. Unfortunately, PM_{10} and nitrogen dioxide limit values have been exceeded very often in some air quality monitoring stations. As discussed in Chapter 4, these atmospheric pollutants are related with PNC levels. Also, as presented in Chapter 2, both road traffic and airports have been pointed as significant sources of UFP. Moreover, maritime transport is also an important source of UFP. Still, there is a lack of studies on passenger in-land ship transport-related UFP emissions.

The developed work allows us to conclude that vehicles are an important contributor to PNC levels, especially in zones with intense traffic flows. Very frequently (as obtained by mode values) PNC levels ranged from $10.2 \times 10^3 \text{ pt.cm}^{-3}$ to $15.6 \times 10^3 \text{ pt.cm}^{-3}$. PNC concentrations associated to ferries were similar, with the most frequent values ranging from $10.1 \times 10^3 \text{ pt.cm}^{-3}$ to $11.7 \times 10^3 \text{ pt.cm}^{-3}$. Aircrafts are responsible for much higher PNC values. In the vicinity of the Lisbon Airport, mode values were higher than 10^5 pt.cm^{-3} (landing path). Zones further away to the airport, lateral to it and under the take-off path, had lower mode values ($12.3 \times 10^3 \text{ pt.cm}^{-3}$ to $17.1 \times 10^3 \text{ pt.cm}^{-3}$). However, they are slightly higher than the ones associated with vehicles and ferries traffic. Regarding peak values (1-minute PNC means), the higher values are found in the vicinity of LA, followed by the vicinity of ferries docks and shores along their pathway, and finally at roadsides.

RQ2: How can we design appropriate monitoring techniques to evaluate UFP levels at roadside, airport landing and take-off pathways, and close to ferries stations?

The specificity of the locations of transport infrastructures in the city of Lisbon and in the surrounding estuary areas, its geography, and the absence of former PNC monitoring campaigns, required a framework methodology that had to combine limitations from both meteorological and locations accessibility. We applied general standard procedures of air quality monitoring, such as:

- 1) Preliminary evaluation – based on literature, identification and selection of the traffic-related main sources of ultrafine particles in Lisbon;
- 2) Selection of best sampling locations – as described in Chapter 3, several sites in the vicinity of the three different sources were chosen, covering the surrounding area (LA), roads with high intensity of traffic, and ferry docks, and
- 3) Selection of specific monitoring periods – sampling periods were chosen according to meteorological forecast and expected traffic intensity.

If the evaluation of the highest levels is the primary goal, sampling has to be carried out downwind of the source. Considering the particularity of fast growing of ultrafine particles once they are released into atmosphere, sampling sites should be as close to the emission sources as possible. Sites successively

further away from the source, will allow to assess the area affected. During sampling periods, complementary information should be also measured or recorded:

- 1) meteorological conditions, in particular wind speed and wind direction;
- 2) vehicles counting and typology:
 - i) Road traffic – differentiation according to fuel source and type of vehicle (light passenger, heavy passenger, taxi, light-duty, heavy-duty, ...);
 - ii) Aircrafts – recording of all take-offs and landings and respective haul type;
 - iii) Ferries – recording of all arrivals and departures and respective model of ferries
- 3) record all specific events which might affect measurements (e.g. tobacco smoke, old automobiles)

Ideally, sampling period should cover a large variety of traffic intensity, hours of the day, and seasons.

We clearly identified “hotspots” related to the three transport types under study. Monitoring campaigns should allow to assess both average and peak exposure of people to UFP, even though in this thesis the main driver was to evaluate the high exposure levels. Therefore, locations close to the sources where people spend a considerable amount of time (e.g. home and work) must be monitored, allowing epidemiological studies to evaluate both long-time and short-time exposures.

RQ3: How do meteorological conditions affect UFP monitoring?

As mentioned in Chapter 1 and detailed in Chapter 2, meteorological conditions affect ambient atmospheric concentration of pollutants. The ability to measure the plume emitted by a source (aircraft, automobile or ferry) strongly depends on the meteorological conditions, namely on the wind direction. The closer to the plume’s centreline we are, the higher PNC we are able to measure and, therefore, identify the maximum PNC levels that population is exposed to. On the other hand, calm wind (breeze) reduces atmospheric pollutants dispersion, and allows measurements of higher PNC levels. Moderate winds, particularly in the case of the plumes emitted by aircrafts, promote a faster transport of their atmospheric pollutants to the ground, lessening dispersion and enabling their peak PNC levels measurement. However, moderate winds tend to reduce PNC readings since the plume easily disperses throughout a larger area and volume. High relative humidity enables fast growth of UFP size and decreases their counting. Precipitation promotes wet deposition and also decreases PNC. Finally, higher temperatures are usually associated with ascendant convective air movements, which also leads to lower PNC levels monitored at the surface.

RQ4: Is it possible to establish and quantify relationships between UFP levels and traffic intensity (vehicles, aircrafts and ferries)?

Our findings clearly indicate that PNC increases with traffic intensity for the different transport modes under evaluation (Pearson's correlation coefficients of 0.76, 0.90 and 0.79 to 0.94, between PNC and number of vehicles, aircrafts and ferries, respectively). In streets where traffic is very intense and flows slower (e.g. Av. da Liberdade), UFP concentrations are systematically high, and the PNC levels depend more on the type and age of the vehicles. Regarding air traffic, take-offs are responsible for higher PNC increases than landings. Up to approximately 1200 m to runway 03, downwind to the airport, 10-minute PNC means increases vary from 26 to 4-fold, when compared to 10-minutes PNC levels recorded without LTO cycles. Also, ferries departures are associated with higher PNC levels than arrivals. The higher 1-minute PNC means are found around the third to fifth minute after a ferry departure, when PNC may increase up to 2.5-fold, compared to the lowest 1-minute PNC mean recorded during the immediate eight minutes after a ferry departure.

RQ5: Regarding road traffic, are there any correlations between UFP concentrations and other pollutants monitored by air quality monitoring stations in the vicinity?

We found strong positive correlation between PNC and PM_{10} ($r = 0.76$) and moderate positive correlation between PNC and nitrogen oxides (NO , NO_2 and NO_x), with Pearson's coefficients of 0.55, 0.51 and 0.59, respectively. We did not find correlations between PNC and other atmospheric pollutants monitored in the AQMS. Particularly, in Entrecampos, we did not find significant correlation between $PM_{2.5}$ and PNC. Unfortunately, this atmospheric pollutant is not measured in AQMS of Av. da Liberdade, the most critical in terms of air quality and where the higher traffic-related PNC levels were found. This fact disabled any deeper conclusions concerning correlations between these two pollutants in traffic-related sites, in Lisbon.

5.5 MAIN CONSTRAINTS AND SUGGESTIONS TO FUTURE WORKS

Despite all the rigor and effort during this work, several limitations and constraints were identified, mostly due to the fact that it was an investigation carried out by only one person and the measuring equipment was handled. We highlight:

- Meteorological data should have been measured and recorded simultaneously to sampling at the same location, allowing a more robust analysis between PNC and meteorological variables, mostly temperature, relative humidity and wind speed and direction;
- Difficulties on accessing areas in the vicinity of the airport (particularly aside and under the take-off path) and ferries' terminals;

- Adverse atmospheric conditions narrowed and prevented several scheduled samplings;
- Data from GERTRUDE system (Lisbon's traffic management system) was scarce, insufficient (e.g. it does not distinguish the type and age of vehicles), and difficult to access (only by request to CML);
- The availability of data from the AQMS network with 15-minutes resolution is difficult to get (only by request to CCDR-LVT). Regarding PM, it is only available with 1-hour resolution which dilutes many events occurred during that period;
- There were no previous studies on PNC in Lisbon to compare the results obtained.

Future works should take into account the results from this research and the main the constraints, especially regarding road traffic-related PNC. Idealistically, for each site, sampling should be performed by teams, or by placing the measuring equipment in a secure location, with supervision, and have it assessing for longer periods. The first hypothesis is particularly mandatory for road traffic measurements, where many complementary data is required, and it is impossible to be accomplished by only one person. The second hypothesis is perfectly suitable for aircrafts and ferries related traffic.

Considering road traffic-related PNC characterization, future works should develop and expand this study, comprising similar assessments and analysis. Given our results, suggested line of work is to replicate this study on other traffic “hotspots”, particularly where nitrogen oxides and PM₁₀ ambient concentrations are known to be frequently exceeded. For comparison, we propose parallel measurements in areas far from the influence of major UFP sources. These combined or disaggregated lines of work would allow to mapping road traffic-related PNC levels in Lisbon and provide background values.

Regarding Lisbon Airport, future studies should focus on assessing PNC levels in residential or densely populated neighbour areas, especially the ones located aside the main runway or under the take-off path. The other less frequent traffic pattern (landing from the north and taking-off to the south) should be also evaluated.

Similar works are required to better characterize the influence on PNC of passenger ferries along shore, both downwind and upwind to the ferries' path. Another important source of UFP, not considered in the present study, is the Lisbon Harbour, particularly the high activity of cruise ships. Future works devoted to maritime transport (including both cruises and cargo) will allow to draw an in-depth knowledge of UFP concentrations in Lisbon and the relative contributions of their main sources.

6 REFERENCES

- ACI (2016). Airports Council International. ACI Annual Report 2016. [Available at: https://issuu.com/aciworlworld/docs/ac_i_annual_report_2016, accessed on October, 2017].
- Ackerman AS, Toon OB, Stevens DE, Heymsfield AJ, Ramanathan V, Welton EJ (2000). Reduction of tropical cloudiness by soot. *Sciences* 288(5468), 1042–1047. <https://doi.org/10.1126/science.288.5468.1042>.
- Agudelo-Castañeda, D. M., Teixeira, E. C., Braga, M., Rolim, S. B. A., Silva, L. F. O., Beddows, D. C. S., ... Querol, X. (2019). Cluster analysis of urban ultrafine particles size distributions. *Atmospheric Pollution Research*, 10(1), 45–52. <https://doi.org/10.1016/j.apr.2018.06.006>.
- Albuquerque, P., Gomes, J., Bordado, J. (2012). Assessment of exposure to airborne ultrafine particles in the urban environment of Lisbon, Portugal. *Journal Of The Air & Waste Management Association*, 62(4), 373-380. <https://doi.org/10.1080/10962247.2012.658957>.
- Alver, F., Saraç, B. A., Alver Şahin, Ü. (2018). Estimating of shipping emissions in the Samsun Port from 2010 to 2015. *Atmospheric Pollution Research*, 9, 822–828. <https://doi.org/10.1016/j.apr.2018.02.003>.
- Anenberg, S., Miller, J., Minjares, R., Du, L., Henze, D., Lacey, F., Malley, C., Emberson, L., Franco, V., Klimont, Z., Heyes, C. (2017). Impacts and mitigation of excess diesel-related NO_x emissions in 11 major vehicle markets. *Nature* 545, 467–471. <https://doi.org/10.1038/nature22086>.
- Annavarapu, R. N., Kathi, S. (2016). Cognitive disorders in children associated with urban vehicular emissions. *Environmental Pollution*, 208 (Part A), 74-78. <https://doi.org/10.1016/j.envpol.2015.09.036>.
- APA (2018). Agência Portuguesa do Ambiente - QualAr - Base de Dados Online sobre Qualidade do Ar – Informações – Qualidade do Ar. Restricted access.
- APA (2019). QualAr – Base de Dados Online sobre a Qualidade de Ar. Agência Portuguesa do Ambiente. [Available at: <https://qualar1.apambiente.pt/qualar/index.php?page=8>, accessed in June, 2019].
- Argyropoulos, G., Samara, C., Voutsas, D., Kouras, A., Manoli, E., Voliotis, A., ... Eleftheriadis, K. (2016). Concentration levels and source apportionment of ultrafine particles in road microenvironments. *Atmospheric Environment*, 129, 68–78. <https://doi.org/10.1016/j.atmosenv.2016.01.009>.
- Atkinson, R.W., Kang, S., Anderson, H.R., Mills, I.C., Walton, H.A. (2014). Epidemiological time series studies of PM_{2.5} and daily mortality and hospital admissions: a systematic review and meta-analysis. *Thorax* 69, 660–665. <https://doi.org/10.1038/jes.2014.63>.
- Babu, S. S., Kompalli, S. K., Moorthy, K. K. (2016). Aerosol number size distributions over a coastal semi urban location: Seasonal changes and ultrafine particle bursts. *Science of the Total Environment*, 563–564, 351–365. <https://doi.org/10.1016/j.scitotenv.2016.03.246>.
- Baldauf, R.W., Devlin, R.B., Gehr, P., Giannelli, R., Hassett-Sipple, B., Jung, H., Martini, G., McDonald, J., Sacks, J.D., Walker, K. (2016). Ultrafine particle metrics and research considerations: review of the 2015 UFP workshop. *Int. J. Environ. Res. Public Health* 13 (11). <https://doi.org/10.3390/ijerph13111054>.
- Becceril-Valle, M., Coz, E., Prévôt, A., Moenik, G., Pandis, S., Sánchez de la Campa, A., Alastuey, A., Diaz, A., Pérez, R., Artiñano, B. (2017). Characterization of atmospheric black carbon and co-pollutants in urban and rural areas of Spain. *Atmospheric Environment*, 169, 36-53. <https://doi.org/10.1016/j.atmosenv.2017.09.014>.
- Beckett, K.P., Freersmith, P.H., Taylor, G. (1998). Urban woodlands: their role in reducing the effects of particulate pollution. *Environ. Pollut.* 99 (3), 347–360. [https://doi.org/10.1016/S0269-7491\(98\)00016-5](https://doi.org/10.1016/S0269-7491(98)00016-5).
- Beelen, R., Hoek, G., Raaschou-Nielsen, O., Stafoggia, M., Andersen, Z. J., Weinmayr, G., ... Schwarze, P. E. (2015). Effects of long-term exposure to air pollution on natural-cause mortality: an analysis of 22 European cohorts within the multicentre ESCAPE project. *Lancet* 383, 785–795. <https://doi.org/10.1289/ehp.1408095>.
- Bharadwaj P, Burney J. (2018). Cognition impact of sand and dust storms highlights future research needs? *Lancet Planet Health*. 2(5): e196–e197. [https://doi.org/10.1016/S2542-5196\(18\)30071-8](https://doi.org/10.1016/S2542-5196(18)30071-8).
- Bohren, C. F., Huffman, D. R. (1998). *Absorption and Scattering of Light by Small Particles*, John Wiley & Sons. 544 pp., Weinheim, Germany. doi:10.1002/9783527618156.

- Booth, B., Bellouin, N. (2015). Climate change: Black carbon and atmospheric feedbacks. *Nature*, 519(7542), 167–168. <https://doi.org/10.1038/519167a>.
- Boucher, O., Randall, D., Artaxo, P., Bretherton, C., Feingold, G., Forster, P., Kerminen, V.-M., Kondo, Y., Liao, H., Lohmann, U. (2013.) Clouds and Aerosols, Climate Change 2013: the Physical Science Basis. Contribution of Working Group I to the Fifth Assessment Report of the Intergovernmental Panel on Climate Change. Cambridge University Press, 571–657. [Available online at <https://www.ipcc.ch/report/ar5/wg1/>, last accessed on January, 2019].
- Brimblecombe, P. (1999). Chapter 2 - Air Pollution and Health History. Editor(s): Stephen T. Holgate, Jonathan M. Samet, Hillel S. Koren, Robert L. Maynard. Air Pollution and Health. Academic Press, 5-18. ISBN 9780123523358. <https://doi.org/10.1016/B978-012352335-8/50077-6>.
- Brines, M., Dall'Osto, M., Beddows, D.C.S., Harrison, R.M., Gómez-Moreno, F., Núñez, L., Artíñano, B., Costabile, F., Gobbi, G.P., Salimi, F., ... Querol, X. (2015). Traffic and nucleation events as main sources of ultrafine particles in high-insolation developed world cities. *Atmos. Chem. Phys.* 15 (10), 5929–5945. <https://doi.org/10.5194/acp-15-5929-2015>.
- Buonanno, G., Giovinco, G., Morawska, L., Stabile, L. (2015). Lung cancer risk of airborne particles for Italian population. *Environmental Research*, 142, 443-451. <https://doi.org/10.1016/j.envres.2015.07.019>.
- Campagna, M., Pili, S., Marcias, G., Angius, N., Cocco, P., Frattolillo, A., Mastino, A., Buonanno, G. (2016). Environmental Exposure to Ultrafine Particles inside and nearby a Military Airport. *Atmosphere*, 7(10), 138. <https://doi.org/10.3390/atmos7100138>.
- Carosino, C., Bein, K., Plummer, L., Castaneda, A., Zhao, Y., Wexler, A., Pinkerton K. (2015). Allergic airway inflammation is differentially exacerbated by daytime and nighttime ultrafine and submicron fine ambient particles: Hemeoxygenase-1 as an indicator of PM-mediated allergic inflammation. *J. Toxicol. Environ. Health A.*, 78(4), 254–266. <https://doi.org/10.1080/15287394.2014.959627>.
- Cattani, G., Di Menno di Bucchianico, A., Gaeta, A., Romani, D., Fontana, L., Iavicoli, I. (2014). Airports and air quality: A critical synthesis of the literature. *Epidemiol. Prev.*, 38(3-4), 254–261.
- CCDR-LVT (2016). O ar e os poluentes atmosféricos. Efeitos das condições meteorológicas. [Available at <http://www.ccdr-lvt.pt/pt/o-ar-e-os-poluente-atmosfericos/8082.htm>. [Last accessed in January, 2019].
- César, A., Nascimento, L., Mantovani, K., Pompeo Vieira, L. (2016). Fine Particulate Matter Estimated By Mathematical Model And Hospitalizations For Pneumonia And Asthma In Children. *Revista Paulista de Pediatria (English Edition)*, 34(1), 18–23. <https://doi.org/10.3390/atmos7100138>.
- Cesari, D., Genga, A., Ielpo, P., Siciliano, M., Mascolo, G., Grasso, F. M., Contini, D. (2014). Source apportionment of PM_{2.5} in the harbour–industrial area of Brindisi (Italy): Identification and estimation of the contribution of in-port ship emissions. *Science of the Total Environment*, 497–498, 392–400. <https://doi.org/10.1016/j.scitotenv.2014.08.007>.
- Cesaroni, G., Badaloni, C., Gariazzo, C., Stafoggia, M., Sozzi, R., Davoli, M., Forastiere, F. (2013). Long-Term Exposure to Urban Air Pollution and Mortality in a Cohort of More than a Million Adults in Rome. *Environmental Health Perspectives*, 121(3), 324–331. <https://doi.org/10.1289/ehp.1205862>.
- Chen, D., Zhao, Y., Nelson, P., Li, Y., Wang, X., Zhou, Y., ... Guo, X. (2016). Estimating ship emissions based on AIS data for port of Tianjin, China. *Atmospheric Environment*, 145, 10–18. <https://doi.org/10.1016/j.atmosenv.2016.08.086>.
- Chen, H.; Goldberg, M. S.; Villeneuve, P. J. (2008). A systematic review of the relation between long-term exposure to ambient air pollution and chronic diseases. *Reviews on Environmental Health*. 23(4), 243–97. <https://www.ncbi.nlm.nih.gov/pubmed/19235364>.
- Chen, H., Kwong, J., Copes, R., Tu, K., Villeneuve, P., van Donkelaar, A., Hystad, P., Martin, R., Murray, B., Jessiman, B., Wilton, A., Kopp, A., Burnett, R. (2017). Living near major roads and the incidence of dementia, Parkinson's disease, and multiple sclerosis: a population-based cohort study. *Lancet* 389, 718–726, [https://doi.org/10.1016/S0140-6736\(16\)32399-6](https://doi.org/10.1016/S0140-6736(16)32399-6).
- Cheung, K. L., Ntziachristos, L., Tzankiozis, T., Schauer, J. J., Samaras, Z., Moore, K. F., and Sioutas, C. (2010). Emissions of particulate trace elements, metals and organic species from gasoline, diesel, and biodiesel passenger vehicles and their relation to oxidative potential. *Aerosol Sci. Tech.*, 44, 500–513, <https://doi.org/10.1080/02786821003758294>.

- Cho, A. K., Sioutas, C., Miguel, A. H., Kumagai, Y., Schmitz, D. A., Singh, M., Eiguren-Fernandez, A., Froines, J. R. (2005). Redox activity of airborne particulate matter at different sites in the Los Angeles Basin. *Environmental Research*, 99, 40. 47. <https://doi.org/10.1016/j.envres.2005.01.00>.
- Chou, C. C.-K., Lee, C.-T., Chen, W.-N., Chang, S.-Y., Chen, T.-K., Lin, C.-Y., Chen, J.-P. (2007). Lidar observations of the diurnal variations in the depth of urban mixing layer: A case study on the air quality deterioration in Taipei, Taiwan. *Science of the Total Environment*, Vol. 374, 156-166. <https://doi.org/10.1016/j.scitotenv.2006.11.049>.
- Chu, D.A., Kaufman, Y.J., Zibordi, G., Chern, J.D., Mao, J., Li, C., Holben, B.N. (2003). Global monitoring of air pollution over land from the earth observing system-terra moderate resolution imaging spectroradiometer (MODIS). *J. Geophys. Res. Atmos.* 108 (4661), D21. <https://doi.org/10.1029/2002JD003179>.
- Cimini, D., Angelis, F. D., Dupont, J.-C., Pal, S., Haeffelin, M. (2013). Mixing layer height retrievals by multichannel microwave radiometer observations. *Atmospheric Measurement Techniques*. Vol. 6, 2941 – 2951. <https://doi.org/10.5194/amt-6-2941-2013>.
- CML (2015). Câmara Municipal de Lisboa – Viver – Mobilidade – Zonas Emissões Reduzidas. Available on <http://www.cm-lisboa.pt/viver/mobilidade/zonas-emissoes-reduzidas>. [Accessed on July 2018].
- Cullinane, K., Cullinane, S. (2013). Atmospheric Emissions from Shipping: The Need for Regulation and Approaches to Compliance. *Transport Reviews*, 33(4), 377–401. <https://doi.org/10.1080/01441647.2013.806604>.
- Daher, N., Saliba, N. A., Shihadeh, A. L., Jaafar, M., Baalbaki, R., Sioutas, C. (2013). Chemical composition of size-resolved particulate matter at near-freeway and urban background sites in the greater Beirut area. *Atmospheric Environment*, 80, 96–106. <https://doi.org/10.1016/j.atmosenv.2013.08.004>.
- Dahl, A., Gharibi, A., Swietlicki, E., Gudmundsson, A., Bohgard, M., Ljungman, A., ... Gustafsson, M. (2006). Traffic-generated emissions of ultrafine particles from pavement–tire interface. *Atmospheric Environment*, 40(7), 1314–1323. <https://doi.org/10.1016/j.atmosenv.2005.10.029>.
- de Hoogh, K., H  ritier, H., Stafoggia, M., K  nzli, N., Kloog, I. (2018). Modelling daily PM_{2.5} concentrations at high spatio-temporal resolution across Switzerland. *Environ. Pollut.* 233, 1147–1154. <https://doi.org/10.1016/j.envpol.2017.10.025>.
- de Jesus, A. L., Rahman, M. M., Mazaheri, M., Thompson, H., Knibbs, L. D., Jeong, C., ... Morawska, L. (2019). Ultrafine particles and PM_{2.5} in the air of cities around the world: Are they representative of each other? *Environment International*, 129, 118–135. <https://doi.org/10.1016/j.envint.2019.05.021>.
- de Nazelle, A., Bode, O., Orjuela, J. (2017). Comparison of air pollution exposures in active vs. passive travel modes in European cities: a quantitative review. *Environ. Int.* 99, 151–160. <https://doi.org/10.1016/j.envint.2016.12.023>.
- de Nazelle, A., Fruin, S., Westerdahl, D., Martinez, D., Ripoll, A., Kubesch, N., Nieuwenhuijsen, M. (2012). A travel mode comparison of commuters' exposures to air pollutants in Barcelona. *Atmospheric Environment*, 59, 151–159. <https://doi.org/10.1016/j.atmosenv.2012.05.013>.
- Decesari, S., Sowlat, M. H., Hasheminassab, S., Sandrini, S., Gilardoni, S., Facchini, M. C., ... Sioutas, C. (2017). Enhanced toxicity of aerosol in fog conditions in the Po Valley, Italy. *ATMOSPHERIC CHEMISTRY AND PHYSICS*, 17(12), 7721–7731. <https://doi.org/10.5194/acp-17-7721-2017>.
- Di, Q., Kloog, I., Koutrakis, P., Schwartz, J., Lyapustin, A., Wang, Y. (2016). Assessing PM_{2.5} Exposures with High Spatiotemporal Resolution across the Continental United States. *Environmental Science and Technology*, 50(9), 4712–4721. <https://doi.org/10.1021/acs.est.5b06121>.
- Donateo, A., Gregoris, E., Gambaro, A., Merico, E., Giua, R., Nocioni, A., Contini, D. (2014). Contribution of harbour activities and ship traffic to PM_{2.5}, particle number concentrations and PAHs in a port city of the Mediterranean Sea (Italy). *Environmental Science & Pollution Research*, 21(15), 9415. <https://doi.org/10.1007/s11356-014-2849-0>.
- dos Santos-Juusela, V., Pet  j  , T., Kousa, A., H  meri, K. (2013). Spatial–temporal variations of particle number concentrations between a busy street and the urban background. *Atmospheric Environment*, 79324-333. <https://doi.org/10.1016/j.atmosenv.2013.05.077>.
- Ebisu, K., Berman, J., Bell, M. (2016). Exposure to coarse particulate matter during gestation and birth weight in the U.S. *Environment International*, 94, pp.519-524. <https://doi.org/10.1016/j.envint.2016.06.011>.
- EEA (2014). Air quality in Europe – 2014 report. [Available at: <https://www.eea.europa.eu/publications/air-quality-in-europe-2014>, last accessed on January, 2019].
- EEA (2015). Air quality in Europe – 2015 report. [Available at: <https://www.eea.europa.eu/publications/air-quality-in-europe-2015>, last accessed on January, 2019].

- EEA (2016). European Environmental Agency. European Aviation Environmental Report 2016. [Available at: <https://ec.europa.eu/transport/sites/transport/files/european-aviation-environmental-report-2016-72dpi.pdf>, accessed on September, 2017].
- EEA (2018a). Air quality in Europe — 2018 report, EEA Report No 12/2018, European Environment Agency. [Available at: <https://www.eea.europa.eu/publications/air-quality-in-europe-2018>, accessed on January, 2019].
- EEA (2018b). Outdoor air quality in urban areas. [Available on <https://www.eea.europa.eu/airs/2018/environment-and-health/outdoor-air-quality-urban-areas>, accessed on January 2019].
- EEA (2018c). Exceedance of air quality standards in urban areas (CSI 004). [Available on <https://www.eea.europa.eu/data-and-maps/indicators/exceedance-of-air-quality-limit-3/assessment-4>, accessed on October 2018].
- Eeftens, M., Phuleria, H. C., Meier, R., Aguilera, I., Corradi, E., Davey, M., ... Tsai, M.-Y. (2015). Spatial and temporal variability of ultrafine particles, NO₂, PM_{2.5}, PM_{2.5} absorbance, PM₁₀ and PM_{coarse} in Swiss study areas. *Atmospheric Environment*, 111, 60–70. <https://doi.org/10.1016/j.atmosenv.2015.03.031>.
- Endresen, Ø., Sørsgård, E., Sundet, J.K., Dalsøren, S.B., Isaksen, I.S., Berglen, T.F., Gravir, G. (2003). Emission from international sea transportation and environmental impact. *J. Geophys. Res.: Atmosphere* 108 (D17). <https://doi.org/10.1029/2002JD002898>.
- Engel-Cox, J.A., Holloman, C.H., Coutant, B.W., Hoff, R.M. (2004). Qualitative and quantitative evaluation of MODIS satellite sensor data for regional and urban scale air quality. *Atmos. Environ.* 38 (16), 2495–2509. <https://doi.org/10.1016/j.atmosenv.2004.01.039>.
- EU (2008). Directive 2008/50/EC of the European Parliament and of the Council of 21 May 2008 on ambient air quality and cleaner air for Europe. [Available at <https://eur-lex.europa.eu/legal-content/en/ALL/?uri=CELEX:32008L0050>, accessed on January, 2019].
- Eurostat (2016). Urban Europe—Statistics on cities, towns and suburbs — Eurostat [Available at: <http://ec.europa.eu/eurostat/documents/3217494/7596823/KS-01-16-691-EN-N.pdf/0abf140c-ccc7-4a7f-b236-682effcde10f>], accessed 14 June, 2018.
- Ezz, W., Mazaheri, M., Robinson, P., Johnson, G., Clifford, S., He, C., Morawska, L., Marks, G. (2015). Ultrafine Particles from Traffic Emissions and Children's Health (UPTech) in Brisbane, Queensland (Australia): Study Design and Implementation. *International Journal of Environmental Research and Public Health*, 12(2), 1687-1702. <https://doi.org/10.3390/ijerph120201687>.
- FCT-NOVA (2017). Inventário de Emissões Atmosféricas da Região de Lisboa e Vale do Tejo | 2011 – 2014. CCDR LVT, Maio 2017. [Available at: <http://www.ccdr-lvt.pt/files/>, accessed on May, 2018].
- Ferreira, A., Cemlyn-Jones, J., Cordeiro, C. (2013). Nanoparticles, nanotechnology and pulmonary nanotoxicology. *Rev. Portuguesa Pneumol.*, 19, 28–37. <https://doi.org/10.1016/j.rppneu.2012.09.003>.
- Ferreira, F., Gomes, P., Tente, H., Carvalho, A., Pereira, P., Monjardino, J. (2015). Air quality improvements following implementation of Lisbon's Low Emission Zone. *Atmospheric Environment*, 12, 2373-381. <https://doi.org/10.1016/j.atmosenv.2015.09.064>.
- Fiore, A.M., Naik, V., Spracklen, D.V., Steiner, A., Unger, N., Prather, M., Bergmann, D., Cameron-Smith, P.J., Cionni, I., Collins, W.J., Eyring, V., Folberth, G.A., Ginoux, P., Horowitz, L.W., Josse, B., Lamarque, J.-F., MacKenzie, I.A., Nagashima, T., O'Connor, F.M., Righi, M., Rumbold, S.T., Shindell, D.T., Skeie, R.B., Sudo, K., Szopa, S., Takemura, T., Zeng, G. (2012). Global air quality and climate. *Chem. Soc. Rev.* 41, 6663–6683. DOI: [10.1039/C2CS35095E](https://doi.org/10.1039/C2CS35095E).
- Fu, M., Ding, Y., Ge, Y., Yu, L., Yin, H., Ye, W., Liang, B. (2013). Real-world emissions of inland ships on the Grand Canal, China. *Atmospheric Environment*, 81, 222–229. <https://doi.org/10.1016/j.atmosenv.2013.08.046>.
- Fujitani, Y., Kumar, P., Tamura, K., Fushimi, A., Hasegawa, S., Takahashi, K., Tanabe, K., Kobayashi, S., Hirano, S., 2012. Seasonal differences of the atmospheric particle size distribution in a metropolitan area in Japan. *Sci. Total Environ.* 437, 339–347. <https://doi.org/10.1016/j.scitotenv.2012.07.085>.
- Fuller, C.H., Brugge, D., Williams, P.L., Mittleman, M.A., Durant, J.L., Spengler, J.D., 2012. Estimation of ultrafine particle concentrations at near-highway residences using data from local and central monitors. *Atmos. Environ.* 57, 257–265. <http://dx.doi.org/10.1016/j.atmosenv.2012.04.004>.
- Gakidou, E., Afshin, A., Abajobir, A. A., Abate, K. H., Abbafati, C., Abbas, K. M., ... Murray, C. J. L. (2017). Global, regional, and national comparative risk assessment of 84 behavioural, environmental and occupational, and

- metabolic risks or clusters of risks, 1990–2016: a systematic analysis for the Global Burden of Disease Study 2016. [https://doi.org/10.1016/S0140-6736\(17\)32366-8](https://doi.org/10.1016/S0140-6736(17)32366-8).
- Gasparotto, J., Somensi, N., Caregnato, F. F., Rabelo, T. K., DaBoit, K., Oliveira, M. L. S., ... Gelain, D. P. (2013). Coal and tire burning mixtures containing ultrafine and nanoparticulate materials induce oxidative stress and inflammatory activation in macrophages. *Science of the Total Environment*, 463–464, 743–753. <https://doi.org/10.1016/j.scitotenv.2013.06.086>.
- Geiser, M., Rothen-Rutishauser, B., Kapp, N., Schürch, S., Kreyling, W., Schulz, H., Semmler, M., Hof, V., Heyder, J., Gehr, P. (2005). Ultrafine Particles Cross Cellular Membranes by Nonphagocytic Mechanisms in Lungs and in Cultured Cells. *Environmental Health Perspectives*, 113(11), 1555–1560. <https://doi.org/10.1289/ehp.8006>.
- Giechaskiel, B., Chirico, R., DeCarlo, P.F., Clairotte, M., Adam, T., Martini, G., Heringa, M.F., Richter, R., Prevot, A.S.H., Baltensperger, U. (2010). Evaluation of the particle measurement Programme (PMP) protocol to remove the vehicles' exhaust aerosol volatile phase. *Sci. Total Environ.* 408 (no. 21), 5106–5116. <http://dx.doi.org/10.1016/j.scitotenv.2010.07.010>.
- Giechaskiel, B., Riccobono, F., Vlachos, T., Mendoza-Villafuerte, P., Suarez-Bertoa, R., Fontaras, G., Bonnel, P., Weiss, M. (2015). Vehicle Emission Factors of Solid Nanoparticles in the Laboratory and on the Road Using Portable Emission Measurement Systems (PEMS). *Front. Environ. Sci.* 3:82. <https://doi.org/10.3389/fenvs.2015.00082>.
- Goel, A., Kumar, P. (2014). A review of fundamental drivers governing the emissions, dispersion and exposure to vehicle-emitted nanoparticles at signalised traffic intersections. *Atmos. Environ.* 97, 316–331. <https://doi.org/10.1016/j.atmosenv.2014.08.037>.
- Goel, A., Kumar, P. (2015). Characterisation of nanoparticle emissions and exposure at traffic intersections through fast-response mobile and sequential measurements. *Atmospheric Environment*, 107, 374–390. <https://doi.org/10.1016/j.atmosenv.2015.02.002>.
- Góis, V., Maciel, H., Torres, P., Mesquita, S., Ferreira, F., Almeida, C., Nogueira, L. (2007). A Detailed Urban Road Traffic Emissions Inventory Model Using Aerial Photography and GPS Survey - 16th Annual International Emission Inventory Conference - Emission Inventories: Integration, Analysis, and Communications. Estados Unidos da América, Raleigh. Maio de 2007. Available at: <https://www3.epa.gov/ttn/chief/conference/ei16/session9/gois.pdf>, accessed on January, 2019].
- Goldberg, D. L., Gupta, P., Wang, K., Jena, C., Zhang, Y., Lu, Z., Streets, D. G. (2019). Using gap-filled MAIAC AOD and WRF-Chem to estimate daily PM_{2.5} concentrations at 1 km resolution in the Eastern United States. *Atmospheric Environment*, 199, 443–452. <https://doi.org/10.1016/j.atmosenv.2018.11.049>.
- Gomes, J., Bordado, J., Albuquerque, P. (2012). Monitoring exposure to airborne ultrafine particles in Lisbon, Portugal. *Inhalation Toxicology*, 24(7), 425–433. <https://doi.org/10.3109/08958378.2012.684077>.
- González, Y., Rodríguez, S. (2013). A comparative study on the ultrafine particle episodes induced by vehicle exhaust: A crude oil refinery and ship emissions. *Atmospheric Research*, 120–121, 43–54. <https://doi.org/10.1016/j.atmosres.2012.08.001>.
- González, Y., Rodríguez, S., Guerra García, J. C., Trujillo, J. L., García, R. (2011). Ultrafine particles pollution in urban coastal air due to ship emissions. *Atmospheric Environment*, 45(28), 4907–4914. <https://doi.org/10.1016/j.atmosenv.2011.06.002>.
- Googlemaps (2018). Google.pt Available at: <https://www.google.pt/maps> [Accessed on April 2018].
- Grana, M., Toschi, N., Vicentini, L., Pietroiusti, A., Magrini, A. (2017). Exposure to ultrafine particles in different transport modes in the city of Rome. *Environmental Pollution*, 228, 201–210. <https://doi.org/10.1016/j.envpol.2017.05.032>.
- Grundström, M., Hak, C., Chen, D., Hallquist, M., Pleijel, H. (2015). Variation and co-variation of PM₁₀, particle number concentration, NO_x and NO₂ in the urban air – Relationships with wind speed, vertical temperature gradient and weather type. *Atmospheric Environment*. Vol. 120, 317 – 327. <https://doi.org/10.1016/j.atmosenv.2015.08.057>.
- Gupta, P., Christopher, S.A. (2009). Particulate matter air quality assessment using integrated surface, satellite, and meteorological products: multiple regression approach. *J. Geophys. Res. Atmos.* 114, D14205. <https://doi.org/10.1029/2008JD011496>.
- Gupta, P., Christopher, S.A., Wang, J., Gehrig, R., Lee, Y.C., Kumar, N. (2006). Satellite remote sensing of particulate matter and air quality assessment over global cities. *Atmos. Environ.* 40 (30), 5880–5892. <https://doi.org/10.1016/j.atmosenv.2006.03.016>.
- Gustafsson, M., Blomqvist, G., Gudmundsson, A., Dahl, A., Swietlicki, E., Bohgard, M., ... Ljungman, A. (2008). Properties and toxicological effects of particles from the interaction between tyres, road pavement and winter

traction material. Science of the Total Environment, 393(2), 226–240. <https://doi.org/10.1016/j.scitotenv.2007.12.030>.

- Habre, R., Zhou, H., Eckel, S. P., Enebish, T., Fruin, S., Bastain, T., Rappaport, E., Gilliland, F. (2018). Short-term effects of airport-associated ultrafine particle exposure on lung function and inflammation in adults with asthma. *Environment International*, 118, 48–59. <https://doi.org/10.1016/j.envint.2018.05.031>.
- Hagler, G. S. W., Lin, M.-Y., Khlystov, A., Baldauf, R. W., Isakov, V., Faircloth, J., Jackson, L. E. (2012). Field investigation of roadside vegetative and structural barrier impact on near-road ultrafine particle concentrations under a variety of wind conditions. *Science of the Total Environment*, 419, 7–15. <https://doi.org/10.1016/j.scitotenv.2011.12.002>.
- Ham, W., Vijayan, A., Schulte, N., Herner, J. D. (2017). Commuter exposure to PM_{2.5}, BC, and UFP in six common transport microenvironments in Sacramento, California. *Atmospheric Environment*, 167, 335–345. <https://doi.org/10.1016/j.atmosenv.2017.08.024>.
- Hama, S. M. L., Cordell, R. L., Kos, G. P. A., Weijers, E. P., Monks, P. S. (2017b). Sub-micron particle number size distribution characteristics at two urban locations in Leicester. *Atmospheric Research*, 194, 1–16. <https://doi.org/10.1016/j.atmosres.2017.04.021>.
- Hama, S. M. L., Cordell, R. L., Monks, P. S. (2017a). Quantifying primary and secondary source contributions to ultrafine particles in the UK urban background. *Atmospheric Environment*, 166, 62–78. <https://doi.org/10.1016/j.atmosenv.2017.07.013>.
- Haywood, J. and Boucher, O. (2000). Estimates of the direct and indirect radiative forcing due to tropospheric aerosols: a review. *Rev. Geophys.*, 38, 513–543. <https://doi.org/10.1029/1999RG000078>.
- He, R.-W., Shirmohammadi, F., Gerlofs-Nijland, M. E., Sioutas, C., Cassee, F. R. (2018). Pro-inflammatory responses to PM_{0.25} from airport and urban traffic emissions. *Science of the Total Environment*, 640–641, 997–1003. <https://doi.org/10.1016/j.scitotenv.2018.05.382>.
- Healy, R. M., O'Connor, I. P., Hellebust, S., Allan, A., Sodeau, J. R., Wenger, J. C. (2009). Characterisation of single particles from in-port ship emissions. *Atmospheric Environment*, 43(40), 6408–6414. <https://doi.org/10.1016/j.atmosenv.2009.07.039>.
- HEI (2013) Review Panel on Ultrafine Particles. HEI Perspectives 3: Understanding the Health Effects of Ambient Ultrafine Particles. Boston, MA: Health Effects Institute. [Available at: <https://www.healtheffects.org/system/files/Perspectives3.pdf>, accessed on September, 2017].
- Hennig, F., Quass, U., Hellack, B., Küpper, M., Kuhlbusch, T. J., Stafoggia, M., Hoffmann, B. (2018). Ultrafine and Fine Particle Number and Surface Area Concentrations and Daily Cause-Specific Mortality in the Ruhr Area, Germany, 2009–2014. *Environmental Health Perspectives*, 126(2), 1–10. <https://doi.org/10.1289/EHP2054>.
- Henriques, R. (2015). Avaliação da implementação da fase III da Zona de Emissões Reduzidas de Lisboa. Dissertação para a obtenção do Grau de Mestre em Engenharia do Ambiente, Perfil de Engenharia de Sistemas Ambientais. Faculdade de Ciências e Tecnologia da Universidade Nova de Lisboa.
- Hodnebrog, Ø., Myhre, G., Samset, B. H. (2014). How shorter black carbon lifetime alters its climate effect. *Nature Communications*, 5(9), 5065. <https://doi.org/10.1038/ncomms6065>.
- Hoek, G., Beelen, R., De Hoogh, K., Vienneau, D., Gulliver, J., Fischer, P., Briggs, D. (2008). A review of land-use regression models to assess spatial variation of outdoor air pollution. *Atmos. Environ.* 42 (33), 7561–7578. <https://doi.org/10.1016/j.atmosenv.2008.05.057>.
- Hofman, J., Staelens, J., Cordell, R., Stroobants, C., Zikova, N., Hama, S., Wyche, K., Kos, G., Van Der Zee, S., Smallbone, K., Weijers, E., Monks, P., Roekens, E. (2016). Ultrafine Particles In Four European Urban Environments: Results from a new continuous long-term monitoring network. *Atmospheric Environment*, 136, pp.68–81. <https://doi.org/10.1016/j.atmosenv.2016.04.010>.
- Holland, M (2014). Cost-benefit Analysis of Final Policy Scenarios for the EU Clean Air Package. Version 2 (Corresponding to IIASA TSAP Report #11, Version 2a). [Available at: http://ec.europa.eu/environment/air/pdf/TSAP_CBA.pdf, accessed on September, 2018].
- Hsu, H., Adamkiewicz, G., Andres Houseman, E., Vallarino, J., Melly, S., Wayson, R., Spengler, J., Levy, J. (2012). The relationship between aviation activities and ultrafine particulate matter concentrations near a mid-sized airport. *Atmospheric Environment*, 50, 328–337. <https://doi.org/10.1016/j.atmosenv.2011.12.002>.

- Hsu, H., Adamkiewicz, G., Houseman, E., Spengler, J., Levy, J. (2014). Using Mobile Monitoring To Characterize Roadway And Aircraft Contributions To Ultrafine Particle Concentrations Near A Mid-Sized Airport. *Atmospheric Environment*, 89, 688–695. <https://doi.org/10.1016/j.atmosenv.2014.02.023>.
- Hsu, H., Adamkiewicz, G., Houseman, E., Zarubiak, D., Spengler, J., Levy, J. (2013). Contributions Of Aircraft Arrivals And Departures To Ultrafine Particle Counts Near Los Angeles International Airport. *Science Of The Total Environment*, 444, 347–355. <https://doi.org/10.1016/j.scitotenv.2012.12.010>.
- Huang, C., Tao, S., Lou, S., Hu, Q., Wang, H., Wang, Q., Li, L., Wang, H., Liu, J., Quan, Y., Zhou, L. (2017). Evaluation of emission factors for light-duty gasoline vehicles based on chassis dynamometer and tunnel studies in Shanghai, China. *Atmospheric Environment*, 169, 193–203. <https://doi.org/10.1016/j.atmosenv.2017.09.020>.
- Hudda, N., Gould, T., Hartin, K., Larson, T., Fruin, S. (2014). Emissions from an International Airport Increase Particle Number Concentrations 4-fold at 10 km Downwind. *Environmental Science and Technology*, 48, pp. 6628 –6635. <https://doi.org/10.1021/es5001566>.
- Hudda, N., Simon, M. C., Zamore, W., Brigge, D., Durant, J. L. (2016). Aviation Emissions Impact Ambient Ultrafine Particle Concentrations in the Greater Boston Area. *Environmental Science and Technology*. American Chemical Society, 50(16), 8514–8521. <https://doi.org/10.1021/acs.est.6b01815>.
- Hudda, N., Simon, M. C., Zamore, W., Durant, J. L. (2018). Aviation-Related Impacts on Ultrafine Particle Number Concentrations Outside and Inside Residences near an Airport. *Environmental Science and Technology*, 52(4). <https://doi.org/10.1021/acs.est.7b05593>.
- Hulskotte, J. H. J., Denier van der Gon, H. A. C. (2010). Fuel consumption and associated emissions from seagoing ships at berth derived from an on-board survey. *Atmospheric Environment*, 44, 1229–1236. <https://doi.org/10.1016/j.atmosenv.2009.10.018>.
- Hystad, P., Villeneuve, P., Goldberg, M., Crouse, D., Johnson, K. (2015). Exposure to traffic-related air pollution and the risk of developing breast cancer among women in eight Canadian provinces: a case-control study. *Environ. Int.* 74, 240–248. <https://doi.org/10.1016/j.envint.2014.09.004>.
- IARC (2014). International Agency for Research on Cancer. Diesel and gasoline engine exhausts and some nitroarenes, IARC Monographs on the Evaluation of Carcinogenic Risks to Humans, Vol. 105. [Available at: <https://monographs.iarc.fr/wp-content/uploads/2018/06/mono105.pdf>, accessed on September, 2017].
- ICAO (2011). Airport Air Quality Manual. [Available at: <https://www.icao.int/environmental-protection/Documents/Publications/FINAL.Doc.9889.1st.Edition.alltext.en.pdf>, accessed on December, 2017].
- INE (2011). Censos 2011. [Available at: <http://mapas.ine.pt/map.phtml>, accessed on December, 2018].
- IPCC (2014). Climate Change 2014: Synthesis Report. Contribution of Working Groups I, II and III to the Fifth Assessment Report of the Intergovernmental Panel on Climate Change [Core Writing Team, R.K. Pachauri and L.A. Meyer (eds.)]. IPCC, Geneva, Switzerland, 151 [Available at: https://www.ipcc.ch/site/assets/uploads/2018/05/SYR_AR5_FINAL_full_wcover.pdf, accessed October, 2018].
- Janhäll, S. (2015). Review on urban vegetation and particle air pollution – Deposition and dispersion. *Atmospheric Environment*, 105, 130–137. <https://doi.org/10.1016/j.atmosenv.2015.01.052>.
- Janssen, N. A. H., Yang, A., Strak, M., Steenhof, M., Hellack, B., Gerlofs-Nijland, M. E., ... Cassee, F. (2014). Oxidative potential of particulate matter collected at sites with different source characteristics. *Science of the Total Environment*, 472, 572–581. <https://doi.org/10.1016/j.scitotenv.2013.11.099>.
- Joerger, V., Pryor, S. (2018). Ultrafine particle number concentrations and size distributions around an elevated highway viaduct. *Atmospheric Pollution Research*, 9714-722. <https://doi.org/10.1016/j.apr.2018.01.008>.
- Karjalainen, P., Pirjola, L., Heikkilä, J., Lähde, T., Tzamkiozis, T., Ntziachristos, L., ... Rönkkö, T. (2014). Exhaust particles of modern gasoline vehicles: A laboratory and an on-road study. *Atmospheric Environment*, 97, 262–270. <https://doi.org/10.1016/j.atmosenv.2014.08.025>.
- Karner, A. A., Eisinger, D. S., Niemeier, D. A. (2010). Near-Roadway Air Quality: Synthesizing the Findings from Real-World Data. *ENVIRONMENTAL SCIENCE & TECHNOLOGY*, 44(14), 5334–5344. <https://doi.org/10.1021/es100008x>.
- Keskinen, J., Ronkko, T. (2010). Can Real-World Diesel Exhaust Particle size Distribution be Reproduced in the Laboratory? A Critical Review. *Journal of the Air & Waste Management Association*, 60: 1245-1255. <https://doi.org/10.3155/1047-3289.60.10.1245>.

- Keuken, M., Moerman, M., Voogt, M., Zandveld, P., Verhagen, H., Stelwagen, U., Jonge de, D. (2016). Particle number concentration near road traffic in Amsterdam (the Netherlands): Comparison of standard and real-world emission factors. *Atmospheric Environment*, 132, 345–355. <https://doi.org/10.1016/j.atmosenv.2016.03.009>.
- Keuken, P., Moerman, M., Zandveld, P., Henzing, J. S., Hoek, G. (2015). Total and Size-Resolved Particle Number and Black Carbon Concentrations In Urban Areas Near Schiphol Airport (the Netherlands). *Atmospheric Environment*, 104, 132–142. <https://doi.org/10.1016/j.atmosenv.2015.01.015>.
- Kim, H., Zhang, Q., Heo, J. (2018). Influence of intense secondary aerosol formation and long-range transport on aerosol chemistry and properties in the Seoul Metropolitan Area during spring time: results from KORUS-AQ. *Atmospheric Chemistry & Physics*, 18(10), 7149. <https://doi.org/10.5194/acp-18-7149-2018>.
- Kim, Y., Guldmann, J.- M. (2011). Impact of traffic flows and wind directions on air pollution concentrations in Seoul, Korea. *Atmospheric Environment*. Vol. 45, 2803 – 2810. <https://doi.org/10.1016/j.atmosenv.2011.02.050>.
- Kittelson, B.D. (1998). Engines and nanoparticles: a review. *Journal of Aerosol Science* 29 (5), 575–588. Retrieved from <https://search.ebscohost.com/login.aspx?direct=true&AuthType=ip,cookie,shib,uid&db=edswsc&AN=000074107300008&lang=pt-pt&site=eds-live&scope=site>.
- Knibbs, L.D., Cole-Hunter, T., Morawska, L. (2011). A review of commuter exposure to ultrafine particles and its health effects. *Atmospheric Environment*, 45(16), 2611–2622. <https://doi.org/10.1016/j.atmosenv.2011.02.065>.
- Köhler, F. (2013). Testing of Particulate Emissions from Positive Ignition Vehicles with Direct Fuel Injection System. Technical Report, 2013-09-26, T\HuV Nord. [Available at: http://www.transportenvironment.org/sites/te/files/publications/TUV-Technical_report.pdf, accessed on December, 2018].
- Kolpakova, A.F., Sharipov, R.N., Kolpakov, F.A. (2017). Air pollution by particulate matter as the risk factor for the cardiovascular diseases. *Gigiena i Sanitariia*, 96:133–137. <https://doi.org/10.1882/0016-9900-2017-96-2-133-137>.
- Kopanakis, I., Chatoutsidou, S. E., Glytsos, T., Lazaridis, M. (2018). Impact from local sources and variability of fine particle number concentration in a coastal sub-urban site. *Atmospheric Research*, 213, 136–148. <https://doi.org/10.1016/j.atmosres.2018.06.002>.
- Kousoulidou, M., L. Ntziachristos, M. G. Mellios, Z. Samaras, (2008). Road-transport emission projections to 2020 in European urban environments. *Atmospheric Environment*, 42 (32), 7465-7475. <https://doi.org/10.1016/j.atmosenv.2008.06.002>.
- Kuhn, T., Krudysz, M., Zhu, Y., Fine, P. M., Hinds, W. C., Froines, J., Sioutas, C. (2005). Volatility of indoor and outdoor ultrafine particulate matter near a freeway. *Journal of Aerosol Science*, 36(3), 291–302. <https://doi.org/10.1016/j.jaerosci.2004.09.006>.
- Kukkonen, J., Karl, M., Keuken, M.P., Denier van der Gon, H.A.C., Denby, B.R., Singh, V., Douros, J., Manders, A., Samaras, Z., Moussiopoulos, N., Jonkers, S., Aarnio, M., Karppinen, A., Kangas, L., Lützenkirchen, S., Petäjä, T., Sokhi, R.S. (2016). Modelling the dispersion of particle numbers in five European cities. *Modelling the dispersion of particle numbers in five European cities. Geoscientific Model Development*, 9(2), 451–478. <https://doi.org/10.5194/gmd-9-451-2016>.
- Kulmala, M., Kerminen, V.-M., Petaja, T., Ding, A. J., Wang, L. (2017). Atmospheric gas-to-particle conversion: why NPF events are observed in megacities? *FARADAY DISCUSSIONS*, 200, 271–288. <https://doi.org/10.1039/c6fd00257a>.
- Kulmala, M., Petäjä, T., Ehn, M., Sipilä, M., Worsnop, D. R., Kerminen, V.-M., Thornton, J. (2014). Chemistry of atmospheric nucleation: On the recent advances on precursor characterization and atmospheric cluster composition in connection with atmospheric new particle formation (Vol. 65). *Annual Reviews Inc.* <https://doi.org/10.1146/annurev-physchem-040412-110014>.
- Kumar, P., Morawska, L., Birmili, W., Paasonen, P., Hu, M., Kulmala, M., Harrison, R.M., Norford, L., Britter, R. (2014). Ultrafine particles in cities. *Environment International* 66, 1-10. <https://doi.org/10.1016/j.envint.2014.01.013>.
- Kumar, P., Robins, A., Vardoulakis, S., Britter, R. (2010). A review of the characteristics of nanoparticles in the urban atmosphere and the prospects for developing regulatory controls. *Atmospheric Environment*, 44(39), 5035–5052. <https://doi.org/10.1016/j.atmosenv.2010.08.016>.
- Kumar, P., Robins, A., Vardoulakis, S., Quincey, P. (2011). Technical challenges in tackling regulatory concerns for urban atmospheric nanoparticles. *Particuology*, 9(6), 566-571. <https://doi.org/10.1016/j.partic.2011.06.002>.

- Lanzinger, S., Schneider, A., Breitner, S., Stafoggia, M., Erzen, I., Dostal, M., Pastorkova, A., Bastian, S., Cyrus, J., Zscheppang, A., Kolodnitska, T., Peters, A. (2016). Associations between ultrafine and fine particles and mortality in five central European cities — Results from the UFireg study. *Environment International*, 8844-52. <https://doi.org/10.1016/j.envint.2015.12.006>.
- Ledoux, F., Roche, C., Cazier, F., Beaugard, C., Courcot, D. (2018). Influence of ship emissions on NO_x, SO₂, O₃ and PM concentrations in a North-Sea harbor in France. *Journal of Environmental Sciences*, 71, 56–66. <https://doi.org/10.1016/j.jes.2018.03.030>.
- Lee, B., Chan, C., Louie, P., Luk, C. (2017). Evaluation of traffic exhaust contributions to ambient carbonaceous submicron particulate matter in an urban roadside environment in Hong Kong. *Atmos Chem Phys*, 17(24), 15121–15135. <https://doi.org/10.5194/acp-17-15121-2017>.
- Lee, K.K., Miller M.R., Shah A.S.V. (2018). Air pollution and stroke. *J Stroke*, 20(1), 2–11. <https://doi.org/10.5853/jos.2017.02894>.
- Lee, M., Kloog, I., Chudnovsky, A., Lyapustin, A., ... Schwartz, J. (2016). Spatiotemporal prediction of fine particulate matter using high-resolution satellite images in the Southeastern US 2003–2011. *J. Expo. Sci. Environ. Epidemiol.* 26, 377–384. DOI: [10.1038/jes.2015.41](https://doi.org/10.1038/jes.2015.41).
- Leitte, A., Schlink, U., Herbarth, O., Wiedensohler, A., Pan, X.-C., Hu, M., ... Franck, U. (2012). Associations between size-segregated particle number concentrations and respiratory mortality in Beijing, China. *International Journal of Environmental Health Research*, 22(2), 119–133. <https://doi.org/10.1080/09603123.2011.605878>.
- Lelieveld, J., Evans, J.S., Fnais, M., Giannadaki, D., Pozzer, A. (2015). The contribution of outdoor air pollution sources to premature mortality on a global scale. *Nature* 525 (7569), 367–371. <https://doi.org/10.1038/nature15371>.
- Liang, B., Ge, Y., Tan, J., Han, X., Gao, L., Hao, L., ... Dai, P. (2013). Comparison of PM emissions from a gasoline direct injected (GDI) vehicle and a port fuel injected (PFI) vehicle measured by electrical low pressure impactor (ELPI) with two fuels: Gasoline and M15 methanol gasoline. *Journal of Aerosol Science*, 57, 22–31. <https://doi.org/10.1016/j.jaerosci.2012.11.008>.
- Liggio, J., Gordon, M., Smallwood, G., Li, S.-M., Stroud, C., Staebler, R., Lu, G., Lee, P., Taylor, B., Brook, J. (2012). Are emissions of black carbon from gasoline vehicles Underestimated? Insights from near and on-road measurements. *Environ. Sci. Technol.* 46, 4819–4828. <https://doi.org/10.1021/es2033845>.
- Lin, J., Liu, W., Yan, I. (2009). Relationship between meteorological conditions and particle size distribution of atmospheric aerosols. *J. Meteorol. Environ.* 25, 1–5.
- Liu, S., Hu, M., Wu, Z., Wehner, B., Wiedensohler, A., Cheng, Y. (2008). Aerosol number size distribution and new particle formation at a rural/coastal site in Pearl River Delta (PRD) of China. *Atmospheric Environment*, 42, 6275–6283. <https://doi.org/10.1016/j.atmosenv.2008.01.063>.
- Liu, Z., Hu, B., Zhang, J., Yu, Y., Wang, Y. (2016). Characteristics of aerosol size distributions and chemical compositions during wintertime pollution episodes in Beijing. *Atmospheric Research*, 168, 1–12. <https://doi.org/10.1016/j.atmosres.2015.08.013>.
- Lohmann, U., Feichter, J. (2005). Global indirect aerosol effects: a review. *Atmospheric Chemistry and Physics*, (3), 715. <https://doi.org/10.5194/acp-5-715-2005>.
- Lonati, G., Cernuschi, S., Sidi, S. (2010). Air quality impact assessment of at-berth ship emissions: Case-study for the project of a new freight port. *Science of the Total Environment*, 409, 192–200. <https://doi.org/10.1016/j.scitotenv.2010.08.029>.
- Lopes, M., Russo, A., Gouveia, C., Ferreira, F. (2019b). Monitoring of ultrafine particles in the surrounding urban area of ferries terminals. *Journal of Environmental Protection*. Vol. 10, 838–860 <https://doi.org/10.4236/jep.2019.106050>.
- Lopes, M., Russo, A., Monjardino, J., Gouveia, C., Ferreira, F. (2019a). Monitoring of ultrafine particles in the surrounding urban area of a civilian airport. *Atmospheric Pollution Research* <https://doi.org/10.1016/j.apr.2019.04.002>.
- López-Aparicio, S., Tønnesen, D., Thanh, T. N., Neilson, H. (2017). Shipping emissions in a Nordic port: Assessment of mitigation strategies. *Transportation Research Part D*, 53, 205–216. <https://doi.org/10.1016/j.trd.2017.04.021>.
- Lou C, Liu H, Li Y, Peng Y, Wang J, Dai L. (2017). Relationships of relative humidity with PM_{2.5} and PM₁₀ in the Yangtze River Delta, China. *Environ. Monit. Assess.* 189 (11), 16. <https://doi.org/10.1007/s10661-017-6281-z>.
- Lough, G.C., Schauer, J.J., Park, J.S., Shafer, M.M., Deminter, J.T., Weinstein, J.P. (2005). Emissions of metals associated with motor vehicle roadways. *Environ. Sci. Technol.* 39 (3), 826e836. <https://doi.org/10.1021/es048715f>.

- Luengo-Oroz, J., Reis, S. (2019). Assessment of cyclists' exposure to ultrafine particles along alternative commuting routes in Edinburgh. *Atmospheric Pollution Research*. <https://doi.org/10.1016/j.apr.2019.01.020>.
- Lyu, X. P., Guo, H., Cheng, H. R., Wang, D. W. (2018). New particle formation and growth at a suburban site and a background site in Hong Kong. *Chemosphere*, 193, 664–674. <https://doi.org/10.1016/j.chemosphere.2017.11.060>.
- Marcazzan, G. M., Vaccaro, S., Valli, G., Vecchi, R. (2001). Characterisation of PM₁₀ and PM_{2.5} particulate matter in the ambient air of Milan (Italy). *Atmospheric Environment*, 35(27), 4639–4650. [https://doi.org/10.1016/S1352-2310\(01\)00124-8](https://doi.org/10.1016/S1352-2310(01)00124-8).
- Marmer, E., Langmann, B. (2005). Impact of ship emissions on the Mediterranean summertime pollution and climate: A regional model study. *Atmospheric Environment*, 39(26), 4659–4669. <https://doi.org/10.1016/j.atmosenv.2005.04.014>.
- Masiol, M., Harrison, R. M. (2014). Review: Aircraft engine exhaust emissions and other airport-related contributions to ambient air pollution: A review. *Atmospheric Environment*, 95, 409–455. <https://doi.org/10.1016/j.atmosenv.2014.05.070>.
- Masiol, M., Vu, T., Beddows, D., Harrison, R. (2016). Source apportionment of wide range particle size spectra and black carbon collected at the airport of Venice (Italy). *Atmospheric Environment*, 139, 13956–74. <https://doi.org/10.1016/j.atmosenv.2016.05.018>.
- Mathissen, M., Scheer, V., Vogt, R., Benter, T. (2011). Investigation on the potential generation of ultrafine particles from the tire-road interface. *Atmospheric Environment*, 45(34), 6172–6179. <https://doi.org/10.1016/j.atmosenv.2011.08.032>.
- Mazaheri, M., Johnson, G. R., Morawska, L. (2009). Particle and gaseous emissions from commercial aircraft at each stage of the landing and takeoff cycle. *Environmental Science and Technology*, 43(2), 441–446. <https://doi.org/10.1021/es8013985>.
- Merico, E., Donato, A., Gambaro, A., Cesari, D., Gregoris, E., Barbaro, E., Dinoi, A., Giovanelli, G., Masieri, S., Contini, D. (2016). Influence of in-port ships emissions to gaseous atmospheric pollutants and to particulate matter of different sizes in a Mediterranean harbour in Italy. *Atmospheric Environment*, 139, 1–10. <https://doi.org/10.1016/j.atmosenv.2016.05.024>.
- Merico, E., Gambaro, A., Argiriou, A., Alebic-Juretic, A., Barbaro, E., Cesari, D., ... Contini, D. (2017). Atmospheric impact of ship traffic in four Adriatic-Ionian port-cities: Comparison and harmonization of different approaches. *Transportation Research Part D*, 50, 431–445. <https://doi.org/10.1016/j.trd.2016.11.016>.
- Miola, A., Ciuffo, B. (2011). Estimating air emissions from ships: Meta-analysis of modelling approaches and available data sources. *Atmospheric Environment*, 45, 2242–2251. <https://doi.org/10.1016/j.atmosenv.2011.01.046>.
- Moldanová, J., Fridell, E., Winnes, H., Holmin-Fridell, S., Boman, J., Jedynska, A., Tishkova, V., Demidjian, B., Joulie, S., Bladt, H., Ivleva, N.P., Niessner, R. (2013). Physical and chemical characterisation of PM emissions from two ships operating in European Emission Control Areas. *Atmospheric Measurement Techniques Discussions*, 6(2), 3931–3982. <https://doi.org/10.5194/amtd-6-3931-2013>.
- Monjardino, J., Barros, N., Ferreira, F., Tente, H., Fontes, T., Pereira, P., Manso, C. (2018). Improving Air Quality in Lisbon: modelling emission abatement scenarios. 1st IFAC Workshop on Integrated Assessment Modelling for Environmental Systems, May 10–11, University of Brescia, Brescia, In IFAC-PapersOnLine (Vol. 51, 61–66). Elsevier B.V. <https://doi.org/10.1016/j.ifacol.2018.06.211>.
- Monteiro A., Ferreira J., Ribeiro I, Fernandes AP, Martins H, Gama C, Miranda A.I. (2015). Air quality over Portugal in 2020, *Atmospheric Pollution Research*, Volume 6, Issue 5, 788–796, <https://doi.org/10.5094/APR.2015.087>
- Morawska, L., Ristovski, Z., Jayaratne, E. R., Keogh, D. U., Ling, X. (2008). Ambient nano and ultrafine particles from motor vehicle emissions: Characteristics, ambient processing and implications on human exposure. *Atmospheric Environment*, 42(35), 8113–8138. <https://doi.org/10.1016/j.atmosenv.2008.07.050>.
- Mordas, G., Plauškaitė, K., Prokopčiuk, N., Dudoitis, V., Bozzetti, C., Ulevicius, V. (2016). Observation of new particle formation on Curonian Spit located between continental Europe and Scandinavia. *Journal of Aerosol Science*, 97, 38–55. <https://doi.org/10.1016/j.jaerosci.2016.03.002>.
- Mousavi, A., Sowlat, M. H., Hasheminassab, S., Polidori, A., Shafer, M. M., Schauer, J. J., Sioutas, C. (2019). Impact of emissions from the Ports of Los Angeles and Long Beach on the oxidative potential of ambient PM_{0.25} measured across the Los Angeles County. *Science of the Total Environment*, 651(Part 1), 638–647. <https://doi.org/10.1016/j.scitotenv.2018.09.155>.

- Mu, C.Y., Tu, Y.Q., Feng, Y. (2011). Effect analysis of meteorological factors on the inhalable particle matter concentration of atmosphere in Hami. *Meteorol. Environ. Sci.* 34, 75-79.
- Mudway, I. S., Dundas, I., Wood, H. E., Marlin, N., Jamaludin, J. B., Bremner, S. A., ... Griffiths, C. J. (2019). Impact of London's low emission zone on air quality and children's respiratory health: a sequential annual cross-sectional study. *The Lancet Public Health*, 4(1), e28–e40. [https://doi.org/10.1016/S2468-2667\(18\)30202-0](https://doi.org/10.1016/S2468-2667(18)30202-0).
- Mühlfeld, C., Rothen-Rutishauser, B., Blank, F., Vanhecke, D., Ochs, M., Gehr, P. (2008). Interactions of nanoparticles with pulmonary structures and cellular responses. *Am J Physiol Lung Cell Mol Physiol* 294: L817–L829. <https://doi.org/10.1152/ajplung.00442.2007>.
- Müller, L., Riediker, M., Wick, P., Mohr, M., Gehr, P., Rothen-Rutishauser, B. (2009). Oxidative stress and inflammation response after nanoparticle exposure: differences between human lung cell J. R. Soc. Interface, 7 (2010), pp. S27-S40. <https://doi.org/10.1098/rsif.2009.0161.focus>.
- Myhre, G., Shindell, D., Bréon, F.-M., Collins, W., Fuglestad, J., Huang, J., Koch, D., Lamarque, J.-F., Lee, D., Mendoza, B. (2013). Anthropogenic and natural radiative forcing. *Climate change* 423.
- Ntziachristos, L., Ning, Z., Geller, M.D., Sioutas, C. (2007). Particle concentration and characteristics near a major freeway with heavy duty diesel traffic. *Environmental Science and Technology* 41, 2223–2230. <https://doi.org/10.1021/es062590s>.
- Nunes, R.A.O., Alvim-Ferraz, M.C.M., Martins, F.G., Sousa, S.I.V. (2017). The activity based methodology to assess ship emissions-A review. *Environ. Pollut.* 231(1), 87–103. <https://doi.org/10.1016/j.envpol.2017.07.099>.
- Ohlwein, S., Kappeler, R., Kutlar Joss, M., Künzli, N., Hoffmann, B. (2019). *Int J Public Health* (2019) 64: 547. <https://doi.org/10.1007/s00038-019-01202-7>.
- Onat, B., Şahin, Ü. A., Uzun, B., Akın, Ö., Özkaya, F., Ayvaz, C. (2019). Determinants of exposure to ultrafine particulate matter, black carbon, and PM_{2.5} in common travel modes in Istanbul. *Atmospheric Environment*, 206, 258–270. <https://doi.org/10.1016/j.atmosenv.2019.02.015>.
- Oudin, A., Forsberg, B., Adolfsson, A. N., Lind, N., Modig, L., Nordin, M., Nordin S; Adolfsson R; Nilsson L. (2016). Traffic-Related Air Pollution and Dementia Incidence in Northern Sweden: A Longitudinal Study. *Environmental Health Perspectives*, 124(3), 306-312. <https://doi.org/10.1289/ehp.1408322>.
- P-Trak® (2013). P-Trak® Ultrafine Particle Counter Model 8525. Operation and Service Manual. (Trakpro TM Data Analysis Software Enclosed). P/N 19803880, Revision M July 2013.
- Pakkanen, T., Kerminen, V., Korhonen, C., Hillamo, R., Aarino, P., Koskentalo, T., Maenhaut, W. (2001). Urban and rural ultrafine (PM_{0.1}) particles in the Helsinki area. *Atmospheric Environment* 35, 4593–4607. [https://doi.org/10.1016/S1352-2310\(01\)00167-4](https://doi.org/10.1016/S1352-2310(01)00167-4).
- Pan, Y., Leifert, A., Ruau, D., Neuss, S., Bornemann, J., Schmid, G., ... Jahnen-Dechent, W. (2009). Gold Nanoparticles of Diameter 1.4 nm Trigger Necrosis by Oxidative Stress and Mitochondrial Damage. *SMALL*, 5(18), 2067–2076. <https://doi.org/10.1002/smll.200900466>.
- Pant, P., Harrison, R. M. (2013). Estimation of the contribution of road traffic emissions to particulate matter concentrations from field measurements: A review. *Atmospheric Environment*, 77, 78–97. <https://doi.org/10.1016/j.atmosenv.2013.04.028>.
- Pateraki, S., Asimakopoulos, D. N., Flocas, H. A., Maggos, T., Vasilakos, C. (2012). The role of meteorology on different sized aerosol fractions (PM₁₀, PM_{2.5}, PM_{2.5–10}). *Science of the Total Environment*, 419, 124–135. <https://doi.org/10.1016/j.scitotenv.2011.12.064>.
- Patton, A. P., Perkins, J., Zamore, W., Levy, J. I., Brugge, D., Durant, J. L. (2014b). Spatial and temporal differences in traffic-related air pollution in three urban neighborhoods near an interstate highway. *Atmospheric Environment*, 99, 309–321. <https://doi.org/10.1016/j.atmosenv.2014.09.072>.
- Patton, A.P., Collins, C., Naumova, E.N., Zamore, W., Brugge, D., Durant, J.L. (2014a). An hourly regression model for ultrafine particles in a near-highway urban area. *Environ. Sci. Technol.* 48, 3272e3280. <http://dx.doi.org/10.1021/es404838k>.
- Patton, A.P., Laumbach, R., Ohman-Strickland, P., Black, K., Alimokhtari, S., Liou, P., Kipen, H. (2016). Scripted drives: a robust protocol for generating exposures to traffic-related air pollution. *Atmos. Environ.* 143, 290–299. <https://doi.org/10.1016/j.atmosenv.2016.08.038>.
- Penttinen, P., Timonen K., Tiittanen, P., Mirme, A., Ruuskanen, J., Pekkanen, J. (2001). Number concentration and size of particles in urban air: Effects on spirometric lung function in adult asthmatic subjects. *Environ. Health Perspect.* 109, 319–323. Retrieved from

<https://search.ebscohost.com/login.aspx?direct=true&AuthType=ip,cookie,shib,uid&db=edswsc&AN=000168413600020&lang=pt-pt&site=eds-live&scope=site>.

- Pérez, N., Pey, J., Reche, C., Cortés, J., Alastuey, A., Querol, X. (2016). Impact of harbour emissions on ambient PM₁₀ and PM_{2.5} in Barcelona (Spain): Evidences of secondary aerosol formation within the urban area. *Science of the Total Environment*, 571, 237–250. <https://doi.org/10.1016/j.scitotenv.2016.07.025>.
- Peters, A., Wichmann, E., Tuch, T., Heinrich, J. e Heyder, J. (1997). Respiratory effects are associated with the number of ultrafine particles. *Am. J. Respir. Crit. Care*, 155, 1376–1383.
- Pey, J., Pérez, N., Cortés, J., Alastuey, A., Querol, X. (2013). Chemical fingerprint and impact of shipping emissions over a western Mediterranean metropolis: Primary and aged contributions. *Science of the Total Environment*, 463–464, 497–507. <https://doi.org/10.1016/j.scitotenv.2013.06.061>.
- Pinault, L. L., Weichenthal, S., Crouse, D. L., Brauer, M., Erickson, A., Donkelaar, A. van, ... Burnett, R. T. (2017). Associations between fine particulate matter and mortality in the 2001 Canadian Census Health and Environment Cohort. *Environmental Research*, 159, 406–415. <https://doi.org/10.1016/j.envres.2017.08.037>.
- Pirjola, L., Paasonen, P., Pfeiffer, D., Hussein, T., Hämeri, K., Koskentalo, T., Virtanen, A., Rönkkö, T., Keskinen, J., Pakkanen, T.A., Hillamo, R.E. (2006). Dispersion of particles and trace gases nearby a city highway: mobile laboratory measurements in Finland. *Atmos. Environ.* 40, 867–879. <https://doi.org/10.1016/j.atmosenv.2005.10.018>.
- Pordata (2018). Base de Dados de Portugal Contemporâneo. Passenger traffic at major airports: Lisbon, Oporto and Faro. [Available at: <https://www.pordata.pt/en/Portugal/Passenger+traffic+at+major+airports+Lisbon++Oporto+and+Faro-3248>, accessed on July, 2019].
- Psanis, C., Triantafyllou, E., Giamarelou, M., Manousakas, M., Eleftheriadis, K., Biskos, G. (2017). Particulate matter pollution from aviation-related activity at a small airport of the Aegean Sea Insular Region. *Science Of The Total Environment*, 596-597, 187-193. <https://doi.org/10.1016/j.scitotenv.2017.04.078>.
- Pushpawela, B., Jayaratne, R., Morawska, L. (2018). Temporal distribution and other characteristics of new particle formation events in an urban environment. *Environmental Pollution*, 233, 552–560. <https://doi.org/10.1016/j.envpol.2017.10.102>.
- Putaud, J. P., Van Dingenen, R., Alastuey, A., Bauer, H., Birmili, W., ..., A., Raes, F. (2010). A European aerosol phenomenology – 3: Physical and chemical characteristics of particulate matter from 60 rural, urban, and kerbside sites across Europe. *Atmospheric Environment*, 44(10), 1308–1320. <https://doi.org/10.1016/j.atmosenv.2009.12.011>.
- Qiu, Z., Wang, W., Zheng, J., Lv, H. (2019). Exposure assessment of cyclists to UFP and PM on urban routes in Xi'an, China. *Environmental Pollution*, 250, 241–250. <https://doi.org/10.1016/j.envpol.2019.03.129>.
- Querol, X., Alastuey, A., Moreno, T., Viana, M. M., Castillo, S., Pey, J., ... de la Campa, A. S. (2008). Spatial and temporal variations in airborne particulate matter (PM₁₀ and PM_{2.5}) across Spain 1999–2005. *Atmos. Environ.* 42, 3964–3979. <https://doi.org/10.1016/j.atmosenv.2006.10.071>.
- Querol, X., Alastuey, A., Pey, J., Cusack, M., Pérez, N., Mihalopoulos, N., ... Koçak, M. (2009). Variability in regional background aerosols within the Mediterranean. *Atmospheric Chemistry & Physics*, 9(14), 4575. Retrieved from <https://search.ebscohost.com/login.aspx?direct=true&AuthType=ip,cookie,shib,uid&db=edb&AN=43691411&lang=pt-pt&site=eds-live&scope=site>.
- Raaschou-Nielsen, O., Andersen, Z.J., Beelen, R., ... Hoek, G (2013). Air pollution and lung cancer incidence in 17 European cohorts: prospective analyses from the European Study of Cohorts for Air Pollution Effects (ESCAPE). *Lancet Oncol.* 14, 813–822. [https://doi.org/10.1016/S1470-2045\(13\)70279-1](https://doi.org/10.1016/S1470-2045(13)70279-1).
- Rahman, M., Mazaheri, M., Clifford, S., Morawska, L. (2017). Estimate of main local sources to ambient ultrafine particle number concentrations in an urban area. *Atmospheric Research*, 194178-189. <https://doi.org/10.1016/j.atmosres.2017.04.036>.
- Ramanathan, V., Crutzen, P., Lelieveld, J., Mitra, A., Althausen, D., Anderson, J., ... Valero, F. (2001). Indian Ocean Experiment: An integrated analysis of the climate forcing and effects of the great Indo-Asian haze. *JOURNAL OF GEOPHYSICAL RESEARCH-ATMOSPHERES*, 106(D22), 28371–28398. Retrieved from <https://search.ebscohost.com/login.aspx?direct=true&AuthType=ip,cookie,shib,uid&db=edswsc&AN=000172355800026&lang=pt-pt&site=eds-live&scope=site>.

- Reche, C., Viana, M., Moreno, T., Querol, X., Alastuey, A., Pey, J., Richard, A. (2011). Peculiarities in atmospheric particle number and size-resolved speciation in an urban area in the western Mediterranean: results from the DAURE campaign. *Atmos. Environ.* 45 (30), 5282e5293. <https://doi.org/10.1016/j.atmosenv.2011.06.059>.
- Rédon, A. M., Salazar, J. F., Palacio, C. A. (2014). Effects of urbanization on the temperature inversion breakup in a mountain valley with implications for air quality. *Journal of Applied Meteorology and Climatology*. Vol. 53, 840 – 858. <https://doi.org/10.1175/JAMC-D-13-0165.1>.
- Ren, J., Cao, X., Liu, J. (2018). Impact of atmospheric particulate matter pollutants to IAQ of airport terminal buildings: A first field study at Tianjin Airport, China. *Atmospheric Environment*, 179, 222–226. <https://doi.org/10.1016/j.atmosenv.2018.02.019>.
- Ren, J., Liu, J., Li, F., Cao, X., Ren, S., Xu, B., Zhu, Y. (2016). A study of ambient fine particles at Tianjin International Airport, China. *Science of the Total Environment*, 556, 126–135. <https://doi.org/10.1016/j.scitotenv.2016.02.186>.
- Renwick, L. C., Donaldson, K., Clouter, A. (2001). Impairment of Alveolar Macrophage Phagocytosis by Ultrafine Particles. *Toxicology and Applied Pharmacology*, 172(2), 119–127. <https://doi.org/10.1006/taap.2001.9128>.
- Riley, E., Gould, T., Hartin, K., Fruin, S., Simpson, C., Yost, M., Larson, T. (2016). Ultrafine particle size as a tracer for aircraft turbine emissions. *Atmospheric Environment*, 139, 20-29. <https://doi.org/10.1016/j.atmosenv.2016.05.016>.
- Rodríguez, S., Cuevas, E., González, Y., Ramos, R., Romero, P.M., Pérez, N., Querol, X., Alastuey, A. (2018). Influence of sea breeze circulation and road traffic emissions on the relationship between particle number, black carbon, PM₁, PM_{2.5} and PM_{2.5-10} concentrations in a coastal city. *Atmospheric Environment*, 42, 6523–6534. <https://doi.org/10.1016/j.atmosenv.2008.04.022>.
- Rönkkö, T., Kuuluvainen, H., Karjalainen, P., Keskinen, J., Hillamo, R., ... Dal Maso, M. (2017). Traffic is a major source of atmospheric nanocluster aerosol. *Proc. Natl. Acad. Sci. Unit. States Am.* 114, 7549–7554. <https://doi.org/10.1073/pnas.1700830114>.
- Russo, A., Lind, P. G., Raischel, F., Trigo, R., Mendes, M. (2014b). Neural network forecast of daily pollution concentration using optimal meteorological data at synoptic and local scales. *Atmospheric Pollution Research* 6 (2015) 540-549 <https://doi.org/10.5094/APR.2015.060>.
- Russo, A., Soares, A.O. (2013). Hybrid Model for Urban Air Pollution Forecasting: A Stochastic Spatio-Temporal Approach. *Mathematical Geosciences* 46, Issue 1, 75-93. <https://doi.org/10.1007/s11004-013-9483-0>.
- Russo, A., Trigo, R., Martins, H., Mendes, M. (2014a). NO₂, PM₁₀ and O₃ urban concentrations and its association with circulation weather types in Portugal. *Atmospheric Environment*, 89, 768-785. <https://doi.org/10.1016/j.atmosenv.2014.02.010>.
- Saffari, A., Daher, N., Shafer, M.M., Schauer, J.J., Sioutas, C. (2013). Seasonal and spatial variation of trace elements and metals in quasi-ultrafine (PM_{0.25}) particles in the Los Angeles metropolitan area and characterization of their sources. *Environ. Pollut.* 181, 14e23. <http://dx.doi.org/10.1016/j.envpol.2013.06.001>.
- Saha, P. K., Zimmerman, N., Malings, C., Hauriyluk, A., Li, Z., Snell, L., ... Presto, A. A. (2019). Quantifying high-resolution spatial variations and local source impacts of urban ultrafine particle concentrations. *Science of the Total Environment*, 655, 473–481. <https://doi.org/10.1016/j.scitotenv.2018.11.197>.
- Saha, P.K., Khlystov, A., Grieshop, A.P. (2018a). Downwind evolution of the volatility and mixing state of near-road aerosols near a US interstate highway. *Atmos. Chem. Phys.* 18 (3), 2139–2154. <https://doi.org/10.5194/acp-18-2139-2018>.
- Saha, P.K., Khlystov, A., Snyder, M.G., Grieshop, A.P. (2018b). Characterization of air pollutant concentrations, fleet emission factors, and dispersion near a North Carolina inter- state freeway across two seasons. *Atmos. Environ.* 177, 143–153. <https://doi.org/10.1016/j.atmosenv.2018.01.019>.
- Samoli, E., Stafoggia, M., Rodopoulou, S., Ostro, B., Declercq, C., Alessandrini, E., ... Forastiere, F. (2013). Associations between Fine and Coarse Particles and Mortality in Mediterranean Cities: Results from the MED-PARTICLES Project. *Environmental Health Perspectives*, 121(8), 932–938. <https://doi.org/10.1289/ehp.1206124>.
- Santos, F. M., Gómez-Losada, Á., Pires, J. C. M. (2019). Impact of the implementation of Lisbon low emission zone on air quality. *Journal of Hazardous Materials*, 365, 632–641. <https://doi.org/10.1016/j.jhazmat.2018.11.061>.
- Sardar, S.B., Fine, P.M., Mayo, P.R., Sioutas, C. (2005). Size-fractionated measurements of ambient ultrafine particle chemical composition in Los Angeles using the NanoMOUDI. *Environmental Science and Technology* 39, 932–944. <https://doi.org/10.1021/es049478j>.

- Schauer, J.J., Lough, G.C., Shafer, M.M., Christensen, W.F., Arndt, M.F., Deminter, J.T., Park, J.-S. (2006). Characterization of Metals Emitted from Motor Vehicles. Research Report 133. Health Effects Institute, Boston MA [Available at <https://www.healtheffects.org/system/files/Schauer.pdf>, accessed on December, 2018].
- Scortichini, M., De Sario, M., de'Donato, F. K., Davoli, M., Michelozzi, P., Stafoggia, M. (2018). Short-Term Effects of Heat on Mortality and Effect Modification by Air Pollution in 25 Italian Cities. *INTERNATIONAL JOURNAL OF ENVIRONMENTAL RESEARCH AND PUBLIC HEALTH*, 15(8). <https://doi.org/10.3390/ijerph15081771>.
- Semmler, M., Seitz, J., Erbe, F., Mayer, P., Heyder, J., Oberdörster, G., Kreyling, W. G. (2004). Long-Term Clearance Kinetics of Inhaled Ultrafine Insoluble Iridium Particles from the Rat Lung, Including Transient Translocation into Secondary Organs. *Inhalation Toxicology*, 16(6/7), 453–459. <https://doi.org/10.1080/08958370490439650>.
- Shah, A., Langrish, J., Nair, H., McAllister, D., Hunter, A., Donaldson, K., Newby, D., Mills, N. (2013). Global association of air pollution and heart failure: a systematic review and meta-analysis. *Lancet*, 382(9897), 1039–1048. [https://doi.org/10.1016/S0140-6736\(13\)60898-3](https://doi.org/10.1016/S0140-6736(13)60898-3).
- Shen, Z.Y., Lu, B., Chen, H.B. (2009). Effects of meteorology condition in precipitation on aerosol concentration in Zhengzhou. *Meteorol. Environ. Sci.* 32, 55–58.
- Shirmohammadi, F., Hasheminassab, S., Saffari, A., Schauer, J. J., Delfino, R. J., Sioutas, C. (2016). Fine and ultrafine particulate organic carbon in the Los Angeles basin: Trends in sources and composition. *Science of the Total Environment*, 541, 1083–1096. <https://doi.org/10.1016/j.scitotenv.2015.09.133>.
- Shirmohammadi, F., Lovett, C., Sowlat, M. H., Mousavi, A., Verma, V., Shafer, M. M., ... Sioutas, C. (2018). Chemical composition and redox activity of PM_{0.25} near Los Angeles International Airport and comparisons to an urban traffic site. *Science of the Total Environment*, 610–611, 1336–1346. <https://doi.org/10.1016/j.scitotenv.2017.08.239>.
- Shirmohammadi, F., Sowlat, M. H., Hasheminassab, S., Saffari, A., Ban-Weiss, G., Sioutas, C. (2017). Emission rates of particle number, mass and black carbon by the Los Angeles International Airport (LAX) and its impact on air quality in Los Angeles. *Atmospheric Environment*, 151, 82–93. <https://doi.org/10.1016/j.atmosenv.2016.12.005>.
- Simon, M. C., Hudda, N., Naumova, E. N., Levy, J. I., Brugge, D., Durant, J. L. (2017). Comparisons of traffic-related ultrafine particle number concentrations measured in two urban areas by central, residential, and mobile monitoring. *Atmospheric Environment*, 169113–127. <https://doi.org/10.1016/j.atmosenv.2017.09.003>.
- Sioutas, C., Delfino, R., Singh, M. (2005). Exposure Assessment for Atmospheric Ultrafine Particles (UFPs) and Implications in Epidemiologic Research. *Environmental Health Perspectives*, 113(8), 947–955. <https://doi.org/10.1289/ehp.7939>.
- Slezakova, K., Alvim-Ferraz, M., Pereira, M. (2012). Elemental characterization of indoor breathable particles at a Portuguese urban hospital. *J. Toxicol. Environ. Health A*, 75(13–15), 909–919. <https://doi.org/10.1080/15287394.2012.690707>.
- Spinazzè, A., Cattaneo, A., C., Peruzzo, C., Cavallo, D. (2014). Modeling Population Exposure to Ultrafine Particles in a Major Italian Urban Area. *International Journal Of Environmental Research And Public Health*, Vol 11, Iss 10, Pp 10641–10662 (2014), (10), 10641. <https://doi.org/10.3390/ijerph111010641>.
- Stafoggia, M., Cattani, G., Forastiere, F., Di Menno di Bucchianico, A., Gaeta, A., Ancona, C. (2016). Particle number concentrations near the Rome-Ciampino city airport. *Atmospheric Environment*, 147, 264–273. <https://doi.org/10.1016/j.atmosenv.2016.09.062>.
- Stafoggia, M., Samoli, E., Alessandrini, E., Cadum, E., Ostro, B., Berti, G., Faustini, A., Jacquemin, B., Linares, C., Pascal, M., Randi, G., Ranzi, A., Stivanello, E., Forastiere, F. (2013). Shortterm associations between fine and coarse particulate matter and hospitalizations in southern Europe: results from the med-particles project. *Environ. Health Perspect.* 121, 1026–1033. <https://doi.org/10.1289/ehp.1206151>.
- Stafoggia, M., Schneider, A., Cyrys, J., Samoli, E., Andersen, J., Bedada, B., Bellander, T., Cattani, G., Eleftheriadis, K., ... Forastiere, F. (2017a). Association between short-term exposure to ultrafine particles and mortality in eight European urban areas. *Epidemiology* 28(2), 172–180. <https://doi.org/10.1097/EDE.0000000000000599>.
- Stafoggia, M., Schwartz, J., Badaloni, C., Bellander, T., Alessandrini, E., Cattani, G., ... Kloog, I. (2017b). Estimation of daily PM₁₀ concentrations in Italy (2006–2012) using finely resolved satellite data, land use variables and meteorology. *Environment International*, 99, 234–244. <https://doi.org/10.1016/j.envint.2016.11.024>.
- Stanek, L., Sacks, J., Dutton, S., Dubois, J. (2011). Attributing health effects to apportioned components and sources of particulate matter: An evaluation of collective results. *Atmospheric Environment*. 45, 5655–5663. <https://doi.org/10.1016/j.atmosenv.2011.07.023>.

- Stanier, C., Khlystov, A., Pandis, S. (2004b). Nucleation events during the Pittsburgh air quality study: description and relation to key meteorological, gas phase, and aerosol parameters. *Aerosol Science and Technology* 38 (S1), 253–264. <https://doi.org/10.1080/02786820390229570>.
- Stanier, C.O., Khlystov, A.Y., Pandis, S.N. (2004a). Ambient aerosol size distributions and number concentrations measured during the Pittsburgh Air Quality Study (PAQS). *Atmos. Environ.* 38, 3275–3284. <https://doi.org/10.1016/j.atmosenv.2004.03.020>.
- Sydlik, U., Bierhals, K., Soufi, M., Abel, J., Schins, R., Unfried, K. (2006). Ultrafine carbon particles induce apoptosis and proliferation in rat lung epithelial cells via specific signaling pathways both using EGF-R. *Am. J. Physiol. Lung Cell Mol. Physiol.*, 291, L725–L733. DOI: [10.1152/ajplung.00131.2006](https://doi.org/10.1152/ajplung.00131.2006).
- Tai, A.P.K., Mickley, L.J., Jacob, D.J. (2010). Correlations between fine particulate matter (PM_{2.5}) and meteorological variables in the United States: implications for the sensitivity of PM_{2.5} to climate change. *Atmos. Environ.* 44 (32), 3976–3984. <https://doi.org/10.1016/j.atmosenv.2010.06.060>.
- Talbi, A., Kerbachi, R., Kerchich, Y., Boughedaoui, M. (2018). Assessment of annual air pollution levels with PM₁, PM_{2.5}, PM₁₀ and associated heavy metals in Algiers, Algeria. *Environmental Pollution*, 232, 252–263. <https://doi.org/10.1016/j.envpol.2017.09.041>.
- Terzano, C., Di Stefano, F., Conti, V., Graziani, E., Petrojanni, A. (2010). Air pollution ultrafine particles: Toxicity beyond the lung. *Eur. Rev. Med. Pharmacol. Sci.*, 14(10), 809–821. Retrieved from <https://search.ebscohost.com/login.aspx?direct=true&AuthType=ip,cookie,shib,uid&db=edspsc&AN=000283750900001&lang=pt-pt&site=eds-live&scope=site>.
- Tsai S-S, Goggins WB, Chiu HF, Yang C-Y. (2003). Evidence for an association between air pollution and daily stroke admissions in Kaohsiung, Taiwan. *Stroke*, 34:2612–2616. DOI: [10.1161/01.STR.0000095564.33543.64](https://doi.org/10.1161/01.STR.0000095564.33543.64).
- UNCTAD (2018). Review of Maritime Transport 2018 (UNCTAD/RMT/2018). [Available at <https://unctad.org/en/pages/PublicationWebflyer.aspx?publicationid=2245>, accessed on January, 2019].
- US-EPA (2009). Proposal to designate an emission control area for nitrogen oxides, sulfur oxides and particulate matter. Technical support document, chapter 3: impacts of shipping emissions on air quality, health and the environment. In: U.S. Environmental Protection Agency (Ed.), Assessment and Standards Division, Office of Transportation and Air Quality [Available at: <https://19january2017snapshot.epa.gov/sites/production/files/2016-09/documents/420r09007.pdf>, accessed on January, 2019].
- Van der Zee, S. C., Dijkema, M. B. A., van der Laan, J., Hoek, G. (2012). The impact of inland ships and recreational boats on measured NO_x and ultrafine particle concentrations along the waterways. *Atmospheric Environment*, 55, 368–376. <https://doi.org/10.1016/j.atmosenv.2012.03.055>.
- Van Poppel, M., Int Panis, L., Govarts, E., Van Houtte, J., Maenhaut, W. (2012). A comparative study of traffic related air pollution next to a motorway and a motorway flyover. *Atmospheric Environment*, 60132–141. <https://doi.org/10.1016/j.atmosenv.2012.06.042>.
- Viana, M., Hammingh, P., Colette, A., Querol, X., Degraeuwe, B., de Vlieger, I., van Aardenne, J. (2014). Impact of maritime transport emissions on coastal air quality in Europe. *Atmos. Environ.* 90, 96e105. <https://doi.org/10.1016/j.atmosenv.2014.03.046>.
- Vu, T., Delgado-Saborit, J., Harrison, R. (2015). Review: particle number size distributions from seven major sources and implications for source apportionment studies. *Atmos. Environ.* 122, 114–132. <https://doi.org/10.1016/j.atmosenv.2015.09.027>.
- Wallace, J., Corr, D., Kanaroglou, P. (2010). Topographic and spatial impacts of temperature inversions on air quality using mobile air pollution surveys. *Science of the Total Environment*. Vol. 408, 5086 – 5096. <https://doi.org/10.1016/j.scitotenv.2010.06.020>.
- Wang, H., Peng, Y., Che, H., Zhang, X., Li, J., Zhang, M. (2018). The impacts of the meteorology features on PM_{2.5} levels during a severe haze episode in central-east China. *Atmospheric Environment*, 177–189. <https://doi.org/10.1016/j.atmosenv.2018.10.001>.
- Wang, J., Christopher, S.A. (2003). Intercomparison between satellite derived aerosol optical thickness and PM_{2.5} mass: implications for air quality studies. *Geophys. Res. Lett.* 30 (21). <https://doi.org/10.1029/2003GL018174>.
- Wang, J., Ni, R., Lin, J., Yan, Y., Hu, Y., Liu, M., Chen, L., Liu, P., Tan, X., ..., Feng, K. (2019). Socioeconomic and atmospheric factors affecting aerosol radiative forcing: Production-based versus consumption-based perspective. *Atmospheric Environment*, 197–207. <https://doi.org/10.1016/j.atmosenv.2018.12.012>.

- Wang, Y., Yifang, Z., Salinas, R., Ramirez, D., Karnae, S., John, K. (2008). Roadside Measurements of Ultrafine Particles at a Busy Urban Intersection. *Journal Of The Air & Waste Management Association (Air & Waste Management Association)*, 58(11), 1449-1457. <https://doi.org/10.3155/1047-3289.58.11.1449>.
- Watson, J.G., Chow, J.C., Park, K., Lowenthal, D.H., Park, K. (2006). Nanoparticle and ultrafine particle events at the Fresno supersite. *J. Air Waste Manage. Assoc.* 56 (4), 417–430. Weichenthal, S., 2012. Selected physiological effects of ultrafine particles in acute cardio-vascular morbidity. *Environ. Res.* 115, 26–36. <https://doi.org/10.1080/10473289.2006.10464526>.
- Westerdahl, D., Fruin, S., Fine, P., Sioutas, C. (2008). The Los Angeles International Airport As A Source Of Ultrafine Particles And Other Pollutants To Nearby Communities. *Atmospheric Environment*, 42(13), 3143-3155. <https://doi.org/10.1016/j.atmosenv.2007.09.006>
- Westerdahl, D., Fruin, S., Sax, T., Fine, P. M., Sioutas, C. (2005). Mobile platform measurements of ultrafine particles and associated pollutant concentrations on freeways and residential streets in Los Angeles. *Atmospheric Environment*, 39(20), 3597–3610. <https://doi.org/10.1016/j.atmosenv.2005.02.034>.
- Westerlund, J., Hallquist, M., Hallquist, Å. M. (2015). Characterization of fleet emissions from ships through multi-individual determination of size-resolved particle emissions in a coastal area. *Atmospheric Environment*, 112, 159–166. <https://doi.org/10.1016/j.atmosenv.2015.04.018>.
- WHO (2005). Health effects of transport-related air pollution: Summary for policy-makers. [Available at: http://www.euro.who.int/_data/assets/pdf_file/0007/74716/e86650sum.pdf, accessed on September, 2017].
- WHO (2006). WHO air quality guidelines for particulate matter, ozone, nitrogen dioxide and sulfur dioxide. Global update 2005, World Health Organization, Regional Office for Europe, Copenhagen. [Available at: http://www.euro.who.int/_data/assets/pdf_file/0005/78638/E90038.pdf?ua=1, accessed on December, 2017].
- WHO (2013). World Health Organization - Health Effects of Particulate Matter. World Health Organization. [Available at: http://www.euro.who.int/_data/assets/pdf_file/0006/189051/Health-effects-of-particulate-matter-final-Eng.pdf, accessed on September, 2017].
- WHO (2014). Burden of disease from Ambient Air Pollution for 2012 – Summary of results.
- WHO (2016). Ambient (outdoor) air quality and health. Fact sheet No 313, updated March 2014, World Health Organization [Available at: <http://www.who.int/mediacentre/factsheets/fs313/en/>, accessed October 2018].
- WHO (2018). Ambient (outdoor) air quality and health. [Available at: [https://www.who.int/en/newsroom/factsheets/detail/ambient-\(outdoor\)-air-quality-and-health](https://www.who.int/en/newsroom/factsheets/detail/ambient-(outdoor)-air-quality-and-health), accessed on January, 2019].
- Wolf, K., Cyrys, J., Hrciníková, T., Gu, J., Kusch, T., Hampel, R., ... Peters, A. (2017). Land use regression modeling of ultrafine particles, ozone, nitrogen oxides and markers of particulate matter pollution in Augsburg, Germany. *Science of the Total Environment*, 579, 1531–1540. <https://doi.org/10.1016/j.scitotenv.2016.11.160>.
- Wu, J.Z., Ge, D.-D., Zhou, L.-F., Hou, L.-Y., Zhou, Y., Li, Q.-Y. (2018). Effects of particulate matter on allergic respiratory diseases. *Chronic Dis Transl Med*, 4:95–102. <https://doi.org/10.1016/j.cdtm.2018.04.001>.
- Zaheer, J., Jeon, J., Lee, S.B., Kim, J.S. (2018). Effect of Particulate Matter on Human Health, Prevention, and Imaging Using PET or SPECT. *Prog Med Phys*, 29(3):81-91. <https://doi.org/10.14316/pmp.2018.29.3.81>.
- Zhang, H., Hoff, R.M., Engel-Cox, J.A. (2009). The relation between Moderate Resolution Imaging Spectroradiometer (MODIS) aerosol optical depth and PM_{2.5} over the United States: a geographical comparison by US Environmental Protection Agency regions. *J. Air Waste Manage.* 59 (11), 1358–1369. <https://doi.org/10.3155/1047-3289.59.11.1358>.
- Zhang, H., Wang, Y., Park, T.-W., Deng, Y. (2017). Quantifying the relationship between extreme air pollution events and extreme weather events. *Atmos. Res.* 188, 64–79. <https://doi.org/10.1016/j.atmosres.2016.11.010>
- Zhang, K.M., Wexler, A.S., Zhu, Y.F., Hinds, W.C., Sioutas, C. (2004). Evolution of particle number distribution near roadways. Part II: the ‘road-to-ambient’ process. *Atmospheric Environment*, 38(38), 6655–6665. <https://doi.org/10.1016/j.atmosenv.2004.06.044>.
- Zhang, T., Zhu, Z., Gong, W., Xiang, H., Fang, R. (2016). Characteristics of Fine Particles in an Urban Atmosphere-Relationships with Meteorological Parameters and Trace Gases. *INTERNATIONAL JOURNAL OF ENVIRONMENTAL RESEARCH AND PUBLIC HEALTH*, 13(8). <https://doi.org/10.3390/ijerph13080807>.
- Zhu, J., Xia, X., Wang, J., Che, H., Chen, H., Zhang, J., Xu, X., Levy, C., Oo, M., Holz, R., Ayoub, M. (2017). Evaluation of aerosol optical depth and aerosol models from VIIRS retrieval algorithms over North China Plain. *Remote Sensing*, 9(5), 432. <https://doi.org/10.3390/rs9050432>.

- Zhu, Y., Fanning, E., Yu, R. C., Zhang, Q., Froines, J. R. (2011). Aircraft emissions and local air quality impacts from takeoff activities at a large International Airport. *ATMOSPHERIC ENVIRONMENT*, 45(36), 6526–6533. <https://doi.org/10.1016/j.atmosenv.2011.08.062>.
- Zhu, Y., Hinds, W., Kim, S., Shen, S., Sioutas, C. (2002a). Study of ultrafine particles near a major highway with heavy duty diesel traffic. *Atmospheric Environment* 36, 4323–4335. [https://doi.org/10.1016/S1352-2310\(02\)00354-0](https://doi.org/10.1016/S1352-2310(02)00354-0).
- Zhu, Y., Hinds, W.C., Kim, S., Sioutas, C. (2002b). Concentration and size distribution of ultrafine particles near a major highway. *Journal of the Air and Waste Management Association* 52 (9), 1032–1042. <https://doi.org/10.1080/10473289.2002.10470842>.
- Zhu, Y., Pudota, J., Collins, D., Allen, D., Clements, A., DenBleyker, A., ..., Michel, E. (2009). Air Pollutant Concentrations Near Three Texas Roadways, Part I: Ultrafine Particles. *Atmospheric Environment*, 43(30), 4513–4522. <https://doi.org/10.1016/j.atmosenv.2009.04.018>.
- Zieger, P., Fierz-Schmidhauser, R., Weingartner, E., Balensperger, U. (2013). Effects of relative humidity on aerosol light scattering: results from different European sites. *Atmospheric Chemistry and Physics*, (21), 10609. <https://doi.org/10.5194/acp-13-10609-2013>.
- Zimmerman, N., Wang, J. M., Jeong, C.-H., Wallace, J. S., Evans, G. J. (2016). Assessing the Climate Trade-Offs of Gasoline Direct Injection Engines. *Environmental Science & Technology*, 50(15), 8385–8392. <https://doi.org/10.1021/acs.est.6b01800>.